



**Technische
Universität
Braunschweig**

Band 1

HYWAG Schriftenreihe



EWATEC-COAST: Technologies for Environmental and Water Protection of Coastal Zones in Vietnam

**Contributions to
4th International Conference for Environment
and Natural Resources — ICENR 2014**

17—18 June 2014

Ho-Chi-Minh City, Viet Nam

Cuvillier-Verlag, Göttingen



HYWAG-Schriftenreihe

Band 1





EWATEC-COAST: Technologies for Environmental and Water Protection of Coastal Zones in Vietnam

**Contributions to
4th International Conference for Environment
and Natural Resources — ICENR 2014**

17—18 June 2014

Ho-Chi-Minh City, Viet Nam

Edited by

Günter Meon, Matthias Pätsch, Nguyen Van Phuoc and Nguyen Hong Quan

Cuvillier-Verlag, Göttingen



Bibliografische Information der Deutschen Nationalbibliothek

Die Deutsche Nationalbibliothek verzeichnet diese Publikation in der Deutschen Nationalbibliografie; detaillierte bibliografische Daten sind im Internet über <http://dnb.d-nb.de> abrufbar.

1. Aufl. - Göttingen : Cuvillier, 2014

© CUVILLIER VERLAG, Göttingen 2014

Nonnenstieg 8, 37075 Göttingen

Telefon: 0551-54724-0

Telefax: 0551-54724-21

www.cuvillier.de

Alle Rechte vorbehalten. Ohne ausdrückliche Genehmigung des Verlages ist es nicht gestattet, das Buch oder Teile daraus auf fotomechanischem Weg (Fotokopie, Mikrokopie) zu vervielfältigen.

1. Auflage, 2014

Gedruckt auf umweltfreundlichem, säurefreiem Papier aus nachhaltiger Forstwirtschaft.

ISBN 978-3-95404-852-6

eISBN 978-3-7369-4852-5



Acknowledgements

The joint research project “Environmental and Water Protection Technologies of Coastal Zones in Vietnam - EWATEC-COAST” (Grants 02WCL1217A-H) was kindly supported by funds provided by the German Federal Ministry of Education and Research (BMBF) and the Vietnam National University, Ho-Chi-Minh City, Viet Nam.



We deeply appreciate the work and assistance of all colleagues in Germany and Vietnam who contributed to this project.

How to cite this document

Citing the complete report:

Meon G., Pättsch M., Phuoc N.V., Quan N.H. (eds.) (2014): EWATEC-COAST: Technologies for Environmental and Water Protection of Coastal Zones in Vietnam. Contributions to 4th International Conference for Environment and Natural Resources, ICENR 2014. Cuvillier, Göttingen, Germany. ISSN: 2363-7218. ISBN: 978-3-95404-852-6

Citing a paper (example):

Fink A. H., Phan V. T., Pinto J. G., van der Linden R., Schubert D., Trinh T. L., and Ngo-Duc T. (2014): Climate change projections and selected impacts for Vietnam. In: Meon G., Pättsch M., Phuoc N.V., Quan N.H. (eds.) (2014): EWATEC-COAST: Technologies for Environmental and Water Protection of Coastal Zones in Vietnam. Contributions to 4th International Conference for Environment and Natural Resources, ICENR 2014. Cuvillier, Göttingen, Germany. ISSN: 2363-7218. ISBN: 978-3-95404-852-6

SPONSORED BY THE



Federal Ministry
of Education
and Research



Vietnam National University

Ho-Chi-Minh City



Institut für Geoökologie
Abt. Umweltsystemanalyse

Hochschule Ostwestfalen-Lippe
University of Applied Sciences



[enviplan@] professional flotation



Funding Measure

International Partnerships for Sustainable Technologies and Services for Climate Protection and the Environment – CLIENT

Project title

EWATEC-COAST: Technologies for Sustainable Protection of Coastal Zones in Vietnam

Reference Code: 02WCL1217A-H

Project duration

01.07.2012 - 30.06.2015

Funding volume of the joint project

3.021.622 €

Coordinator and contact

Technische Universität
Carolo-Wilhelmina zu Braunschweig
Prof. Dr.-Ing. Günter Meon
Leichtweiß-Institut für Wasserbau
Beethovenstraße 51a
38106 Braunschweig, Germany
Tel: 0531-391-3950
Email: ewatec@tu-bs.de
Web: www.tu-braunschweig.de/ewatec

Project Partners in Germany

Hochschule Ostwestfalen-Lippe
Universität zu Köln
Universität Siegen
enviplan Ingenieurgesellschaft mbH
A3 Water Solutions GmbH
IWUD – Ingenieure für Wasser, Umwelt und Datenverarbeitung GmbH
Institut für Wassermanagement IfW GmbH

Project Partner in Vietnam

Viet Nam National University HCMC – IER
Hanoi University of Science
Nhon Trach Industry Zone, Dong Nai Province
Dang Tu Ky Leather Company
Department of Natural Resources and Environment
DONRE
Provinces Dong Nai, Ba Ria–Vung Tau and HCMC
Can Gio Mangrove Protection Forest Management Board

Publisher

EWATEC-COAST Working Group

Editorial work and design

LWI

Printing

Cuvellier Verlag Göttingen

Cover photo credits

EWATEC-COAST, Volker Pick



Content

Authors	Title	Page
	Foreword by the Editors	
Meon, G. & Phuoc, N.V.	BMBF-VNU-joint research project “Environmental and Water Protection Technologies of Coastal Zones in Vietnam” (EWATEC-COAST)	1
Phan, V.T. et al.	Observed Climate Variations and Change in Vietnam	20
Fink, A.H. et al.	Climate change projections and selected impacts for Vietnam	35
Massmeyer, K. et al.	Modelling of atmospheric dispersion and deposition in industrial areas - Comparison of different modelling approaches -	57
Lorenz, M. et al.	Ecohydrological modeling of the Thi Vai Catchment in South Vietnam	83
Prilop, K. et al.	Integrated water quality monitoring of the Thi Vai River: an assessment of historical and current situation	97
Prilop, K. et al.	A 3D-hydrodynamic and water quality model of the Thi Vai river under strongly tidal effect	111
Lam, Q. D. et al.	The evaluation of groundwater level variations in a coastal zone using groundwater software FEFLOW	124
Anh, N. H. et al.	Accumulation of contaminants in mangrove species <i>Rhizophora apiculata</i> along ThiVai River in the South of Vietnam	138
Costa-Böddeker, S. et al.	Spatial distribution of diatom assemblages in surface sediments of a deltaic coastal zone in Southern Vietnam	157
Dangendorf, S. et al.	On analyzing the marine-hydrological boundary conditions for the flood risk in the Thi-Vai region	181
Fettig, J. & Pick, V.	Treatment of tannery wastewater by enhanced biological processes – preliminary results	194
Oldenburg, M.	Membrane bio-reactors for wastewater treatment - Principles and Design	204
Damann, R.	Municipal and Industrial Wastewater Treatment by Microflotation	214





Dear readers,

We are glad to present hereby the scientific and technical contributions of the EWATEC-COAST working groups to the 4th VNU - HCM International Conference for Environment and Natural Resources ICENR 2014 with a focus on “green growth, climate change and protection of the coastal environment”. This conference was held in June 2014 in Ho-Chi-Minh City (HCMC), Vietnam, and hosted by the Institute for Environment and Resources (IER) of the Vietnam National University Ho-Chi-Minh City (VNU-HCMC).

EWATEC-COAST is the name of our German-Vietnamese joint project dealing with “technologies for environmental and water protection of coastal zones in Vietnam under climate change conditions”. The project is coordinated by the University of Braunschweig, Germany. Main Vietnamese partner is the IER. The project is funded by the German Federal Ministry of Education and Research (BMBF) as a part of the funding initiative CLIENT, and by the VNU-HCMC. The project is financed for a period of three years. It started in fall 2012.

Presentations of the project scope and of intermediate results were embedded in the scientific programme of the ICENR 2014. More than 200 scientists, government officials, national and international experts and the engineering practice joined the conference. The excellent development of German-Vietnamese cooperation was appreciated by the Vietnamese Deputy Minister of Natural Resources and Environment (MONRE), Assoc. Prof. Bui Cach Tuyen, and the Consul General, German Consulate General of Ho-Chi-Minh City, Dr. Hans-Dieter Stell, in their welcome notes.

It is the rapid growth of economy and population that puts massive environmental pressure on river catchments in Vietnam. The joint project EWATEC-COAST focuses on one of the most jeopardized zones of Vietnam, the highly polluted inland water and estuary system of the Thi Vai river basin and the adjacent Can Gio mangrove forest, an UNESCO world biosphere reserve.

Both areas are located south-eastern of Ho-Chi-Minh City. In the past, various companies, which are mostly located in industrial zones along the river, discharged wastewater without treatment into the river system. The Thi Vai river was therefore considered as ecologically dead. Most recently, the water quality of the river has been slightly improved because first control initiatives have been realized. A comprehensive strategy for the sustainable rehabilitation is still missing.



EWATEC-COAST will significantly contribute to find ecologically and economically sound solutions for the rehabilitation of the affected water bodies, the fauna and the flora with focus on mangroves. Climate change impacts, in particular the impact of the sea water level on coastal protection and the inland water system will be considered. Main task is the development and application of a model-based "management system" for sustainable water and environmental protection of the affected coastal zone. The system will serve for decision making. Another important task is the development and optimization of innovative process technology for industrial waste water treatment in the industrial zones of the Thi Vai river basin.

The management system will be implemented at provincial and municipal authorities as well as research institutions and primarily serve as a planning framework. The project concept can be transferred to other regions of Vietnam and to other countries. First project results are very promising and confirm the suitability of the overall project strategy. Excellent perspectives for economic, scientific and technical exploitation of results are expected.

In this book we have compiled the contributions of nearly all German and Vietnamese project partners of EWATEC-COAST presented at the ICENR and hence present a comprehensive overview about the preliminarily findings that have been gained throughout focused research work since the beginning of the project.

We hope you enjoy reading this issue.

Yours sincerely

Günter Meon, Matthias Pätsch, Nguyen Van Phuoc and Nguyen Hong Quan
Braunschweig, Germany, and Ho-Chi-Minh City, Vietnam,

10 October 2014



BMBF-VNU-joint research project “Environmental and Water Protection Technologies of Coastal Zones in Vietnam” (EWATEC-COAST)

Günter Meon ⁽¹⁾ and Nguyen Van Phuoc ⁽²⁾

¹University of Braunschweig; Leichtweiss-Institute for Hydraulics and Water Resources; Dept. of Hydrology, Water Management and Water Protection; Beethovenstraße 51a, D-38106 Braunschweig, Germany;

²IER, VNU-HCMC, 142 To Hien Thanh Str., Distr. 10, Ho-Chi-Minh City, Vietnam

Abstract

The project “EWATEC-COAST” (Technologies for environmental and water protection of coastal zones in Vietnam under climate change conditions) started in autumn, 2012. The project is funded by the German Federal Ministry of Education and Research (BMBF) as a part of the funding programme “CLIENT” and by the Vietnam National University of Ho-Chi-Minh City (VNU-HCMC). Study areas are the highly polluted inland water and estuary system of the Thi Vai river and the adjacent Can Gio mangrove forest. Both areas are located south-east of Ho-Chi-Minh City. In the past, various companies, which are mostly situated in industrial zones along the river, discharged wastewater without treatment into the river system. The Thi Vai river was therefore considered as ecologically dead. Most recently, the water quality of the river has been slightly improved because first control initiatives have been realized. A comprehensive strategy for the sustainable rehabilitation is still missing. EWATEC-COAST will significantly contribute to find ecologically and economically sound solutions for the rehabilitation of the affected water bodies, the fauna and the flora with focus on mangroves. Furthermore climate change impacts will be considered. Main task is the development and application of a model-based “management system” for sustainable water and environmental protection of the affected coastal zone. The system will serve for decision making. Components of the integrative system are meteorological data series for the past, present and future including climate change, and data on the quantity and quality of surface water and ground water systems, the mangrove ecosystem, aquatic organisms and coastal protection. Another



important task is the development and implementation of innovative water technology for the treatment of tannery wastewater. For this, a multi-stage pilot plant has been put in operation in an industrial zone located in the project region. The management system will be implemented at provincial and municipal authorities as well as research institutions and primarily serve as a planning framework. The project concept can be transferred to other regions of Vietnam and to other countries. First project results are very promising and confirm the suitability of the overall project strategy. Excellent perspectives for economic, scientific and technical exploitation of results are expected.

Key Words: EWATEC-COST, Vietnam, climate change, hydrologic modelling, hydrodynamic modelling, water quality modelling, Thi Vai river, Can Gio mangrove forest, coastal zone, environmental and water protection, tannery waste water.



1. Introduction

The country of Vietnam has more than 3000 km of coastline. Parts of the coast are frequently affected by devastating storm floods, often in combination with inland flood waters. The loss of lives, the economic losses and environmental damages are substantial. In addition to the threat caused by natural disasters, the environmental conditions have deteriorated significantly since the economic opening of the country in 1990 due to industrialization along many rivers and littorals. This critical situation is overlaid with the climate change and its consequences. For most of the coastal areas, these consequences with respect to the rise of the sea level and increasing extreme inland flood waters and low waters, respectively, have not been scientifically quantified. Moreover there is a lack of sustainable technologies in many areas – for example for the integrated management of surface and groundwater resources or for an efficient treatment of industrial wastewater. Water authorities and municipalities usually do not use well proved planning tools like management concepts or even model-based management systems for an integrated and sustainable water management. In the joint German-Vietnamese research project EWATEC-COAST (Technologies for environmental and water protection of coastal zones in Vietnam under climate change conditions), technologies and service tools for the sustainable improvement of an affected coastal zone located in southern Vietnam will be developed and provided. This project has been running since September 2012 and will last until about September 2015. The project is funded by the German Federal Ministry of Education and Research (BMBF) and the Vietnam National University of Ho-Chi-Minh City (VNU-HCMC). The research area of this project is the Thi Vai river landscape and the adjacent Can Gio Mangrove forest both being located about 2 hours south-east of HCMC. The German project partners are coordinated by the Leichtweiss Institute (LWI) for Hydraulics and Water Resources of the University of Braunschweig. The Vietnamese project coordinator is the Institute for Environment and Resources (IER) of the VNU-HCM.

The main objective of the project is (1) the development and application of a model-based "management system" for the sustainable protection of water, environment and human beings in coastal zones and (2) implementation of water technology with focus on industrial waste water man-

agement. The results of the water technology part will be accounted for by the management system. This planning instrument enables to identify and optimize combined measures for a sustainable improvement of the environmental and living conditions of the designated coastal zone. Anthropogenic influences as well as the natural climate variability and future climate change will be examined within the project. The project concept can be transferred to other concerned regions.

2. Project Area

The project area covers the Thi Vai river basin and the Can Gio mangrove forest in South Vietnam (Figure 1).



Figure 1. Project area "Thi Vai river" and "Can Gio mangrove forest ", modified map from Google 2011

The river has a length of 37 km from the Ba Ky weir to the sea mouth. The mean temperature of the Thi Vai catchment is about 28°C, the mean annual rainfall amounts to about 1800 mm. The area is affected by the tropical monsoon climate with a rainy season from May to November and a dry season from December to April. The whole river is strongly affected by tide. The Ba Ky weir has the task to prevent the salt intrusion into the upper part of the Thi Vai river. Towards downstream, the width of the



main river bed increases significantly up to 900 m. In addition to the main reach, several meandering subreaches exist. The river system is exposed to the strong tide. The daily tidal range is about 3 m. The strong tide effect hinders the transport of polluted inland river water into the sea. Until 2009, the Thi Vai basin was considered as a “hot spot” with regard to surface water pollution in Vietnam. The main reason was and still is the release of untreated industrial wastewater into the river system. From about 1994 to 2008, the large Vedan company released highly concentrated waste water into the main river. Thanks to a partially improved control and punishment campaigns by local and superior authorities, the surface water quality of Thi Vai River has slightly improved in the recent years. A comprehensive strategy for a sustainable rehabilitation is still missing. Consequently, planning instruments and their implementation and application are essential for the region.

The Can Gio mangrove forest is located about 40 km south-east of Ho-Chi-Minh City and is a UNESCO biosphere reserve. It is about 760 km² in size and is adjacent to the Thi Vai river basin. The forest also serves as a protection barrier against storm floods which threaten Ho-Chi-Minh City. In recent years this nature reserve was ecologically damaged by erosion and sedimentation along the coastal zones, by aquacultures, inflowing untreated wastewater and oil spills. Parts of the soil had been chemically changed due to the reduced freshwater inflow from inland, saltwater intrusion from the sea and an increasing evaporation. Large parts of the trees and other resources in the Can Gio mangrove forest have therefore disappeared. Because of the expected rise of the sea level due to climate change and increasing pollution loads from the inland, a sustainable protection of this nature reserve is urgently needed.

3. Structure of the EWATEC-COAST project

The EWATEC-COST project is divided into 9 subprojects (SP) according to Figure 2. Components of the modelling-based subprojects are combined in SP 9 “development and application of a model-based management system for the sustainable protection of water, environment and human beings in coastal zones”. The SP 8 includes the installation, operation and optimization of a pilot plant for the treatment of wastewater from a tannery locat-



ed in an industrial zone at the Thi Vai river. Results of SP 8 will be considered in the management system.

Within the present project phase, the management system will reach the following working level:

- Analysis of the past up to the current state.
- Prediction of the effects of future climate changes and other factors on water and environment “without measures”.

The system will be transferred to the Vietnamese users, in particular to the Departments of Natural Resources and Environment (DONRE) of the concerned provinces, to municipalities and other institutions. The project partners will support the local users to develop planning variants “with measures” including environmental technologies against water pollution and adaptation measures to meet the climate change. It is foreseen that the management system will be extended in a future project phase to cover all relevant planning variants “with measures”.

It is emphasized that the development of the management system is accompanied by a supervisory group consisting of the future users - mainly DONRE personnel – and national and international advisors.

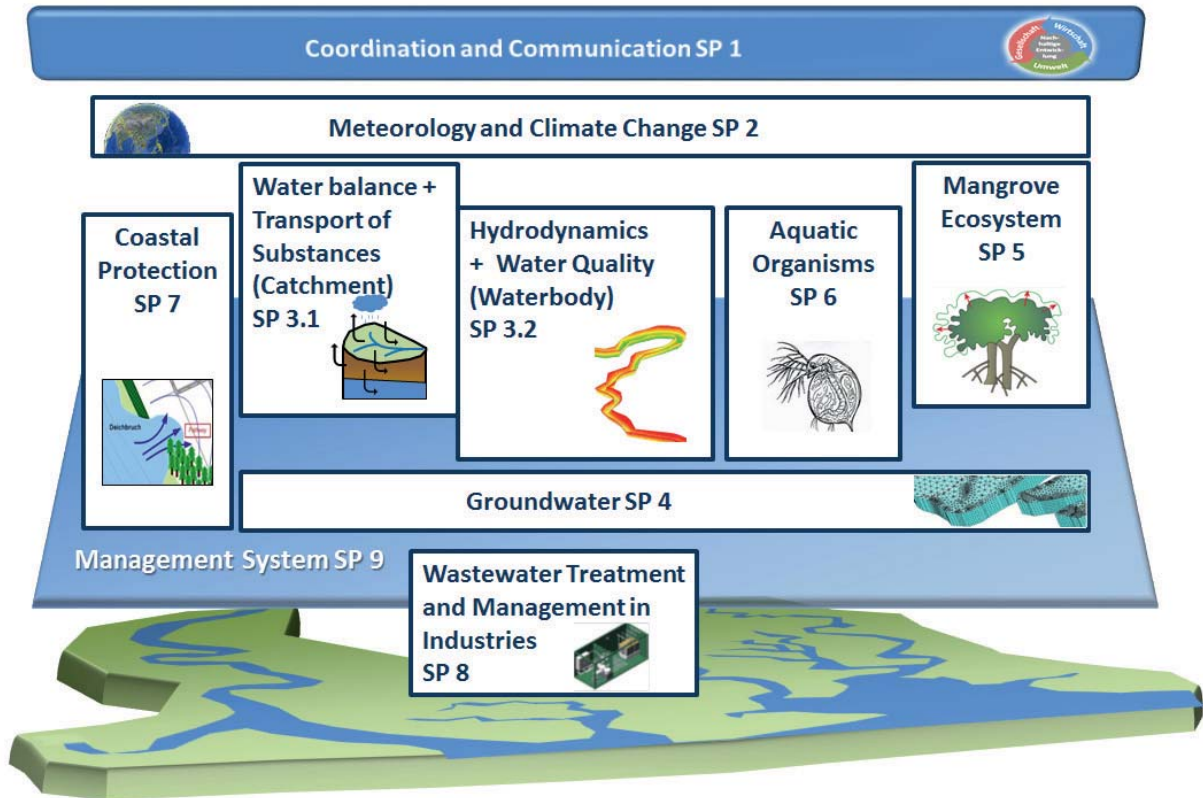


Figure 2. Structure of the joint research project EWATEC-COAST with a total of 9 subprojects

4. Subprojects

Subproject 1 has the task of professional and administrative coordination for the whole project. It is important to pay special attention to the successful content-related and methodological cross-linkage of the subprojects and cooperation between the Vietnamese and the German partners. Within the project, an EWATEC-COAST contact group (ECCG) was established. The group consists of members of the Vietnamese and German project coordinators who ensure that questions, problems or exchanges between the responsible scientists in the different subprojects can be continuously communicated. The ECCG is thus able to convey between the partners, to support existing contacts, as well as to build new contacts between German and Vietnamese partners. In addition, the ECCG cooperates with the stakeholders and the interested Vietnamese public such as Ministry of Natural Resources and Environment (MONRE), provincial Departments of Natural Resources and Environment (DONRE) and with the supervisory group mentioned in chapter 3 with the aim of developing an implementation plan of the project results.



Subproject 2 "meteorology and climate change" is linked to all subprojects in the management system (Figure 3). Weather and climate information (including precipitation, temperature, evaporation, air humidity, wind, radiation, sunshine duration) had been created as meteorological data series for the current situation (past to present) and for the future (approx. 2040-2070) by using state-of-the-arts methods. Meteorological data being available from the region and from international databases had been collected in cooperation with Vietnamese climate researchers. Using this data, the climate and its variability and extreme events were analyzed. In the next step, a statistic-dynamic downscaling based on the COSMO Climate Local Model (CLM) for the Thi Vai basin and the mangrove area has been conducted. The obtained long-term data series are being further refined with the help of a probabilistic regionalization. The results are used as an input for the water budget and water quality modelling in SP 3, groundwater modelling in SP 4, analysis of sea level in SP 7 and investigations of the mangrove ecosystem in SP 5. Particular emphasis is given on an appropriate spatial and temporal resolution of the climate data, as well as on quantitative and qualitative precision regarding the spatial projection. Hence, a relevant research focus is the quantification of uncertainty of scenario data by taking into account the different meteorological regional models and various greenhouse gas scenarios. The meteorological data sets will finally be provided to SP 9. Furthermore SP 2 includes air pollutant modelling for the research area. The assessment of air quality with increasing air pollution as a result of the population and industrial growth provides the basis for the development of technologies to improve environmental and living conditions in the coastal region.

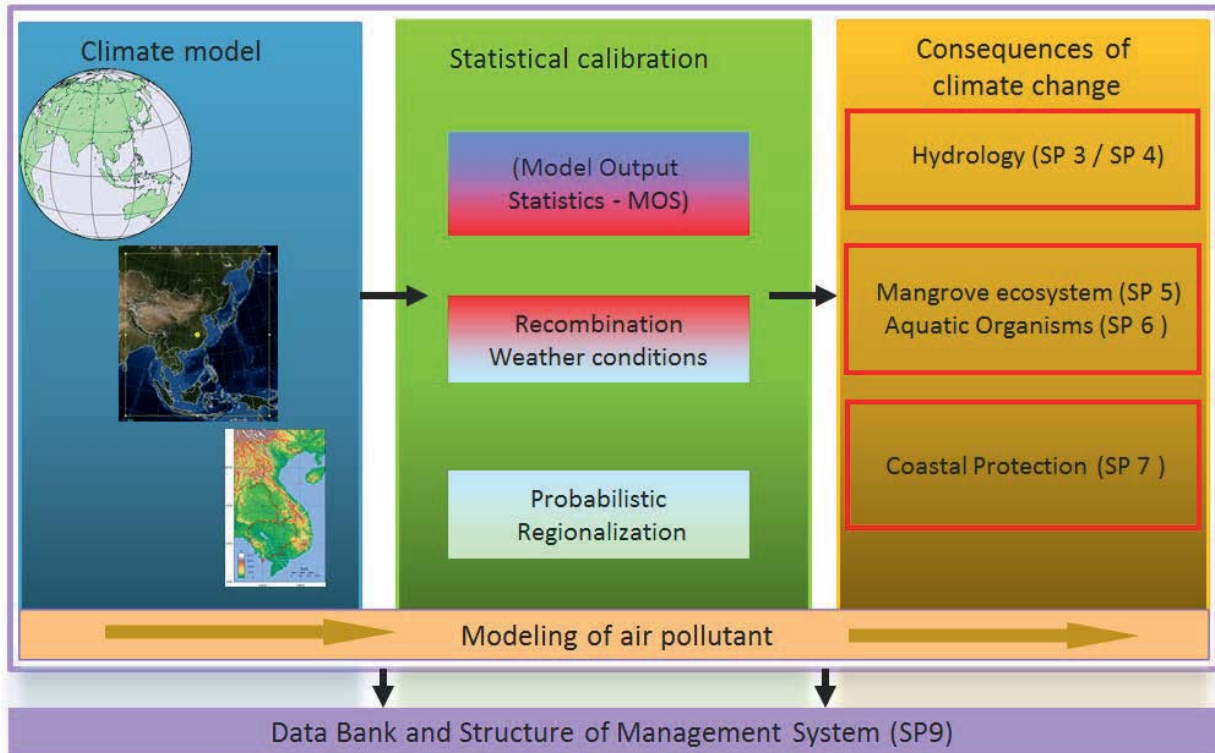


Figure 3. Working scheme of SP 2 "Meteorology and climate change"

Subproject 3 "surface water" is the core subproject for the water management system, since it includes the modelling of water resources with a focus on surface water quantity and quality (Figure 4). The SP 3 is thus closely related to all subprojects of the management system. The main objective of SP 3 is the development and application of a linked model system for long-term-continuum simulation. In this system, a model for the hydrological water balance and transport of substances (point and non-point sources) from the catchment into the river for the whole catchment area of the Thi Vai river has been developed. For this the model PANTA RHEI programmed by the Leichtweiss Institute, University of Braunschweig (see Riedel et al., 2011) was selected. This ecohydrological model or hydrological water quality model will be coupled with a hydrodynamic water quality model (DELFT3D, see Deltares, 2014) for the main river.

In addition to the meteorological data being available from SP 2, SP 3 requires series of hydrometric data and water quality data for calibration. These data were not available at the beginning of the project. Consequently, a monitoring program was performed. It consists of the installa-



tion and operation of 7 hydrometric stations – 3 at relevant tributaries, 4 along the main river - since early 2013 for a continuous measurement of the water level. With the help of ADCP technique, rating curves had been elaborated to transform the water level into discharge – a challenging task because of the strong tide and because of the increasing width of the main river bed towards the river mouth. For the water quality, water samples were taken at all stations in short time intervals and analyzed in a project laboratory which was installed in the industrial zone close to the pilot plant. The water quality measurement will end at the end of June 2014, and the water level measurement will last until the end of March 2015.

In the meantime, the models had been built up. The models are being individually calibrated with the measured data. After that, the models will be coupled in cooperation with SP 9 to form the management system. Process equations will be adjusted to the specific circumstances of the river. For the real situation (past to present) and future scenarios (2040-2070), meteorological time series will be provided by SP 2, and time series of the sea water level by SP 7. The wastewater pollutants load from point sources was collected from the provincial DONREs in cooperation with the Vietnamese partner institute IER. As a result, the impact of anthropogenic influences and climate change will be quantified for the variant "without measures". The data, the model system and the results will be integrated in the management system (SP 9). After implementation of the management system at various users, the project partners will help the local users to set up first scenarios respectively planning variants "with measures". Extension of the management system to deal with the latter variants is envisaged in a consecutive project phase.

Concurrently, SP 3 serves as an interface to SP 8 "water technology". Cleaning effects achieved with the pilot plant in of SP 8 will be integrated in the model chain of SP 3 at all existing sites of tannery factories. But also effects of (future) treatment facilities for other types of wastewater, e.g. from firms producing tapioca starch, will be considered. For the latter, results from the completed German-Vietnamese research project TAP-IOCA (Meon et al., 2013; Le Huyen et al., 2012) will be used.

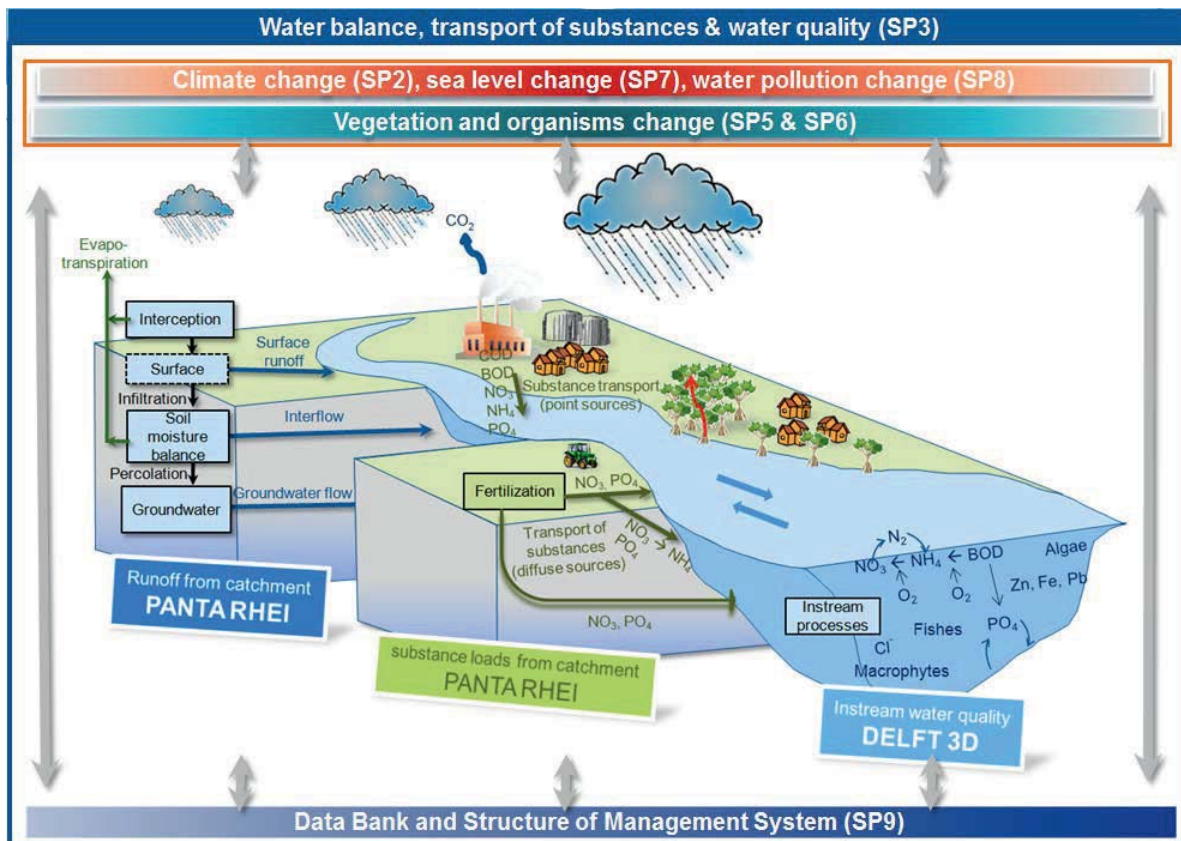


Figure 4. Working scheme of SP 3 "surface water"

Subproject 4 "ground water" is mainly linked with SP 3. The main objective is the development and the application of a regional groundwater model for relevant parts of the Thi Vai river basin. Due to the heavily pollution of surface water in the research area, groundwater is intensively used for domestic water supply, irrigation and for industrial water supply. The overexploitation of water, the salt intrusion in conjunction with changing climatic conditions requires a sustainable groundwater management as part of an integrated water resources management. The working scheme of SP4 is displayed in Figure 5.

Because of the weak data situation, own groundwater observation stations were established and are being operated together with the Vietnamese partners. In parallel the hydrogeological model FEFLOW (DHI-WASY, 2014) was set up. First results will be showed during the conference. The simulation for the current situation and the future situation is carried for the same periods as in the SP 3.

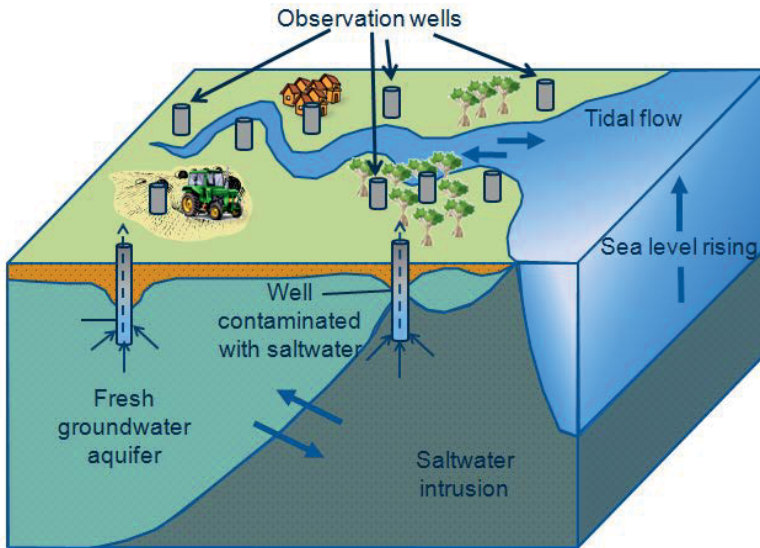


Figure 5. Working scheme of SP 4 "ground water"

In **subproject 5** "mangrove ecosystem", mangrove trees and forests are investigated with focus on their functioning as natural wetlands for the cleaning of polluted river water in the estuary system. Aim is to develop a model for the propagation and the degradation of pollutants by phytoremediation within a river basin (Figure 6). For this purpose, the processes describing the absorption of substances by roots, their distribution and degradation were already implemented in a local (point) mangrove model which represents a single mangrove tree. On the basis of the local model a simplified reactor model is being developed. The reactor model is characterized by the composition of the mangrove ecosystem, stocking density, soil properties, salinity and the hydrological regime. The next step is the upscaling from the reactor scale to a larger landscape scale (mangrove catchment) which includes simplified mass transport in the river system. In addition, the option of coupling the landscape model with the complex water quality model of SP 3 will be examined.

For the calibration of the local scale model, local field measurements regarding the degradation are being carried out together with the Vietnamese partners. Totally, 6 plot stations on the forest site and located along the Thi Vai river and 6 other plot stations located inside the Can Gio mangrove forest were selected. Vegetation and soil samples of these 12 stations were taken and analyzed in Germany. In addition, a greenhouse was

constructed in July 2013 in collaboration with the IER. The purpose of the greenhouse is to test the capacity of mangrove trees in taking up contaminants. The first samples were harvested in November 2013 and analyzed by the IER. The landscape model should be able to predict the pollution in the Thi Vai River in dependency of the remediation potential of mangrove forests. The results are required for the development and quantification of protection technologies which can be quantified within the management system.

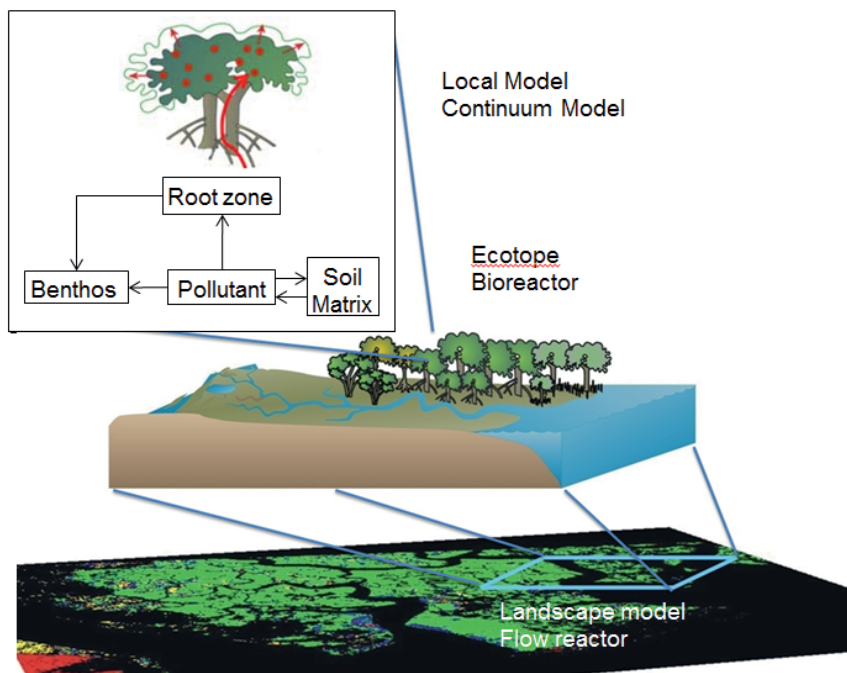


Figure 6. Working scheme of SP 5 "mangrove ecosystem"

In **subproject 6** "aquatic organisms" long time information (one to several decades) about water quality and water balance are derived by analysis of aquatic organisms (Figure 7). This information supplements the data inventory of water quality data. It can be compared with the new data from the monitoring program and the results of model simulations of SP 3. Within SP 6, sediment samples from the mangrove forests and the Thi Vai river estuary were taken. Physical parameters, nutrient contents and heavy metal were measured at the laboratory of IER. Species of aquatic organisms had been analyzed. On the basis of fossil species associations from continuously deposited sediments and the geochemical sig-

nature of the sediments, the development of the mangrove and estuarine ecosystem for the past decades is planned to be reconstructed.

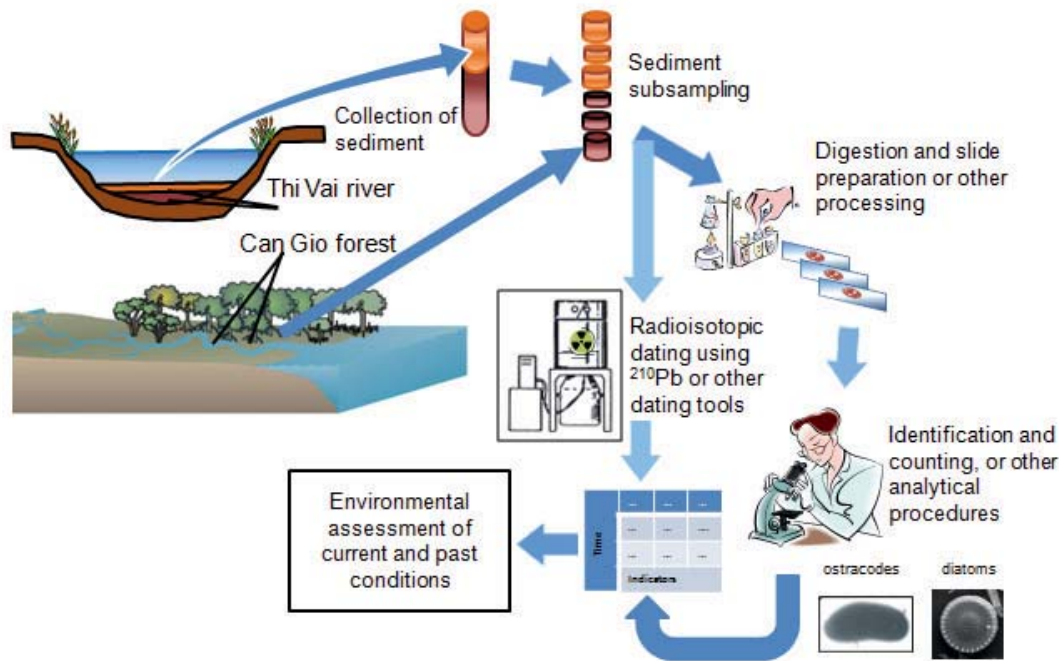


Figure 7. Working scheme of SP 6 "aquatic organisms"

The focus of subproject 7 "coastal protection" is on hydrological system and risk analysis of the coastal subarea stretching along the project region. Climatic and anthropogenic changes in the study area will be taken into account (Figure 8). The systems analysis is essential to develop a sustainable coastal protection strategy. Like in the other subprojects, existing data series of the corresponding sea water level were firstly collected and evaluated. These data are used as boundary conditions for the models of SP 3, 4 and 5. Based on time series analysis of these data, statistical analysis of the mean sea level (MSL) and of extreme discharge values observed in the Dong Nai river basin had been derived. These values were then transferred to the Thi Vai river basin. Both analyses are statistically superimposed for the purpose of identifying seaside and inland extreme situations and creating forecasts. The results are incorporated as boundary conditions in the hydrodynamic calculations of extreme flood inundations (landfall of tropical cyclones) in the coastal zone by means of DELFT 3D. For future extreme events in the coastal and estuary flood zones, the expected annual risk of loss of life and the annual economic risk costs will be estimated. For this purpose specific damage val-

ues are required and will be set up together with Vietnamese partners in the region. Quantitative risk indices such as the annual hazard and potential for damage for the period "past to present" and period "future without measures" will be determined. These parameters are used for a first development of technical and natural protection technologies. This work is strongly supported by Vietnamese partners at the VNU-HCMC. The integrative analysis of overlapping inland and sea-side extreme events, but also the modelling of the protective effect of existing mangrove forests to the reduction of the spread of storm surges in the coastal zone is a scientific challenge.

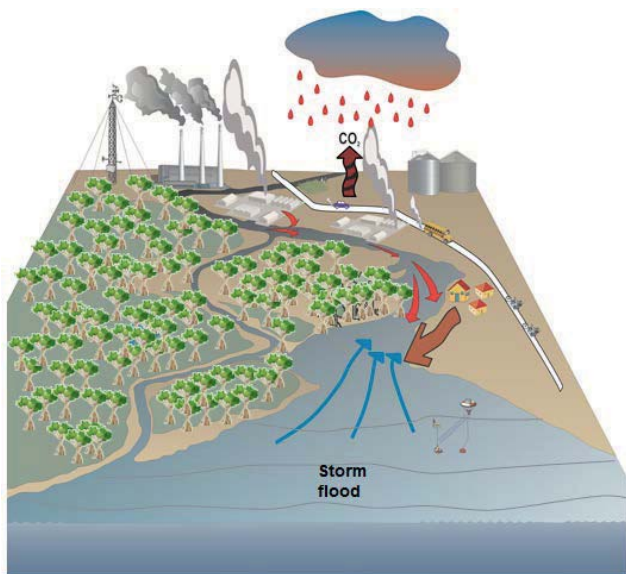


Figure 8. Working scheme of SP 7 "coastal protection"

Subproject 8 "industrial water management" refers to industrial waste water treatment and process water optimization. In this subproject, a pilot plant for leather wastewater treatment using German process engineering was developed. The pilot plant is now being further adapted to the on-site conditions and optimized during the project. A membrane bioreactor was built in Germany and shipped to Vietnam. It arrived in Vietnam in April 2013. Existing parts of the pilot plant from the former TAPIOKA project (Huyen Le et al., 2012) – in particular the anaerobic reactor (type EGSB) and a microflotation equipment - were removed from the old pilot plant location in the Tay Ninh province to the selected leather factory. This factory is located in an industrial zone located at the upper

Thi Vai river, province Dong Nai. The process technology which was taken over had to be adapted to the new demands. The entire pilot plant including associated laboratory equipment was put into operation in May 2013. With this pilot plant, the ability of an extensive cleaning of tannery wastewater including the safe removal of pollutants like sulfide-sulfur and chromium is now being investigated. To achieve an optimal adaptation to the sewage situation on site, the original treatment concept was modified. In the new concept (Figure 9), pretreatment of the wastewater is processed by microflotation technique (dissolved air flotation). After that, the treatment train is divided into two lines: In line 1 the wastewater after microflotation is treated by the anaerobic reactor (type EGSB). In line 2 the membrane bioreactor is put behind the flotation stage. The effluent from the membrane bioreactors which is virtually solids-free will be tested to be recirculated into the water cycle of the tannery.

The results will be part of the expected know-how transfer. Information thus obtained will be fed into the SP 3 "surface water" and in the management system.

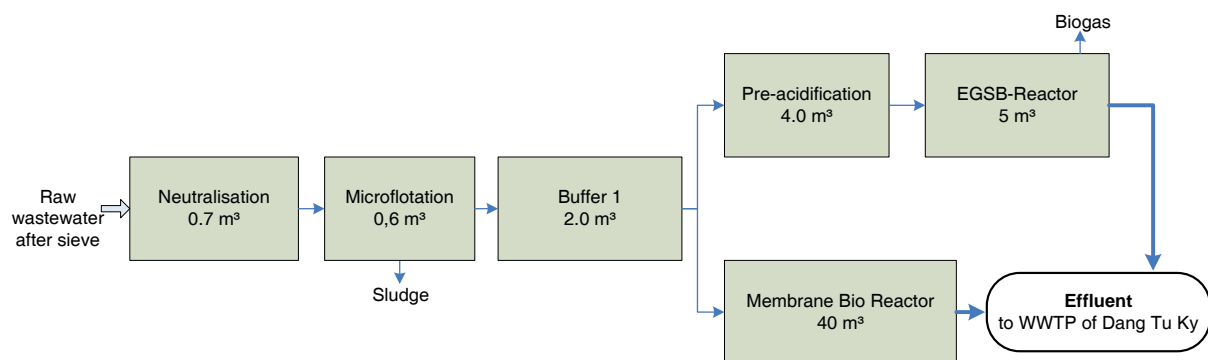


Figure 9. Working scheme of SP 8 "industrial water management"

Subproject 9 "management system" has a cross divisional function for the entire project. Several mathematical models of the other subprojects will be coupled with the help of SP 9. An effective model-based expert system where the main components are the software platform, the database, a model control unit, analysis and display routines will be provided. At the end of this project phase, the system will be available in a prototype version that contains parameterized results of model applications for time level 1 (past to present) and level 2 (future without measures). In-



egrated model applications will be controlled individually or in a linked mode. For applications, various input data sets will be integrated into the system. To meet the project objectives, the system is structured in a way that relevant data, which are collected and processed by other subprojects, can be acquired centrally. This data - as a part of a system data base - will be made available to the user by a uniform interface. Procedures will be designed to control the different model systems of the subprojects and to couple them on demand. On this basis, data and model results from (coupled) simulations will be presented for the current situation and the forecast for different situations "without measures respectively action". It is foreseen that the management system will be extended in a future project phase to cover all relevant planning variants "with measures respectively action". The proposed management system is a dynamic system. It will be structured in such a way that any realized simulations can be stored and visualized. Parameterized results of precalculated variants can be read out directly. Individual applications can be defined by qualified users and be processed by the system.

5. First results and outlook

All subprojects gained first results which show promising progress in the project to develop the management system. The detailed results can be found in other papers of the ICENR 2014 conference. In this paper, only some intermediate results concerning the water quantity and water quality of the Thi Vai River will be shown.

Figure 10 shows the measured and simulated water level of the Thi Vai river at the station Vedan located at the (upper) middle reach in May 2013. The discharge at the station Phy My located at the (lower) middle reach is reproduced in Figure 11. Enormous tide effects cause the strong variability of water level and discharge. In the middle reach, maximum discharges vary between about $+8.000 \text{ m}^3/\text{s}$ and $-8.000 \text{ m}^3/\text{s}$. The simulation was performed with the model DELFT3D and confirms that the selected model can represent the river dynamics and the tide effect very well.

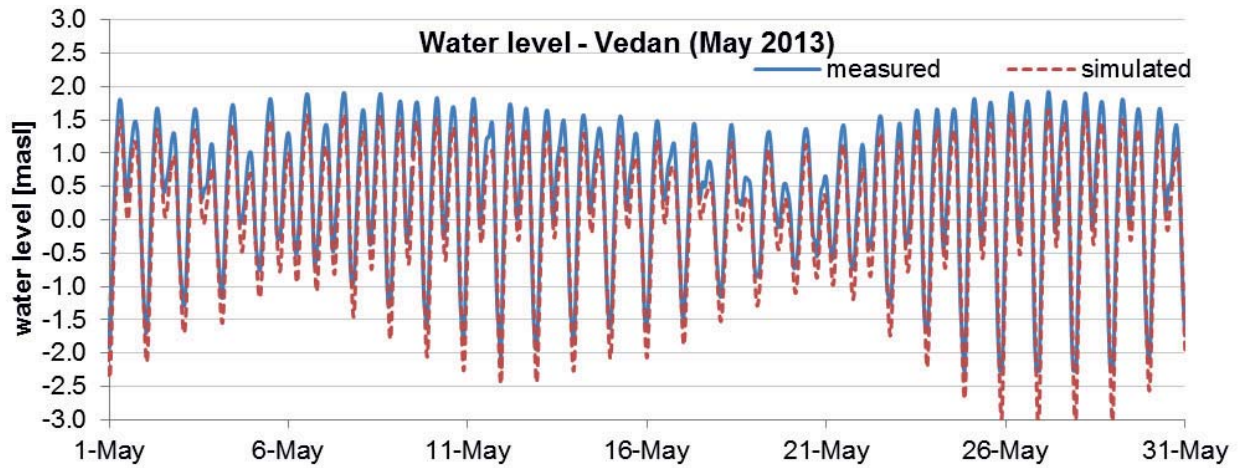


Figure 10. Measured and simulated water levels at the Thi Vai river, station Vedan, in May and October 2013.

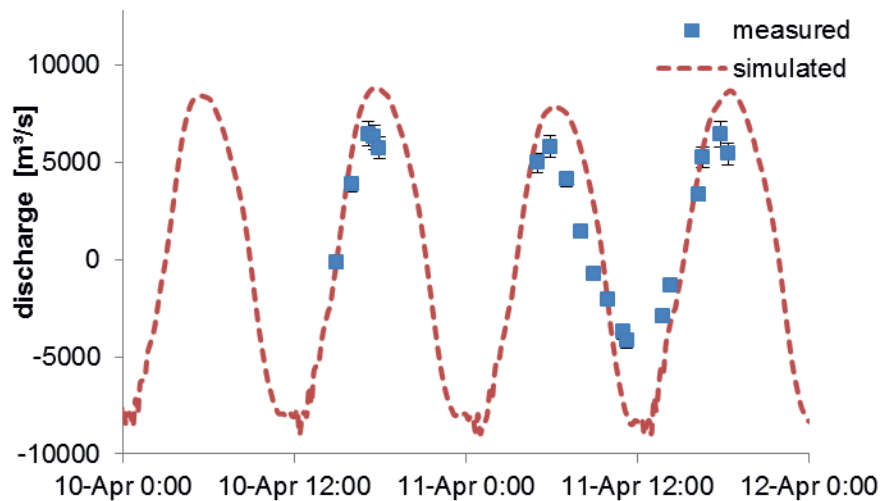


Figure 11. Measured and simulated discharges at the Thi Vai river, Phi My station, from 10 to 12 April 2013.

Concerning the water quality and according to observed parameters, improvement of the water quality has taken place, but signs of pollution like high nitrite concentrations and low dissolved oxygen concentrations still exist (Figure 12).

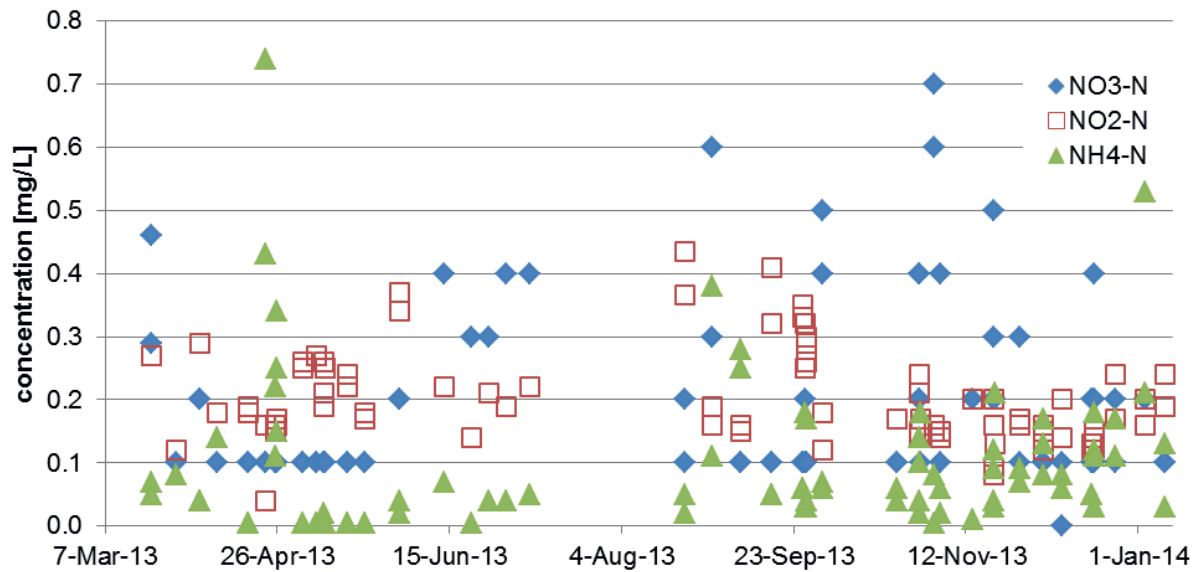


Figure 12. Measured concentrations of NO₃-N, NO₂-N and NH₄-N at the Thi Vai river, station Vedan.

References

- [1] Deltares (2014): see Website: <http://oss.deltares.nl/web/delft3d>
- [2] DHI-WASY (2014): see Website: <http://www.feflow.info/>
- [3] Le, T.T.Huyen., Lorenz, M., Prilop, K., Lam, Q. D., Meon, G. (2012): An eco-hydraulic model system for water management of the Saigon river system under tide effect. Proceedings of the "9th International Symposium on Eco-hydraulics". September 17th - 21st 2012. Vienna, Austria.
- [4] Meon, G., Le, T.T.H., Fettig, J., Nguyen, P. (2013): Water pollution management in the vicinity of the Lower Mekong Basin: German-Vietnamese research projects "TAPIOCA" and "EWATEC-Coast". Proceedings of the Environmental Mekong Symposium, Ho-Chi-Minh City, 5-7 March 2013.
- [5] Riedel, G., Meon, G., Förster, K., Lange, S., Lichtenberg, T., Anhalt, M. (2011): Panta Rhei –Hydrologisches Modellsystem für Forschung und Praxis in Niedersachsen. In: Blöschl, G., Merz, R. (Hrsg.): Hydrologie & Wasserwirtschaft - von der Theorie zur Praxis. Forum für Hydrologie und Wasserbewirtschaftung, Heft 30.11.



Observed Climate Variations and Change in Vietnam

Phan V. T.¹, Fink A. H.², Ngo-Duc T.¹, Trinh T. L.¹, Pinto J. G.^{3,4},
van der Linden R.³, Schubert D.^{3,5}

¹Department of Meteorology, Hanoi University of Science, Vietnam National University, Hanoi, Vietnam

²Institute for Meteorology and Climate Research, Karlsruhe Institute of Technology, Karlsruhe, Germany

³Institute for Geophysics and Meteorology, University of Cologne, Cologne, Germany

⁴Department of Meteorology, University of Reading, Reading, United Kingdom

⁵Department of Environmental Engineering and Applied Computer Sciences, University of Applied Science, Höxter, Germany

Abstract

In this study, observed changes of temperature, rainfall, and some extreme climate indices in Vietnam were investigated by using daily observations during the period 1961-2012. The observed data were collected from 80 meteorological stations for temperature, and from 170 stations for rainfall over the seven climatological sub-regions of Vietnam. Results show that there were insignificant differences between the trends of changes obtained from the 1961-2011 and 1979-2012 periods. Near-surface temperature, including mean (T_{2m}), maximum (T_x) and minimum temperature (T_m), increased consistently at almost all stations. T_m increased faster than T_x. Temperature also increased faster in winter than in summer. Consequently, the number of hot days and warm nights increased whereas the number of cold days, cold nights and cool days decreased. In the northern regions, temperature tended to slightly decrease in May but significantly increased in June.

Annual rainfall decreased in the northern area of Vietnam, while it increased at almost all stations in the central regions, and had insignificant trends in the southern sub-region. Changes in some extreme rainfall indices were likely consistent with changes in annual rainfall. Monthly rainfall in the central regions significantly increased from August to December. Rainfall generally increased in May and decreased in June over almost all country.

Key Words: climate change, extreme events, trend analysis



1. Introduction

From the late 19th century, the average near-surface temperature has globally increased by about 0.74°C (IPCC, 2007). However the warming was not uniform for all places on the globe; some places were even slightly colder than before (IPCC, 2007). In some arid areas such as the Southwest United States, Southwest Asia, Central Asia, or Australia, the rate of warming was believed to be slightly higher than the warming rate over the continents, therefore higher than the global average rate (Hulme, 1996). The rise of global temperatures might lead to changes in atmospheric and oceanic circulations that consequently cause changes in rainfall patterns and other extreme climate phenomena. Global warming could also alter bio-climatic conditions. Agricultural production in some areas might be heavily impacted due to the increase in the frequency and intensity of droughts that could occur even in the areas with increasing precipitation. Therefore, in the context of the current global warming, assessing climate change (CC) is of particular importance. The results of the assessment provide a scientific basis for evaluating the impacts of CC, hence mitigation and adaption measures can be designed and implemented. At regional and national scales, the assessments of climate change were usually conducted following two steps: 1) Assessing climate change based on the observed data; and 2) Projecting future climate.

Vietnam's climate is mainly influenced by summer monsoon (also called southwest monsoon, from May to October) and winter monsoon (or northeast monsoon, from November-April). Additionally, the impact of the Inter-Tropical Convergence Zone as well as other tropical disturbances in the interaction with the topography also play an important role. In the past recent years, several studies about the changes of climate conditions in Vietnam have been conducted (eg. Ho et al., 2009; Phan et al., 2009; Phan et al., 2010; Ho et al., 2011; Ngo-Duc et al., 2012; Nguyen, 2008). However, further evaluations of the changes of temperature, rainfall and their mechanism of changes are still needed. In this study, observed daily data during the period 1961-2012 are used to examine the changes of temperature and rainfall characteristics for the whole territory of Vietnam. Detailed description of the data and methodology are presented in Section 2. Sections 3 and 4 present the analysis results and conclusions, respectively.

2. Data and methods

The following daily observed variables were collected from the meteorological station network of Vietnam: 1) rainfall (R); 2) near-surface air temperature (T2m); 3) daily maximum near-surface air temperature (Tx); and 4) daily minimum near-surface air temperature (Tm). Figure 1 shows the number of stations where data were available. The collected data were sparse before 1979. There are totally about only 60 stations in the network with more than 50 years of data. In truth, there are about 120 to 170 stations in Vietnam with more than 60 years of data but their use for research purposes was still limited because the data had not been fully digitized. Since 1978, the number of meteorological stations with available data has significantly increased. There are about 80 and 150 stations for temperature and rainfall, respectively. Therefore in order to compare the spatial distribution as well as the changes of temperature and rainfall over time, two periods were separately used in this study: 1) 1961-2012 for stations with at least 45 years of data; and 2) 1979-2012 for stations with at least 30 years of data.

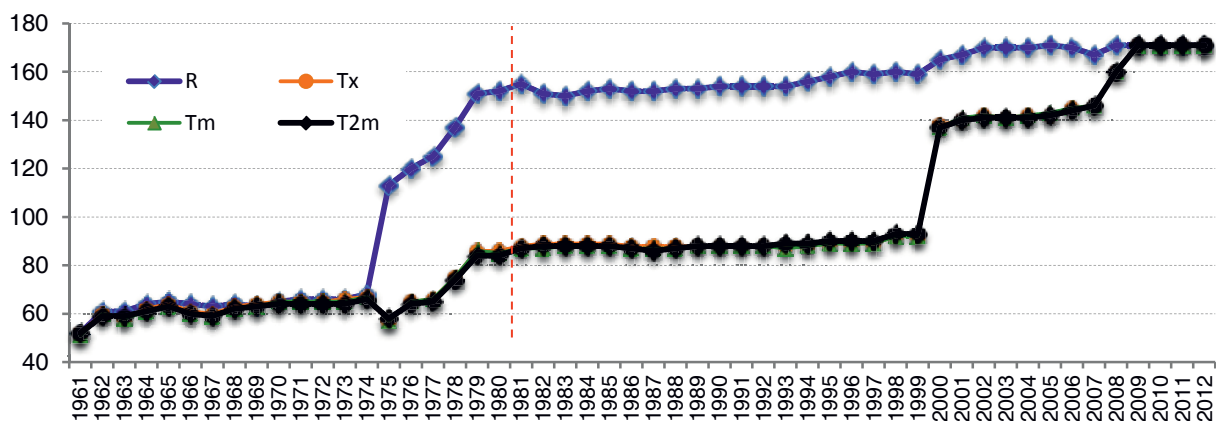


Figure 1. Number of meteorological stations used in this study over time. The vertical axis indicates the number of stations; the horizontal axis indicates the observed period from 1961 to 2012.

The data were provided by the Data Center of the National Hydro-Meteorological Service of Vietnam, which belongs to the Ministry of Natural Resources and Environment. The missing data and the data with detected errors are excluded in the analysis. Monthly (annual) temperature



and rainfall are only estimated if there are more than 25 (330) days in the month (year) with available data. This is equivalent to 80% (90%) of data availability.

The trends of changes of climate characteristics are estimated using the Sen's slope (Sen, 1968) and the non-parametric Mann-Kendall test (Kendall, 1975).

Table 1 shows several climate variables derived from temperature and rainfall. Those variables are analysed and discussed in Section 3.

Table 1. Climate variables derived from temperature and rainfall. A rainy day is the day where its total rainfall is greater than or equal to 0.1 mm.

No	Variables	
1	Annual average near-surface temperature	T2m
2	Monthly average near-surface temperature	Tmon
3	Annual average value of daily maximum near-surface temperature	Tx
4	Annual maximum value of daily maximum near-surface temperature	TXx
5	Annual average value of daily minimum near-surface temperature	Tm
6	Annual minimum value of daily minimum near-surface temperature	TNn
7	Number of hot days (days with $T_x \geq 35^\circ\text{C}$)	Tx35
8	Number of cold days (days with $T_m \leq 15^\circ\text{C}$)	T2m15
9	Annual count of days when $T_x > 90$ percentile	TX90p
10	Annual count of days when $T_m < 10$ percentile	TN10p
11	Total annual rainfall	R
12	Total monthly rainfall	Rmon
13	Annual count of rainy days	R01Ann
14	Total rainfall during the summer monsoon season (May-October)	RSum
15	Total rainfall during the winter monsoon season (November-April)	RWin
16	Number of rainy days during the summer monsoon season (May-October)	R01Sum
17	Number of rainy days during the winter monsoon season (November-April)	R01Win
18	Annual maximum 1 day rainfall	Rx1day
19	Number of days when rainfall $> 50\text{mm}$	R50
20	Number of days when rainfall > 95 percentile	R95p



3. Observed climate variability and change for Vietnam

3.1. Changes in temperature characteristics

Figure 2 shows the Sen's slope for the trends of T2m, Tx and Tm for both periods 1961-2012 and 1979-2012. Over the whole territory of Vietnam, temperature has increased steadily and substantially in the last decades. Most uptrends satisfied the 10% significance level. Except Hue station, the increase of T2m and Tm agreed well over all climate zones as well as for the two periods. Tx had decreasing tendencies at about one third of the stations in Central Highlands, South and South Central Vietnam during 1979-2012 although the trends hardly satisfied the 10 % significance level. Figure 3 shows in more detail the changing tendencies of T2m at each station. The trends of T2m averaged over Vietnam were almost equal to 0.18°C per decade for both periods. However, the trend of T2m and Tm in the southern part of Vietnam was significantly greater during the 1979-2012 period compared with 1961-2012 while in the northern part, the temperature increase in the period 1961-2012 seemed a little larger than that in the period 1979-2012.

The trend of annual minimum value of daily minimum temperature (TNn) was entirely consistent with that of annual T2m, whereas annual maximum value of daily maximum temperature (TXx) had some decreasing trends at a number of stations in the northwest region, and in the southern area, especially in the Central Highlands (Figure 4). It was previously reported that TXx in the southern region (from 16.0°N equatorward) was usually identified during March-April together with severe drought conditions. The decreasing trend of TXx in these regions was probably related to the extended impacts of winter monsoon activities to the lower latitudes. Yet another possibility could be linked to the occurrences of abnormal rainfall events and/or other in the corresponding period, which consequently reduced the maximum daily temperature.

The trends of annual count of days with maximum temperature greater than 90 percentile (TX90p) and annual count of days with minimum temperature less than 10 percentile (TN10p) had insignificant differences between the two data periods. TN10p decreased for both periods with a higher decreasing rate in the southern part compared with that in the North. These North-South differences in the trends of TN10p were signifi-

cantly greater for the period 1979-2012 compared with 1961-2012. The changes of TX90p were consistent with those of TXx, which showed increasing trends in the northern regions and significant decreases in the Central Highlands and at some stations in the southern areas. The trends of number of hot days (Tx35) and number of cold days (T2m15) were essentially similar to those of TX90p and TN10p, respectively, except for the southern region where most T2m15 had zero values.

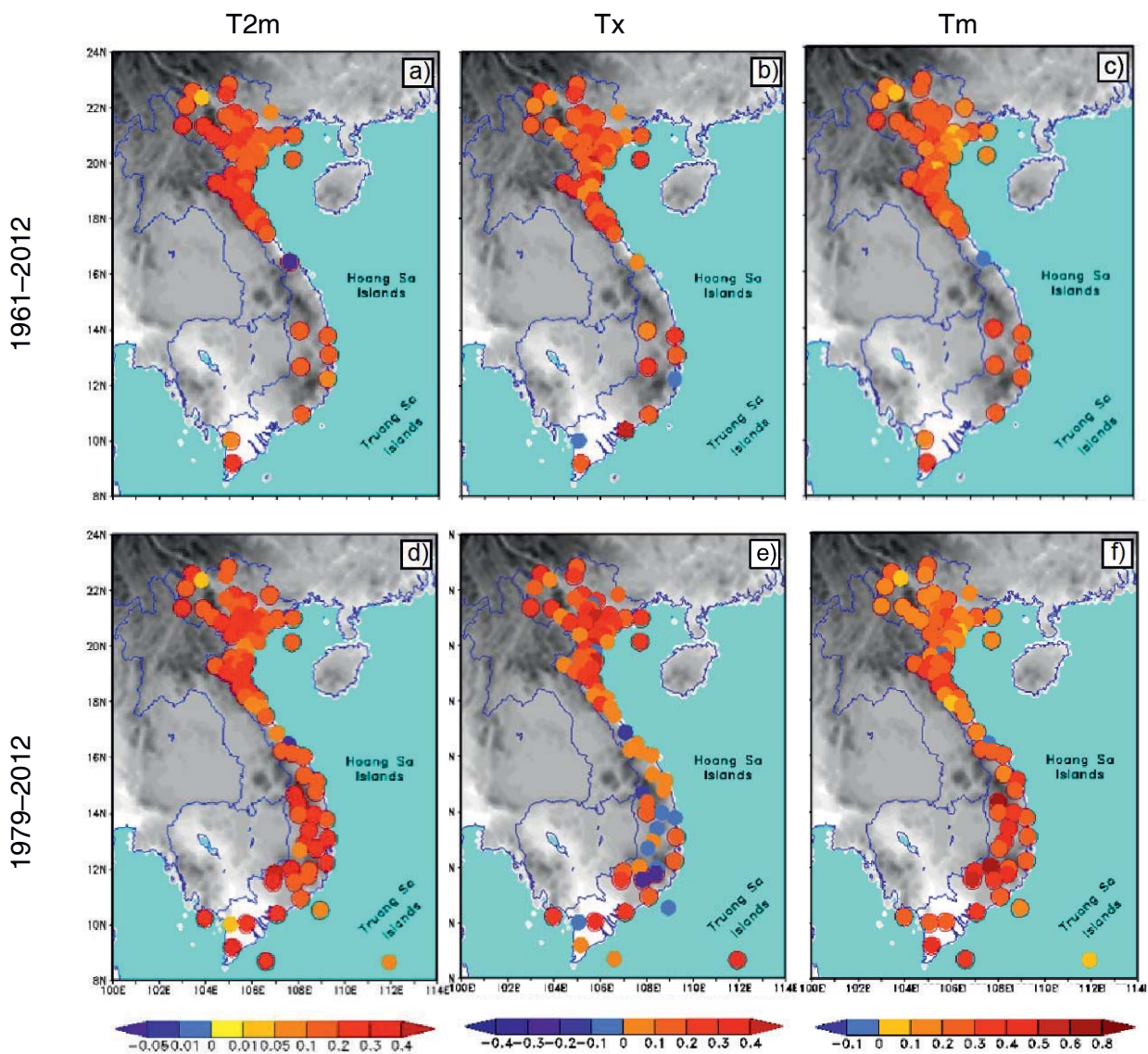


Figure 2. Sen's slopes of annual average near-surface temperature (T2m), annual average value of daily maximum temperature (Tx) and annual value of daily minimum temperature (Tm) for the period 1961-2012 (a, b, c) and 1979-2012 (d, e, f) in °C per decade. The dots with circles indicate where the trends satisfy the 10% significance test.

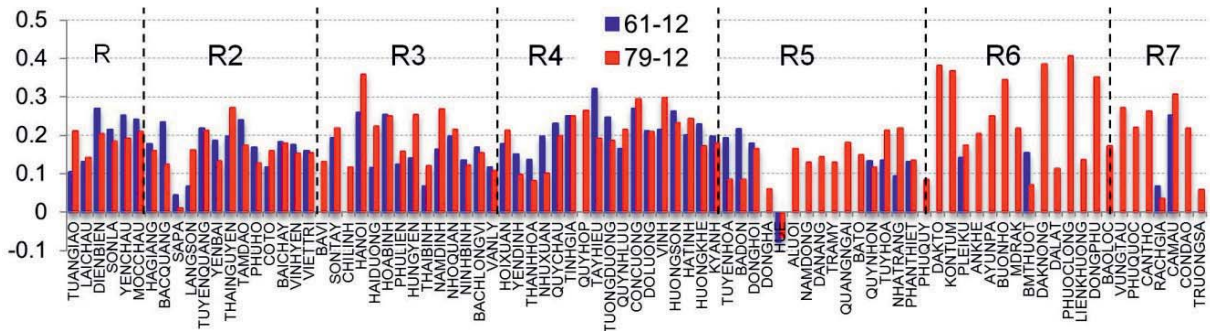


Figure 3. Sen's slopes of T_{2m} (°C/decade) of the two phases from 1961 to 2012 and from 1979 to 2012. R1-R7 are sub-regions: R1: North West; R2: North East; R3: North Delta; R4: North Central; R5: South Central; R6: Central Highlands; R7: South.

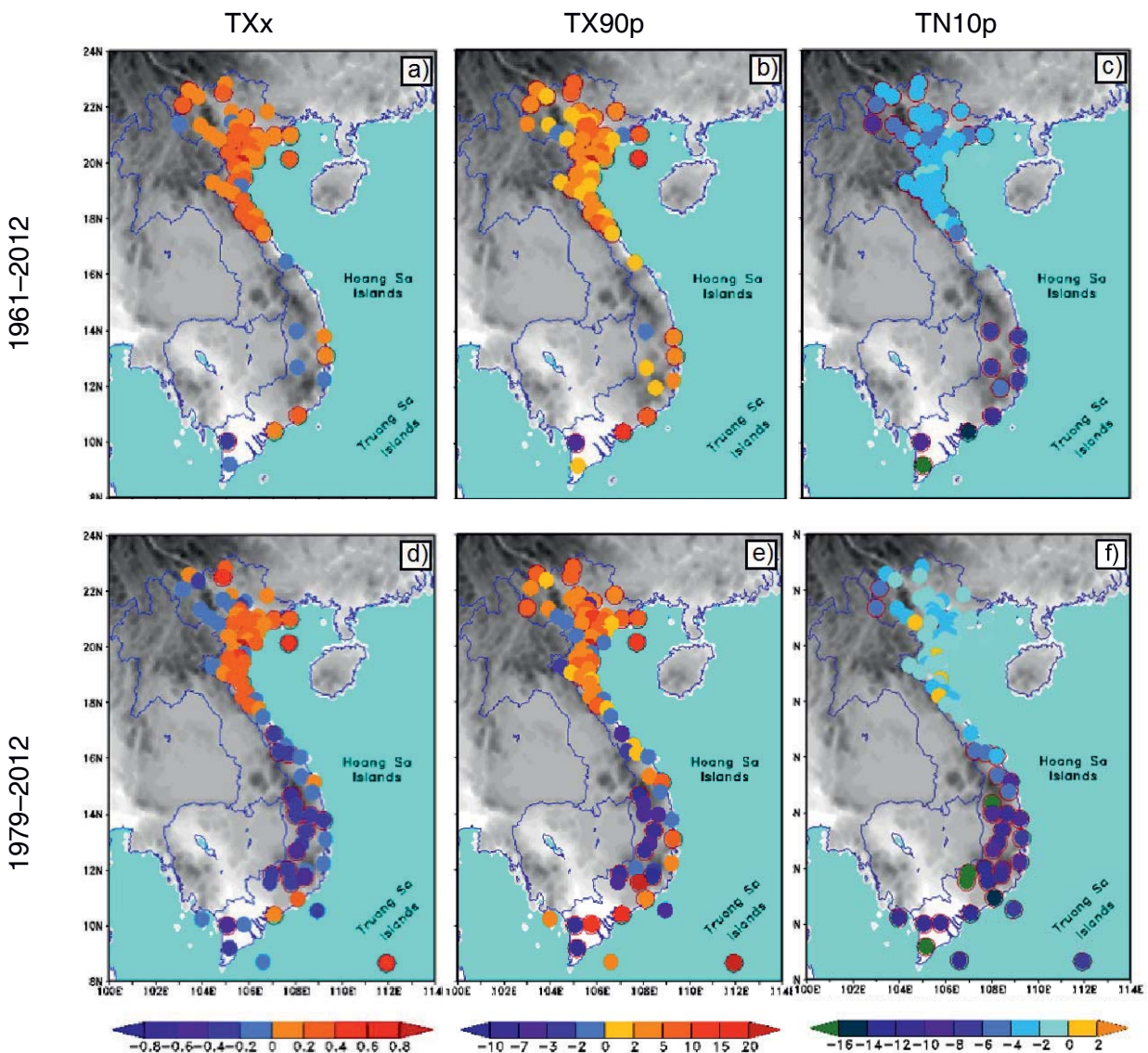


Figure 4. Similar to Figure 2 but for the annual maximum value of maximum daily temperature (TXx) in °C per decade, annual count of days with maximum temperatures greater than 90 percentile (TX90p) and annual count of days with minimum temperatures less than 10 percentile (TN10p) in days per decade.



Figure 5 represents the trends of T2m for each month, reflected in the value of the Sen's slope averaged over all stations for both 1961-2012 and 1979-2012 periods. Results for the period 1961-2012 indicated that the trend of temperature in May in Vietnam was almost unchanged and the stations of the northern part showed some decreasing trends (Figure 6). The temperature increase in summer was less than that in winter. The decrease in May temperature and strong increase in June temperature detected in the northern stations (Figure 5-6) might be related to seasonal changes or shifts in modes of monsoon activities over the area.

There was a noticeable difference in temperature trends in January and December between the period 1979-2012 and the period 1961-2012. While the trend of January-T2m during the 1979-2012 period was near zero, the trend of December-T2m was surprisingly high (greater than 0.4°C per decade). The differences in the T2m trends between the two periods are more clearly shown in Figure 6. One should note that these differences mainly occurred in the northern stations. The near-zero trend of January-temperature might be related to an increase in the frequency of cold events in recent years. The strong upward trend of T2m in the first half of the winter months (October-December) could be an indicator for the delayed activities of winter monsoon. This hypothesis deserves will be further investigated in the near future.

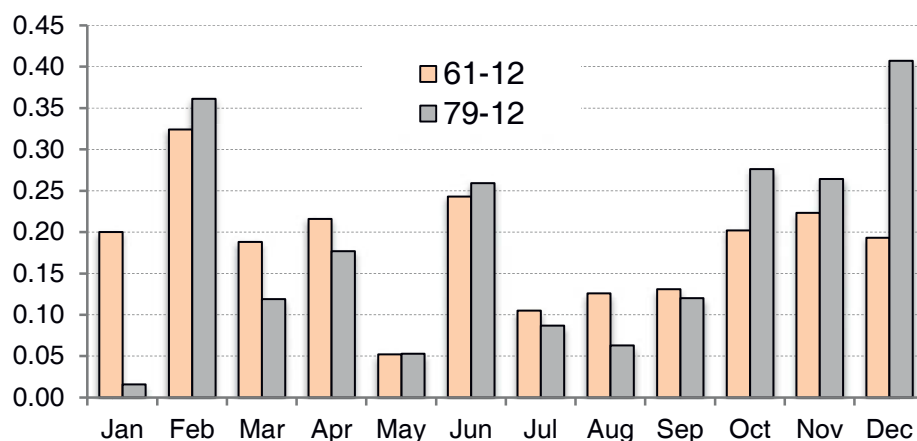


Figure 5. Seasonal variation of the Sen's slopes of T2m (°C/decade) averaged over all stations.

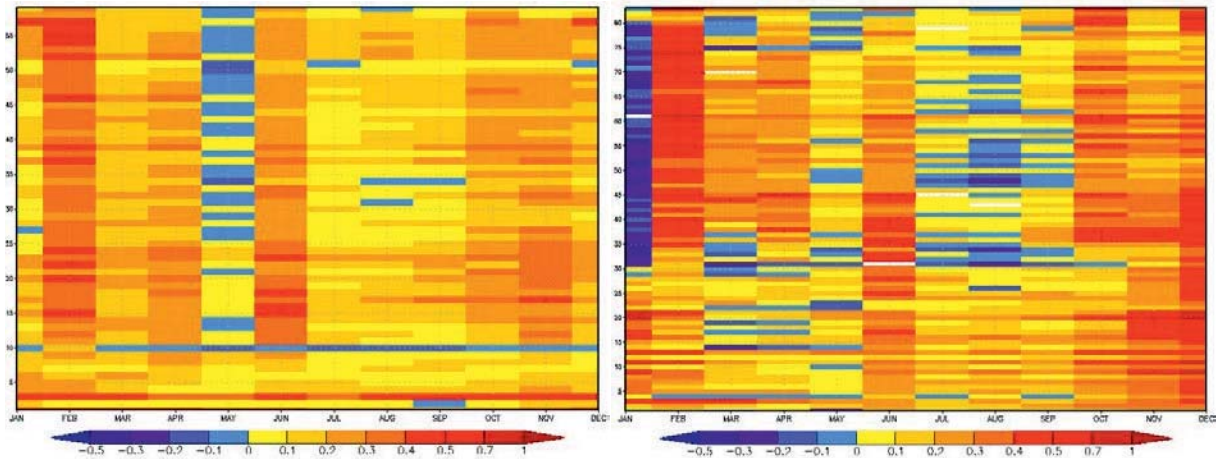


Figure 6. Seasonal variations of the Sen's slopes of T2m ($^{\circ}\text{C}/\text{decade}$) at each station arranged from South to North in Y axis for the periods 1961-2012 (left) and 1979-2012 (right). Number on the vertical axis shows the station number from South to North.

3.2. Changes in rainfall characteristics

The changes of rainfall, including annual rainfall and rainfall in the monsoon seasons were fairly consistent, showing that rainfall tended to decrease in the northern climates (from 16°N northward) and increased in the southern area, especially in the South Central region (R5) for both periods (Figure 7, Figure 9). The decrease (increase) rates of rainfall in the northern (southern) regions were generally small with a majority of stations having the absolute changing rate of less than 5% per decade. The trends of rainfall estimated for the two periods were also of notable differences. The 1961-2012 trend was relatively less than that of the period 1979-2012. During the later period, there were a number of northern stations with decreasing rates (reaching -10% per decade), while the upward trends in some southern stations are detected (up to 10 to 15% per decade). From 1979 to 2012, there were a number of rainfall stations in the South having a decreasing trend of rainfall in the summer monsoon season but a sharply increasing trend in the winter monsoon season.

The changing tendencies of the annual count of rainy days (R01Ann), of the rainy days within the summer monsoon season (R01Sum) and of the rainy days within the winter monsoon season (R01Win) were basically consistent with the change of rainfall (Figure 8), except for the North (South) Central region where rainfall tended to decrease (increase) while the number of rainy days increased (decreased). The upward trend in

rainfall together with the downward trend in the number of rainy days in the rainy season in some parts of the South Central Coast and Highlands of Vietnam may lead to increased risks of flooding. As will be shown below, days and periods with intense rainfall indeed increased in southern Vietnam. On the other hand, an increase in rainfall and in number of rainy days in the dry season might not contribute much to the increase in annual rainfall but could have an important impact on crop structuring in agriculture and aquaculture.

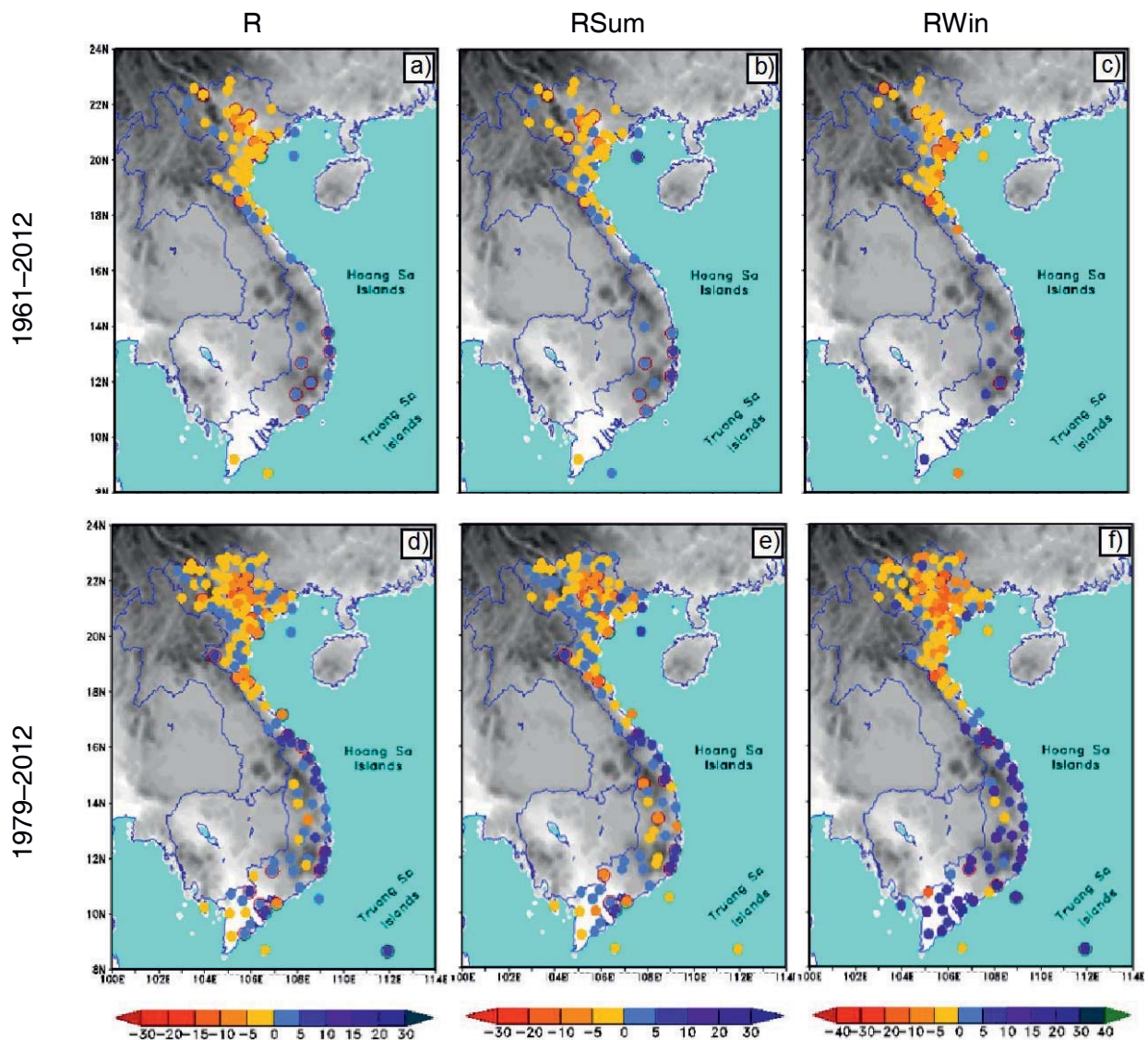


Figure 7. Same as Figure 2 but for annual rainfall amount (R), summer monsoon rainfall amount (RSum) and winter monsoon rainfall amount (RWin) in % per decade.



Figure 10 shows the seasonal variability of the rainfall trend at each station. The order of the stations is arranged on the Y axis from R7 to R1 and from South to North. One can realize the consistency of the trends estimated from the two different periods. The alternating increase and decrease in the trend of rainfall across the months suggest a shift in seasonal rainfall regimes that could be associated with the monsoon activities over Vietnam. Averaging over Vietnam, the trends (for both increasing and decreasing ones) during the period 1979-2012 were stronger than that of the period 1961-2012. The difference was most pronounced in December, of which the trend for the period 1961-2012 was near zero, while that for the later period tended to increase by more than 8% per decade. Except for December, both periods indicated upward trends in January, March, May and July and decreasing trends in February, June and October.

The changes in rainfall regime can also be realized through the trends Rx1day, R50 and R95p (Figure 11). In Vietnam, a heavy rainy day is defined when daily rainfall is greater than or equal to 50mm. When daily rainfall exceeds 95 percentile (R95p) or 99 percentile (R99p), it is considered as an extreme rainy day. In this study, only R95p was analyzed. One can see that the trends of RX1day, R95p and R50 were basically similar to the trend of annual rainfall, i.e. all three variables had downward trends in the northern regions and upward trends in the southern part, particularly in the South Central region of Vietnam (Figure 11). Results based on the 1979-2012 data series showed that most of the additional stations (compared with the period 1961-2012) in the southern part had decreasing trends for all three variables. However, those decreasing trends were generally small.

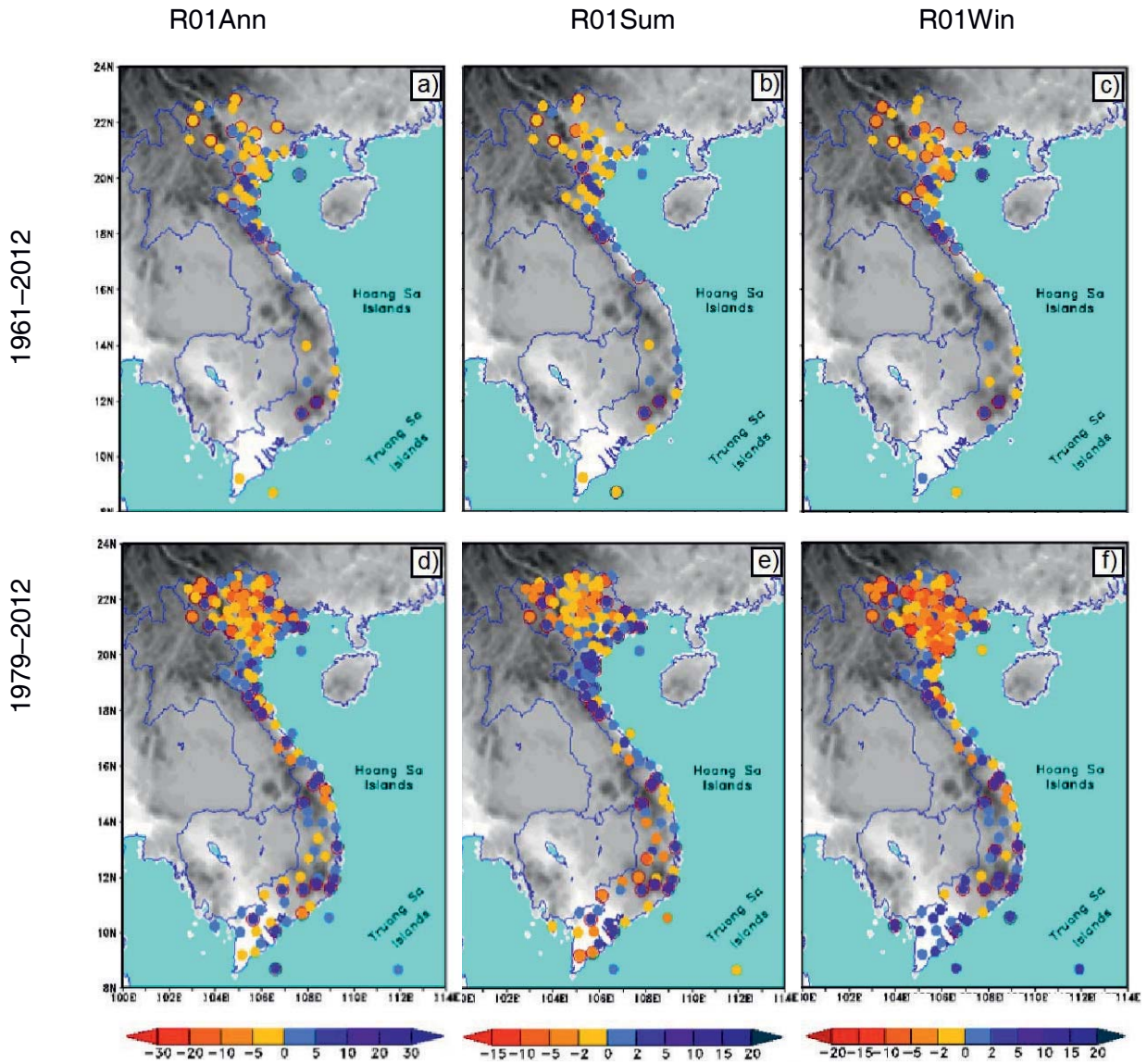


Figure 8. Same as Figure 2 but for number of annual rainfall days (R01Ann), summer monsoon rainfall days (R01Sum) and winter monsoon rainfall days (R01Win) in % per decade.

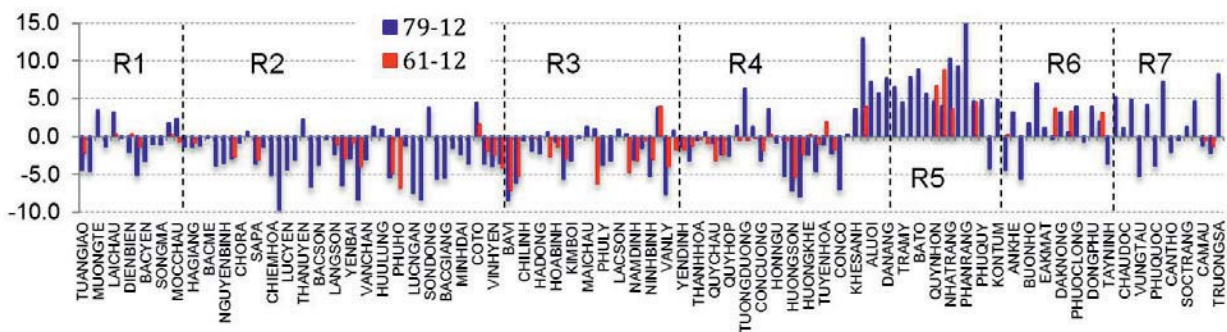


Figure 9. Same as Figure 3 but for annual rainfall amount (%/decade).

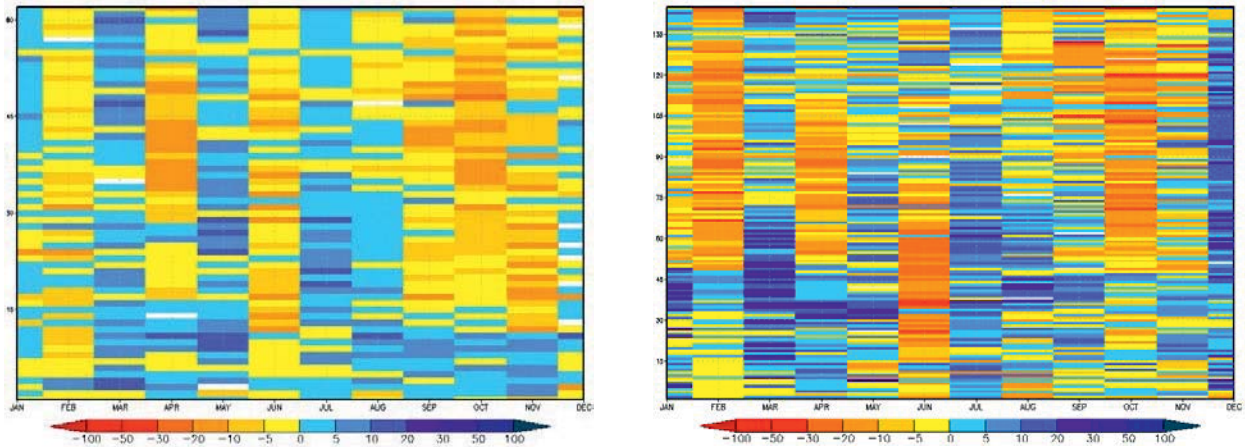


Figure 10. Same as Figure 6 but for annual rainfall amount (%/decade).

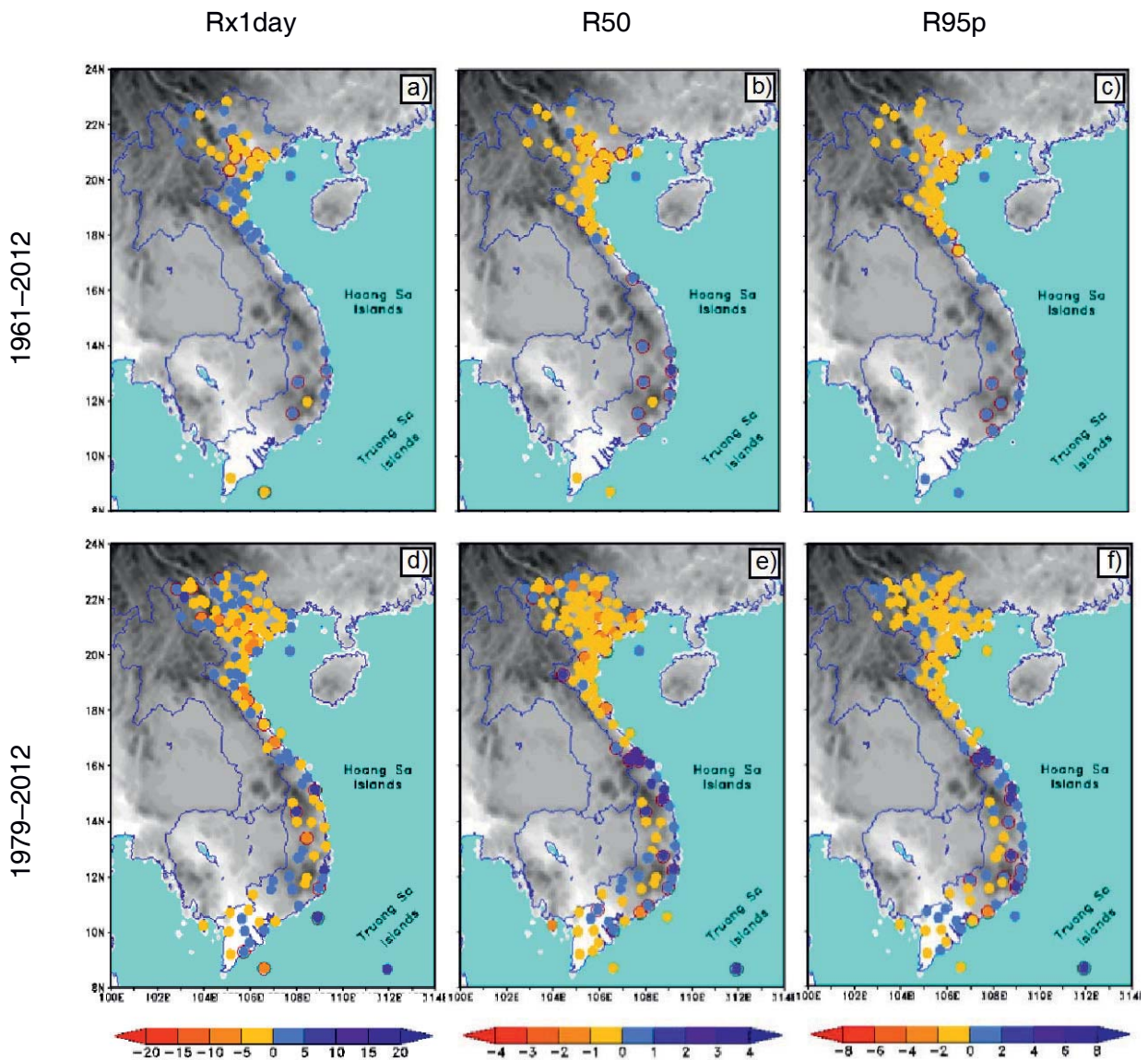


Figure 11. Same as Figure 2 but for maximum daily rainfall (Rx1day) in % per decade, number of heavy rainfall days (R50) and number of extreme rainfall days (R95p) in days per decade.



4. Summary and future plans

In this study, it was shown that near-surface temperatures including mean (T_{2m}), maximum (T_x) and minimum temperature (T_m) have increased consistently at almost all stations in Vietnam in the last decades. The increasing rate was faster in winter than in summer, and faster for T_{2m} and T_m than for T_x. Consequently, the number of hot days increased whereas the number of cold nights decreased. In the northern regions, temperature tended to slightly decrease in May but significantly increased in June. Between the two periods 1979-2012 and 1961-2012, there was a noticeable difference in temperature trends in January and December, which could be an indicator for the delayed activities of winter monsoon in recent decades. This hypothesis deserves further detailed investigations in the near future.

This study also confirmed that annual rainfall decreased in the northern area of Vietnam, while it increased at almost all stations in the central regions, and had insignificant trends in the southern sub-region. The trends of rainfall estimated for 1961-2012 were relatively less than that of the period 1979-2012. Rainfall generally increased in May and decreased in June over almost all Vietnam. Changes in some extreme rainfall indices were likely consistent with changes in annual rainfall.

The unusual change of temperature in May over the northern part of Vietnam might be related to the changes of the summer monsoon and/or the extension of the winter monsoon over Vietnam. These and other aspects will be explored in future studies, focussing on the driving mechanisms for the identified changes.

References

- [1] Fink A. H., Phan V. T., Pinto J. G., van der Linden R., Schubert D., Trinh T. L., and Ngo-Duc T. (2014): Climate change projections and selected impacts for Vietnam. 4th VNU – HCM International Conference for Environment and Natural Resources ICENR 2014.
- [2] Ho T. M. H., Phan V. T. (2009): Magnitude and trend in extreme monthly temperature in Vietnam in period of 1961-2007. *Journal of Science, Vietnam National University, Hanoi*, 25, 3S, 412–422.



- [3] Ho, T. M. H., Phan V. T., Le N. Q., Nguyen Q. T. (2011): Extreme climatic events over Vietnam from observational data and RegCM3 projections. *Clim. Res.*, 49, 87–100.
- [4] Hulme M. (1996): Recent climatic change in the world's drylands. *Geophys. Res. Lett.*, 23, 61–64.
- [5] IPCC (2007): *Climate Change 2007: The Scientific Basis, Contribution of Working Group I to the Fourth Assessment Report of the Intergovernmental Panel on Climate Change*, Cambridge University Press, Cambridge, United Kingdom and New York, NY, USA.
- [6] Kendall M. G. (1975): *Rank Correlation Methods*, Charles Griffin, London, 272 pp.
- [7] Ngo-Duc T., Kieu C., Phan V. T., and Thatcher M. (2012): Evaluating performance of three regional climate models and their ensemble combination in projecting future climate in Vietnam, *Climate Res.*, under revision.
- [8] Nguyen D. N. (2008): *Climate Change*. Science and Technology Publisher, Hanoi.
- [9] Phan V. T., Ngo-Duc T., Ho T. M. H. (2009): Seasonal and interannual variations of surface climate elements over Vietnam, *Climate Res.*, 40, 1, 49–60.
- [10] Phan V. T. (2010): *Impacts of Global Climate Change on the Extreme Climate Events in Viet Nam, Predictability and Adaptation Strategies*. Technical report of National Project, code KC08.29/06-10
- [11] Sen P. K. (1968): Estimates of the Regression Coefficient Based on Kendall's Tau, *J. Am. Stat. Assoc.*, 63, 324, 1379–1389.



Climate change projections and selected impacts for Vietnam

Fink A. H.¹, Phan V. T.², Pinto J. G.^{3,4}, van der Linden R.³,
Schubert D.^{3,5}, Trinh T. L.² and Ngo-Duc T.²

¹ Institute for Meteorology and Climate Research, Karlsruhe Institute of Technology, Karlsruhe, Germany

² Department of Meteorology, Hanoi University of Science, Vietnam National University, Hanoi, Vietnam

³ Institute for Geophysics and Meteorology, University of Cologne, Cologne, Germany

⁴ Department of Meteorology, University of Reading, Reading, United Kingdom

⁵ Department of Environmental Engineering and Applied Computer Sciences, University of Applied Science, Höxter, Germany

Abstract

In September 2013, the 5th Assessment Report (5AR) of the International Panel on Climate Change (IPCC) has been released. Taking the 5AR climate change scenarios into account, the World Bank published an earlier report on climate change and its impacts on selected hot spot regions, including Southeast Asia. Currently, dynamical and statistical-dynamical downscaling efforts are underway to obtain higher resolution and more robust regional climate change projections for tropical Southeast Asia, including Vietnam. Such initiatives are formalized under the World Meteorological Organization (WMO) Coordinated Regional Dynamic Downscaling Experiment (CORDEX) East Asia and Southeast Asia and also take place in climate change impact projects such as the joint Vietnamese-German project “Environmental and Water Protection Technologies of Coastal Zones in Vietnam (EWATEC-COAST)”. In this contribution, the latest assessments for changes in temperature, precipitation, sea level, and tropical cyclones (TCs) under the 5AR Representative Concentration Pathway (RCP) scenarios 4.5 and 8.5 are reviewed. Special emphasis is put on changes in extreme events like heat waves and/or heavy precipitation. A regional focus is Vietnam south of 16°N.

A continued increase in mean near surface temperature is projected, reaching up to 5°C at the end of this century in northern Vietnam under the high greenhouse-gas forcing scenario RCP8.5. Overall, projected changes in annual precipitation are small, but there is a tendency of



more rainfall in the boreal winter dry season. Unprecedented heat waves and an increase in extreme precipitation events are projected by both global and regional climate models. Globally, TCs are projected to decrease in number, but an increase in intensity of peak winds and rainfall in the inner core region is estimated. Though an assessment of changes in land-falling frequency in Vietnam is uncertain due to difficulties in assessing changes in TC tracks, some work indicates a reduction in the number of land-falling TCs in Vietnam. Sea level may rise by 75-100 cm until the end of the century with the Vietnamese coastline experiencing 10-15% higher rise than on global average. Given the large rice and aquaculture production in the Mekong and Red River Deltas, that are both prone to TC-related storm surges and flooding, this poses a challenge to foodsecurity and protection of coastal population and assets.

Key Words: climate change, extreme events, climate modeling, regionalization, downscaling

1. Introduction

Vietnam is affected by the powerful Asian-Australian Monsoon (AAM) system. In Chapter 14 of the most recent 5th Assessment Report (5AR) of the Intergovernmental Panel on Climate Change (IPCC; Christensen et al., 2013), the AAM system is subdivided into the East Asian Summer (EAS), the Southern Asia Summer (SAS), and the Australian-Maritime Continent (AUSMC) monsoon systems (Figure 1).

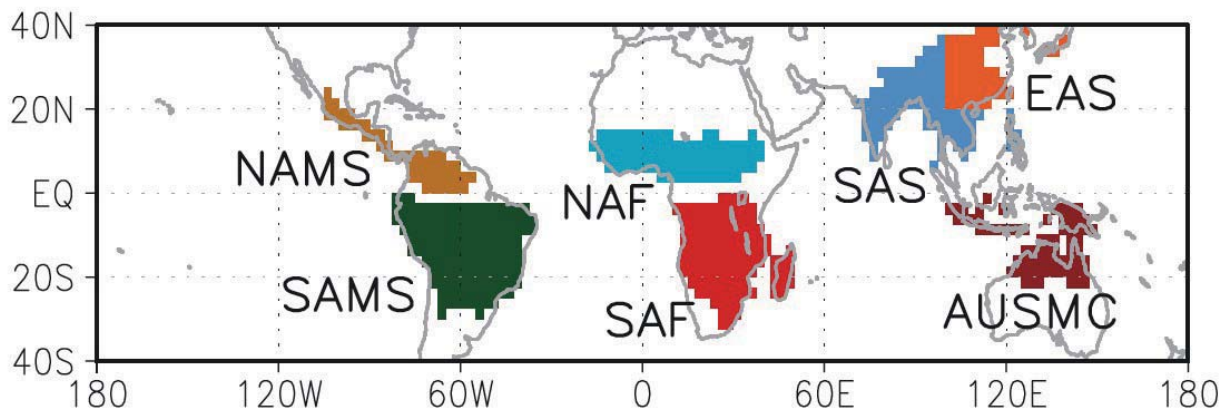


Figure 1. Regional land monsoon domain based on 26 CMIP5 multi-model mean precipitation with a common $2.5^\circ \times 2.5^\circ$ grid in the present-day (1986–2005). Northern hemisphere monsoon domains: North America Monsoon System (NAMS), North Africa (NAF), Southern Asia Summer (SAS) and East Asian Summer (EAS); Southern hemisphere monsoon domains: South America Monsoon System (SAMS), South Africa (SAF), and Australian-Maritime Continent (AUSMC). Christensen et al. (2013).

The Indochina peninsula is part of the SAS monsoon system. Rainfall and its distribution over the season is the most important climate variable of the AAM in terms of socioeconomic impacts. Boreal summer rainfall projections for the SAS monsoon (Figure 2) until the end of the 21st century are quite typical for the behavior of the global monsoon systems; average May-September rainfall (P_{av}) increases slightly by up to 10% (Figs. 2a and 2b), with increasing variability (P_{sd}), precipitation intensity (SDII and R5d) and longer monsoon duration (DUR) due to an earlier onset (ONS) and later withdrawal (RET) of the monsoon. Expectedly, these changes are more pronounced for the strongest radiative forcing scenario, the RCP8.5 (Representative Concentration Pathway; 8.5 W/m^2 radiative



forcing at the end of the 21st century) scenario. Unlike for the global monsoon system, the global General Circulation Models (GCMs), that participated in the Coupled Model Intercomparison Project Phase 5 (CMIP5) and are the basis of many 5AR projections, do not show a coherent trend towards longer dry spells during the wet season (CDD) for the SAS monsoon (Figure 2b). The more regional, and spatially and temporally higher resolved climate projection are requested to be, the more uncertain they are since observed regional climate variability and change generally represents a complex convolution of natural and anthropogenic factors. The latter includes local land use and cover changes (LUCC) and aerosol emissions. The CMIP5 GCMs are too coarse to resolve regional circulations due to, for example, complex terrain. In addition, several small-scale, but important atmospheric phenomena are not resolved, as for example tropical cyclones (TCs). Some CMIP5 models also have a very rudimentary treatment of aerosol effects and LUCC. To partly overcome these deficiencies, the World Meteorological Organisation (WMO) launched the Coordinated Regional Dynamic Downscaling Experiment (CORDEX; Giorgi et al., 2009). One of the experiments includes the East Asian region from 70°E to 160°E and 15°S to 60°N. The joint Vietnamese-German project "Environmental and Water Protection Technologies of Coastal Zones in Vietnam (EWATEC-COAST)" will conduct a further regionalization for central and southern Vietnam using a statistical-dynamical approach. In Section 2, we show the application of the COSMO-CLM (COntortium for Small scale MOdelling in Climate Mode) Regional Climate Model (RCM) to the CORDEX East Asia domain. Initial validation of this and five other CORDEX East Asia RCM runs for the period 1998-2008 will be shown. Section 3 furnishes details of the statistical-dynamical downscaling approach. The contribution will continue in Section 4 with a summary of findings for climate change in Vietnam based on the latest IPCC and World Bank reports. Finally, an outlook is given to future work within the EWATEC-COAST project.

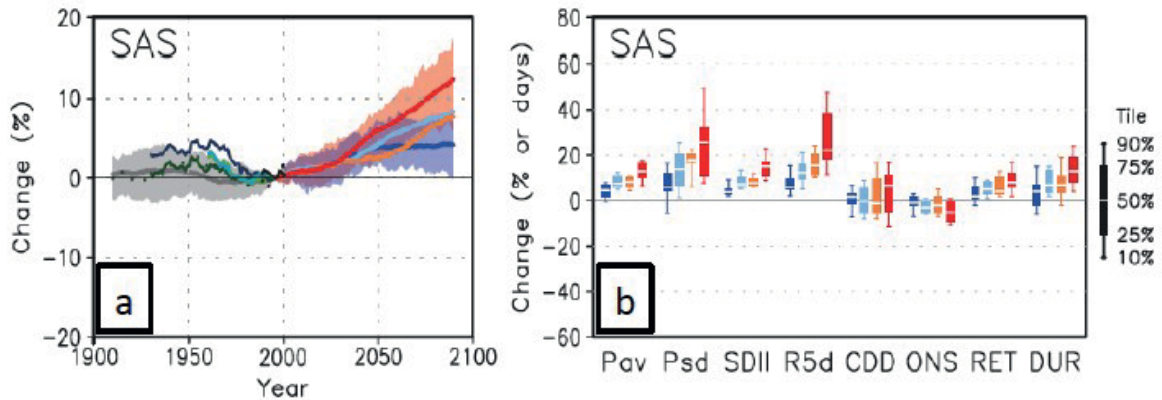


Figure 2. Changes in May-September precipitation indices over the regional land monsoon domain of Southern Asia (SAS) based on CMIP5 multi-models. (a) Time series of observed and model-simulated summer precipitation anomalies (%) relative to the present-day average. All the time series are smoothed with a 20-year running mean. For the time series of simulations, all model averages are shown by thick lines for the historical (grey; 40 models), RCP2.6 (dark blue; 24 models), RCP4.5 (light blue; 34 models), RCP6.0 (orange; 20 models), and RCP8.5 scenarios (red; 32 models). Their intervals between 10th and 90th percentiles are shown by shading for RCP2.6 and RCP8.5 scenarios. For the time series of observations (dotted and solid lines before about 2005), various data sets have been used. (b) Projected changes for the future (2080-2099) relative to the present-day average (1986-2005) in averaged precipitation (Pav), standard deviation of interannual variability in seasonal average precipitation (Psd), simple precipitation daily intensity index (SDII), seasonal maximum 5-day precipitation total (R5d), seasonal maximum consecutive dry days (CDD), monsoon onset date (ONS), retreat date (RET), and duration (DUR), under the RCP2.6 (18 models), RCP4.5 (24 models), RCP6.0 (14 models) and RCP8.5 scenarios (26 models). Units are % in Pav, Psd, SDII, R5d, and CDD; days in ONS, RET, and DUR. Box-whisker plots show the 10th, 25th, 50th, 75th and 90th percentiles. Christensen et al. (2013).

2. Model and data

2.1 Model description and setup

The COSMO limited-area model of the German Weather Forecast Service (DWD) is used in its Climate Mode (version 4.8) as an RCM to perform the dynamical downscaling. The COSMO-CLM is a three-dimensional, non-hydrostatic atmospheric circulation model and has been applied to several domains, spatial scales as well as to various climatological and meteorological phenomena (Rockel et al. 2008). The prognostic equations

for wind, temperature, pressure, specific humidity, cloud water and cloud ice content are solved on an Arakawa-C grid (Arakawa and Lamb 1977) on a rotated geographical coordinate system. The precipitation is treated as a diagnostic variable and is parameterized by a bulk microphysics approach. For the moist convection parameterization the Tiedke scheme (Tiedke, 1989) is used. The radiative transfer scheme by Ritter and Geleyn (1992) is applied and is called once per hour. For this study we have used 35 vertical levels, with the upper most layer increased to 30 km above sea level. The lower height of the damping layer was increased from 11 km to the approximate height of the tropical tropopause in 18 km. A horizontal grid resolution of 0.44° is used with 219 points from West to East and 183 points from South to North, including the sponge zone with 8 points at each side. The domain roughly ranges from 15°S to 55°N and from 70°E to 160°E (Figure 3). The simulation has been driven by the European Centre for Medium-Range Weather Forecast (ECMWF) ERA-Interim reanalysis (Dee et al. 2011) for the period 1979 – 2010.

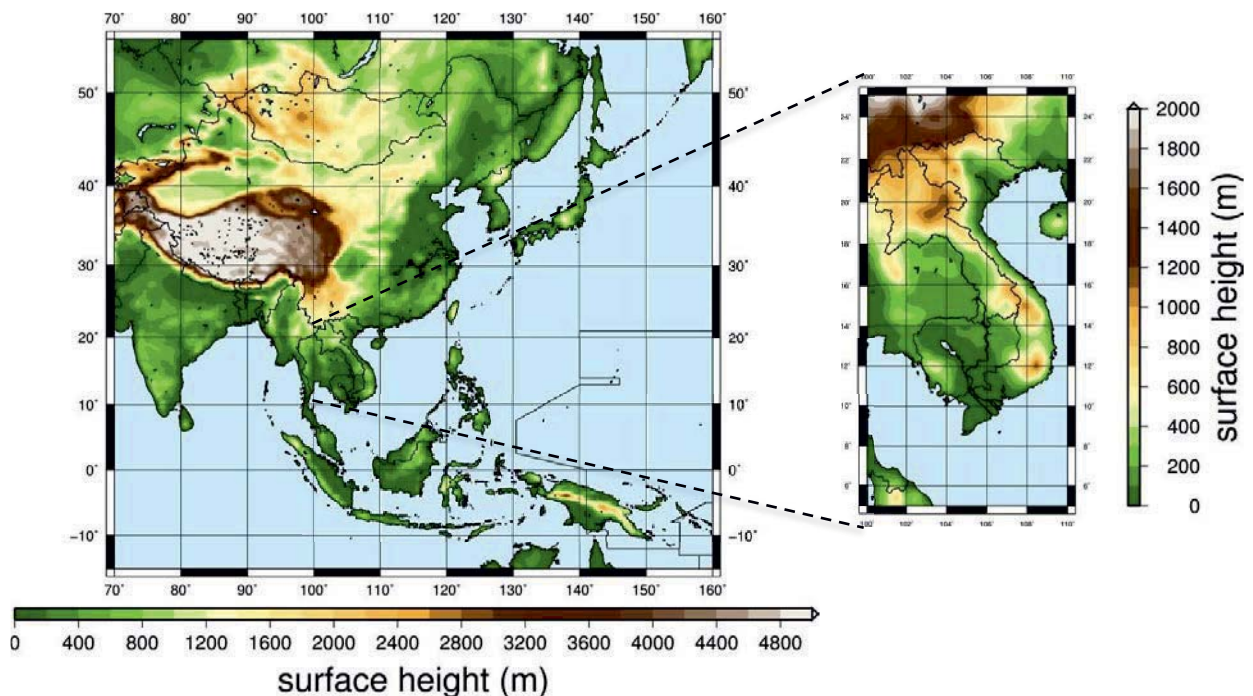


Figure 3. Surface height (m) in the model domain for COSMO-CLM simulations. The domain includes lateral sponge zones of 8 grid points in each direction.

2.2 Observational datasets

To quantify the model performance in terms of rainfall, we use different datasets, which are either ground based (e.g. rain gauge data interpolated to a regular grid), satellite products, or reanalysis data. A summary of data sets is given in Table 1.

Table 1: Data sets used for evaluation of model experiments

NAME	TYPE	VARIABLE	TIME PERIOD	TIME RES.	SPATIAL RES.
ERA-Interim	Reanalysis	Precipitation	1979 – 2010	6- hourly	0.75°
TRMM V7	Satellite	Precipitation	1998 – 2010	3- hourly	0.25°
APHRODITE	Rain gauges	Precipitation	1979 – 2007	daily	0.25°
GPCC	Rain gauges	Precipitation	1979 – 2010	monthly	0.5°

2.3 Evaluating existing CORDEX East Asia experiments

Although GCMs are able to reproduce the main characteristics of monsoon circulation over the tropics, there is still a need for higher resolved simulations. Regional climate downscaling, either dynamical, statistical, or a combination of both, has the potential to improve the representation of the monsoon circulation. These higher resolved experiments produce regional climate information that is frequently used in impact and adaption studies. The World Climate Research Program (WCRP) CORDEX Program will produce an ensemble of dynamical downscaling forced with different GCMs from the CMIP5 archive. For East Asia there are four institutions involved, namely Yonsei National University (YSU), Kongju National University (KNU), Seoul National University (SNU), and National Institute of Meteorological Research (NIMR), which produce regional climate information for impact studies. These institutions are making use of different RCMs, involving various parameterizations of land-surface processes and moist convection. The specifications for the RCMs are listed in Table 2.



Table 2. RCMs participating the CORDEX Program in East Asia including their physical packages. Note that COSMO-CLM is not participating in the CORDEX Program. All models have a grid resolution of 0.44°, corresponding to about 50 km.

Summary of physical parameterization in HadGEM3-RA	
Institution	National Center of Meteorological Research (NIMR)
Land Surface Model	Second version of UK Met. Office surface exchange scheme (MOSES II), nine surface types and coastal tiling
Boundary Layer	Nonlocal mixing scheme for unstable layers and local Richardson number scheme for stable layers
Convection	Entrainment and Detrainment rates for convection (Grant and Brown, 1999)
Radiation	General 2-stream radiation (Edward and Slingo, 1996)
Summary of physical parameterization in WRF	
Institution	Seoul National University (SNU)
Land Surface Model	Unified NOAH Land surface Model
Boundary Layer	YSU boundary layer scheme (Hong et al., 2006)
Convection	Cumulus Convection Scheme (Kain and Fritsch, 1990), 1-D Entrainment/Detrainment cloud model derived from Fritsch – Chapell cumulus scheme
Radiation	Rapid Radiative Transfer Model (RRTM) for longwave radiation and shortwave transfer scheme after Dudhia (1989)
Summary of physical parameterization in MM5	
Institution	Seoul National University (SNU)
Land Surface Model	Third version of Community Land Model of National Center for Atmospheric Research (NCAR-CLM3) up to 15 layers for soil
Boundary Layer	YSU boundary layer scheme (Hong et al., 2006)
Convection	Cumulus Convection Scheme (Kain and Fritsch, 1990), 1-D Entrainment/Detrainment cloud model derived from Fritsch – Chapell cumulus scheme
Radiation	Second version of Community Climate Model (CCM2) for radiative transfer after Briegleb (1992)
Summary of physical parameterization in RegCM4	
Institution	Kongju National University (KNU)
Land Surface Model	Third version of Community Land Model (CLM3) with 5 primary sub-grid land cover types
Boundary Layer	Air mass transformation model (ATM) one-dimensional, multilayer boundary layer after Holtslag et al. (1990)
Convection	MIT-Emanuel cumulus parameterization scheme
Radiation	Third version of Community Climate Model (CCM2) for radiative transfer after Kiehl et al. (1996)
Summary of physical parameterization in RSM	
Institution	Yonsei National University (YSU)
Land Surface Model	Land surface-hydrological model after Chen and Dudhia (2001), with four layers
Boundary Layer	Yonsei University planetary boundary layer scheme after Hong et al. (2006)
Convection	Simplified Arakawa-Schubert cumulus convection parameterization
Radiation	Shortwave and longwave radiation parameterizations after Chou (1992) and Chou et al. (1999)
Summary of physical parameterization in COSMO-CLM	
Institution	German Weather Service (DWD)
Land Surface Model	Multilayer land surface model (TERRA-ML) with 10 layers up to 11 km
Convection	Cumulus convection parameterization after Tiedtke (1989)
Radiation	Radiative transfer scheme after Ritter and Geleyn (1992)



For evaluation, the period 1998 – 2008 was used. All RCMs are forced with the same observational data sets at the boundary zone. Although there are strict standards in the CORDEX Program concerning the domain size, the RCMs differ in the central longitude and latitude and the number of grid points in S-N as well in E-W direction. Within the EWATEC-COAST project the available CORDEX East Asia runs are analyzed with reference to the present climate as well as to climate variability. In terms of future climate projection, foci lie on the RCP4.5 and RCP8.5 scenarios that are somewhat similar to the IPCC SRES scenarios A1B and B1.

Verification of dynamical downscaling of precipitation

Generally, dynamical downscaling is expected to improve the spatial patterns of precipitation due to its high-resolution topography and/or physical representation. Figure 4 illustrates the mean precipitation bias between the RCMs from Table 2 compared to TRMM for the timeframe 1998-2008. In addition the precipitation bias between the reanalysis and satellite product is shown in Figure 4. Overall the experiments differ in precipitation bias in terms of magnitude and location. For the HadGEM3-RA (Figure 4b) RCM the driest biases occur over the Bay of Bengal and parts of Indonesia with up to 5 mm/d.

Most parts of Vietnam also show a negative bias except for northern Vietnam with a weak positive bias of up to 2 mm/d. For the RegCM4 (Figure 4c) experiment the situation changes. Over Vietnam there is a larger wet bias of up to 4 mm/d. This may be due to the different application of the land surface model and parameterization of moist convection. Within the EWATEC-COAST project we also simulate an evaluation experiment using the ERA-Interim reanalysis for boundary conditions and following the CORDEX East Asia terms. The results can be seen in Figure 4f. Most parts of Indonesia and Malaysia show a negative bias when compared to TRMM. Also for most parts of Vietnam there is a dry bias between 1 and 4 mm/d.

In the next step we calculate the ensemble mean of all RCM members (Figure 4g).

High negative biases remain over the western coastline of Indonesia and parts of Malaysia while the bias over Vietnam is substantially reduced, with an overall small positive bias of up to 1 mm/d.

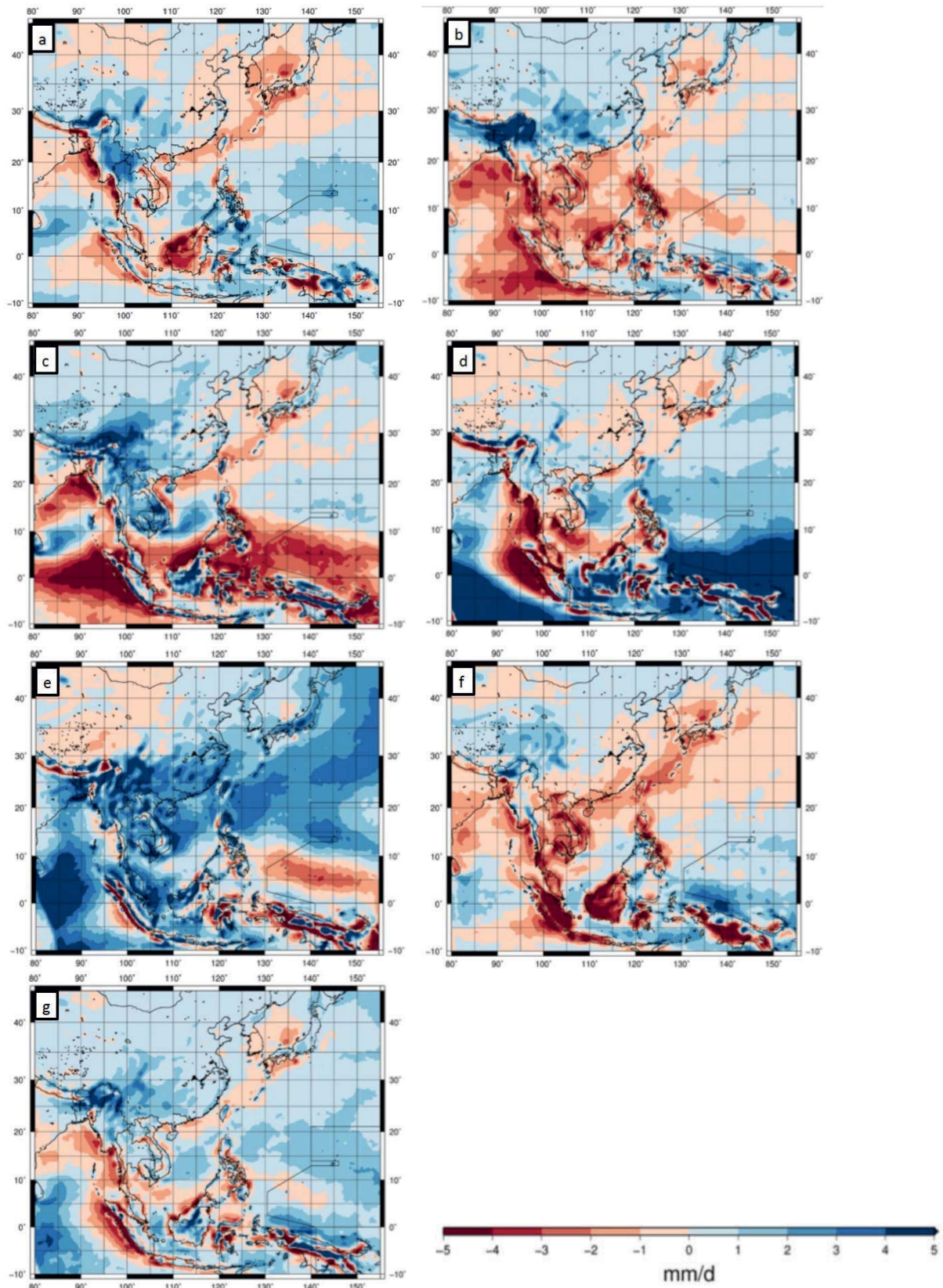


Figure 4. RCM bias for precipitation in mm per day (mm/d) against TRMM for a) ERA-Interim reanalysis, b) HadGEM3-RA, c) RegCM4, d) WRF, e) RSM, f) COSMO-CLM and g) ENSEMBLE. The calculation is based on the period 1998-2008.



Since we are interested in reflecting climatological features in Vietnam within the EWATEC-COAST project, the 11-year average bias is calculated for 3 subdomains, namely North Vietnam (101–108°E, 18–24°N), Central Vietnam (103–110°E, 12–18°N) and South Vietnam (104–110°E, 7–12°N). Results of observed model biases for the three regions are shown in Table 3.

Table 3. Mean bias (mm/d) of precipitation for three subdomains of all RCM members against TRMM. Additionally the bias for the ensemble is calculated (last column).

	HadGEM3	RegCM4	WRF	RSM	CLM	Ensemble
North VN.	-0.3	1.1	0.1	2.9	-1.6	0.6
Central VN.	-2.0	1.4	-0.1	2.8	-2.5	0.4
South VN.	-1.5	1.5	-1.9	1.9	-1.1	-0.1

3. Statistical-dynamical downscaling approach

In general, there are three frequently used methods to receive meteorological features on the regional scale. Firstly, the purely dynamical downscaling approach, which is using RCM simulations for providing climatological information on the regional scale. The driving data is derived from GCM output or (re-)analysis fields. A specific location is defined and the RCM is forced with driving fields from the GCM. The results are finer-scale projections, which are informed by both regional climate factors and large-scale processes from the global model. Most GCMs show systematic biases (IPCC, 2013). Thus, an efficient bias correction for the target region is mandatory. While dynamical downscaling with RCMs is an important tool for impact studies, it is also a very costly approach in terms of computing time and resources, A second way for downscaling climate data uses statistical methods (e. g. weather generators; Maraun et al. 2010). The general strategy of this method is to establish a statistical relationship between large-scale variables simulated by the GCMs and the local climate conditions from pre-

sent-day observations. Nevertheless this strategy does not account for any physical processes on the local scale and assume statistical stationarity that cannot necessarily be adopted for future climate settings. Within the EWATEC-COAST project we are using a third approach that is a combination of the two downscaling methods. The so-called statistical-dynamical downscaling combines the advantages of the dynamical and statistical downscaling approaches (Fuentes and Heimann 2000). With this approach we do not need to run the RCM for a long time period. Instead, we define weather classes that do have a relationship to tropical phenomena on the large scale. These weather classes are divided into clusters and for each cluster we run the RCM. The modeled tropical phenomena on the small scale are weighted with the occurrence of the cluster found on the large scale. In a final step we recombine the modeled clusters. For future projections, only the changes in cluster frequency are considered to weight the RCM results. This method combines the advantage of considering the physical processes in the atmosphere and of saving computational time. The procedure is summarized in Figure 5. The application of the cluster analysis within the EWATEC-COAST project follows the procedure of Pope et al. (2009) using wind field, temperature and humidity observations at 16 pressure levels from radiosonde data near Ho-Chi-Minh City.

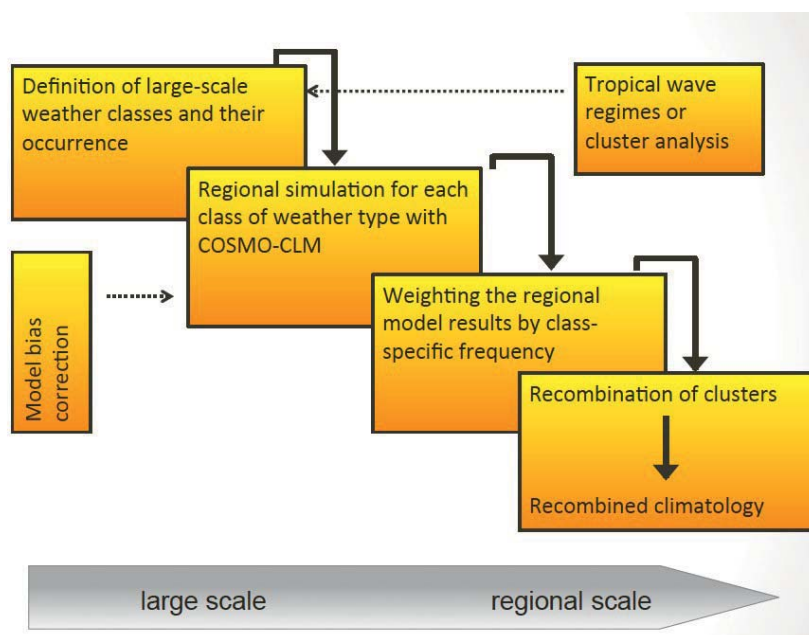


Figure 5. Schematic flow chart describing the different steps of the statistical-dynamical downscaling approach.



4. Observed climate variability and change for Vietnam

4.1 Observed trends

Southeast Asia is characterized by a complex orography and land-sea contrasts (Figure 3). Observed trends show a mean temperature increase at an average rate between 0.14°C and 0.20°C per decade since the 1960s (Tangang et al., 2007). For Vietnam, a rate of about $0.26^{\circ}\text{C}/\text{decade}$ since 1971 is discernable (Nguyen et al., 2013). Since the global positive observed trend is near 0.13°C per decade, the observed warming for Southeast Asia and Vietnam is almost twice as large. Additionally there are trends with a rising number of hot days and warm nights, and a decline in cooler weather (cf. companion abstract by Phan et al., 2014; Manton et al., 2001; Caesar et al., 2011). For precipitation there is a positive trend of heavy rainfall events in central Vietnam (see companion abstract by Phan et al., 2014) and a light negative trend of moderate rainfall events (Lau and Wu, 2007). For TCs there is no long-term trend observable, neither in frequency nor in intensity. The number of land-falling TCs in Vietnam and the Philippines does not display a significant long-term trend over the 20th century (Chan and Xu, 2009). However, for the Philippines, there is a negative correlation with El Niño-Southern Oscillation (ENSO), with less land-falling TCs during ENSO warm events. During the same time, Western North Pacific TCs exhibited a weak increase in intensity (IPCC, 2013) and a significant co-variation with ENSO, with a tendency toward more intense TCs during El Niño years (Camargo and Sobel, 2005).

4.2 Projected trends

CMIP5 models indicate an increase of temperature in both boreal winter and summer over East Asia for RCPs 2.6, 4.5 and 8.5. The strongest warming in June-August is expected in northern Vietnam, with a multi-model mean projecting up to 5°C under RCP8.5 (Figure 6, top right). The expected future warming is large compared to the local year-to-year natural variability. The monthly temperature distribution of almost all land areas over Southeast Asia shifts by six standard deviations. Even under low emission scenario there is still a shift up to four standard deviations (Figure 6, bottom left). The strongest increases in extreme tem-

peratures are found in Indonesia, the southern Philippine Islands, and southern Vietnam. Almost half of the summer months are beyond the 5-sigma level, the statistically definition of an unprecedented heat wave, under the lowest emission scenario (Figure 7 bottom left) and roughly all summer months beyond the 5-sigma level in RCP8.5 (Figure 7 bottom right). Thus, a present-day 5-sigma event would be a cold event in the projected climate in 2071–2099. Figure 7 (top row) shows that the majority of the summer months would be usually hot (> 3 -sigma) by the end of this century. It should be noted that in the inner tropics, due to a low natural year-to-year variability in mean summer temperatures, a temperature increase of smaller amplitude when compared to mid-latitudes satisfies the criteria of “unusual” and “unprecedented” heat waves. Nonetheless, flora and fauna have no past experience with such increased temperatures and urban heat islands in megacities might aggravate the effects on human health.

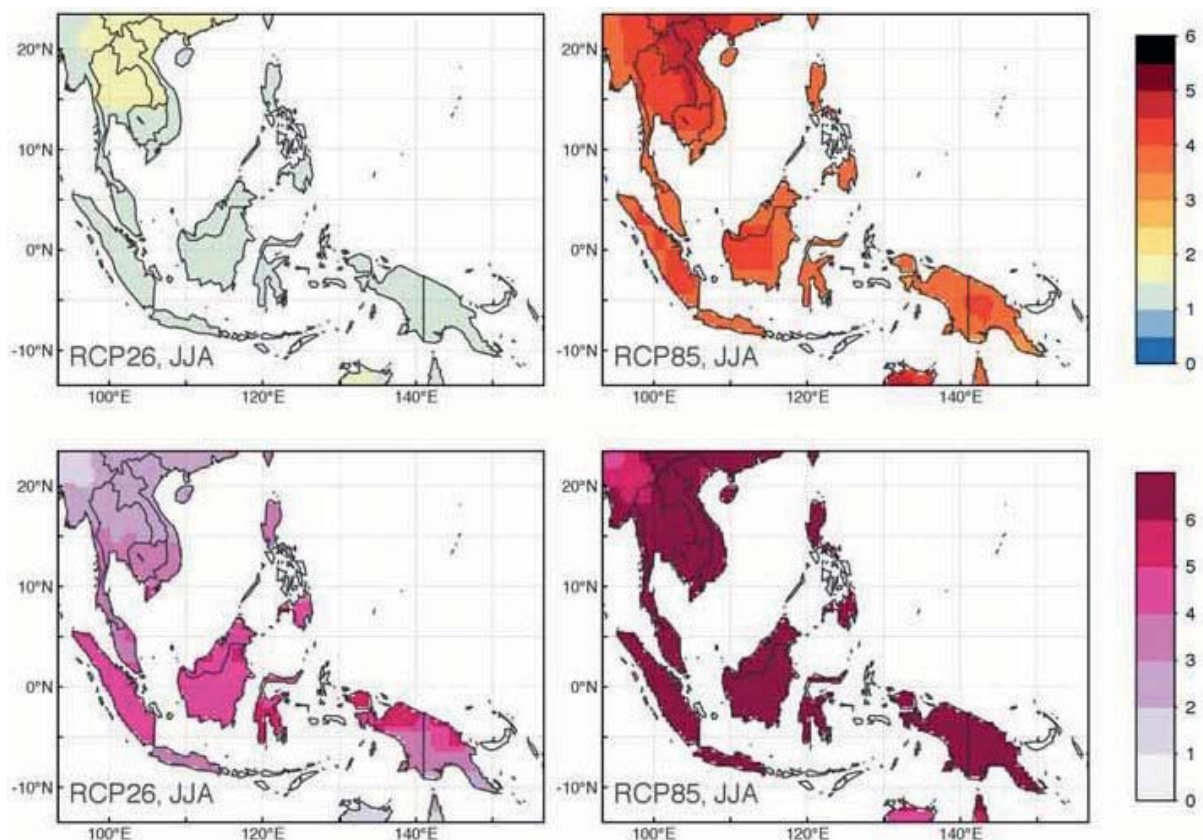


Figure 6. JJA temperature anomalies in °C (top row) are averaged over the time period 2071 – 2099 relative to 1951 – 1980, and normalized by the local standard deviation over Southeast Asia (bottom row). World Bank. 2013. Turn Down the Heat: Climate Extremes, Regional Impacts, and the Case of Resilience.

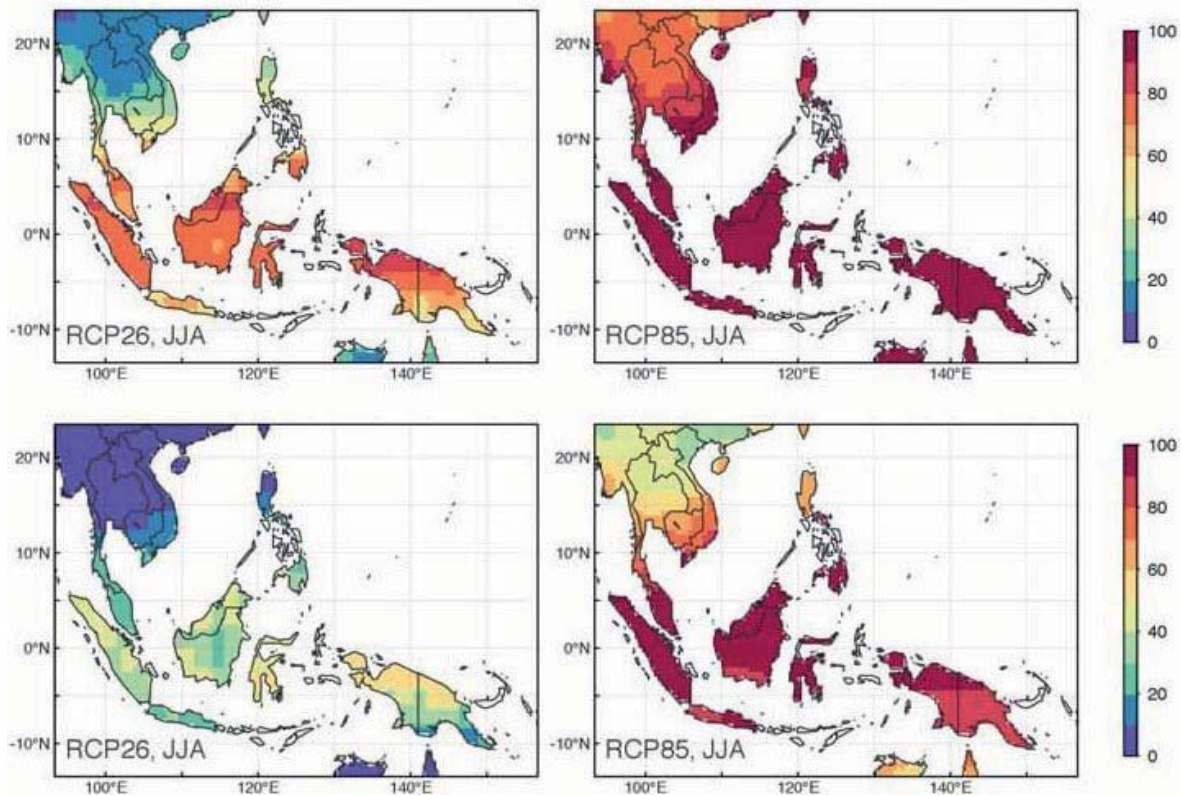


Figure 7. Multi-model mean of the percentage of boreal summer months in the time 2071 – 2099 with temperatures greater than 3σ (unusual heat waves, top row) and 5σ (unprecedented heat waves, bottom row) over Southeast Asia. World Bank. 2013. Turn Down the Heat: Climate Extremes, Regional Impacts, and the Case of Resilience.

Due to the enhanced moisture convergence in a warmer climate (Ding et al., 2007) an increase of summer precipitation in amount and intensity is expected over East Asia, under RCPs 2.6, 4.5 and 8.5 in CMIP5 models (Figure 8). In the winter months, there are slight differences in projected precipitation. While the CMIP5 models under RCP4.5 exhibit a slight positive trend over Vietnam, the CMIP3 models detect a decreasing trend in 2080 – 2099 (Figure 8). The present consensus assessment of changes in Western North Pacific TCs (Christensen et al., 2013) is displayed in Figure 9a. A robust signal is the increase in the inner core precipitation amounts (Figure 9a, IV) that is due to enhanced moisture flux convergence. Most models indicate a decrease in the total number of TCs (Figure 9a, I) due to drier mid-tropospheric levels and decreased vertical mass flux in deep convection.

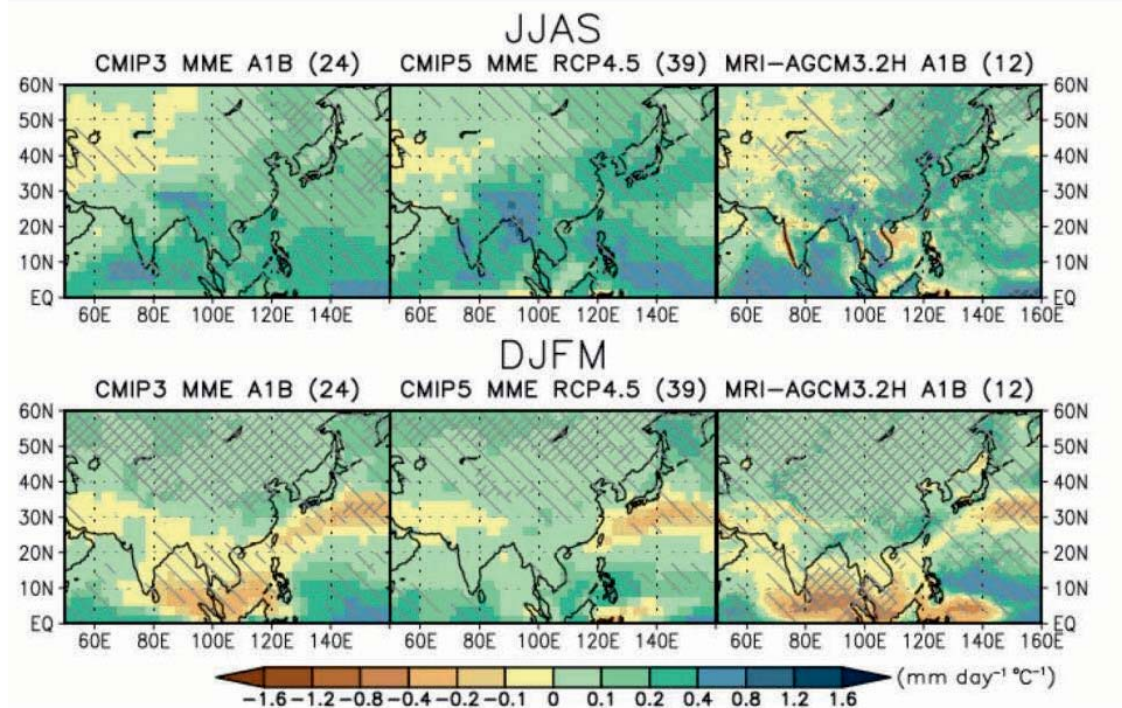


Figure 8. Precipitation changes for Central, North, East and South Asia in 2080 – 2099 with respect to 1986 – 2005 in (top) June to September and (bottom) December to March in the SRES A1B scenario with 24 CMIP3 models (left), and in the RCP4.5 scenario with 39 CMIP5 models (middle). Right figures are the precipitation changes in 2075 – 2099 with respect to 1979 – 2003 in the SRES A1B scenario with the 12-member 60 km mesh Atmospheric General Circulation Model (AGCM3.2). Precipitation is normalized by the global annual mean surface air temperature changes in each scenario. Light hatching denotes where more than 66% of members have the same sign with the ensemble mean changes, while dense hatching denotes where more than 90% of members have the same sign with the ensemble mean changes. Christensen et al., (2013).

The higher sea surface temperatures and warmer tropospheric temperatures could, however, allow some storms to attain higher peak intensities due to larger storm moisture contents and latent heating by condensation (Figure 9a, III, cf. Christensen et al. (2013), and references therein). No consensus exists as to track changes in the Western North Pacific including the South China Sea. In the present climate, ENSO modulates TC tracks in the North Pacific, but low confidence exists as to future changes in ENSO variability. Figure 9b shows changes in the Genesis Potential Index (GPI; Emanuel and Nolan, 2004) computed from very high time-scale experiments with the ECHAM5 GCM under the IPCC 4th AR SRES A1B scenario; it is clearly evident that large parts of the South

China Sea are less conducive to tropical cyclogenesis at the end of the 21st century. This is mainly due to increased wind shear and a drier mid-troposphere (Lucia, 2012). Though this might suggest less land-falling TCs along the Vietnamese coast, the GPI does not reflect TC track densities and other studies do not confirm the result.

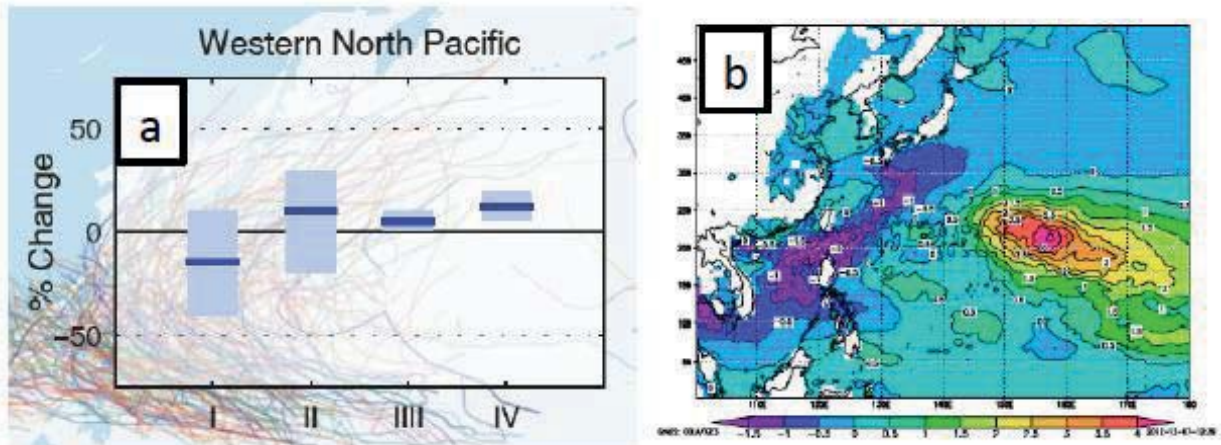


Figure 9. (a) General consensus assessment of numerical experiments. All values represent expected percent change in the average over the period 2081–2100 relative to 2000–2019, under an A1B-like scenario, based on expert judgment after subjective normalization of the model projections. Four metrics were considered: the percent change in (I) the total annual frequency of tropical storms, (II) the annual frequency of Category 4 and 5 storms, (III) the mean Lifetime Maximum Intensity (LMI; the maximum intensity achieved during a storm’s lifetime) and (IV) the precipitation rate within 200 km of storm center at the time of LMI. For each metric plotted, the solid blue line is the best guess of the expected percent change, and the colored bar provides the 67% (likely) confidence interval for this value. After Christensen et al., 2013.

(b) Differences (2071-2100 relative to 1961-1990) in the annual TC Genesis Potential Index (Emanuel and Nolan, 2004) in the Western North Pacific in the 21st century based on the ECHAM5/MPI-OM A1B simulations. Lucia (2012).

While projections in temperature and precipitation characteristics did not change much between IPCC 4AR and 5AR, observed increased melting of Greenland and Antarctic ice sheets lead the experts to substantially increase global sea-level rise assessments. In addition, due to the location close to the equator, sea-level rise at Southeast Asian coastlines is projected by the end of the 21st century to be 10-15% higher than the global

mean. Figure 10 shows time series for different locations in Southeast Asia.

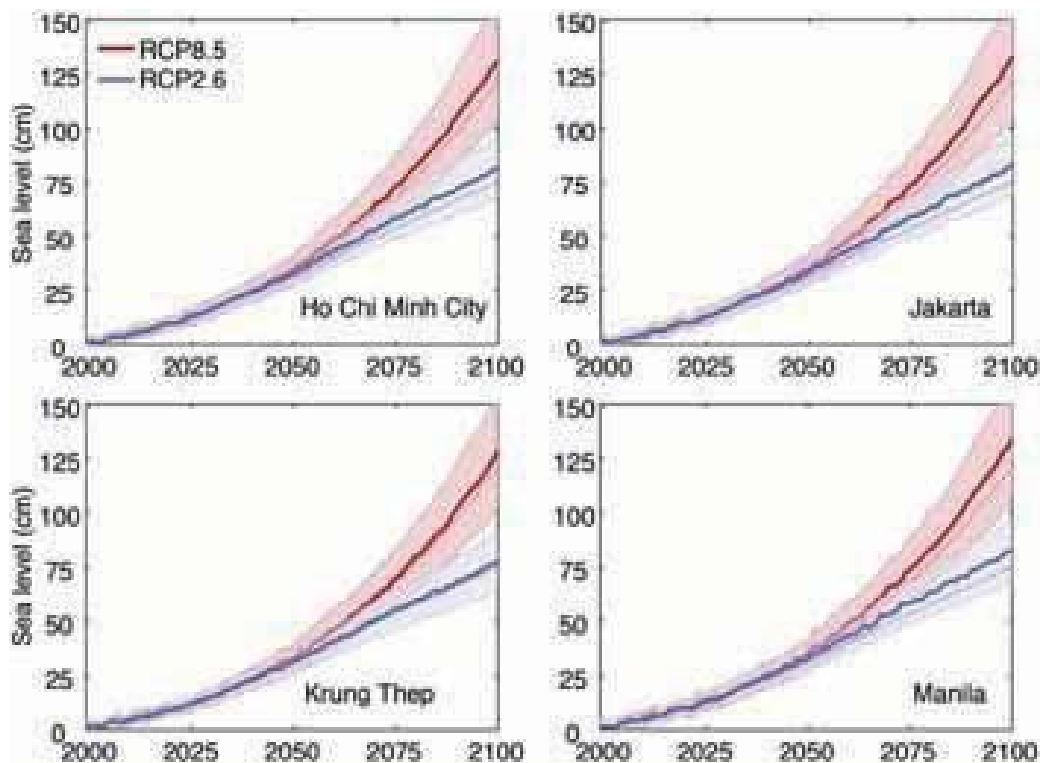


Figure 10. Local sea-level rise above mean 1986 – 2005 sea level as a result of global climate change. Shaded areas indicate 66% uncertainty range and dashed lines indicate the global mean sea-level rise. Blue lines under RCP2.6 scenario and red line under RCP8.5 scenario. Adapted from World Bank. 2013. Turn Down the Heat: Climate Extremes, Regional Impacts, and the Case of Resilience.

For Ho-Chi-Minh City, sea-level rise is projected to be considerable higher than the global mean. By the end of the 21st century, a sea level rise of up to 125 cm in RCP8.5 and 75 cm in RCP2.6 is expected. These assessments are obtained from the semi-empirical model published in the World Bank report (World Bank, 2013) and are thus higher than those in the IPCC reports that largely consider GCM results. It should be stressed, however, that an expert group of ice sheet experts (Bamber and Aspinall, 2013) and recent findings (e.g. Rignot et al., 2014) suggests that even the assessments from semi-empirical models can turn out to be conservative due to the instabilities of the Greenland and West Ant-



arctic ice sheets, of which increasing observational evidence exists. The sea-level rise will aggravate storm surges from tropical cyclones, even if their land-falling intensity in Vietnam will not change, and enhance salt water intrusions into the Mekong and Red River deltas. Land subsidence due to human and natural causes in the Ho-Chi-Minh area is another factor. The World Bank report concludes that in “Ho-Chi-Minh City up to 60% of the built-up area is projected to be exposed to 1 m sea-level rise” around the 2080s (World Bank, 2013).

5. Summary and future plans

In this work we presented a short overview of the observed and projected climate change projection for South East Asia, as reported in the IPCC 5AR and World Bank reports. The strongest warming is expected in northern Vietnam, with up to 5°C to the end of the 21st century for the highest emission scenario. The summer precipitation is projected to increase while for the winter months there are differences between CMIP3 and CMIP5 models. The latest CMIP5 models project an increase in winter rainfall, though no consensus exists amongst models. Sea level may rise by 75-100 cm until the end of this century with the Vietnamese coastline experiencing 10-15% higher rise than on global average. Due to the complex terrain and land-sea distribution of Southeast Asia, it is necessary to obtain climatological information on the local scale. Within the EWATEC-COAST project we will use a statistical-dynamical downscaling approach to reach high-resolution (i.e. up to 1x1 km grid resolution) meteorological time series over the Thi Vai river area in southern Vietnam for the present and for future scenarios. For the dynamical part, we will use the COSMO-CLM regional model of the German Weather Forecast Service (DWD). The RCM will be forced by CORDEX East Asia RCM projections and – if available – RCM runs from the Southeast Asian CORDEX initiative.

References

- [1] Arakawa A. and Lamb V. R. (1977): Computational design of the basic dynamical process of the UCLA general circulation model. *Methods In Computational Physics*, Vol 17, Academic Press, 173-265.



- [2] Bamber J. L. and Aspinall W. P. (2013): An expert judgement of future sea-level rise from ice sheets. *Nature Clim. Change*, 3, 424-427.
- [3] Caesar J. et al., (2011): Changes in temperature and precipitation extremes over the Indo-Pacific region from 1971 to 2005. *Int. J. of Climatol.*, 31(6),791–801.
- [4] Camargo S. and Sobel A. (2005): Western North Pacific tropical cyclone intensity and ENSO. *Journal of Climate*, 18, 2996–3006.
- [5] Chan J. C. L., and Xu M. (2009): Inter-annual and inter-decadal variations of land-falling tropical cyclones in East Asia. Part I: Time series analysis. *Int. J. Climatol.*, 29, 1285–1293.
- [6] Chen F. and Dudhia J. (2001): Coupling and advanced land surface-hydrology model with the Penn State-NCAR MM5 modeling system. Part I: Model implementation and sensitivity. *Mon. Wea. Rev.*, 129, 569-585.
- [7] Chou M. D. (1992): A solar radiation model for use in climate studies, *J. Atmos. Sci.*, 49,762-772.
- [8] Chou M. D., Lee K. T., Tsay S. C. and Fu Q. (1999): Parameterization for cloud longwave scattering for use in atmospheric models. *J. Climate*, 12, 159-169.
- [9] Christensen J.H., Krishna Kumar K., Aldrian E., An S. I., Cavalcanti I. F. A., de Castro M., Dong W., Goswami P., Hall A., Kanyanga J. K., Kitoh A., Kosin J., Lau N. C., Renwick J., Stephenson D.B., Xie S. P. and Zhou T. (2013): Climate Phenomena and their Relevance for Future Regional Climate Change. In: *Climate Change 2013: The Physical Science Basis. Contribution of Working Group I to the Fifth Assessment Report of the Intergovernmental Panel on Climate Change* [Stocker, T.F., Qin D., Plattner G. K., Tignor M., Allen S. K., Boschung J., Nauels A., Xia Y., Bex V. and Midgley P.M. (eds.)]. Cambridge University Press, Cambridge, United Kingdom and New York, NY, USA.
- [10] Ding Y., Ren G., Zhao Z., Xu Y., Luo Y., Li Q., and Zhang J. (2007): Detection, causes and projection of climate change over China: An overview of recent progress. *Adv. Atmos. Sci.*
- [11] Dee et al. (2011): The ERA-Interim reanalysis: configuration and performance of the data assimilation system. *Quarterly Journal of the Royal Meteorological Society*, 137 (2011), pp.553–597.
- [12] Dudhia J. (1989): Numerical Study of Convection Observed during the Winter Monsoon Experiment Using a Mesoscale Two-Dimensional Model. *J. Atmos. Sci.* 46, 3077-3107.



- [13] Edward J. M. and Slingo, A. (1996): Studies with a flexible new radiation code. 1: Choosing a configuration for a large-scale model. *Quart. J. Royal Meteorol. Soc.*, 122,689-719.
- [14] Emanuel K. A. and Nolan D.S. (2004): Tropical cyclone activity and global climate. *Proceeding of 26th Conference on Hurricanes and Tropical Meteorology*, 240–241.
- [15] Fuentes, U. and Heimann, D. (2000): An improved statistical-dynamical downscaling scheme and its application to the Alpine precipitation climatology. *Theor. Appl. Climatol.*, 65, 119-135.
- [16] Giorgi F., Jones C. und Asrar, G. R. (2009): Addressing climate information needs at the regional level: The CORDEX framework. *WMO Bulletin*, 58(3): 175–182.
- [17] Grant A. L. M. and Brown, A. R. (1999): A similarity hypothesis for shallow-cumulus transport. *Q. J. Roy. Meteorol. Soc.*, 125, 1913-1936, 1999.
- [18] Holtslag A. A. M., De Bruijin E. I. F., and Pan H. L. (1990): A high resolution air mass transformation model for short-range weather forecasting. *Mon. Wea. Rev.*, 118, 1561-1575.
- [19] Hong S. Y., Noh Y., and Dudhia J. (2006): A new vertical diffusion package with an explicit treatment of entrainment processes. *Mon. Weather Rev.*
- [20] Intergovernmental Panel on Climate Change (IPCC). (2013): Managing the risks of extreme events and disasters to advance climate change adaptation A Special Report of Working Groups I and II of the Intergovernmental Panel on Climate Change. (C. B. Field, V. Barros, T. F. Stocker, D. Qin, D. J. Dokken, K. L. Ebi, M. D. Mastrandrea, et al., Eds.) (pp. 1–582). Cambridge, United Kingdom and New York, NY, USA: Cambridge University Press.
- [21] Kain J. S., and Fritsch K., (1990): A One-dimensional Entrainment/Detrainment Plume Model and its application in convective parameterization. *J. Atmos. Sci.*, 47, 2784-2802.
- [22] Kiehl J. T., Hack J. J., Bonan G. B., Boville B. A., Briegleb B. P., Williamson D. L., and Rasch P. J. 1(996): Description of NCAR Community Climate Model (CCM3). NCAR Tech. Note NCAR/TN-420+STR, 152 pp.
- [23] Lucia A. S. (2012): Recent and future trends of tropical cyclones and impacts in the West Pacific. Unpublished Master Thesis within the "International Master of Environmental Sciences" study at the University of Cologne, 100 p.



- [24] Manton M. J., Della-Marta P. M., Haylock M. R., Hennessy K. J., Nicholls N., Chambers L. E., Collins D. A., et al. (2001): Trends in extreme daily rainfall and temperature in Southeast Asia and the South Pacific: 1961–1998. *Int. J. of Climatol.*, 21(3), 269–284.
- [25] Maraun et al., (2010): Precipitation downscaling under climate change. Recent developments to bridge the gap between dynamical models and the end user. *Rev. Geophys.*, 48 (3).
- [26] Nguyen D.-Q., Renwick J., & McGregor J. (2013): Variations of surface temperature and rainfall in Vietnam from 1971 to 2010. *Int. J. of Climatol.* 34, pp 249-264.
- [27] Phan V. T., Fink A. H., Ngo-Duc T., Trinh T. L., Pinto J. G., van der Linden R., Schubert D. (2014): Observed Climate Variations and Change in Vietnam. 4th VNU – HCM International Conference for Environment and Natural Resources ICENR 2014.
- [28] Pope M., Jakob, C., Reeder M. J. (2009): Objective Classification of Tropical Mesoscale Convective Systems. *J. Climate*, 22, 5797–5808.
- [29] Ritter B., and Geleyn J. F. (1992): A Comprehensive Radiation Scheme for Numerical Weather Prediction Models and Potential Applications in Climate Simulations. *Mon. Wea. Rev.*, 120, 303-325.
- [30] Rignot E., Mouginot J., Seroussi H., and Scheuchl B. (2014): Widespread, rapid grounding line retreat of Pine Island, Thwaites, Smith and Kohler glaciers, West Antarctica from 1992-2011. *Geophys. Res. Lett.*, 41, pp. 3501-3509.
- [31] Rockel B., Will A., Hense A. (2008): Special issue: Regional climate modeling with COSMO- CLM (CCLM) *Meteorologische Zeitschrift*, 17, pp. 347–348.
- [32] Tangang, F. T., Juneng, L., and Ahmad, S. (2007): Trend and interannual variability of temperature in Malaysia: 1961–2002. *Theor. Appl. Climatol.*, 89, 127–141.
- [33] Tiedtke, M. (1983): The sensitivity of the time-mean large-scale flow to cumulus convection in the ECMWF model: Workshop on convection in large-scale models, ECMWF, 297-316.
- [34] World Bank. (2013): Turn Down the Heat: Climate Extremes, Regional Impacts, and the Case for Resilience. A report for the World Bank by the Potsdam Institute for Climate Impact Research and Climate Analytics. Washington, DC:World Bank.



Modelling of atmospheric dispersion and deposition in industrial areas

- Comparison of different modelling approaches -

Klaus Massmeyer¹, Bang Quoc Ho², Cao Minh Ngoc², David Schubert¹

¹ Department of Environmental Engineering and Applied Informatics, University of Applied Sciences Ostwestfalen-Lippe, An der Wilhelmshoehe 44, D 37671 Hoexter
klaus.massmeyer@hs-owl.de

² Institute for Environment and Resources / Vietnam National University in Ho-Chi-Minh City; 142 To Hien Thanh, Ward 14, District 10, Ho-Chi-Minh City

Abstract

Modelling of atmospheric dispersion processes is necessary in order to follow national or international instructions on air quality control. A variety of different models and turbulence parameterizations exists to calculate atmospheric dispersion of emissions in the near field of industrial sources. The aim of this paper is the intercomparison of two different dispersion models used in Vietnam and Germany.

In Vietnam a Gaussian type of model is used based on the Pasquill turbulence parameters whereas in Germany Appendix 3 of the German regulation "Technical Instruction on Air Quality Control" (TA Luft) demands for dispersion calculations a Lagrangian particle model in compliance with the German guideline VDI 3945 Part 3 [1]. In Germany time series or statistics of meteorological parameters like diffusion category, wind speed and wind direction are used to calculate the distribution of ground level concentration of emissions (e.g. SO₂, NO_x, particulate matter), Vietnamese calculations are focused on specified case studies of single meteorological conditions.

For normalized source terms and five different source heights covering typical stack heights in industrial areas of the Thi Vai region, both types of models have been used for specified meteorological conditions covering unstable, neutral as well as stable atmospheric stratifications. The comparison of the two types of models is focused on the maximum concentration of a pollutant and the distance at which this concentration occurs.

It could be shown that based on the Lagrangian particle model including turbulence parameterization based on Monin Obukhov similarity theory



the results of the Gaussian model for low release heights in an area with low roughness length can be reproduced very often within some 10 %, larger deviations up to a factor of two have been found for extreme stable and unstable stratification of the atmosphere. The same holds for elevated releases in an area with high roughness length.

The Lagrangian model has in addition been validated against different dispersion experiments. It shows a satisfactory performance compared to the (Gaussian) model and experimental results with varying boundary conditions (emission height, roughness length) being independent of specific dispersion experiments, which have been the basic input to the specific dispersion parameters of a Gaussian model.

Key Words: Dispersion modelling, turbulence parameterization, model intercomparison, maximum ground level concentration



1. Introduction

Air pollution control is handled via National Technical Regulations on ambient air quality which stipulate limit values of basic parameters including sulfur dioxide (SO₂), carbon monoxide (CO), nitrogen oxides (NO_x), ozone (O₃), suspended dust, PM 10 dust (dust > 10 μm) and lead (Pb) in the ambient air (e.g. [2], [3]). The limit values of the basic parameters in the ambient air used in Vietnam and Germany are specified in Table 1. Often the limit values in both countries are identical or only slight differences exist. Only limit values are listed for Germany, other values (alarm etc.) exist, but are not listed for consistency reasons.

In the context of planning a new facility, model calculations of atmospheric dispersion have to be carried out in order to identify what will be the maximum concentration of pollutants and their distance from the source/location and to compare the pollutants concentrations with the limit values.

Table 1. Limit values of the basic parameters of the ambient air in Vietnam [2] (German values are given in parenthesis [3]). Unit: micrograms per cubic meter (μg/m³). Note: Mark (-) is not defined.

Parameter	Average 1 hour	Average 3 hours	Average 24 hours	Average year
SO ₂	350 (350 max. 24 times/a)	-	125 (125 - max. 3 times/a)	50 (50)
CO	30000 (-)	10000 (10000 - 8 hours)	-	-
NO ₂	200 (200 - max. 18 times/a)	-	100 (-)	40 (40)
O ₃	200 (-)	120 (-)	-	-
Suspended dust (TSP)	300 (-)	-	200 (-)	100 (-)
Dust > 10 μm (PM10)	-	-	150 (50 - max. 35 times/a)	50 (40)
Pb	-	-	1.5 (-)	0.5 (0.5)



For the calculation of a single stationary atmospheric concentration distribution of a pollutant dispersion models have to be equipped with a set of input parameters:

- source strength,
- source height (depending on the emission conditions - exit velocity and source temperature in comparison to the ambient temperature - in addition to the geometrical source height mechanical and or thermal lift of the plume has to be taken into account) and
- meteorological information concerning
- wind direction,
- wind speed and
- atmospheric stability/turbulence intensity.

Wind speed and turbulence intensity have a pronounced effect on the atmospheric dilution/diffusion process. The turbulence intensity is commonly parameterized either based on diffusion categories (named A for very unstable atmospheric stratification to F for very stable atmospheric stratification) or following the Monin Obukhov similarity theory, which enables a continuous stability parameterization based on the Monin Obukhov length and site specific parameters like the roughness length and the displacement height.

In Germany preferably meteorological time series with an hourly resolution (covering a minimum duration of one year which should be representative for the long term dispersion conditions) are used as an input for the dispersion model. Average concentration values and exceeding frequencies of concentration values can be analysed on the calculation grid of the model and at specified locations if necessary. If only a three dimensional frequency distribution of diffusion category, wind speed and wind direction is available as input, horizontal fields of yearly mean concentrations can be calculated.

In Vietnam representative meteorological conditions (most frequent ones) and those leading to high concentrations (normally happening in hot season) – are used for the calculations.

The Institute for Environment and Resources in Ho-Chi-Minh City, Vietnam has compiled an emission inventory for more than 50 different emission sources in the Thi Vai region. Data have been collected for CO₂-, CO-, SO₂-, NO_x-, TSP- and THC/VOC-emissions including emission flow, emis-



sion temperature, diameter and height of the sources/stacks. In future applications this emission inventory will be used for model intercomparison.

To understand the basic performance of the two (national) approaches/models applied for air quality control in Vietnam and Germany in a first step comparative calculations have been carried out for five different source heights (10, 20, 50, 100 and 180 m), six stability categories (A – F) and six different modelling approaches (Gaussian model with five different sets of dispersion parameters (following Pasquill-Gifford (PG), Briggs urban and Briggs rural parameterization, Brookhaven National Laboratory (BNL) (all described in [4]) and Juelich-Karlsruhe parameter set (JK) [5]) and one Lagrangian type of model. Because dry deposition is handled via the concept of deposition velocity in both models the results found for maximum airborne concentration and their positions can be

2. Vietnamese and German dispersion model

In Vietnam and Germany different models for the dispersion calculations in the context of air quality control are in use. The Gaussian plume model is widely used in Vietnam. Atmospheric stability is classified by stability classes/diffusion categories and the wind speed in the source height is calculated based on a power law formula. The exponent of the power law formula can be chosen for terrain with low or high surface roughness. In Germany up to 2001 a Gaussian model has been used too for air quality control applications (in some technical guidelines dealing with specialized aspects of environmental protection this Gaussian plume model is still recommended (e.g. [5]) but since 2002 a Lagrangian particle model has to be used. This type of model has more capabilities in adaption to special boundary conditions within an application. The dispersion parameters of the German Gaussian model have been derived from dispersion experiments in Germany at the research centers of Juelich and Karlsruhe. Parameter sets for three different source heights have been published [5]. They are representative for rough terrain. In the following subchapters the models are described in more detail.



2.1 Vietnamese dispersion model

In Vietnam a Gaussian model for a stationary plume is used. The near surface ($z=0$ m) concentration at a source distance x and y meter away from the plume centerline can be calculated based on the following formula:

$$C(x, y, z = 0) = \frac{Q}{\pi \sigma_y \sigma_z u} \exp\left(-\frac{y^2}{2\sigma_y^2}\right) \exp\left(-\frac{H_e^2}{2\sigma_z^2}\right) \quad (1)$$

with: C pollutant concentration (g/m^3)
Q source strength (g/s)
u wind velocity (m/s)
 H_e effective source height (m) – geometrical source height plus mechanical and/or thermal lift of the plume
 $\sigma_{y,z}$ dispersion parameters for horizontal (y) and vertical (z) direction (m)

The dispersion parameters σ_y and σ_z are specified according to the atmospheric stability classes and the distant dependent formulation of Pasquill (these parameters are based on dispersion experiments carried out during the Prairie grass experimental series with a source height of 0.46 m, meteorological averaging times of 10 minutes in an area of low roughness length (max. 0.03 m) and sampling distances of max. 800 m) [6]. The stability class can be derived following the scheme given in Table 2.



Table 2. Estimation of stability classes based on meteorological observations following Pasquill (in [4]).

Wind speed at 10 m (m/s)	Day			Night	
	strong sunlight	medium sunlight	weak sunlight	much clouds cloud cover > 4/8	less clouds cloud cover <= 3/8
< 2	A	A – B	B	E	F
2 - 3	A – B	B	C	E	F
3 - 5	B	B – C	C	D	E
5 - 6	C	C – D	D	D	D
> 6	D	D	D	D	D

Usually the wind speed in the effective source height H_e is used for concentration calculations. Based on wind speed measurements in height z_1 (usually 10 m above ground) the wind speed in height H_e can be calculated via:

$$u(H_e) = u(z_1)(H_e/z_1)^p \quad (2)$$

The exponent p varies with the atmospheric stability as shown in Table 3 following Irwin [7]. The data given in Table 3 are used for rough terrain. If the domain has a low surface roughness the exponent is reduced to 56 % of the tabulated values. This results in different values compared to Irwin [7], who also recommends values for rural terrain, which are given in parenthesis in Table 3.

Table 3. Exponent for the wind speed profile for urban conditions following Irwin [7]. In parenthesis profile exponents for rural terrain are given [7].

Diffusion category	A	B	C	D	E	F
Profile exponent	0.15 (0.07)	0.15 (0.07)	0.20 (0.10)	0.25 (0.15)	0.40 (0.35)	0.60 (0.55)

2.2 German Model

Until 2001 in Germany a Gaussian model has been used for air quality control. The dispersion parameters have been derived from German dispersion experiments at the research centers of Juelich and Karlsruhe (JK).



Within this experimental series source heights between 50 and 180 m have been used (in detail: parameter sets are available for the source heights 50, 100 and 180 m. For source heights between these heights interpolation formulas exist. For source heights above 180 m the parameters of 180 m have to be used, for source heights below 50 m the parameters of 50 m should be used [5]). The terrain around Juelich and Karlsruhe can be classified as rough (roughness length ≈ 1 m), the averaging times of the meteorological data have been between 30 and 60 minutes, therefore – in comparison to the PG-parameterization used in Vietnam – covering also parts of the lower frequencies in the turbulence spectrum. The sampling distances have extended to 10 – 15 km leewards of the source. In the German Gaussian model, the wind speed in the source height has to be used as an input which can be calculated using the same formula like in the Vietnamese model but with a different set of exponents (0.09 (A) – 0.20 (B) – 0.22 (C) – 0.28 (D) – 0.37 (E) – 0.42 (F)) which have been derived via long term measurements at the meteorological towers at the research centers of Juelich and Karlsruhe. The height of the towers are 120 m for Juelich and 180 m for Karlsruhe.

Since 2002 a Lagrangian type of dispersion model (AUSTAL/ARTM) is used in Germany based on a turbulence parameterization following the Monin-Obukhov similarity theory. The dispersion model is a realization of the guideline VDI 3945/Part 3 [1]. The computer program AUSTAL2000 is a reference implementation of the specifications given in appendix 3 of the German regulation TA Luft [3]. A program description is available [8].

In the Lagrangian model wind speed and turbulence profiles are calculated via similarity theory (based on a one dimensional boundary layer model) and the particles are transported (advected and diluted) by the wind and turbulence data at their actual position. The dispersion model can be coupled with a diagnostic or prognostic mesoscale wind field model if the terrain is not flat.

Vietnamese and German models can handle plume rise due to mechanical and thermal lift. However this aspect is not in our focus here.



3. Model intercomparison

3.1 Setup

The comparative calculations with the different dispersion parameterizations (for the Gaussian model) and the Lagrangian model have been carried out to show the variability of the atmospheric concentration of a pollutant near the surface for different atmospheric stabilities and source heights and the differences between the results following alternative parameterization/modelling schemes.

To keep the boundary conditions for the calculations following the Gaussian formula as simple as possible, in a first step the source strength has been set to a value of 1 g/s and the wind speed has been set to 1 m/s.

In a second step the PG- and JK-parameterizations have been used together with wind speed calculated for the source heights under consideration and assuming a value of 1 m/s in 10 m height using the power law formula (2) given in section 2. For the Vietnamese approach the PG dispersion parameters and the profile exponents from Table 3 modified for flat terrain have been used. The conversion factors for the wind speed in the different source heights are given in Table 4.

The results of the comparative concentration calculations are given in chapter 3.2.



Table 4. Conversion factors for wind speed in heights of 20, 50, 100 and 180 m in the Gaussian model (wind speed in 10 m height: 1 m/s). Vietnamese wind profile upper part, German wind profile lower part of the Table

Source height/10 m				
	2	5	10	18
Vietn. profile exponent (low roughness)				
0.08	1.06	1.14	1.20	1.26
0.08	1.06	1.14	1.20	1.26
0.11	1.08	1.19	1.29	1.37
0.14	1.10	1.25	1.38	1.50
0.22	1.17	1.43	1.66	1.89
0.34	1.27	1.73	2.19	2.67

Source height/10 m				
	2	5	10	18
Germ. profile exponent (high roughness)				
0.09	1.06	1.16	1.23	1.30
0.20	1.15	1.38	1.59	1.78
0.22	1.17	1.43	1.66	1.89
0.28	1.21	1.57	1.91	2.25
0.37	1.29	1.81	2.34	2.91
0.42	1.34	1.97	2.63	3.37

3.1 Concentration maxima and their source distances

In tables 5 – 9 the results of the model calculations are shown. For a source height of 10 m (Table 5) the wind speed used in the model is the same as the value measured in 10 m height. Therefore no additional concentration data in parenthesis are given in Table 5. In Tables 6 – 9 the Gaussian model has been applied with two wind speeds, a reference value



of 1 m/s for all parameterizations and a value at the source height connected to a wind speed profile for the PG- and JK-parameterizations (see chapter 2 and Table 4).

The results of the Lagrangian model AUSTAL/ARTM and 10 m source height have been calculated for the two roughness lengths given in Table 5 in order to underline that the roughness length is an input parameter of the model and to show the sensitivity of the model results to this parameter. The results of AUSTAL/ARTM can only be compared to the results of Gaussian model calculations based on the wind speed in source height because this is the normal mode of operation of the Gaussian models in Vietnam and Germany. The results of AUSTAL/ARTM for low roughness length should be compared to the Gaussian model and PG-parameters because this fits to the basic dispersion experiments for this parameterization. The results for the high roughness length should be compared to Gaussian JK-results for the same reasons.

Table 5. Source height 10 m: maximum ground level concentration of a pollutant in (g/m³) and its position (source distance in m) calculated with a Gaussian model (source strength 1 g/s and wind speed 1 m/s) and five different dispersion parameterizations and the Lagrangian model AUSTAL/ARTM. AUSTAL/ARTM has been setup for a high ($z_0=1.0$ m) and low roughness length ($z_0 = 0.03$ m).

Parameter system Diffusion category	Pasquill-Gifford (PG) low roughness		Juelich-Karlsruhe (JK) high roughness		Briggs urban [9]		Briggs rural [9]		BNL [10]		AUSTAL/ARTM $z_0=1.0$ m $z_0=0.03$ m	
	Cmax (g/m ³)	Position (m)	Cmax (g/m ³)	Position (m)	Cmax (g/m ³)	Position (m)	Cmax (g/m ³)	Position (m)	Cmax (g/m ³)	Position (m)	Cmax (g/m ³)	Position (m)
A - Cmax (g/m ³) Position (m)	1.09 10 ⁻³ 60		7.54 10 ⁻⁴ 30		1.79 10 ⁻³ 30		2.07 10 ⁻³ 40		2.33 10 ⁻³ 20		1.24 10 ⁻³ 23	7.45 10 ⁻⁴ 45
B - Cmax (g/m ³) Position (m)	1.17 10 ⁻³ 70		9.63 10 ⁻⁴ 40		1.79 10 ⁻³ 30		1.76 10 ⁻³ 60		- -		1.61 10 ⁻³ 23	9.00 10 ⁻⁴ 57
C - Cmax (g/m ³) Position (m)	1.27 10 ⁻³ 100		1.19 10 ⁻³ 50		2.09 10 ⁻³ 40		1.70 10 ⁻³ 90		2.10 10 ⁻³ 40		1.96 10 ⁻³ 23	1.23 10 ⁻³ 79
D - Cmax (g/m ³) Position (m)	1.32 10 ⁻³ 160		1.17 10 ⁻³ 50		2.05 10 ⁻³ 50		1.62 10 ⁻³ 130		1.61 10 ⁻³ 90		2.22 10 ⁻³ 45	1.79 10 ⁻³ 125
E - Cmax (g/m ³) Position (m)	1.26 10 ⁻³ 230		8.40 10 ⁻⁴ 70		1.72 10 ⁻³ 90		1.10 10 ⁻³ 250		- -		2.39 10 ⁻³ 45	1.39 10 ⁻³ 194
F - Cmax (g/m ³) Position (m)	1.19 10 ⁻³ 380		3.28 10 ⁻⁴ 160		1.72 10 ⁻³ 90		8.35 10 ⁻⁴ 490		4.53 10 ⁻⁴ 830		2.65 10 ⁻³ 45	5.27 10 ⁻⁴ 677

Table 6. Source height 20 m: maximum ground level concentration of a pollutant in (g/m³) and its position (source distance in m) calculated with a Gaussian model (source strength 1 g/s and wind speed 1 m/s) and five different dispersion parameterizations and the Lagrangian model AUSTAL/ARTM. The values in parenthesis have been calculated with the wind speed in source height.

Parameter system	Pasquill-Gifford (PG)	Juelich-Karlsruhe (JK)	Briggs urban [9]	Briggs rural [9]	BNL [10]	AUSTAL/ARTM
Diffusion category	low roughness	high roughness				$z_0=1.0\text{ m}$
A – C _{max} (g/m ³)	3.04 10 ⁻⁴ (2.86 10 ⁻⁴)	2.43 10 ⁻⁴ (2.29 10 ⁻⁴)	4.56 10 ⁻⁴	5.34 10 ⁻⁴	6.00 10 ⁻⁴	1.76 10 ⁻⁴
Position (m)	120	40	60	70	50	42
B – C _{max} (g/m ³)	3.03 10 ⁻⁴ (2.86 10 ⁻⁴)	2.85 10 ⁻⁴ (2.39 10 ⁻⁴)	4.56 10 ⁻⁴	4.42 10 ⁻⁴	-	2.37 10 ⁻⁴
Position (m)	140	80	60	120	-	71
C – C _{max} (g/m ³)	3.21 10 ⁻⁴ (2.97 10 ⁻⁴)	3.43 10 ⁻⁴ (2.93 10 ⁻⁴)	5.40 10 ⁻⁴	4.22 10 ⁻⁴	5.37 10 ⁻⁴	2.92 10 ⁻⁴
Position (m)	210	90	70	180	80	99
D – C _{max} (g/m ³)	3.09 10 ⁻⁴ (2.81 10 ⁻⁴)	3.17 10 ⁻⁴ (2.62 10 ⁻⁴)	5.14 10 ⁻⁴	3.75 10 ⁻⁴	4.03 10 ⁻⁴	3.39 10 ⁻⁴
Position (m)	350	120	100	270	210	99
E – C _{max} (g/m ³)	2.85 10 ⁻⁴ (2.44 10 ⁻⁴)	2.14 10 ⁻⁴ (1.66 10 ⁻⁴)	4.35 10 ⁻⁴	2.59 10 ⁻⁴	-	3.34 10 ⁻⁴
Position (m)	510	170	180	530	-	127
F – C _{max} (g/m ³)	2.50 10 ⁻⁴ (1.97 10 ⁻⁴)	7.73 10 ⁻⁵ (5.77 10 ⁻⁵)	4.35 10 ⁻⁴	1.84 10 ⁻⁴	1.13 10 ⁻⁴	3.27 10 ⁻⁴
Position (m)	880	450	180	1110	2190	199

Table 7. Source height 50 m: maximum ground level concentration of a pollutant in (g/m³) and its position (source distance in m) calculated with a Gaussian model (source strength 1 g/s and wind speed 1 m/s) and five different dispersion parameterizations and the Lagrangian model AUSTAL/ARTM. The values in parenthesis have been calculated with the wind speed in source height.

Parameter system Diffusion category	low roughness		high roughness		Briggs urban [9]	Briggs rural [9]	BNL [10]	AUSTAL/ARTM
	Pasquill-Gifford (PG)	Juelich-Karlsruhe (JK)	Briggs urban [9]	Briggs rural [9]				$z_0=1.0\text{ m}$
A - Cmax (g/m ³)	6.14 10 ⁻⁵ (5.39 10 ⁻⁵)	5.32 10 ⁻⁵ (4.59 10 ⁻⁵)	7.71 10 ⁻⁵	8.59 10 ⁻⁵	9.59 10 ⁻⁵			2.41 10 ⁻⁵
Position (m)	240	100	140	180	130			177
B - Cmax (g/m ³)	5.31 10 ⁻⁵ (4.66 10 ⁻⁵)	5.83 10 ⁻⁵ (4.22 10 ⁻⁵)	7.71 10 ⁻⁵	7.13 10 ⁻⁵	-			2.68 10 ⁻⁵
Position (m)	350	170	140	300	-			248
C - Cmax (g/m ³)	5.23 10 ⁻⁵ (4.40 10 ⁻⁵)	6.53 10 ⁻⁵ (4.57 10 ⁻⁵)	8.81 10 ⁻⁵	6.67 10 ⁻⁵	8.59 10 ⁻⁵			3.05 10 ⁻⁵
Position (m)	550	230	180	460	230			389
D - Cmax (g/m ³)	4.13 10 ⁻⁵ (3.30 10 ⁻⁵)	5.64 10 ⁻⁵ (3.59 10 ⁻⁵)	8.29 10 ⁻⁵	4.84 10 ⁻⁵	6.44 10 ⁻⁵			3.21 10 ⁻⁵
Position (m)	1070	330	260	810	670			496
E - Cmax (g/m ³)	3.39 10 ⁻⁵ (2.37 10 ⁻⁵)	3.50 10 ⁻⁵ (1.93 10 ⁻⁵)	7.17 10 ⁻⁵	3.36 10 ⁻⁵	-			2.62 10 ⁻⁵
Position (m)	1720	560	460	1600	-			715
F - Cmax (g/m ³)	2.34 10 ⁻⁵ (1.35 10 ⁻⁵)	1.15 10 ⁻⁵ (5.84 10 ⁻⁶)	7.17 10 ⁻⁵	1.85 10 ⁻⁵	1.81 10 ⁻⁵			1.30 10 ⁻⁵
Position (m)	3540	1820	460	4080	7980			1355

Table 8. Source height 100 m: maximum ground level concentration of a pollutant in (g/m³) and its position (source distance in m) calculated with a Gaussian model (source strength 1 g/s and wind speed 1 m/s) and five different dispersion parameterizations and the Lagrangian model AUSTAL/ARTM. The values in parenthesis have been calculated with the wind speed in source height.

Parameter system		Pasquill-Gifford (PG)	Juelich-Karlsruhe (JK)	Briggs urban [9]	Briggs rural [9]	BNL [10]	AUSTAL/ARTM
		low roughness	high roughness	$z_0=1.0\text{ m}$			
Diffusion category							
A - Cmax	(g/m ³)	1.97 10 ⁻⁵ (1.64 10 ⁻⁵)	7.88 10 ⁻⁶ (6.41 10 ⁻⁶)	2.08 10 ⁻⁵	2.17 10 ⁻⁵	2.40 10 ⁻⁵	6.86 10 ⁻⁶
	Position (m)	390	240	270	360	290	354
B - Cmax	(g/m ³)	1.47 10 ⁻⁵ (1.23 10 ⁻⁵)	1.08 10 ⁻⁵ (6.80 10 ⁻⁶)	2.08 10 ⁻⁵	1.81 10 ⁻⁵	-	6.61 10 ⁻⁶
	Position (m)	690	420	270	590	-	495
C - Cmax	(g/m ³)	1.33 10 ⁻⁵ (1.03 10 ⁻⁵)	1.47 10 ⁻⁵ (8.86 10 ⁻⁶)	2.28 10 ⁻⁵	1.63 10 ⁻⁵	2.15 10 ⁻⁵	6.74 10 ⁻⁶
	Position (m)	1170	590	360	960	510	852
D - Cmax	(g/m ³)	8.11 10 ⁻⁶ (5.88 10 ⁻⁶)	1.23 10 ⁻⁵ (6.44 10 ⁻⁶)	2.10 10 ⁻⁵	9.14 10 ⁻⁶	1.61 10 ⁻⁵	5.87 10 ⁻⁶
	Position (m)	2880	920	550	2190	1640	1070
E - Cmax	(g/m ³)	5.35 10 ⁻⁶ (3.22 10 ⁻⁶)	7.64 10 ⁻⁶ (3.27 10 ⁻⁶)	1.87 10 ⁻⁵	5.43 10 ⁻⁶	-	2.82 10 ⁻⁶
	Position (m)	5470	1880	970	4560	-	2303
F - Cmax	(g/m ³)	2.53 10 ⁻⁶ (1.16 10 ⁻⁷)	3.49 10 ⁻⁷ (1.33 10 ⁻⁷)	1.87 10 ⁻⁵	1.39 10 ⁻⁶	3.93 10 ⁻⁶	4.03 10 ⁻⁷
	Position (m)	> 15000	7880	970	> 15000	> 15000	5028

Table 9. Source height 180 m: maximum ground level concentration of a pollutant in (g/m³) and its position (source distance) calculated with a Gaussian model (source strength 1 g/s and wind speed 1 m/s) and five different dispersion parameterizations and the Lagrangian model AUSTAL/ARTM. The values in parenthesis have been calculated with the wind speed in source height.

Parameter system	Pasquill-Gifford	Juelich-Karlsruhe	Briggs urban [9]	Briggs rural [9]	BNL [10]	AUSTAL/ARTM
Diffusion category						$z_0=1.0 \text{ m}$
A - C _{max} (g/m ³)	7.83 10 ⁻⁶ (6.21 10 ⁻⁶)	8.12 10 ⁻⁶ (6.25 10 ⁻⁶)	7.10 10 ⁻⁶	6.78 10 ⁻⁶	7.41 10 ⁻⁶	2.65 10 ⁻⁶
Position (m)	570	320	460	640	550	636
B - C _{max} (g/m ³)	5.01 10 ⁻⁶ (3.98 10 ⁻⁶)	7.91 10 ⁻⁶ (4.44 10 ⁻⁶)	7.10 10 ⁻⁶	5.70 10 ⁻⁶	-	2.36 10 ⁻⁶
Position (m)	1200	560	460	1070	-	891
C - C _{max} (g/m ³)	4.18 10 ⁻⁶ (3.05 10 ⁻⁶)	6.34 10 ⁻⁶ (3.35 10 ⁻⁶)	7.37 10 ⁻⁶	4.89 10 ⁻⁶	6.63 10 ⁻⁶	2.17 10 ⁻⁶
Position (m)	2220	1280	650	1830	1020	1533
D - C _{max} (g/m ³)	1.89 10 ⁻⁶ (1.26 10 ⁻⁶)	2.68 10 ⁻⁶ (1.19 10 ⁻⁶)	6.57 10 ⁻⁶	2.11 10 ⁻⁶	4.97 10 ⁻⁶	1.38 10 ⁻⁶
Position (m)	7430	3420	1050	6050	3480	2471
E - C _{max} (g/m ³)	8.89 10 ⁻⁷ (4.70 10 ⁻⁷)	4.04 10 ⁻⁷ (1.39 10 ⁻⁷)	6.13 10 ⁻⁶	6.08 10 ⁻⁷	-	2.84 10 ⁻⁷
Position (m)	> 15000	13970	1850	14960	-	8889
F - C _{max} (g/m ³)	4.60 10 ⁻⁸ (1.72 10 ⁻⁹)	6.28 10 ⁻⁸ (1.86 10 ⁻⁸)	6.13 10 ⁻⁶	3.88 10 ⁻⁹	1.02 10 ⁻⁷	-
Position (m)	> 15000	> 49000	1850	> 15000	> 15000	out of range



The PG- and JK-parameters are based on diffusion experiments with different source heights, different roughness lengths, different sampling times of the meteorological data and different sampling distances from the source. Therefore it is not surprising, that a comparison of the results of the Gaussian models leads to differences in maximum concentration data and differences in the position of the maxima. On the other hand the Lagrangian model can handle different source heights, atmospheric stabilities and roughness lengths as input parameters. In Table 10 the bias in the maximum concentration data and the position of C_{max} of the Lagrangian model is shown in comparison to the results of the PG-parameterization for the source height of 10 m and in comparison to the JK-parameterization for the source heights of 50, 100 and 180 m. The bias is calculated as follows:

$$\text{Bias } C_{max} = (C_{maxAUSTAL} - C_{maxGAUSSIAN})/C_{maxGAUSSIAN} \quad (3)$$

$$\text{Bias } C_{maxdist} = (C_{maxdistAUSTAL} - C_{maxdistGAUSSIAN})/C_{maxdistGAUSSIAN} \quad (4)$$

Assuming that the PG-Parameterization is the best guess for real dispersion for near surface release (10 m) in areas of low roughness length and the JK-parameterization is the best approximation to real dispersion for elevated release in regions with high roughness lengths the bias of AUSTAL/ARTM is calculated for all atmospheric stabilities and for the source heights of 10, 50, 100 and 180 m. The results are displayed in Table 10 and will be discussed in chapter 4.

Application of the AUSTAL/ARTM-model results in slightly lower concentration data compared to the Gaussian model except for elevated release and stable stratification of the atmosphere where an overestimation by a factor of two is possible. Looking at the position of the concentration maxima AUSTAL/ARTM and the Gaussian model agree within some 10 %. For low release height and low roughness length the concentration maxima with AUSTAL/ARTM have been found closer to the source compared to the Gaussian results, for elevated release in rough terrain the AUSTAL/ARTM maxima have been found at greater source distances compared to the Gaussian model.



Table 10. Bias of the AUSTAL/ARTM-results compared to the PG- and JK- dispersion parameterization of a Gaussian model. Upper part: bias of the maximum concentration data, lower part: bias of the source distance of maximum concentration

Bias Cmax Diff. category	AUSTAL– PG 10 m	AUSTAL– JK 50 m	AUSTAL– JK 100 m	AUSTAL– JK 180 m
A	-0.32	-0.47	0.07	-0.58
B	-0.23	-0.36	-0.03	-0.47
C	-0.03	-0.33	-0.24	-0.35
D	0.36	-0.11	-0.09	0.16
E	0.10	0.36	-0.14	-0.80
F	-0.56	1.23	2.03	-
Bias Cmaxdist Diff. category	AUSTAL– PG 10 m	AUSTAL– JK 50 m	AUSTAL– JK 100 m	AUSTAL– JK 180 m
A	-0.25	0.77	0.48	0.99
B	-0.19	0.46	0.18	0.59
C	-0.21	0.69	0.44	0.20
D	-0.22	0.50	0.16	-0.28
E	-0.15	0.28	0.23	-0.57
F	0.78	-0.26	-0.36	-

4. Discussion

The results for the Gaussian model using different sets of diffusion parameters (for source strength 1 g/s and wind speed of 1 m/s) show that the general qualitative behaviour within each parameterization scheme is similar:

- for a fixed diffusion category the maximum concentration of a pollutant decreases with increasing source height
- the source distance of the maximum concentration of a pollutant increases with source height



- for a fixed source height the source distance of the maximum concentration of a pollutant increases with stabilization of the atmospheric boundary layer (variation from stability class A to F).

A quantitative comparison of the results should be carried out based on the PG-parameterization for 10 m source height and based on the JK-parameterization for the source heights of 50 m, 100 m and 180 m (as reference results).

For a source height of 10 m and within one diffusion category differences of the maximum concentration data of a pollutant C_{max} between all the parameterization schemes (compared to the PG-parameterization) up to a factor of two have been found for unstable to stable stratification. This is equivalent to bias values in the range from -0,5 to +1. For diffusion category F a factor of three or even larger can occur.

For larger source heights (≥ 50 m) the deviation of the maximum concentration data of a pollutant from the JK-parameterization results are within a factor of two for unstable and neutral stratification. For stable stratification and 180 m emission height differences up to a factor of ten can occur. These differences result due to the varying turbulence parameterization schemes that in turn are depending on diffusion experiments with different/specific setups. The local roughness length is one important parameter acting on C_{max} and influencing the position of the concentration maximum. Only with a very few exceptions for very unstable stratification a comparison of both Briggs schemes show that for higher roughness length (urban case) the C_{max} -data within one diffusion category are higher than for lower roughness length (rural case). During stable stratification of the atmosphere the only mechanism, which generates turbulence is mechanic production via surface roughness. In regions with low surface roughness vertical turbulence intensity is small and vertical diffusion is weak. So the plume reaches the ground far away from the source and shows low maximum concentration values because the horizontal dilution is acting continuously during the (slow) vertical spread of the plume.

Looking at the position of the maximum concentration of a pollutant a factor of three between the different approaches is not unusual, some-



times larger sometimes smaller. The largest differences again occur under stable stratification.

The PG-scheme gives C_{max} positions, which are similar to the results of the Briggs rural scheme whereas the JK-parameters lead to comparable C_{max} distances based on the Briggs urban scheme. Remembering the experimental conditions during the underlying dispersion experiments for deriving the parameterizations the PG-parameters should be typical for low roughness length – as the rural Briggs scheme – and the JK-parameters have been derived from experiments at locations with higher roughness lengths – like the Briggs urban parameters -.

In addition to the roughness length other effects may be important in deriving parameterization schemes from diffusion experiments as pointed out earlier (source height, averaging times, etc.). But these effects will not be discussed here.

Within the new German modelling approach via the Lagrangian particle model AUSTAL/ARTM a one dimensional boundary layer model is available for calculation of wind speed and turbulence profiles. The local roughness length is an input parameter for this model. The results of AUSTAL/ARTM-model have been compared to the Gaussian results with PG- and JK- parameterizations. Comparisons with the PG-results have been done with a roughness length of 0.03 m and comparisons with JK-data have been carried out with AUSTAL/ARTM runs with roughness length of 1.0 m.

The bias data in Table 10 show that for the majority of combinations of atmospheric stratification and source heights with AUSTAL/ARTM it is possible to calculate results (maximum concentration and its source distance) for the PG- and JK-situations which differ by less than 50 % (except for the very stable situations where a bias of 2 is possible in the concentration data).

The particle model has also been tested against dispersion experiments (wind tunnel data and Prairie grass experiments). The tests are documented in a guideline [11]. A revision of this parameterization (especially for stable stratification and for high sources) is prepared by a working group and will be published at the end of 2014.



5. Validation

The approaches described here for a turbulence parameterization of a Lagrangian dispersion model have been compared to results from wind tunnel measurements and dispersion experiments [11]. Validation examples and validation data are available in [12].

5.1 Experiments in a wind tunnel

For a roughness length $z_0 = 0.7$ m and source heights of 60 m and 100 m, near surface measurements of concentration distribution $c(x, y, 0)$ are available for a neutral stratified wind tunnel. By cross wind integration, the variable $c_y(x)$ was determined.

Figure 1 presents the standardised concentration $C_y = c_y H u_q / Q$ (source strength Q , source height H , wind velocity at source height u_q) as a function of source distance. Further details in [11].

“For an emission height of 60 m, the curve of the Lagrangian model indicates a slightly conservative result. For all evaluated source distances, the standardised concentration data of the wind tunnel experiment lie below the calculated comparison data” [11]. The position of the measured concentration maximum lies at a slightly lower source distance to the concentration values of the model.

“For a height of emission of 100 m, the calculated values of the concentration increase fit quite well to the measured values derived from experimental data. The concentration maximum is slightly overestimated when calculated on the basis of the proposed parameterisation of this guideline in comparison to the measured maximum. The source distance of the calculated maximum is located slightly further away from the observed data” [11].

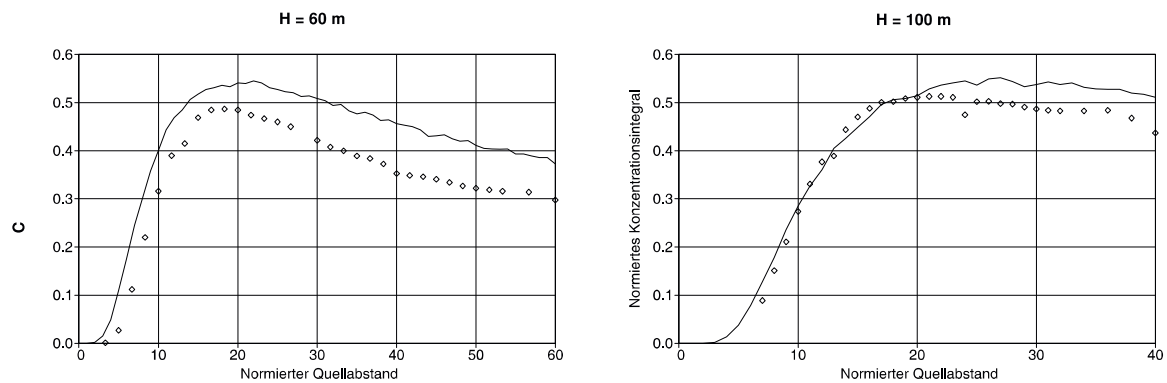


Figure 1. Comparison of the cross wind integrated concentration as a function of the normalized source distance (measurement data wind tunnel (open lozenges), model calculations (continuous curve)) for source height 60 m and 100 m. [12]

5.2 Prairie Grass experiments

“The Prairie Grass experiments were carried out in 1956 in O’Neill, Nebraska/USA. For three source distances (50 m, 200 m and 800 m), the following variables of measurement and calculation values were compared:

- cross wind integrated concentration and
- plume width

The experimental results are displayed in Figures 2 and 3, the reciprocal Monin-Obukhov length $1/L$ was used as a stability parameter (open lozenge = \wedge measurement values; red lozenge = \wedge model results). The plume widths are quite well described by the parameterisation for the entire stability range. For stable to neutral stratification, the calculated and observed values show a satisfying agreement for standardised concentration data. The turbulent vertical exchange is described close to reality by the parameterisation. In the range of unstable stratification and for larger source distances, the differences between measurement and calculation results are more pronounced. A large scatter of the measured data occurs. The stratification of the atmosphere was extremely convective in parts though the emitted tracer was effectively transported into upper regions of the atmosphere” [11].

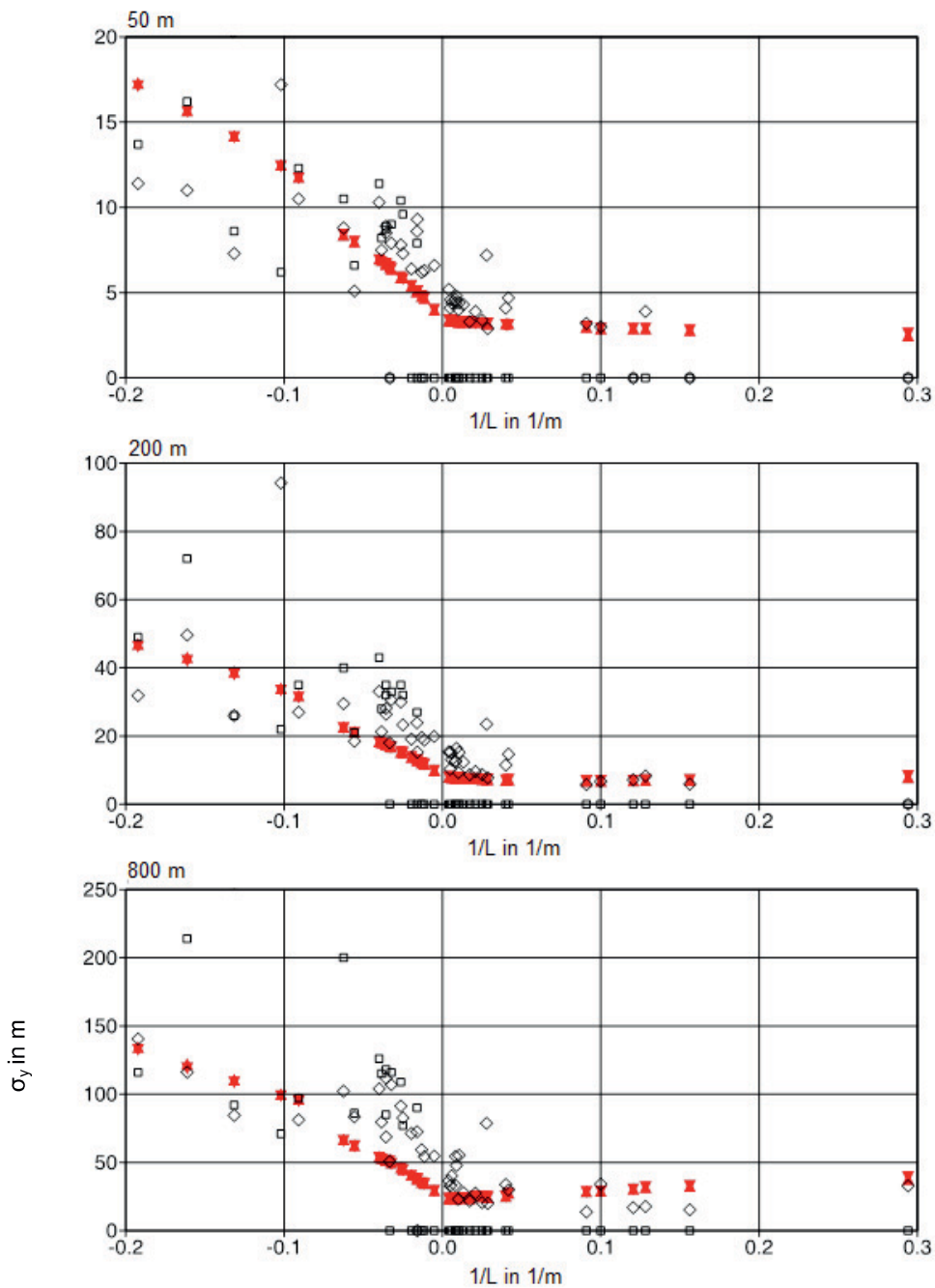


Figure 2. Comparison of trace element plume widths established during the Prairie-Grass experiments for three source distances as a function of the reciprocal Monin-Obukhov length (open lozenge: measurement values, red lozenge: model results) [12]

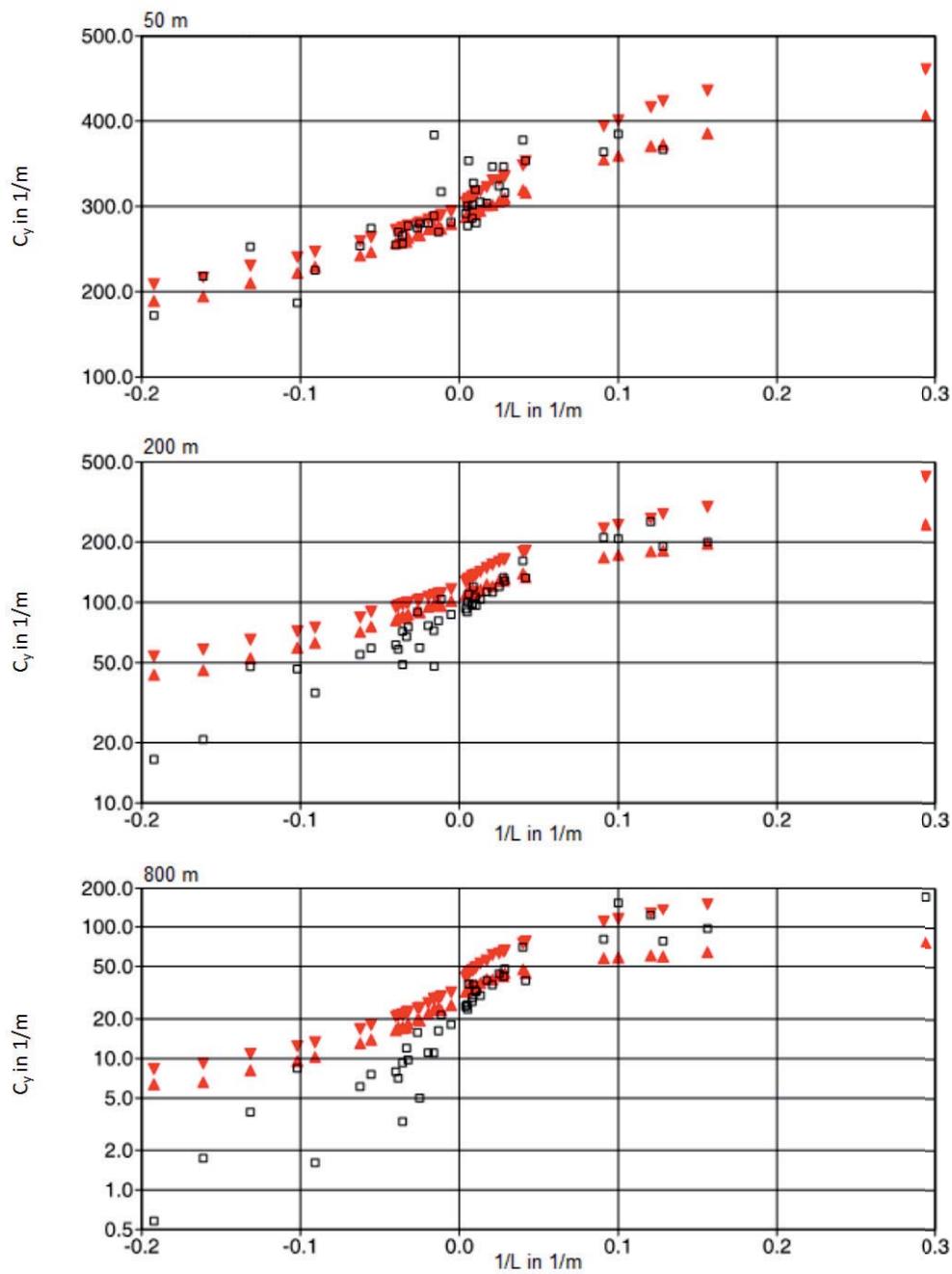


Figure 3. Comparison of integrated trace element concentrations as established during the Prairie-Grass experiments for three source distances as a function of the reciprocal Monin-Obukhov length (open lozenge: measurement values, red lozenge: model results) [12]



6. Summary

For a wide range of source heights and diffusion categories five different parameterization schemes for a Gaussian type plume model and a Lagrangian type particle model have been compared focussing on the maximum concentration value and its position leewards of a point source. Pronounced scattering of the model results have been found, especially for stable atmospheric stratification. One reason for the differences could be attributed to the roughness length, which has a strong influence on the turbulence structure in the atmospheric boundary layer.

It could be shown that based on the Lagrangian particle model including turbulence parameterization based on Monin Obukhov similarity theory the results of the Gaussian models for low release heights in an area with low roughness length can be reproduced within some 10 %. The same holds for elevated releases in an area with high roughness length.

The assessment of atmospheric dispersion within air pollution control strategies / licensing procedures at sites covering a large range of surface roughness and possible source heights should be done with a turbulence parameterization based on site specific roughness length and the source height as explicit input parameters. A similarity based approach validated against concentration distributions is available together with a computer program via the German guideline Technische Anleitung zur Reinhaltung der Luft [3]. It is ready for inspection and further testing for applications in Vietnam.

References

- [1] Verein Deutscher Ingenieure [Ed.] (2000): Environmental meteorology – Atmospheric dispersion models – Particle model. VDI 3945, part 3, VDI/DIN-Handbuch Reinhaltung der Luft, Bd. 1b.
- [2] QCVN 05 : 2013/BTNMT. Vietnam National Ambient Air Standards. Socialist Republic of Vietnam, Ha Noi 2013.
- [3] Technische Anleitung zur Reinhaltung der Luft (TA-Luft) in Germany (available (17.5.2014)): http://www.verwaltungsvorschriften-im-internet.de/bsvwvbund_24072002_IGI2501391.htm).



- [4] Hanna SR, Briggs GA, Hosker RP Jr (1982): Handbook on atmospheric diffusion. Technical information center, US department of energy, DOE/TIC-11223 (DE82002045).
- [5] Bundesministerium für Umwelt, Naturschutz und Reaktorsicherheit [Ed.] (2012): Allgemeine Verwaltungsvorschrift zu § 47 Strahlenschutzverordnung: Ermittlung der Strahlenexposition durch die Ableitung radioaktiver Stoffe aus Anlagen oder Einrichtungen – vom 28. August 2012), BAnz AT 05.09.2012 B1 /(available (17.5.2014)):
http://www.verwaltungsvorschriften-im-internet.de/bsvwvbund_28082012_RSII.htm.
- [6] Gifford FA (1976): Turbulent diffusion typing schemes. A review. Nucl. safety, vol. 17 (1), p. 71.
- [7] Irwin, JS (1979): Estimating plume dispersion – A recommended generalized scheme. Preprints of fourth symposium on turbulence, diffusion and air pollution, Reno, Nev., Jan. 15-18, pp. 62-69, American Meteorological Society, Boston Mass.
- [8] AUSTAL2000, download (available 17.5.2014):
<http://www.austal2000.de/en/home.html>.
- [9] Briggs GA (1973): Diffusion estimation of small emissions. Atmospheric turbulence and diffusion laboratory: ATDL Contribution, file no. 79.
- [10] Smith ME (1968): Recommended guide for the prediction of the dispersion of airborne effluents. New York: American Society of Mechanical Engineers.
- [11] Verein Deutscher Ingenieure [Ed.] (2002); Environmental meteorology – Turbulence parameters for dispersion models supported by measurement data. VDI 3783, part 8, VDI/DIN-Handbuch Reinhaltung der Luft, Bd. 1b.
- [12] Verein Deutscher Ingenieure [Ed.] (2002): Validierungsbeispiele zur VDI Richtlinie 3783, Blatt 8:
<http://www.vdi.de/technik/fachthemen/reinhaltung-der-luft/technische-regeln/vdi-richtlinien-fb-ii/rl-programme/richtlinie-vdi-3783-blatt-8-validierungsbeispiel/>.



Ecohydrological modeling of the Thi Vai Catchment in South Vietnam

Malte Lorenz¹, Karen Prilop¹, Mai Toan Thang², Huyen Le¹, Nguyen Duy Hieu², Günter Meon¹, Nguyen Hong Quan²

¹ Leichtweiß-Institute for Hydraulic Engineering and Water Resources, Department of Hydrology, Water Management and Water Pollution Control, University of Braunschweig, Beethovenstr. 51a, D-38106 Braunschweig, Germany, Malte.Lorenz@tu-bs.de

² Institute for Environment and Resources (IER) - Vietnam National University of Ho-Chi-Minh City, 142 To Hien Thanh, District 10, Ho-Chi-Minh City, Viet Nam

Abstract

The joint research project “Environmental and Water Protection Technologies of Coastal Zones in Vietnam EWATEC-COAST” is funded by the German Ministry of Research and Education (BMBF) and the Vietnam National University of Ho-Chi-Minh City and is focused on the Thi Vai River catchment.

The overall objective of the research project is the development, supply and use of water and environmental technologies and service tools in the framework of a management system. The Thi Vai River has a catchment size of about 625 km² and a length of 32 km. The middle and lower parts of the river form an estuary, strongly affected by the tide. Since 1990 the Thi Vai River is facing heavy water quality problems due to the discharge of mainly untreated industrial waste water. Beside the high density of industrial parks along the Thi Vai River, the catchment is characterized by intensive agriculture, mainly rubber plantations (42 % of the catchment area). The water of the Thi Vai River cannot be used for irrigation and industrial or domestic purposes, because of its naturally high salinity. In consequence, the water quantity and quality of the main tributaries of the Thi Vai River is very important for the fresh water supply for irrigation and industrial or domestic purposes. The presented work is focused on the ecohydrological modeling of the water quantity and quality of the main tributaries of the Thi Vai River. It is the aim of this work to model and evaluate discharge and nutrient loads of the main tributaries and diffuse inflow and diffuse nutrient loads of the catchment into the Thi Vai River.

Within the project a monitoring system for water quantity and quality was installed along the Thi Vai River and its main tributaries the Bun Mon, Ca



and Cau Vac River. The monitoring was started in March 2013 and is still in progress. At the three tributary stations discharge is derived from water level data logged every 15 minutes. Physical and chemical water quality parameters are obtained every week at each monitoring station.

The hydrology and the water quality of the investigated tributaries of the Thi Vai River are modeled with the rainfall runoff model Panta Rhei. Within the project the model Panta Rhei is extended with process routines for terrestrial biogeochemical cycles (carbon, nitrogen and phosphorus) and routines for instream water quality. As the Thi Vai catchment is strongly influenced by the monsoon, there is a pronounced change of precipitation during the year, resulting in large variability of environmental conditions like flash floods during rainy season and heavy droughts during dry season. The high variability of environmental conditions has a strong impact on the temporal patterns of soil organic matter decomposition and nutrient leaching. To deal with this, the soil microbial biomass is in the focus of the terrestrial biogeochemical model, linking the carbon, nitrogen and phosphorous cycle in soils

Key Words: ecohydrological modelling, water quality, hydrology, nutrient transport



1. Introduction

The presented study is part of the joint research project “Environmental and Water Protection Technologies of Coastal Zones in Vietnam EWATEC-COAST” funded by the German Ministry of Research and Education (BMBF) and the Vietnam National University of Ho-Chi-Minh City.

In focus of the research project is the Thi Vai River and its catchment. Since 1990 the Thi Vai River is facing heavy water quality problems due to the discharge of huge amounts of mainly untreated industrial waste water. Since 2008 the water quality of the Thi Vai River could be improved by a first introduction of treatment plants, but is still facing problems [1,2]. The Thi Vai River is an estuary influenced by tide. The water of the Thi Vai River cannot be used for irrigation and industrial or domestic purposes, because of its naturally high salinity. In consequence, the water quantity and quality of the main tributaries of the Thi Vai River is very important for the fresh water supply for irrigation and industrial or domestic purposes.

The overall objective of the research project is the development, supply and use of water and environmental technologies and service tools in the framework of a management system.

The management system includes coupled models for the description of water quantity and quality of surface waters, simulating the water balance, the transport of pollutants into receiving water bodies and the water quality of rivers. The models need to be highly distributed in time and space, be capable of modeling effects of different treatment facilities on point sources and deal with management practices on diffuse source input from agricultural sources. In doing so, the interactions of the measures and the overall impact on the water quality can be quantified at any location of the river system, and suitable planning variants can be elaborated [3, 4]. Because of the tidal influence on the Thi Vai River, the application of a hydrodynamic water quality model is necessary to adequately simulate temporal and spatial patterns of the water quantity and quality of the Thi Vai River [3]. The hydrodynamic water quality model needs input information about the discharge and substance loads of its tributaries in an adequate temporal resolution. For the simulation of the catchment dis-



charge and substance loads an ecohydrological model is coupled with the hydrodynamic water quality model [5].

The application of the hydrodynamic water quality model of the Thi Vai River is described in the accompanying paper "A 3D-hydrodynamic and water quality model of the Thi Vai River under strongly tidal effect".

The presented work is focused on the ecohydrological modeling of the water quantity and quality of the main tributaries of the Thi Vai River. It is the aim of this work to simulate and evaluate discharge and nutrient loads of the main tributaries and diffuse inflow and diffuse nutrient loads of the catchment into the Thi Vai River. The simulated discharge and nutrient loads are boundary conditions for the hydrodynamic water quality model of the Thi Vai River. Furthermore, the ecohydrological model of the Thi Vai Catchment can be used to evaluate scenarios, predicting the effects of future developments of climate, landuse or point sources on the water quantity and quality of the Thi Vai River [4].

2. Study area and approach

2.1 Study area

The study area Thi Vai catchment has a size of about 625 km² and is located in the provinces Dong Nai, Ba Ria-Vung Tau and Ho-Chi-Minh City in South Vietnam. The Thi Vai River has a length of 32 km and is an estuary under semi diurnal tidal regime. The main tributaries are the Bung Mon, Suoi Ca and Cau Vac River (Figure 1). The catchment is affected by tropical monsoon climate, with a characteristic rainy season from May to November and dry season from December to April. The mean annual rainfall is 1800 mm, whereof 80% fall in rainy season.

Beside the high density of industrial parks along the Thi Vai River (10 % of the catchment area), the catchment is characterized by intense agriculture, mainly rubber plantations (42 % of the catchment area). Other important crops and landuses in the catchment are rice (5 %), annual plants (6.7 %), mangrove forest (7 %) and country housing areas (10 %).

The soils in the catchment are dominated by acidic soil types like Acrisols (arenic Acrisol 23.4 %, ferric Acrisol 9.4 %, gleyic Acrisol 8.3 % and plintic

acrisol 8.1 %), other important soil types are rhodic ferrasols (14.7 %) and thionic fluvisols (10.9 %).

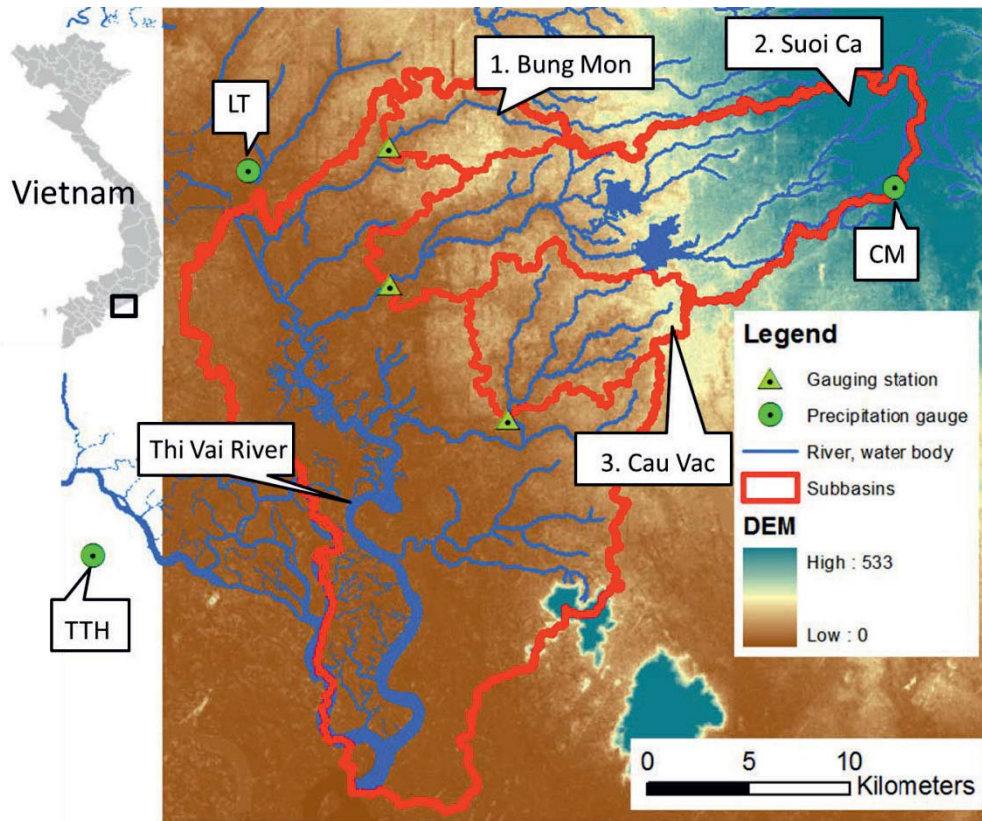


Figure 1. The Thi Vai River catchment, including the investigated subcatchments: 1. Bung Mon, 2. Suoi Ca and 3. Cau Vac and available precipitation gauges Long Thanh (LT), Cam My (CM) and Tam Thon Hiep (TTH).

2.2 Collection of data

Only sparse historical discharge and water quality data of the investigated subcatchments were available. These historical data was collected at single events only during the dry season, discharge and water quality data was not available during the rainy season. To achieve all necessary data, a monitoring of water quantity and quality was established at the main tributaries of the Thi Vai River and at the Thi Vai River. The monitoring of the Thi Vai River is described in detail in the accompanying paper “Integrated water quality monitoring of the Thi Vai river: an assessment of historical and current situation”. The positions of the gauging stations at the main tributaries were chosen on the basis of two main criteria: 1) the gauging station has to be unaffected by tidal influence, to allow the development of an unambiguous stage discharge relationship and 2) the



station needs to be accessible relatively easily, since most areas of the catchment do not have a well-developed infrastructure (Figure 1).

The Monitoring was initialized in March 2013 and is still in progress. At each station the water level is logged automatically every 15 minutes to detect flash floods that can occur during the rainy season, caused by convective rainfall events with high intensities and short duration and a characteristically short time of runoff concentration of the catchments. During 2013 20 to 30 discharge measurements were done at each station, to develop a stage discharge relationship for every station.

Water samples, for the analysis of river water quality, were taken once a week. For each sample the parameters NH_4 , NO_2 , NO_3 , total nitrogen, PO_4 , total phosphorus and iron (2+ and 3+) were quantified spectrometrically (NOVA 60, Merck). The total suspended solids (TSS) were analysed gravimetrically. Water physical parameters like temperature, pH, conductivity, turbidity and dissolved oxygen were collected by a multiparameter sonde (V2 6600, YSI).

Additionally field investigations of soil and landuse were performed, to improve available maps of soil and landuse.

2.3 Model set up and calibration

The software Panta Rhei was applied to simulate the hydrology of the Thi Vai Catchment. Pantha Rhei is a deterministic, semi-distributed hydrological model for single event or long-term simulations which has been developed at the University of Braunschweig [6]. Within the model the catchment is divided into sub catchments, which consist of hydrologic similar units (HSU). The HSU are created by overlapping topography, landuse and soil maps. Artificial structures like reservoirs, retention structures, culverts and junctions can be included into the watershed model. Panta Rhei has a flexible modular structure. Depending on the availability of data and modeling purpose, different modules of varying complexity could be selected for the simulation of hydrological processes (e.g. interception, evapotranspiration, etc.). A GIS interface enables the direct import of sub-catchment areas, pre and post processing and calibration options. The simulation time step can range from minutes, to hours, to one day, specified by the user. Currently Panta Rhei is applied for hydrologic design, flood forecasting and climate impact studies.

In the framework of the joint research project EWATEC-COAST Panta Rhei is extended to an ecohydrological model, being capable to simulate water and mass balance. The extended model includes modules for: terrestrial biogeochemical cycles (carbon, nitrogen and phosphorus), crop growth, crop manager, erosion and instream water quality. At the point of submission of the paper the testing of the developed ecohydrological modules were still in progress. Hence, this paper will focus on the hydrological part of the work.

Only three precipitation gauges with daily data for the year 2013 were available, surrounding the Thi Vai catchment (Figure 1). For the calibration of flow, discharge data derived from water level data for the period of March 2013 to December 2013 was available in a high temporal resolution of 15 minutes for the gauging stations Bung Mon, Suoi Ca and Cau Vac (Figure 1). Unfortunately the water level logger at Suoi Ca station was stolen, resulting in missing data from July to August 2013.

Despite the low density of precipitation gauges with daily data, a modeling time step of one hour was chosen. This was done for two reasons: 1) Because of the mainly convective rainfall events with high intensities and short duration and characteristically short time of runoff concentration of the investigated subcatchments [7] and 2) Because of the demand of the coupled hydrodynamic water quality model for boundary conditions with a minimum time step of one hour. The satellite derived rainfall products CMORPH and TRMM [8, 9] were used to disaggregate the daily precipitation data to hourly data, using the temporal distribution of the satellite derived rainfall measurements [10].

3. Results and discussion

3.1 Water quality assessment

The water quality of the investigated subcatchments was evaluated based on the water quality monitoring data from March 2013 to December 2013. Monitoring results for selected water quality parameters are summarized in Figure 2. All water quality parameters are compared against the Vietnamese water quality standard QCVN 08: 2008/BTNMT A2 [11]. Apart from some single measurements, all the measured phosphate and nitrate

concentrations are below the threshold concentration of 0.2 mg PO₄-P/l and 5 mg NO₃-N/l at all three stations (Figure 2 b, e).

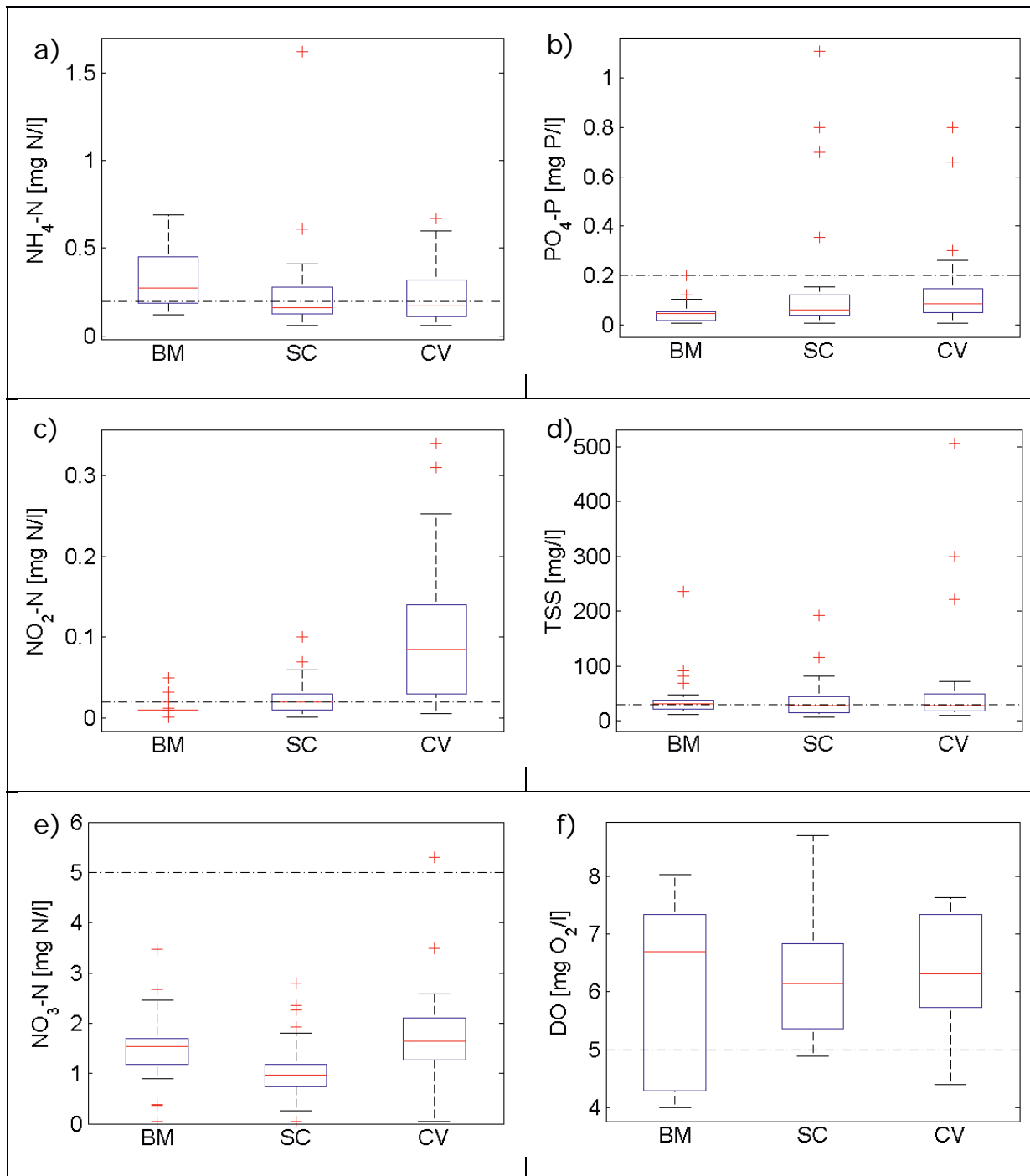


Figure 2. Results of the water quality monitoring at the stations Bung Mon (BM), Suoi Ca (SC) and Cau Vac (CV), from March 2013 to December 2013, for the parameters a) ammonia (NH₄-N), b) phosphate (PO₄-P), c) nitrite (NO₂-N), d) total suspended solids (TSS), e) nitrate (NO₃-N) and f) dissolved oxygen (DO). The dashed line shows the threshold concentration following the Vietnamese standard QCVN 08: 2008/BTNMT A2 (in mg/l: NH₄-N = 0.2, PO₄-P = 0.2, NO₂-N = 0.02, TSS = 30, NO₃-N = 5, DO = 5).

In the case of ammonia the threshold concentration of 0.2 mg NH₄-N/l is exceeded at Bung Mon for 74 %, at Suoi Ca for 37 % and at Cau Vac for 53 % of the measurements (Figure 2 a).

Also nitrite shows elevated concentrations in comparison to the threshold concentration of 0.02 mg NO₂-N/l (Figure 2 c). At Bung Mon are 5 %, at Suoi Ca are 32 % and at Cau Vac are 76 % of the NO₂-N measurements higher than the threshold concentration. Plotting the concentrations of NH₄, NO₂, NO₃ and PO₄ vs. the discharge for each station (data not shown) indicates that diffuse sources are the dominant source for nutrient input into the investigated rivers [12]. Elevated concentrations of NH₄ and NO₂ and comparable low concentrations of NO₃ are indicating an inhibition of the nitrification process. Nitrification is very sensitive in respect to pH. An optimal nitrification rate is reached at a pH of 7 to 8.5 and is declining to nearly zero at a pH below 5 [13], however small nitrification rates are documented for acidic soils with pH ranging from 3 to 4.5 [14]. The mean pH of river water is 6.6, 7.3 and 7.2 at Bung Mon, Suoi Ca and Cau Vac station, respectively. The river water pH shows no indication for inhibition of nitrification in the river water. But the soil investigation in the sub-catchments shows that the pH of the top soils is ranging between 3.5 and 4.5, indicating a strong inhibition of nitrification in the soils of the investigated catchments. There is no information about pH in the lower soil available.

The comparison of TSS measurements with the threshold concentration of 30 mg/l shows that 58 % of the TSS measurements at Bung Mon, 48 % of the TSS measurement at Suoi Ca and 50 % of the TSS measurements at Cau Vac are higher than the threshold concentration (Figure 2 d). Also the elevated concentrations of TSS are mainly related to diffuse sources, due to erosion events caused by intensive precipitation during the rainy season. During the field investigations, signs for high erosion rates were documented at several places over the investigated catchment. Particularly rubber plantations are showing signs of elevated erosion, because of lacking ground cover under the trees.

Only 8 % of the DO measurements at Suoi Ca and 11 % at Cau Vac are lower than the threshold concentration of 5 mg O₂/l, however at station Bung Mon are 35 % of the DO measurements lower than the threshold concentration (Figure 2 f).

3.2 Hydrological modeling

The results of the hydrological modeling are shown in Figure 3. The goodness of fit was evaluated using the coefficient of determination R^2 and the Nash-Sutcliffe efficiency E [14]. On an hourly time step R^2 and E are: 0.48 and 0.36 for Bung Mon, 0.5 and 0.46 for Suoi Ca and 0.48 and 0.35 for Cau Vac station. Aggregated to a daily time step R^2 and E are: 0.69 and 0.66 for Bung Mon, 0.58 and 0.54 for Suoi Ca and 0.7 and 0.67 for Cau Vac station. Taking in account the simulation time step of one hour, the simulation results show a moderate agreement with the measured discharges. Single rainfall events are captured very well by the model, in response to the hourly disaggregation of the daily precipitation measurements, using the temporal distribution derived from the satellite data. In contrast, some measured discharge peaks are missed completely, because of non-detected precipitation events, resulting in a lowering of the goodness of fit. The lacking precision of the simulation can be attributed to the low density of precipitation gauges. In total only three precipitation gauges are available for the investigated subcatchments (Figure 1). The distance between the precipitation gauges is ranging from 20 to 40 km. The correlation of the measured rainfall of the three precipitation gauges shows a low correlation between the gauges (Table 1). This reflects the highly convective rainfall patterns, which are characteristic for tropical catchments. In consequence, small scale storm events, affecting the investigated subcatchments, are often not recorded by the available precipitation gauges, resulting in an underestimation of single discharge events. Furthermore, single local storm events with high intensities in the area of the precipitation gauges can result in a massive overestimation of single discharge peaks, if these events are interpolated to obtain areal precipitation.

Table 1. Correlation between precipitation gauges Long Thanh (LT), Tam Thon Hiep (TTH), Cam My (CM)

	<i>LT</i>	<i>TTH</i>	<i>CM</i>
<i>LT</i>	1		
<i>TTH</i>	0.55	1	
<i>CM</i>	0.43	0.45	1

The comparison of the simulated and measured cumulative discharge of the stations Bung Mon (Figure 3 a) and Cau Vac (Figure 3 c) show that the cumulative discharge is matched very well during the simulation period.

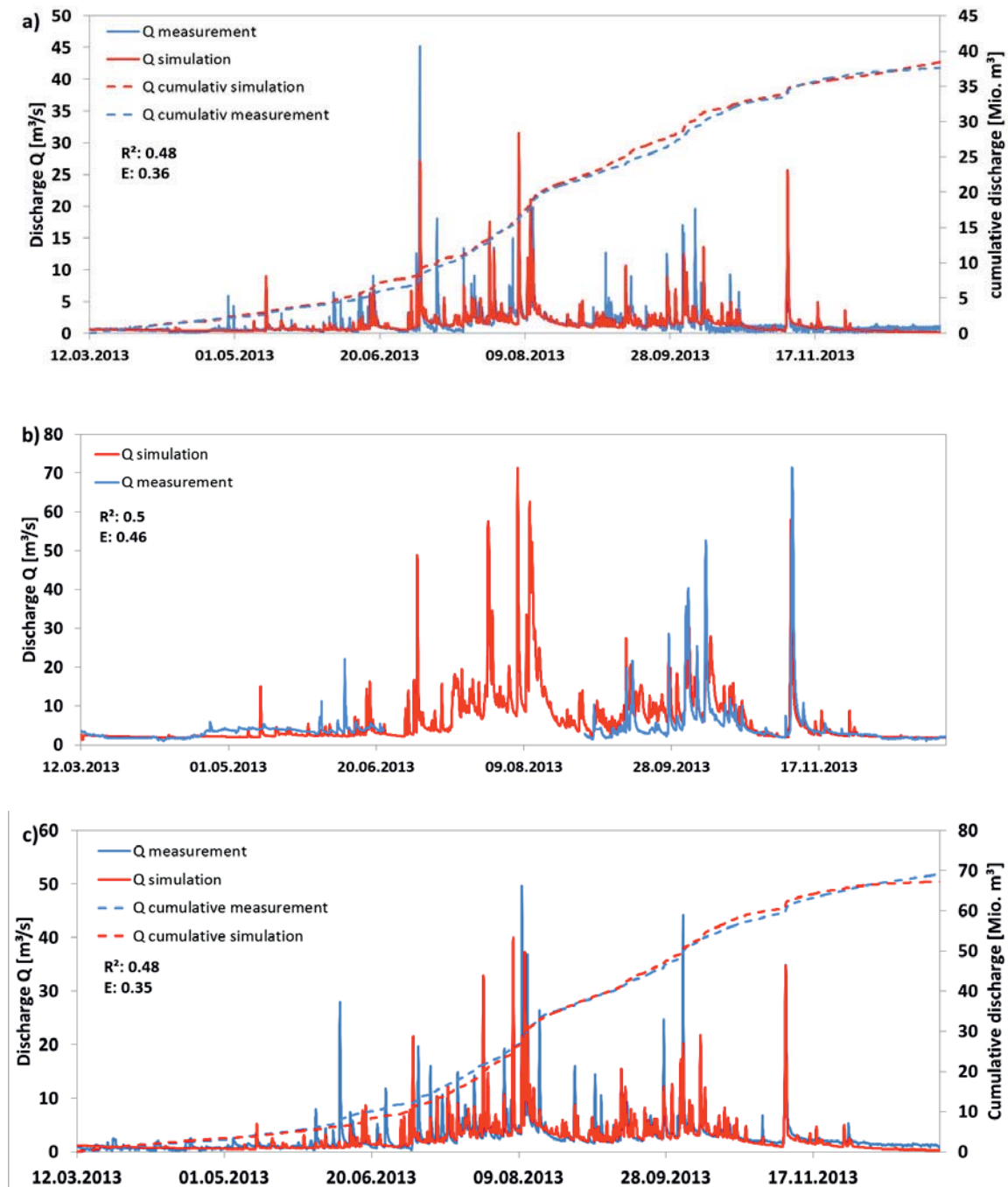


Figure 3. Comparison of simulated and measured hydrographs of the stations a) Bung Mon, b) Suoi Ca, c) Cau Vac.

However, the comparison of the simulated and measured cumulative discharge of the stations Bung Mon and Cau Vac shows also a slight underestimation of discharge during the dry season and an overestimation of discharge in the rainy season. The comparison of the duration curves of the station Bung Mon (Figure 4 a) and Cau Vac (Figure 4 b) shows a good agreement of the exceedance time of the simulated and the measured discharge, although the peak runoff is underestimated at both stations, because of insufficient rainfall data. This indicates in total, that the seasonal patterns and hydrological characteristics of the investigated catchments can be accurately simulated.

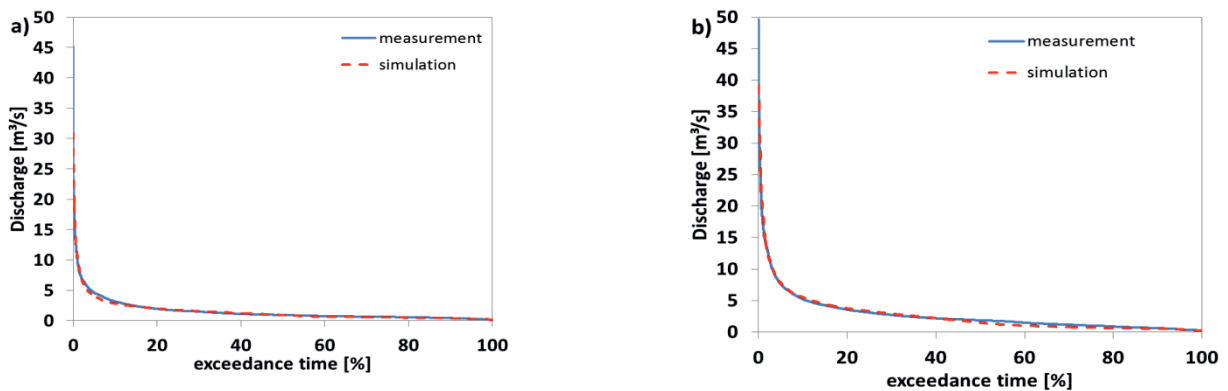


Figure 4. Comparison of simulated and measured duration curves of the stations a) Bung Mon and b) Cau Vac.

4. Outlook and conclusions

The Panta Rhei model was applied successfully to simulate the discharge of the investigated catchments of the main tributaries of the Thi Vai River. The seasonal discharge patterns and the hydrological characteristics of the investigated catchments are simulated accurately by the hydrological model. Also single discharge events are simulated well at an hourly time step, in response to the temporal disaggregation of daily precipitation data due to the temporal distribution of satellite derived rainfall data. Because of the low density of precipitation gauges, single discharge events are over or underestimated, resulting in a lower goodness of fit at a higher temporal resolution. Nevertheless, the general hydrological behaviour of the investigated subcatchments is simulated in a reliable way and the



hydrological model will supply realistic boundary conditions for the hydrodynamic water quality model.

At the point of submission of the paper the testing of the developed ecohydrological modules for terrestrial biogeochemical cycles (carbon, nitrogen and phosphorous), crop growth and management, erosion and in-stream water quality were still in progress and will be presented in future studies.

References

- [1] Nguyen, H.P., Pham, H.T. (2011): The dark side of development in Vietnam: Lessons from the Killing of the Thi vai River. *Journal of Macromarketing* 32(1), 74-86.
- [2] Institute of Environment and Natural Resources (IER) (2006): Báo cáo kết quả thực hiện Nhiệm vụ KIỂM SOÁT Ô NHIỄM MÔI TRƯỜNG LƯU VỰC SÔNG THỊ VẢI ("Report about the controlling of the environment pollution in the Thi Vai Catchment"). Vietnam National University of Ho-Chi-Minh City.
- [3] Le TTH, Lorenz M, Prilop P, Lam Q D and Meon G.(2012): An Ecohydraulic Model System for Water Management of the Saigon River System under Tide Effect. Proceedings of the "9th International Symposium on Ecohydraulics". September 17th - 21st 2012. Vienna Austria.
- [4] Meon G, Le TTH, Fettig J, Nguyen P (2013): Water pollution management in the vicinity of the Lower Mekong Basin: German-Vietnamese research projects "TAPIOCA" and "EWATEC-Coast". Proceedings of the Environmental Mekong Symposium, Ho-Chi-Minh City, 5-7 March 2013.
- [5] Debele B, Srinivasan R and Parlange J-Y (2008): Coupling upland watershed and downstream water body hydrodynamic and water quality models (SWAT and CE-QUAL-W2) for better water resources management in complex river basins. *Environ Model Assess*, Vol. 13, No. 1, pp 135-153.
- [6] Förster K, Gelleszun M and Meon G (2012): A weather dependent approach to estimate the annual course of vegetation parameters for water balance simulations on the meso- and macroscale. *Adv. Geosci.*, 32, 15-21.
- [7] Quan N H, Meon G (2013): Nutrient Dynamics during Flood Events in Tropical Catchments: A Case Study in Southern Vietnam. *Clean – Soil, Air, Water* 2014, 42 (9999), 1–10.



- [8] Cohen Liechti T, Matos J P, Boillat J-L and Schleiss A J (2012): Comparison and evaluation of satellite derived precipitation products for hydrological modeling of the Zambezi River Basin. *Hydrol. Earth Syst. Sci.*, 16, 489–500
- [9] Kidd C and Levizzani V (2011): Status of satellite precipitation retrievals. *Hydrol. Earth Syst. Sci.*, 15, 1109–1116.
- [10] Gebremichael M and Hossain F (2010): *Satellite Rainfall Applications for Surface Hydrology*. Springer Dordrecht Heidelberg London New York.
- [11] QCVN 09:2008/BTNMT (2008): National Regulation on Surface Water Quality. Vietnamese Government
- [12] Bowes M J, T. Smith J T, Jarviea H P and Neal C (2008): Modelling of phosphorus inputs to rivers from diffuse and point sources. *Science of the total environment*. 395 (2008) 125–138.
- [13] Grunditz C and Dalhammar G (2001): Development of Nitrification Inhibition Assays using Pure Cultures of Nitrosomonas and Nitrobacter. *Wat. Res.* Vol. 35, No. 2, pp. 433±440.
- [14] De Boer W, Kowalchuk G A (2001): Nitrification in acid soils: microorganisms and mechanisms. *Soil Biology & Biochemistry* 33 (2001) 853-866
- [15] Krause p, Boyle D P and Båse F (2005): Comparison of different efficiency criteria for hydrological model assessment. *Advances in Geosciences*, 5, 89–97.



Integrated water quality monitoring of the Thi Vai River: An assessment of historical and current situation

Karen Prilop¹, Nguyen Hong Quan^{2*}, Malte Lorenz¹, Huyen Le¹, Le Thi Hien² and Günter Meon¹

¹ Leichtweiß-Institute for Hydraulic Engineering and Water Resources, Department of Hydrology, Water Management and Water Pollution Control, University of Braunschweig, Beethovenstr. 51a, D-38106 Braunschweig, Germany, email: malte.lorenz@tu-bs.de,

² Institute for Environment and Resources (IER) - Vietnam National University of Ho-Chi-Minh City, 142 To Hien Thanh, District 10, Ho-Chi-Minh City, Viet Nam, email: hongquanmt@yahoo.com (*corresponding author), hienev01@yahoo.com

Abstract

In Vietnam the Thi Vai River was considered as one of the spots with the heaviest water pollution, which was induced by industrial wastewater discharges, especially by untreated wastewater of the Vedan company during the years 1994 to 2008. However, thanks to the consideration on water quality management from local to national authorities, especially the controlling and reducing of wastewater discharges to the river, the surface water quality of Thi Vai River, situated in South Vietnam, has been improved in the recent years.

The assessment of the water quality status from the past to present of the Thi Vai River is very essential for water quality management. Within the joint research project "Environmental and Water Protection Technologies of Coastal Zones in Vietnam EWATEC-COAST" funded by the German Ministry of Research and Education (BMBF) and the Vietnam National University of Ho-Chi-Minh City a model-based water management system for the Thi Vai River is developed. The availability and further the evaluation of water quality and quantity data is one necessary basis for this objective.

Firstly, historical data from different sources, especially from some recent projects carried out by the Institute for Environment and Resources (IER) - Vietnam National University of Ho-Chi-Minh City, has been collected and evaluated. Apart other signs of pollutions, very low concentrations of dissolved oxygen and very high concentrations of ammonia were detected in



the past. An extreme pollution was recorded in the upper reaches, whereas a lower pollution level existed in the lower reaches.

Next, within the BMBF research project EWATEC-COAST, subproject 3 "Surface Water", the scientists from the Leichtweiss-Institute, TU Braunschweig (Germany) have implemented a monitoring system for water quantity and quality at the Thi Vai River and its main tributaries. The monitoring data provide detailed data for the complex Thi Vai River, which is strongly affected by tide. Previous results indicate that the water quality has improved in comparison to the past until 2008. Nevertheless still signs of pollution exist. High nitrite concentrations, elevated ammonia concentrations as well as partly low oxygen concentrations still occur.

Key Words: water quality, river monitoring, tide



1. Introduction

Untreated and poorly treated wastewater from ports and industrial zones was discharged to the Thi Vai River in the past. A section of about 9 km (from the tributary Suoi Ca River to the My Xuan industrial zone) were seriously polluted. This section was regarded as ecologically dead: Fish, shrimps and other aquatic species hardly existed and only plankton and algae species adapted to high nutrient contents occurred [1, 2, 3]. After determining the illegal discharge of waste water by the company Vedan as one of the main factors for the impairment of the water quality of the Thi Vai in 2008, the water quality has been improved by investments in waste water treatment systems and better controls.

Assessment of water quality status from the past to present of the Thi Vai River is very essential for the water quality management. A main objective of the joint research project "Environmental and Water Protection Technologies of Coastal Zones in Vietnam EWATEC-COAST" funded by the German Ministry of Research and Education (BMBWF) and the Vietnam National University of Ho-Chi-Minh City, is the development of a model-based water management system. The hydrodynamic and water quality model of the Thi Vai River is the issue of the accompanying paper "A 3D-hydrodynamic and water quality model of the Thi Vai River under strongly tidal effect". Measured data of water quantity and water quality are the prerequisite for the water management system. Within the project a monitoring system along the Thi Vai River and at the main tributaries was implemented in 2013 and still continues. Previous results for the Thi Vai main river will be presented and compared with the historical situation. Monitoring results for the main tributaries are presented in the accompanying paper "Ecohydrological modeling of the Thi Vai Catchment in South Vietnam".

2. Study area

The Thi Vai River is situated in South Vietnam and its main river flows from the Ba Ky weir about 37 km before entering the East Sea. The whole main river is strongly affected by tide with a tidal range of approx. 3 m. Therefore the water is brackish and the measured salinities reach in the lower reaches up to 30 ppt. In the upper reaches the salinity is more var-



ible and depends on the tide and the amount of fresh water inflow. Main tributaries of the Thi Vai River are the Bung Mon, Suoi Ca and Cau Vac River. In the South the Go Gia River and Thi Vai River meet.

The Thi Vai catchment, located in the provinces Dong Nai, Ba Ria-Vung Tau and Ho-Chi-Minh City, covers approx. an area of 625 km². The mean temperature is about 28°C and the average yearly rain fall is approx. 1800 mm. The area is affected by the tropical monsoon climate with a rainy season from May to November and a dry season from December to April.

Mangrove forest lines at the west bank. Also the Can Gio mangrove forest, a UNESCO biosphere reserve, is adjacent to the Thi Vai River basin in the West. In contrast the east bank is dominated by ports and industrial areas. There are 14 industrial zones situated in the catchment. The location of nine of them is shown in Figure 1. Further industrial zones (Nhon Trach II, III, V and VI and Vinatex Tan T o) are located in the west of the upper river reach. Its waste waters also enter into the Thi Vai River. There were only few industries before 1993. In 1993 the company Vedan became officially operative. Then, more and more companies and industrial zones were established at the Thi Vai catchment since 1996.

Recording to an investigation form a cooperation of MONRE and the People Committes of Ba Ria-Vung Tau and Dong Nai in 2006, most production sites and industrial zones had not installed or had incorrectly installed approved wastewater treatment procedures: All in all 49 out of 77 production sites had a wastewater treatment system, but only 12 had a system, that meet the national standard. In case of the industrial zones 8 of 12 had not implemented a wastewater treatment system that meets a sufficient degree of purification [2].

In September 2008, the illegal discharging of untreated waste water directly into the river by the company Vedan was detected. The waste water was transported through an 800-meter long underground system. The investigators concluded that Vedan Vietnam discharged untreated wastewater for 14 years (1994-2008) at a rate of 105,600 cubic meters per month [4]. Therefore Vedan was mainly responsible for the pollution of the Thi Vai River.

In contrast to the situation in the past, there is now a consideration of water quality management from local to national authorities at the Thi Vai River. Better controlling and investments in waste water treatment reduce the industrial pollutant load into the river. The waste waters of many companies are transported to central waste water treatment plants of the industrial zones.

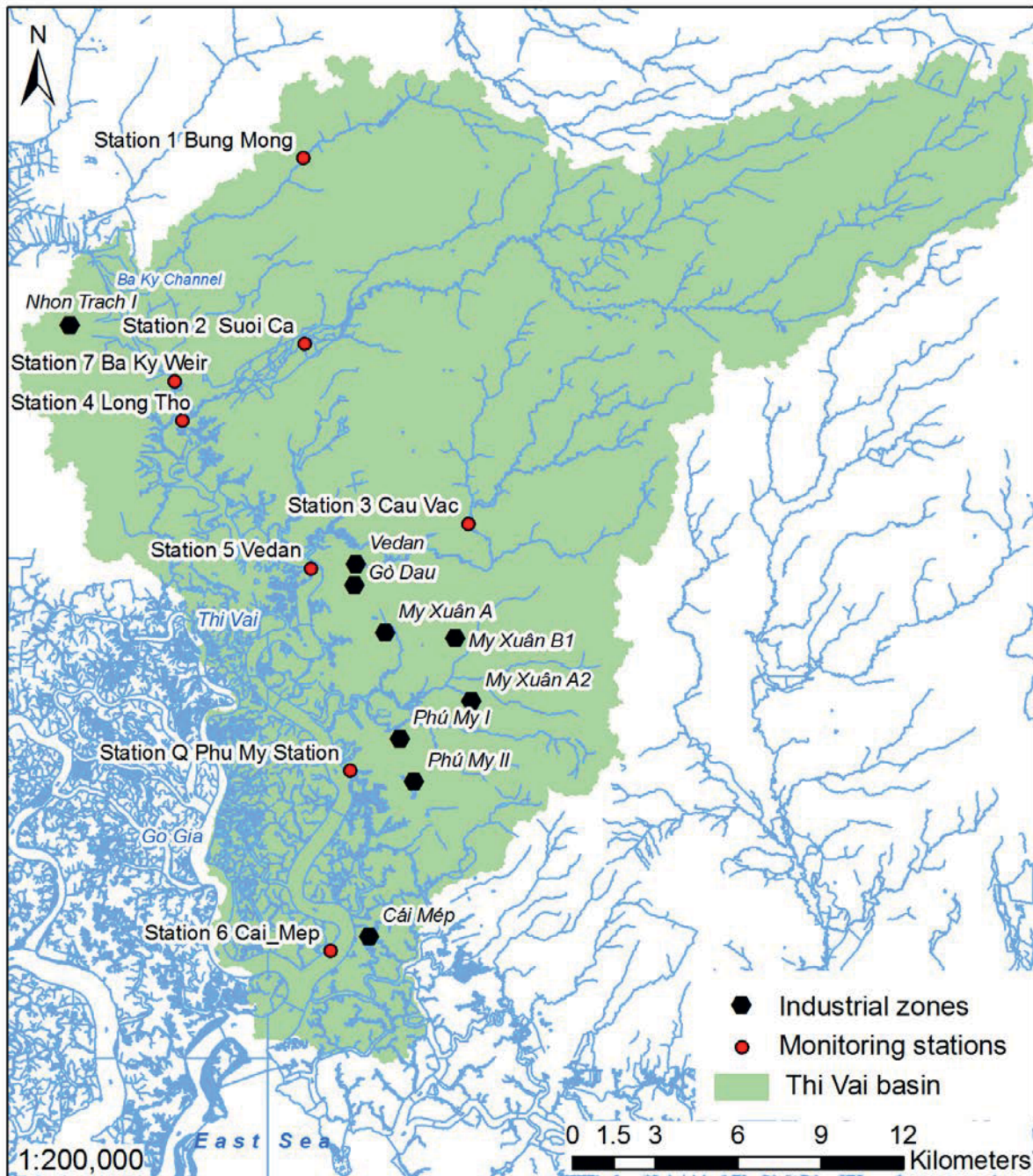


Figure 1: Monitoring stations and industrial zones in the Thi Vai River catchment.



Besides the industrial waste waters, other sources of pollution are municipal waste waters and aquacultures, especially of shrimp farms. Furthermore, the Thi Vai River is polluted by diffuse substance loads of agriculture, oil as well as waste of ships.

3. Monitoring system

The monitoring at the Thi Vai River was implemented in March 2013 by the Leichtweiss-Institute (TU Braunschweig, Germany). At three monitoring stations along the river, namely Long Tho, Vedan and Cai Mep the water level as well as the water temperature is recorded continually since middle of March. Furthermore the conductivity is recorded at Cai Mep since the middle of March and at Long Tho and Vedan since the middle of September. At Phu My discharge measurements of the Thi Vai River have been performed.

Water samples and measurements with a multiparameter water quality sonde are conducted at the stations Long Tho, Vedan and Phu My weekly, at Vedan and Phu My in two depths (surface and mostly 5 m depth). Additionally to the regular weekly measurements, intensive tide samplings (5 samples within 12 hours) have been performed. The water quality monitoring will be continued till summer 2014. Parameters like dissolved oxygen (DO), salinity, pH and turbidity are measured with the sonde. The water samples are tested in the laboratory for the following parameters: acidity, alkalinity, ammonia, nitrate, nitrite, phosphate, total phosphorus, silicate, iron and total suspended solids (TSS). Apart from acidity, alkalinity and total suspended solids the most parameters are analysed by a photometer.

4. Water quality in the past

Water quality data of the past were provided by the Institute for Environment and Resources (IER) - Vietnam National University of Ho-Chi-Minh City. The past data are often limited in term of temporal and spatial scale.

Selected results of a water quality investigation by the IER in May 2006 are listed in Table 1 [1]. The river was divided into three zones, according to the level of pollution. The section from the area of the inflow of Suoi Ca



River to the industrial zone My Xuan was indicated as extremely polluted: Dissolved oxygen concentrations were extremely reduced with values often below 1 mg L^{-1} . The concentrations of the biological oxygen demand (BOD_5) and the chemical oxygen demand (COD) were very high. Furthermore the ammonia concentration was extremely elevated. Also high concentrations of lead (Pb) and mercury (Hg) were detected at some measuring points. The sediments show high concentrations of many pollutants like chrome (Cr) and Nickel (Ni). The diversity of phytoplankton and zooplankton in the zone 1 was lower than at the other river section.

Low concentrations of dissolved oxygen as well as very high concentrations of ammonia occurred also in the strong polluted zone 2 from My Xuan to the port of Phu My. The concentrations of BOD_5 and COD were also elevated, but lower than in zone 1.

In contrast to the zones 1 and 2, the concentrations of dissolved oxygen are significant higher in zone 3, apart from the Phu My port. Moreover the ammonia (NH_4) concentration was smaller in this zone, although still too high. The values of BOD_5 were considerably reduced in this area in comparison to the upper reaches, but COD occurred still on a high level.

Table 1. Minimum and maximum values of water quality parameters from an investigation at the Thi Vai River in May 2006 [1] (LOD = Limit of detection)

Parameter in [mg/L]	Zone 1 (extremely polluted)		Zone 2 (strong polluted)		Zone 3 (clean to moderate polluted)	
	Long Tho-My Xuan		My Xuan-Phu My		Phu My-Cai Mep	
	Min	Max	Min	Max	Min	Max
DO	0.02	1.13	0.10	1.53	0.86	5.01
BOD_5	8	19	2	13	1	4
COD [mg/L]	72	120	19	88	9	40
$\text{NH}_4\text{-N}$	2.69	9.78	0.78	9.78	0.13	2.13
Pb	0.023	0.11	0.02	0.062	0.022	0.053
Hg	< LOD	0.047	< LOD	0.012	< LOD	0.009

Figure 2 implicates the big differences of the dissolved oxygen concentrations depending on the river section in the years 2006 to 2009: The concentrations are constantly low near the company Vedan, whereas the concentrations are more variable and on a higher level towards the sea (Cang Phu My, Cang Cai Mep). Near Vedan the parameter dissolved oxygen is below the VN standard B2 of the national technical regulation on surface water quality from 2008 (QCVN 08: 2008/BTNMT) nearly throughout the whole investigation period. The standard B2 of QCVN 08: 2008/BTNMT is valid for shipping and other purposes, which need only a low water quality.

Furthermore the concentrations of $\text{NH}_4\text{-N}$ is much higher at Vedan than at the sections near Phu My and Cai Mep in the same period, as Figure 3 shows. It is noticeable, that the level of $\text{NH}_4\text{-N}$ decreases during 2006 to 2009. After 2008, when the illegal discharge of water water by the company Vedan was detected, the amount of $\text{NH}_4\text{-N}$ decreased distinctly and satisfies temporarily the standard value B2.

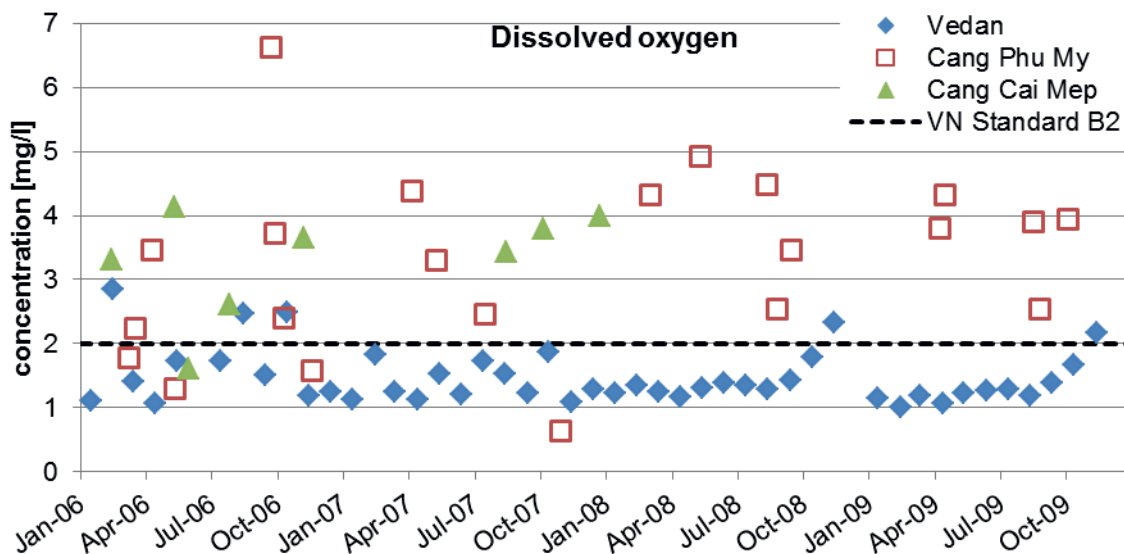


Figure 2: Measured concentrations of dissolved oxygen at different river sections from 2006 to 2009. The standard B2 of QCVN 08: 2008/BTNMT for dissolved oxygen is marked.

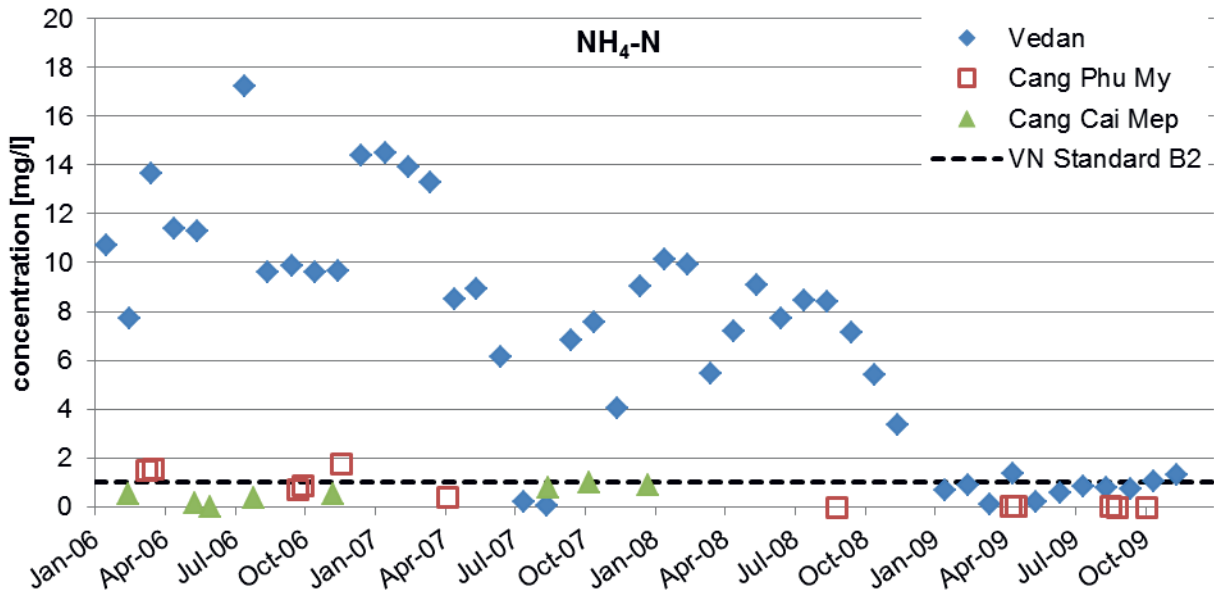


Figure 3: Measured concentrations of NH₄-N at different river sections from 2006 to 2009. The standard B2 of QCVN 08: 2008/BTNMT for NH₄-N is marked.

5. Results of the current monitoring system

The current recorded water temperatures of the Thi Vai are around 30°C and the pH ranges mostly between 6 and 8 and therefore close neutral.

The monitored water levels show, that the whole river up to Long Tho is strongly affected by semidiurnal tide. The tidal amplitude is about 2-4 meters. The water levels at the stations Cai Mep and Vedan during three days in May 2013 are shown as an example in Figure 4. Comparing the water levels at high tide and low tide a higher tidal range at Vedan can be noted. The water level at Long Tho is similar to the water level at Vedan.

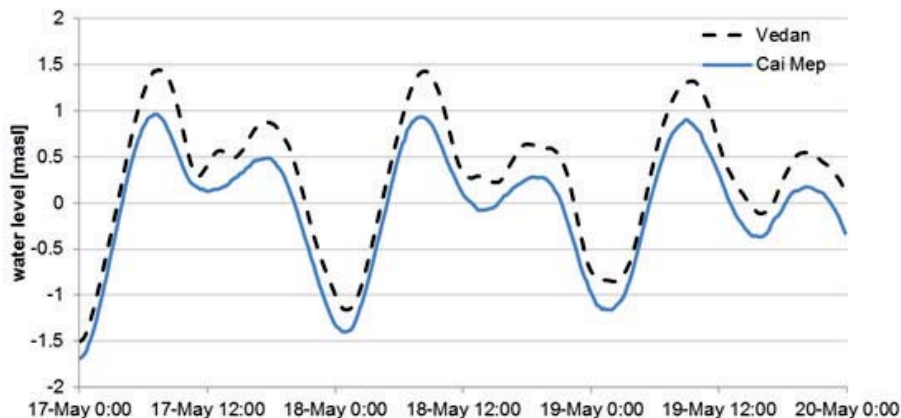


Figure 4: Recorded water levels at the stations Vedan and Cai Mep on the 17-19 May 2013.

Figure 5 shows the water level and the electrical conductivities at Long Tho in comparison. There is a clear relationship between the two parameters: high conductivities and consequently high salinities at high water levels and low conductivities, respectively salinities at low water levels. Besides the salinity at Long Tho is very variable, as a range of conductivities from 0 to 30 ms cm^{-1} (corresponding to approx. salinities of 0 to 14 ppt) indicates. However no obvious relationship between nutrient concentrations and the phase of the tide, respectively water level has been detected by the intensive tide sampling yet.

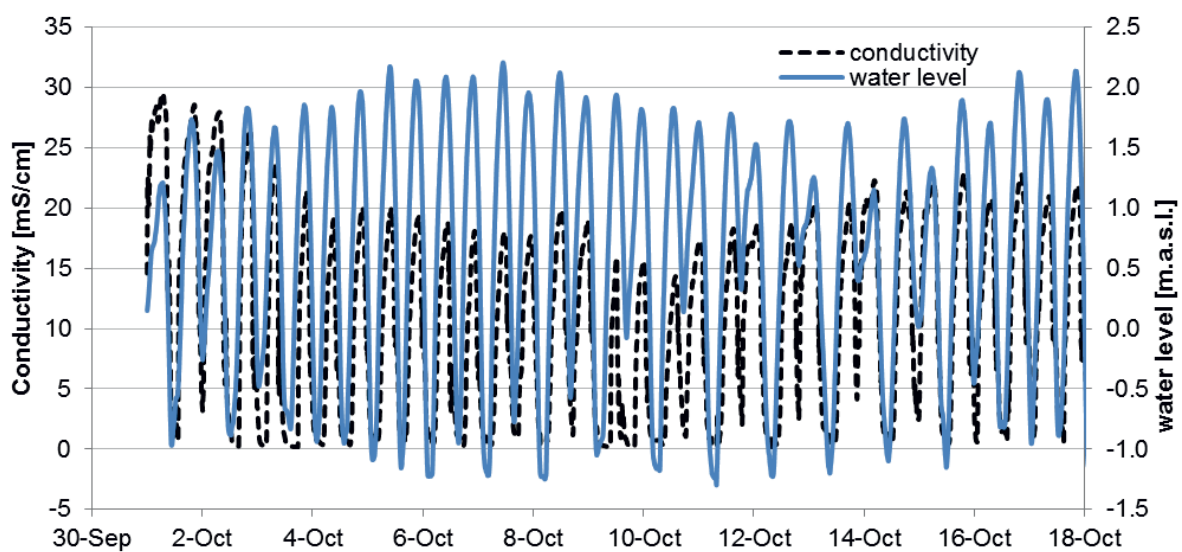


Figure 5: Recorded water levels and electrical conductivities at the station Long Tho in October 2013.

In Table 2 the mean and extreme values of nutrients and dissolved oxygen are compared with summarized results of several previous investigations, which data was provided by the IER. The compared data in past and present were measured in a similar river section. Furthermore the values, which do not meet the standard B2 of the national technical regulation on surface water quality from 2008 (QCVN 08: 2008/BTNMT [5]), are marked in grey. In addition values, which meet this low standard, but do not meet the higher standard of the “national technical regulation in surface water quality for protection of aquatic lifes” (QCVN 38:2011/BTNMT [6]), are marked in light grey.



The concentration of dissolved oxygen has significantly increased at all three stations since 2008. Regarding the whole river, most currently detected values meet both mentioned standards. But there are differences between the river sections and low dissolved oxygen concentrations have been measured occasionally, especially at Long Tho. So 38% of the recorded dissolved oxygen concentrations at Long Tho since March 2013 are below 4 mg L^{-1} , which is the limit value of QCVN 38:2011/BTNMT. In contrast the amount of measured data below 4 mg L^{-1} oxygen is about 14% at Vedan and smaller than 2% at Phu My. The mean recorded saturation of dissolved oxygen ranges between 64% at Long Tho and 86% at Phu My.

Furthermore the pollution with NH_4 has decreased extremely in comparison to the time until 2008, when there were concentrations, which correspond to a multiple of the both mentioned standards ($1 \text{ mg NH}_4\text{-N L}^{-1}$). This downward trend has been indicated before by the historical monitoring data from 2006 to 2009. Nevertheless for 11% of the samples at Long Tho, taken in course of the current monitoring system, $\text{NH}_4\text{-N}$ concentrations exceed 1 mg L^{-1} . The local differences of the parameters $\text{NH}_4\text{-N}$ and dissolved oxygen indicate that the water quality increase from upstream to downstream as in the past.

The values of nitrate are mostly low. In contrast the concentrations of nitrite, which naturally occurs in very low concentrations, are still on a high level. Figure 6 illustrate that the concentrations of nitrate-nitrogen ($\text{NO}_3\text{-N}$) and nitrite-nitrogen ($\text{NO}_2\text{-N}$) are often at the same level. This indicates that the nitrification do not pass off completely, although mostly relative high concentrations of dissolved oxygen concentrations have been measured.



Table 2. Mean and maximum, respectively minimum values of nutrients and dissolved oxygen (DO) in the past and present. Values marked dark grey fail the VN standard B2 of QCVN 08: 2008/BTNMT [5] and the VN standard of QCVN 38:2011/BTNMT [6]. Values marked light grey fail the standard of QCVN 38:2011/BTNMT, but satisfy the standard B2 of QCVN 08: 2008/BTNMT.

		Long Tho		Vedan		Phu My	
		2000-2008	03/13-04/14	2005-2008	03/13-04/14	2001-2008	03/13-04/14
DO [mg/L]	Mean	3.1	4.5	1.6	4.8	3.0	5.5
	Min	0	1.4	1.1	3.0	0.5	2.8
NH ₄ -N [mg/L]	Mean	3.7	0.5	7.8	0.1	2.3	0.1
	Max	7.8	3.0	17.4	0.7	9.7	0.5
NO ₂ -N [mg/L]	Mean	0.04	0.11	0.07	0.19	0.12	0.09
	Max	0.31	0.59	1.51	0.43	0.48	0.32
NO ₃ -N [mg/L]	Mean	0.5	0.5	3.0	0.2	0.5	0.2
	Max	4.1	9.0	28.3	0.7	3.0	0.7
PO ₄ -P [mg/L]	Mean	-	0.05	-	0.03	-	0.03
	Max	-	0.46	-	0.13	-	0.10
TP [mg/L]	Mean	0.2	0.2	0.3	0.1	0.5	0.1
	Max	2.3	3.1	1.8	1.3	3.5	3.2

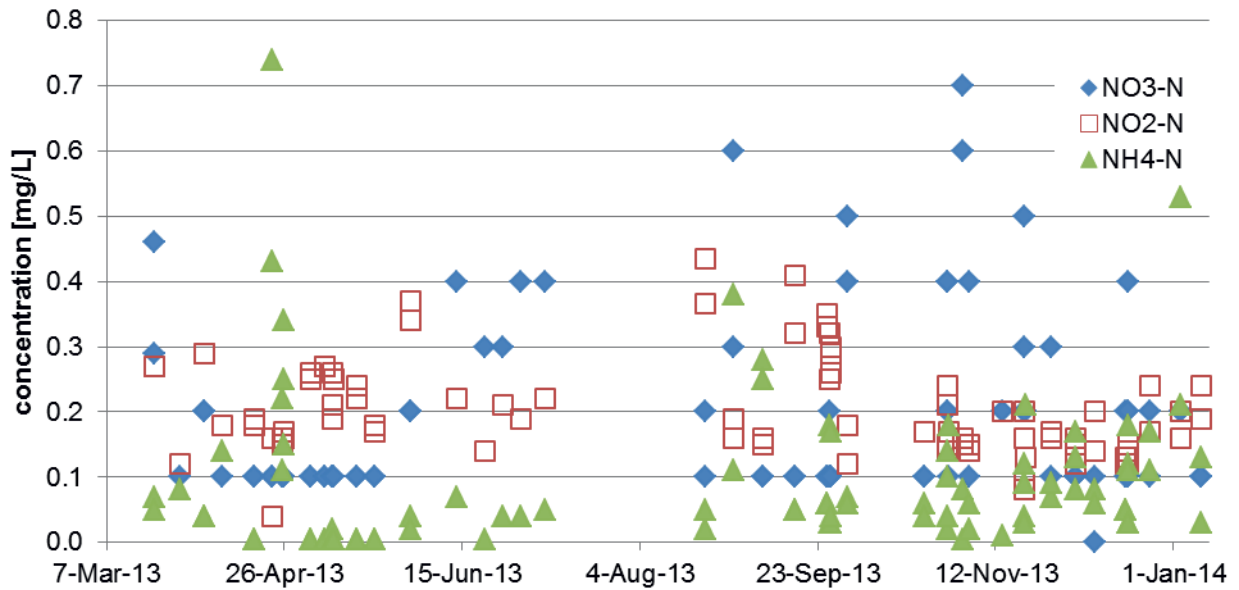


Figure 6: Measured concentrations of $\text{NO}_3\text{-N}$, $\text{NO}_2\text{-N}$ and $\text{NH}_4\text{-N}$ at the station Vedan. Regarding total phosphorus (TP) the concentrations are still on the same level. The concentrations of orthophosphate-phosphorus ($\text{PO}_4\text{-P}$) satisfy the standard B2 of QCVN 08: 2008/BTNMT with maximum 0.5 mg P L^{-1} , whereas there is no standard defined for $\text{PO}_4\text{-P}$ in QCVN 38:2011/BTNMT.

6. Conclusion and outlook

The mentioned results indicate that the pollution of the Thi Vai River with organic matter and nutrients has decreased in the last years. Higher concentrations of dissolved oxygen and lower concentrations of ammonia, in comparison to the past until 2008, are detected. Before, untreated or poorly treated waste water, especially of the company Vedan was the main reason for a locally extreme pollution. The improvement of water quality is attributed to better controls and the installation of wastewater treatment plants at the industrial zones.

Nevertheless still signs of pollution, like high nitrite concentrations, elevated ammonia concentrations and partly low oxygen concentrations, exist. The reasons for the incomplete process of nitrification have to be investigated. The data of the current monitoring system will be further evaluated. A continuous monitoring of the water quality is also important for the Thi Vai River in the future, so that deficits can be detected.



References

- [1] Institute of Environment and Natural Resources (IER) (2006): Báo cáo kết quả thực hiện Nhiệm vụ KIỂM SOÁT Ô NHIỄM MÔI TRƯỜNG LƯU VỰC SÔNG THỊ VẢI (“Report about the controlling of the environment pollution in the Thi Vai Catchment”). Vietnam National University of Ho-Chi-Minh City.
- [2] World Bank, MoNRE and DANIDA (2006): Vietnam Environment Monitor 2006 - Water quality in Viet Nam with a focus on the Cau, Nhue Day and Dong Nai River Basins.
- [3] MoNRE (2006): Environment Report of Vietnam 2006 – the current state of water environment in 3 river basis of Ca, Nhue-Day and Dong Nai River systems. Hanoi.
- [4] Nguyen, H.P., Pham, H.T. (2011): The dark side of development in Vietnam: Lessons from the Killing of the Thi vai River. Journal of Macromarketing 32(1), 74-86.
- [5] Vietnamese Government (2008): QCVN 08: 2008/BTNMT, “National technical regulation on surface water quality”.
- [6] Vietnamese Government (2011): QCVN 38:2011/BTNMT, “National technical regulation in surface water quality for protection of aquatic lifes”.



A 3D-hydrodynamic and water quality model of the Thi Vai river under strongly tidal effect

Karen Prilop¹, Malte Lorenz¹, Huyen Le¹, Ngo Quang Hieu², Günter Meon¹
and Nguyen Hong Quan²

¹ Leichtweiß-Institute for Hydraulic Engineering and Water Resources, Department of Hydrology, Water Management and Water Pollution Control, University of Braunschweig, Beethovenstr. 51a, D-38106 Braunschweig, Germany, email: malte.lorenz@tu-bs.de, huyen.le@tu-bs.de, g.meon@tu-bs.de

² Institute for Environment and Resources (IER) - Vietnam National University of Ho-Chi-Minh City, 142 To Hien Thanh, District 10, Ho-Chi-Minh City, Viet Nam, email: nquanghieu.ngo@gmail.com, hongquanmt@yahoo.com

Abstract

The Thi Vai main river in South Vietnam flows from the Ba Ky weir about 37 km before entering the East Sea and is strongly affected by the tide. Its catchment, located in the provinces Dong Nai, Ba Ria-Vung Tau and Ho-Chi-Minh City, covers approx. an area of 625 km². A lot of industries are situated in this catchment.

In the past, the Thi Vai river was strongly polluted by industrial wastewater discharges, especially by untreated wastewater of the Vedan company during the years 1994 to 2008. As a result, the Thi Vai river has been considered ecologically dead. In the recent years the water quality in the Thi Vai area has been managed considerably more. As a consequence, the water quality has been improved partly in the recent past, especially due to the investments in wastewater treatment systems.

In the course of the joint research project "Environmental and Water Protection Technologies of Coastal Zones in Vietnam EWATEC-COAST" a two and three-dimensional hydrodynamic and water quality model Delft3D has been applied for the Thi Vai river: The hydrodynamic results including temperature and salinity, which are firstly modelled in the program Delft3D-Flow, deliver input data for modelling the water quality in the program Delft3D-WAQ. The discharge, water level, temperature, salinity as well as concentrations of nutrients and dissolved oxygen are simulated. The simulation of water level shows good results. Furthermore previous results for the discharge, temperature and salinity simulation are presented. A simulation experiment with a tracer input indicates that pollutants



are trapped into the estuary due to the tide and can remain several days in a river reach.

In the next step, this hydrodynamic water quality model Delft3D will be linked with the ecohydrological water and mass balance model PANTA RHEI, which is covering the upstream catchment. The calibrated model system will be used for long-term past to present simulations and future scenarios.

Key Words: hydrodynamic modelling, water quality modelling, estuary



1. Introduction

The joint research project “Environmental and Water Protection Technologies of Coastal Zones in Vietnam EWATEC-COAST” funded by the German Ministry of Research and Education (BMBF) and the Vietnam National University of Ho-Chi-Minh City is focussed on the Thi Vai river basin and the Can Gio mangrove forest in South Vietnam. One important objective of the project is the development of a model-based water management system. As main part of the subproject 3 “Surface Water” a linked model system is evolved and applied, which comprised of a hydrological water and mass balance model and a hydrodynamic and water quality model. For the hydrodynamic water quality model, which is adapted to the Thi Vai river, the multi-dimensional (2D or 3D) simulation program DELFT3D, developed by Deltares, has been chosen. The application of the hydrological water and mass balance model PANTA RHEI to the Thi Vai catchment is described in the accompanying paper “Ecohydrological modeling of the Thi Vai Catchment in South Vietnam”.

A monitoring program with measurements of water levels, discharges and water quality parameters started in March 2013 and still continues. Previous results of the monitoring system are outlined in the accompanying paper “*Integrated water quality monitoring of the Thi Vai River: an assessment of historical and current situation*”. The measured data will be used for the calibration of the presented model.

The calibrated model system will be used for long-term past to present simulations, as wells as future scenarios, which include climate and (other) anthropogenic changes of the water supply.

2. Study area

The Thi Vai main river in South Vietnam flows from the Ba Ky weir about 37 km before entering the East Sea. It is located in the northern tropics (10°29’N, 107°10’E) with mean temperatures of 28°C and a yearly rainfall of approx. 1800 mm. The area is affected by the tropical monsoon climate with a rainy season from May to November and a dry season from December to April.



The whole main river is strongly affected by tide and therefore forms a long estuary. The width of the Thi vai river ranges from about 300 m in the upper reaches to 900 m in the lower reaches. The elevation of the river bed decreases downstream and reaches 30 meter below sea level near the port Cai Mep. The water is brackish, the measured salinities reaches in the lower reaches up to 30 ppt. In the upper reaches the salinity is more variable and depends on the tide. The Thi Vai catchment, located in the provinces Dong Nai, Ba Ria-Vung Tau and Ho-Chi-Minh City, covers approx. an area of 625 km². One of the industrial core areas of South Vietnam is situated in the catchment: There are about 14 industrial zones located in the catchment. In the past the Thi Vai river was strongly polluted by industrial wastewater discharges, especially by untreated wastewater of the Vedan company during the years 1994 to 2008 [1]. An approx. 9 km long river section downstream the tributary Suoi Ca was extremely polluted as, for example, very low concentrations of dissolved oxygen (often < 1mg/L) show [2]. Nowadays, the pollution level is lower, but, as showed by the current monitoring program, the water quality remains impaired for several parameters.

The eastern bank is dominated by ports and industrial areas. In contrast, the western bank is covered by mangrove forest. The Can Gio mangrove forest, a UNESCO biosphere reserve, is adjacent to the Thi Vai river basin in the West.

Entering the Ganh Rai bay, a shallow and relative separated bay, the Thi Vai river is regarded as a rather closed system, so that pollutants could hardly be transported out of the river into the ocean [3].

3. Model set up

The used model system DELFT3D includes two programs: the hydrodynamic (and transport) simulation program DELFT3D-FLOW and the water quality program DELFT3D-WAQ (also named D-Water-Quality). DELFT3D-FLOW is able to calculate non-steady flow and transports due to tidal and meteorological forcing in 2D and 3D [4]. A wide range of substances can be simulated by DELFT3D-WAQ, which solves the mass balance equations containing advection, diffusion and reactions [5]. The information on the flow field for DELFT3D-WAQ is derived from DELFT3D-FLOW.

3.1 Hydrodynamic Model

The model area comprises the lower reaches of the canal Ba Ky and the Thi Vai river up to the port Cai Mep. The modelled river length of the Thi Vai main river accounts for approx. 30 km.

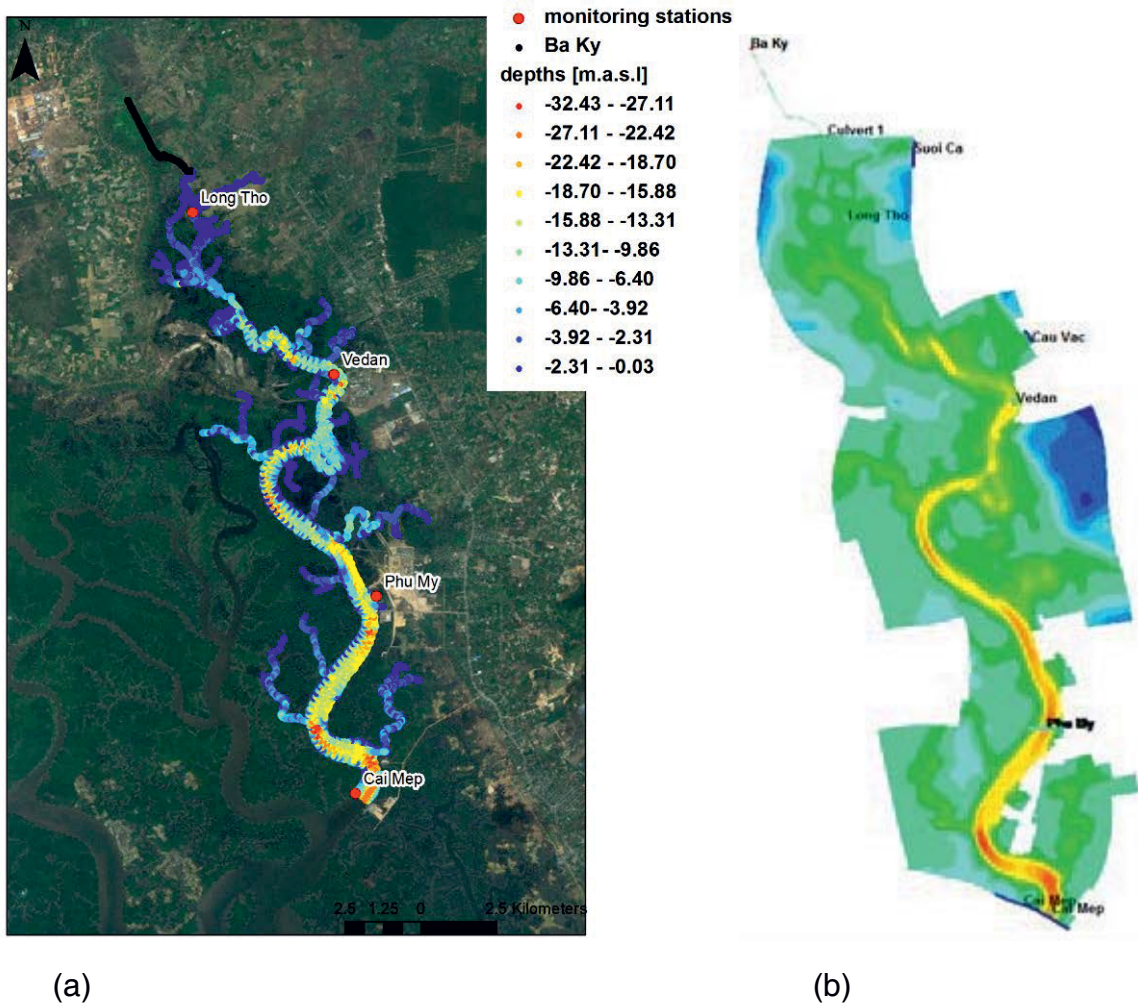


Figure 1. The measured depths of the Thi Vai river (a) and derived depth information for DELFT3D (b).

Creating a grid is the first step to set up the model. This was done by the program RGFGRID, which is integrated in the model suite DELFT3D. The grid in the current version consists about app. 23400 grid cells. The average grid width is about 76 m in the general flow direction and about 55 m vertical to the flow direction. Furthermore the maximal grid width is about 252 m in the general flow direction and about 168 m vertical to the flow direction.



Then the bathymetry has been built by interpolating measured depths of the Thi Vai with the help of the program QUICKIN, which is also one integrated tool of DELFT3D. Nearly all used river depths were measured by the Bach Kho construction equipment company in 2013 on behalf of the Leichtweiss-Institute, TU Braunschweig. For the last segment in the south of the Thi Vai River old measured depths, provided by the IER in HCMC, were applied. Altitude information with much lower density, which also was provided by the IER in HCMC, was used for the surrounding area of the Thi Vai. Figure 1 shows the measured depths of the Thi Vai and the derived depth information for DELFT3D. One can choose between 2D and 3D simulations by defining the number of layers: 1 layer for a 2D simulation and several layers for 3D simulations.

The discharge of the tributary Bung Mon via Ba Ky channel, the discharge of the tributary Suoi Ca and the discharge of the tributary Cau Vac are the upper boundary conditions for the flow at the current version of the model. The measured water levels of the monitoring station Cai Mep form the lower boundary condition. Furthermore the salinity and temperature must be defined for the boundaries. The discharge data of the tributaries has been calculated from measured water levels of the main tributaries using a stage discharge curve, which was set up by discharge measurements done in the course of the project. Also first simulations with discharges delivered by the hydrological model PANTA RHEI has run successfully. In the model the channel Ba Ky is separated from the main Thi Vai River by a thin dam. The water discharge into the river at low tide is realised by an implemented culvert. This represents the Ba Ky Weir.

The water level data of the lower boundary have a high resolution with time steps of 10 minutes, so that the tide can be well reproduced. The correct simulation of the water level and discharges depends primarily on the lower boundary, whereas the upper boundaries have less influence. Regarding the simulations of future scenarios water levels for the boundary condition of Cai Mep are supposed to be obtained by transforming simulated water levels at the coast by DELFT3D, which is implemented by the subproject 7 "Coastal Protection" (Universität Siegen).

The main calibration parameter for the hydrodynamic is the bottom roughness, which has an influence in reproducing the correct tide phase and height. In Delft3D-Flow it is possible to input a roughness file defining



spatially variable values of bottom roughness. In the current version Manning values appear in a range of 0.015 to 0.1 s m^{-1/3}.

In Delft3D-Flow one can choose between different heat flux models to model the water temperature and the evaporation. The required input for the used heat flux model 1 ("Absolute flux, total solar radiation) are time dependent data for the shortwave radiation for a clear sky, for the air temperature and for the relative humidity as well as constant values for the sky cloudiness and the water surface area, which is exposed to the wind. The incoming short wave radiation is available for the station Nha Be in Vietnam. Because of the absence of better data, these data are used, although these do not refer to a clear sky. The use of other heat flux models like the ocean heat flux model seems to be less suitable for the Thi Vai River. Furthermore time dependent data for wind speed and wind direction as well as for the quantity of rainfall are defined. The meteorological data originate from meteorological and rain stations, which are located near the river. At the current version the rain data of the rain station Long Thanh and meteorological data of the station Bien Hoa are used. Meteorological data for different future climate scenarios will be delivered by the subproject 2 "Meteorology and Climate Change" (Universität zu Köln).

3.2 Water quality model

The calibrated hydrodynamic results, including the modelled salinities and temperatures, of DELFT3D-FLOW serve as an input for the water quality model DELFT3D-WAQ. Together with DELFT3D-FLOW, 2D and 3D simulations are possible in DELFT3D-WAQ.

DELFT3D offers a wide range of modelled substances, which can be combined. Substances included in the water quality program are among others the pH, the phytoplankton, nutrients, organic matter and heavy metals. In the so-called process library one can choose the substances and also the processes, which will be simulated as well as the parameters of the processes, which should be editable. Primarily the nutrients and the dissolved oxygen are supposed to be modelled for the Thi Vai River.

At the moment the DELFT3D-WAQ model is built up and tested. The wastewater discharges of the industrial zones and of single companies, which wastewater is not channelled into central wastewater treatment



systems of the industrial zones, are, implemented in the water quality model. Nutrients loads of the catchment area through the tributaries will be delivered by the water and mass balance model PANTA RHEI. Measured chemical and physical water quality parameters, collected during the on-going monitoring program since March 2013, will be used for calibrating the model.

4. Results

First simulations offer satisfactory to very good results for the water level: Figure 2 shows the measured and simulated water level at the monitoring station Long Tho in May and October 2013.

In May the phase of tide is overall well reproduced, but the peaks at high tide are a slightly underestimated. The coefficient of determination (R^2) is 0.87 and the Nash-Sutcliffe-Efficiency 0.79 for Long Tho in this month. It must be considered, that the measured values at low tide are partly deficient, because very low water levels have not been detected by the water level logger.

The agreement between measured and simulated water levels is very high in October, when the high tidepeaks are also well simulated. Some simulated water levels in October are not displayed, because there are missing data for the lower boundary condition Cai Mep and therefore there are no correct simulation results for these periods. This problem will be solved by a regression between water levels of Vung Tau, a station at the coast, and water levels of Cai Mep, so that missing values for Cai Mep can be generated. For the periods in October, for which correct data for the lower boundary condition is present, the coefficient of determination (R^2) is 0.88 and the Nash-Sutcliffe-Efficiency is 0.87.

The simulated discharges are within a similar range like the measured values for the discharge, as shown in Figure 3. The discharge data were measured at the station Phu My by an ADCP (Acoustic Doppler Current Profiler). A problem is that on the one hand, the measurement of the discharge of the whole cross section needs some time (approx. 25 minutes), and on the other hand, the discharge is changing very fast because of the tide. Therefore there are probably deviations between measured and actual discharges. So a comparison between simulated and the original

measured discharge data is aggravated. However, the modelled discharge data seem to be in a realistic range.

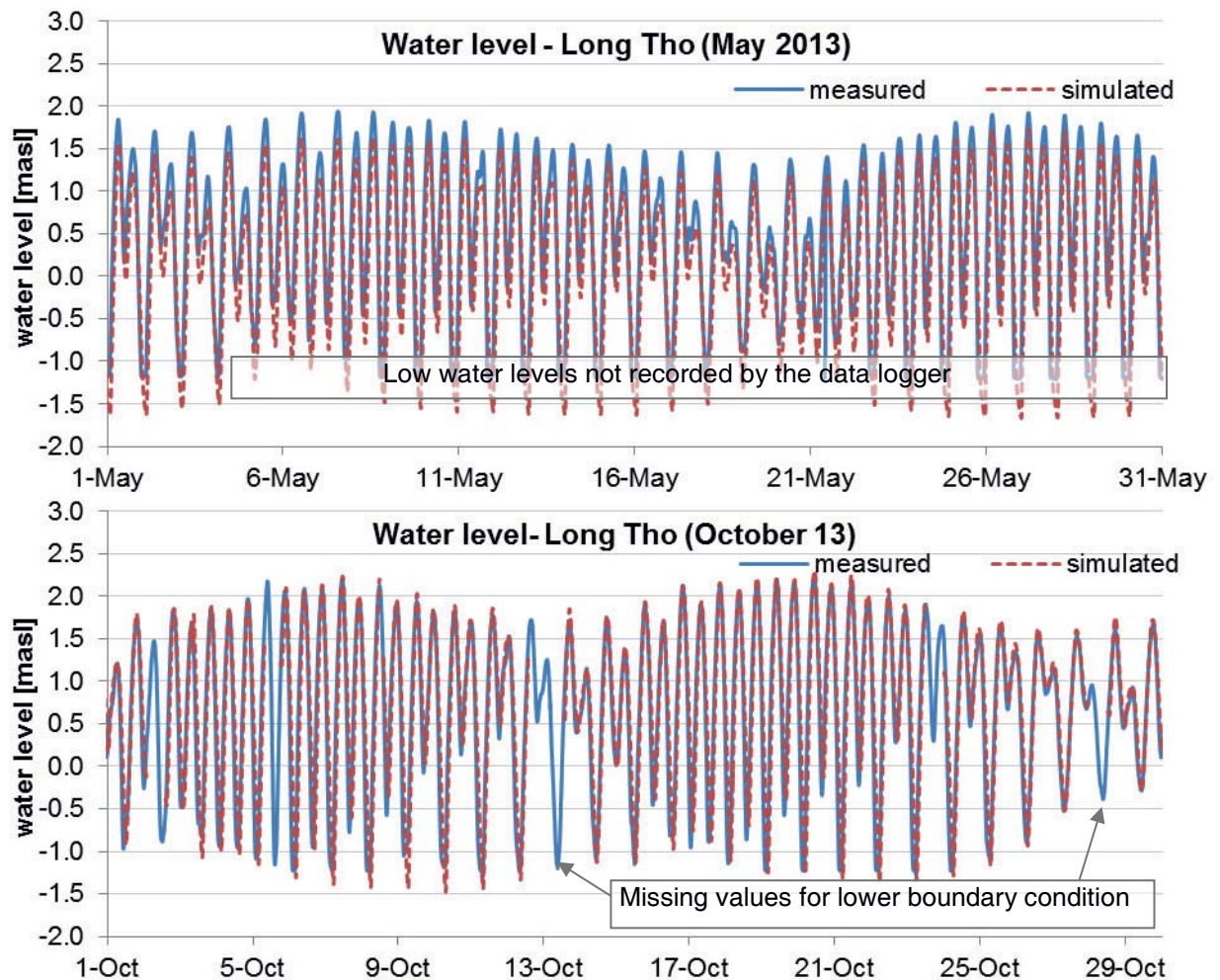


Figure 2. Measured and simulated water levels at the station Long Tho in May and October 2013.

The Figure 4 shows results for the Heat Flux model 1 (absolute flux, total solar radiation). As noted before, there is a difference between the required solar radiation data, namely the shortwave radiation for a clear sky and the measured input data, the incoming shortwave radiation. Another imprecision of the input data is, that only mean daily values are available for the temperature and so diurnal changes are not represented exactly. Despite these inaccuracies of the input data, the results for the station Long Tho are all in all good, as Figure 4 shows. It has also to be considered that, the depth of the measured water temperature varies, depends on the actual water levels, because the data logger has a fixed position.

For this reason the measured water temperatures have an additional variation. The measured water temperatures are compared with a depth averaged temperature of the 2D model.

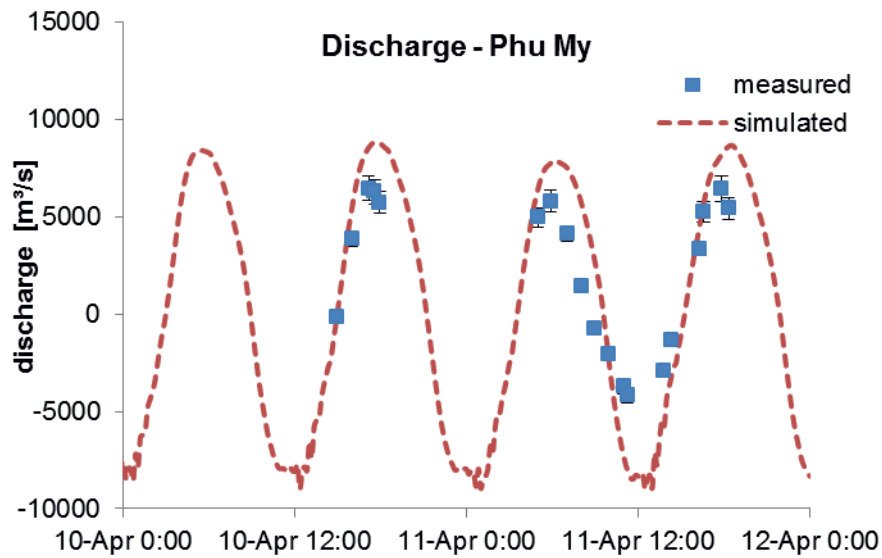


Figure 3. Measured and simulated discharges at the Phu My on 10-12. April 2013.

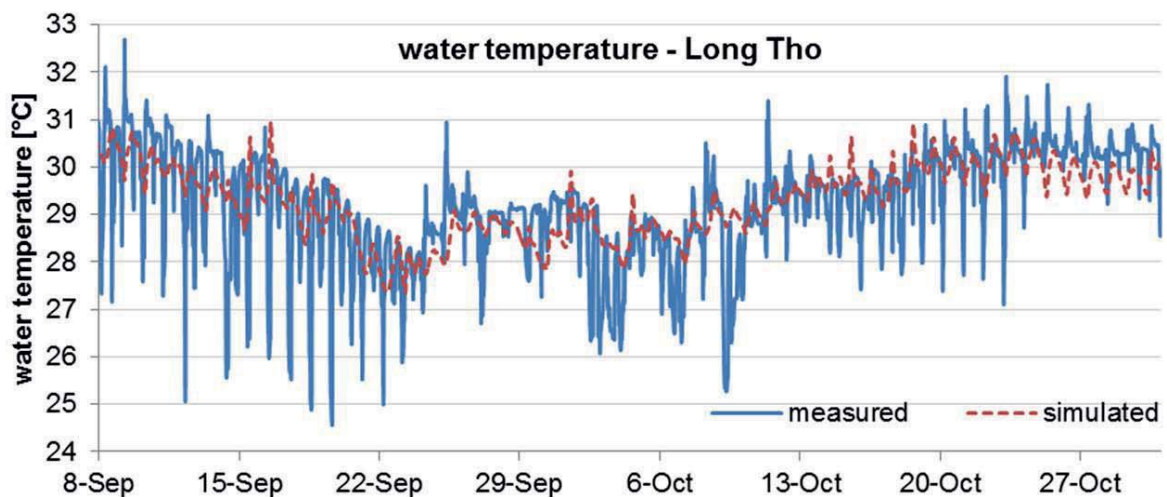


Figure 4. Measured and simulated discharges at the Phu My on 10-12. April 2013.

By simulating a tracer in DELFT3D-Flow it is possible to reproduce a possible transport of a pollutant discharged into the Thi Vai river. Figure 5 shows the spreading of a tracer at different points of time after a tracer input in the upper reaches of the Thi Vai river on 15 April 2013 at 6 am. It

is obvious, that the tracer is transported downstream and upstream and remains mainly in the upper reaches for several days. The tracer is spread, but do not reach the lower reaches respectively the sea. Also after 10 days the tracer is mainly recorded in the upper reaches. This is an indication that pollutants, which are discharged into the river and are not degraded, could remain for a long time in the river. In consequence the risk of a local high pollution level is increased, especially in the upper and middle reaches. These results correspond to the situation in the past, when a river section was extremely polluted by wastewater discharges, whereas other sections of the river had not such a high pollution level.

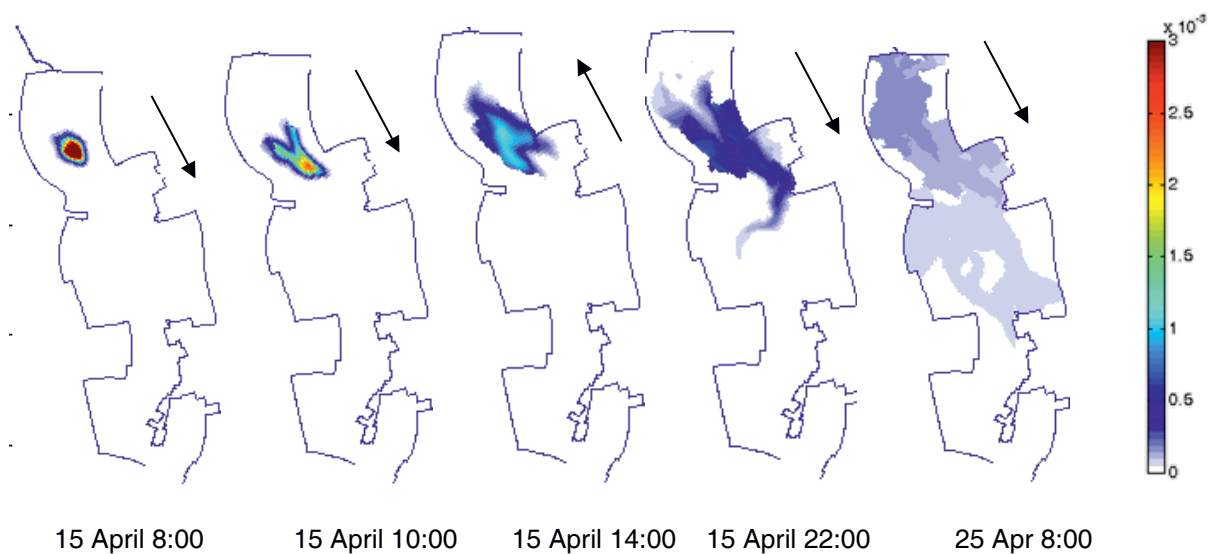


Figure 5. Simulation of a tracer by DELFT3D-Flow. The arrows show the main flow directions.

As mention before, one can choose between a two dimensional (depth averaged) and a three dimensional modelling in DELFT3D-Flow. The 3D-simulations are much more time-consuming, but interesting for the consideration of vertical differences, like for example, of salinity. In Figure 6 the velocities and salinities of two time points are shown in a vertical profile: once before high tide with a flow landwards (negative velocities) and once two hours later after high tide with a flow towards the sea (positive velocities).

The shown cross-section, located in the middle reaches upstream of Phu My, has a water depth of 18 m and a total width of 1.2 km. At the first time point there is now big vertical gradient according to velocities and

salinities. In contrast, there is a significant decrease of velocity from the center of the channel to the bank.

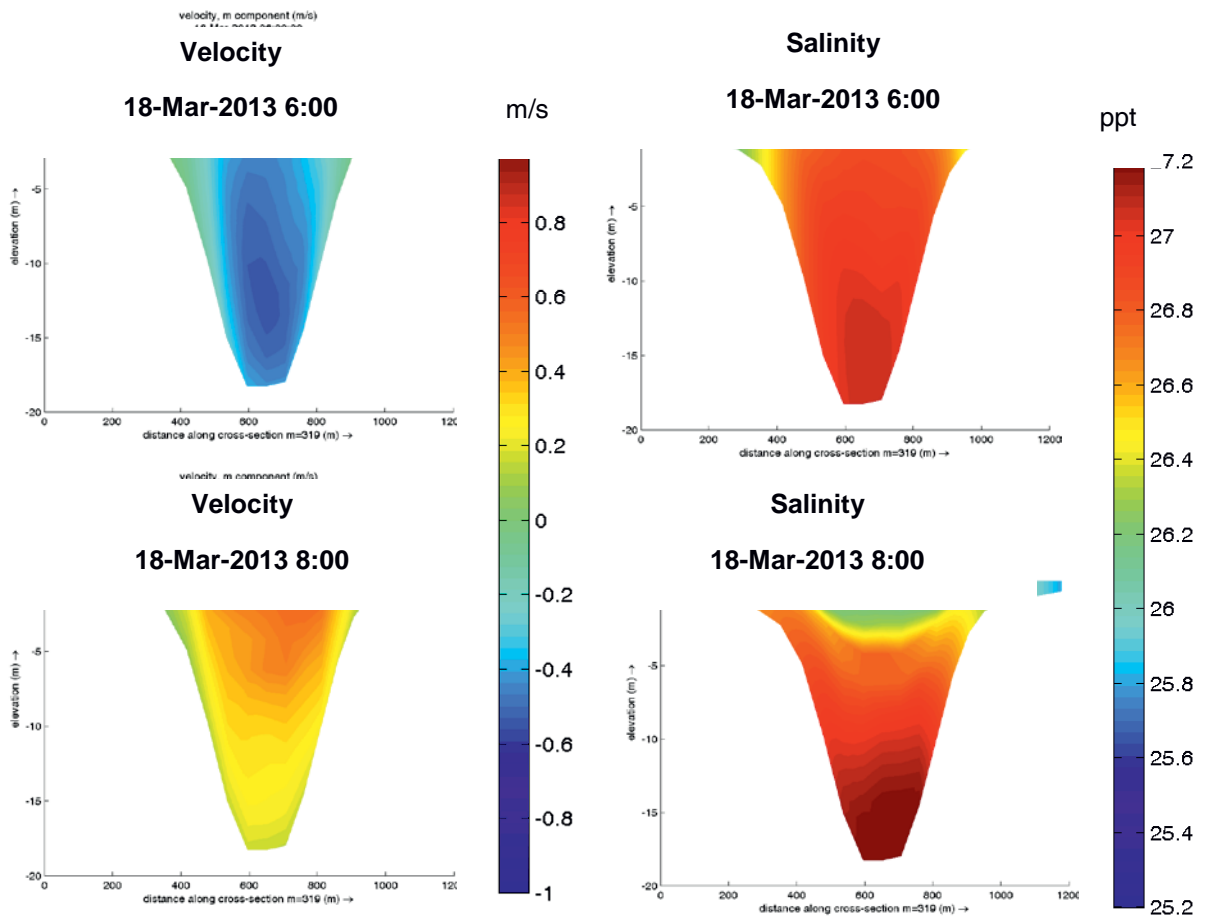


Figure 6. Velocities and salinities along a cross section upstream of the monitoring station Phu My.

At the bank, respectively at the flat areas, the velocity is approx. 0 m/s. Also the salinities are lower at the flat bank areas at this time. Two hours later, the velocities towards the sea decrease with increasing depth and towards the banks. The salinities increase slightly with decreasing depth.

5. Conclusion and outlook

Previous results show, that the DELFT3D-FLOW model for the Thi Vai River is suitable to simulate the hydrodynamic of the river and thereby can deliver a realistic hydrodynamic impulse for the water quality model. Furthermore the DELFT3D model can help to understand, how pollutants are transported or remain in the river (sections). The completion and calibration of the water quality model in DELFT3D is one important step in the



near future, so that the transport relevant biochemical processes can be reproduced and investigated.

The overall objective is the finalisation of the combined model system for the Thi Vai river catchment including the water and mass balance model PANTA RHEI and the hydrodynamic and water quality model DELFT3D. This model system is a part of the integrated management system for the project area. It will be also used for long-term past to present simulations as well as for simulations of future scenarios concerning climate and anthropogenic changes. The required climate data and the water level data at the coast for the latter purpose will be delivered by other subprojects within the joint research project "EWATEC-COAST".

References

- [1] Nguyen, H.P., Pham, H.T. (2011): The dark side of development in Vietnam: Lessons from the Killing of the Thi vai River. *Journal of Macromarketing* 32(1), 74-86.
- [2] Institute of Environment and Natural Resources (IER) (2006): Báo cáo kết quả thực hiện Nhiệm vụ KIỂM SOÁT Ô NHIỄM MÔI TRƯỜNG LƯU VỰC SÔNG THỊ VẢI ("Report about the controlling of the environment pollution in the Thi Vai Catchment"). Vietnam National University of Ho-Chi-Minh City.
- [3] Ban Quản Lý Chương Trình Tăng Cường Năng Lực Quản Lý Môi Trường Và Quản Lý Đất Đai tỉnh BRVT (2007): Báo cáo Hợp phần triển khai kế hoạch bảo vệ môi trường lưu vực sông Thị Vải. Report about the implementation of environment protection plans in the catchment of Thi Vai River. Vietnam.
- [4] Deltares (2013): DELFT3D-Flow, Simulation of multi-dimensional hydrodynamic flows and transport phenomena, including sediments. User Manual Hydro-Morphodynamic, Version 3.15.30932. Delft, Netherlands.
- [5] Deltares (2013): D-Water Quality, Versatile water quality modelling in 1D, 2D or 3D systems including physical, (bio)chemical and biological processes. User Manual D-Water Quality, Version 4.99.31050. Delft, Netherlands.



The evaluation of groundwater level variations in a coastal zone using groundwater software FEFLOW

Quang Dung Lam¹, Matthias Pätsch², Günter Meon³, Stephan Lange⁴

¹ Institut for Water Management IfW GmbH, Köterei 13H, 38108 Braunschweig, Germany; Email: dunglam1510@yahoo.de

² Department of Hydrology, Water Management and Water Protection, University of Braunschweig, Beethovenstr. 51a, D-38106 Braunschweig, Germany;

³ Department of Hydrology, Water Management and Water Protection, University of Braunschweig, Beethovenstr. 51a, D-38106 Braunschweig, Germany;

⁴ Institut for Water Management IfW GmbH, Köterei 13H, 38108 Braunschweig, Germany

Abstract

The assessments of groundwater behavior at regional scales are necessary to achieve the sustainable water resources management. Groundwater is often abundant resource. However, over-use of groundwater can cause adverse impacts on human users and on the environment such as a lowering of the water table and saltwater intrusion. The aims of this study are to identify the capacities of applying a groundwater model for simulating the groundwater flow and to assess the mutual interaction between river water and groundwater level.

The study area is located in the coastal zone of Ba Ria-Vung Tau province, Vietnam. The river Thi Vai has a total length of 76 km and rises from Long Thanh district (Dong Nai province) to Ba Ria-Vung Tau province and then flows into Ganh Rai bay. The domain model covers approximately 500 km². The stratigraphic formations in the investigated area can be distinguished into 4 hydrogeological units, including Holocene, upper Pleistocene, lower and middle Pleistocene, and Pliocen. The main materials of these aquifers are fine sandy loam, silt, sandy silt, coarse sand and fine gravel and pebbles. Groundwater flow is not only influenced by water surface and topography of land surface, but also by tidal level and other activities of groundwater exploitation from abstraction wells.

A 3-D finite element model (FEFLOW) is useful tools for simulating groundwater flow in river catchment. The necessary information on the geological formations, rivers, hydraulic parameters, land use, and climate



data as well as abstraction wells are implemented in the model set-up. The study revealed that FEFLOW performed satisfactorily in simulating groundwater flow in a coastal area. The model results also demonstrated that groundwater levels at the areas close to the Thi Vai river are slightly to significantly influenced by the change of water level in Thi Vai river. The results of the study provide useful information regarding the groundwater behavior of different aquifers aiming for better understanding and management of the groundwater development in the study area.

Keywords: *Groundwater, hydrogeology, FEFLOW*



1. Introduction

Groundwater is one of the most important natural resources in many places around the world. It is a source of industries, agriculture, and drinking water to communities. Therefore, the sustainable management of groundwater resources will play an important role in the future development of a country, especially when rising demand for drinking water (Mende et al., 2007). Due to increasing the requirements for various purposes of water supply, the abstraction of groundwater has rapidly and continuously increased in the last decades. Excessive water withdrawal from groundwater aquifers can directly affect the availability of groundwater and decline groundwater levels in aquifers (Phien-wej et al., 2006; Shamsudduha et al., 2009). Several studies reported that declining groundwater levels have a number of adverse impacts on the groundwater environment due to additional recharge from wastewater sources, leaking sewers, and saline water intrusions (Hoque et al., 2007; Berg et al., 2007; Paniconi et al., 2001; Perera et al., 2010). In addition, the overexploitation of groundwater can also cause land subsidence problems. Timothy (2006) stated that about 80% of serious land subsidence problems have been affected by the excessive extraction of groundwater.

In coastal zones, surface water quality degradation resulting from saline water intrusion is a common issue of concern (Werner and Simmons, 2008). Therefore, groundwater is considered to be the main sources of these areas. The assessment of groundwater behaviors is needed to achieve sustainable management of the water resources. Some previous studies have looked at the changes in groundwater level based on the monitoring data (Almedeij and Al_Ruwaih, 2006; Hoque et al., 2007; Akther et al., 2009). These studies mainly used different methods such as the linear regression, seasonal trend decomposition to detect the trend in groundwater levels.

In combination with traditional hydraulic monitoring methods, mathematical modeling has emerged as an important tool used to depict groundwater flow in aquifers. Globally, groundwater models are used broadly to assess various groundwater aquifers in the world: Chen (2002) used MODFLOW (McDonald and Harbaugh, 1988) and PEST_ASP (Doherty, 2001) model to investigate groundwater balance at North Stradbroke Island,



Queensland, Australia. Sekhar et al, (2004) used groundwater model to assess groundwater flow of Gundal Sub-basin in Kabini River Basin, India and indicated that water levels in the excessive groundwater depletion zones are sustained at the present level due to the inflows from the adjacent Nugu river basin. In this study, a numerical groundwater flow model FEFLOW (Finite Element Subsurface Flow and Transport Simulation System, Diersch (1979), version 6.1) is developed to understand the current groundwater behaviors in a coastal zone of Vietnam and to assess the variations of groundwater level in complex aquifers which are directly affected by overexploitation of groundwater and Tidal.

2. The study area

The study area is located in the Thi Vai catchment and its vicinity, Ba Ria-Vung Tau province, Vietnam, covering an area of 500 km² (Figure 1). This region has potential for convergence of economic development of the Sea such as gas, seafood, and sea ports. The whole Thi Vai river has a length of 76 km which originates in Dong Nai province and then flows into the East Sea. The area is affected by tropical monsoon climate, with a characteristic rainy season from May to October and dry season from November to April. The mean annual rainfall is 1500 mm, whereof 80% fall in rainy season. The average annual temperature is 27 degrees Celsius, the lowest month is about 24.8 degrees Celsius, and the highest is about 28.6 degrees Celsius. In this area, the number of sunshine hours is very high, estimated to be 2400 hours per year.

Regarding the topography of the Thi Vai area, the extreme Northeast parts of the area has maximum elevations, ranging from 32 to 48 m above mean sea level (asl). In general, the elevations gently slope towards the Western and the Southern area.

In this area, apart from surface water which is mainly supplied by Thi Vai river, groundwater serves as the main source of agriculture, industry, and drinking water. Groundwater in the area situates at a depth of 10-90 m with the average flow capacity from 10-20 m³/s (PCP, 2010). The stratigraphic formations in the investigated area can be divided into four hydrogeological units, namely Holocene, upper Pleistocene, lower and mid-

dle Pleistocene, and Pliocen. The soil compositions in aquifers are mainly fine sandy loam, silt, sandy silt, coarse sand and fine gravel and pebbles.

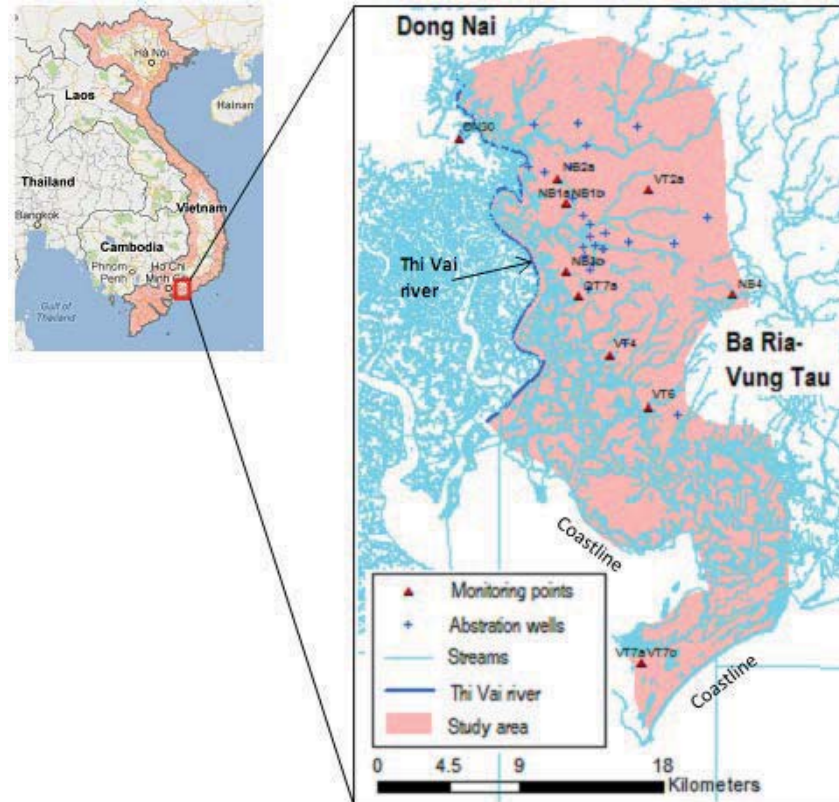


Figure 1. Location of the study area in Ba Ria-Vung Tau province, Vietnam

3. Model conceptualization and development

3.1 Groundwater level

A network of 12 existing observation wells was selected for groundwater monitoring (Figure 1). The locations of these monitoring wells are concentrated mainly along the Thi Vai river. The groundwater monitoring program was initiated in April 2013. The groundwater levels are being automatically recorded with 15 minute intervals at all observation points under a EWATEC-COAST (Environmental and Water Protection Technologies of Coastal Zones in Vietnam) project. The depth of monitoring wells range between 5 and 50 m and these tap the first to the seven layers of the porous aquifers. The elevation of the groundwater table ranges from 34 m asl at the Northeastern to 0.1 m asl at the Southern part of the study area.



3.2. Aquifer geometry

The information of geologic including geological maps, cross section and well logs were combined with information on hydrogeologic properties to define hydrostratigraphic units for the conceptual model (Anderson and Woessner, 2002). There are 55 existing boreholes drilled in the area during the time from 1960 to 2010. The lithology data from those boreholes were utilized for sketching horizontal and vertical disposition of aquifers and aquitards in the study area to the highest depth of 83 m beneath the land surface.

In this area, the sedimentation regime and the sea level transgressions and regressions have caused large variations in aquifers consisting of Holocene (qh), upper Pleistocene (qp³), lower and middle Pleistocene (qp²), and Pliocen (n²). The Holocene aquifer occurs at the surface of almost the whole area and consists of clayed silt, fine sand and organic matters. The boreholes installed in this aquifer mainly shallow boreholes, with the depths from several meters to 16 m. The upper Pleistocene, mainly overlain by the Holocene aquifer, is also distributed widely throughout the whole area. This aquifer can be divided into two parts. The top part is an aquitard layer, consisting of silt, clay or silt clay. The lower part is an aquifer including fine to coarse sand, having a thickness from 2 to 17 m. Similar to the Pleistocene aquifer, the lower and middle Pleistocene aquifer can be divided into two parts. The top part is an aquitard layer consisting of clay or silty clay. The lower part is a confined aquifer, consisting of fine to coarse sand, having the average thickness from 4 to 15 m. The lowest aquifer is Pliocen, a confined aquifer, consisting of fine to coarse sand, having the average thickness from 2 to 34 m.

3.3. Aquifer parameters

The parameters such as hydraulic conductivity and specific yield/specific storage are key factors influencing groundwater flow in the aquifers. In addition, in-transfer and out-transfer rate are also important factors controlling the water movements between the Thi Vai river and groundwater level. Due to the lack of input data, these parameters assigned in different aquifers were derived from Mekong Delta projects (Uppenberg et al., 1997). The hydraulic conductivity and the porosity



values assigned to the model ranged between 12 and 41 m/day and between 0.001 and 0.02, respectively.

3.4. Groundwater recharge and abstraction wells

Most groundwater recharge results from precipitation infiltration and runoff in the middle mountain ranges. Based on climate data, land use, soils, topography, and current management practices, groundwater recharge was obtained using the hydrological model PANTA RHEI which has been developed by the Department of Hydrology, Water Management and Water protection, Leichweiss Institute for Hydraulic Engineering and Water Resources, University of Braunschweig. Those calculated values were integrated into the first layer of the groundwater model.

There are 21 existing abstraction wells in the study area (Figure 1). The groundwater abstraction is mainly used for industrial zones and drinking. According to the report of Groundwater Monitoring of Ba Ria-Vung Tau (DONRE_Ba Ria-Vung Tau), the groundwater supply for drinking, industries, and agriculture ranges from 413 to 51.575 m³/day, of which the groundwater used by TanThanh District is 51.575 m³/day, followed by Ba Ria Town (27.029 m³/day) and Vung Tau City (413 m³/day). Because the pumping duration and rate have not been measured so far, pumping rate ranging from 1500 m³/day to 2500 m³/day were assumed in this study.

3.5. Model development

The groundwater model FEFLOW was used in the present study. FEFLOW is a computer program that numerically solves the three-dimensional groundwater flow equation for a porous medium by using a finite element method. The FEFLOW model is composed of three parts consisting of (1) the designation of finite element mesh; (2) 3D designation of slices and layers; and (3) problem editor to specify the parameters needed for simulation.

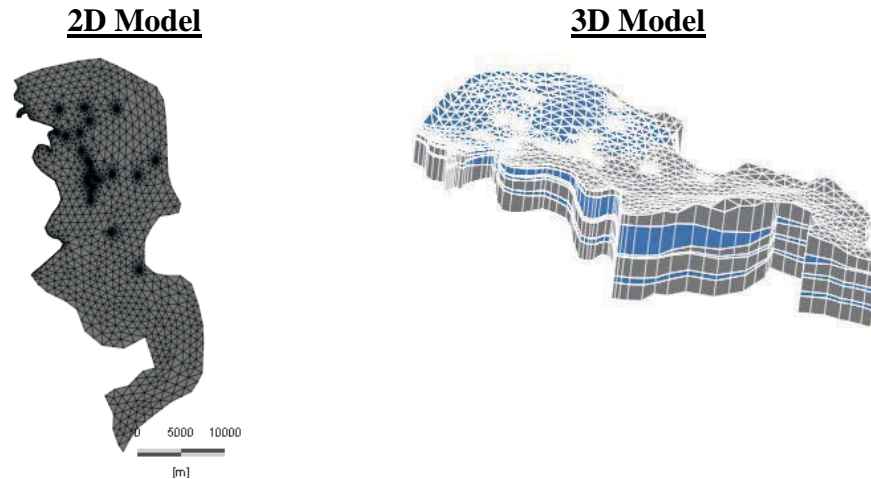


Figure 2. Finite element meshes in horizontal plane (left) and three dimension model (right)

The model domain is divided into 25186 meshes elements and 15104 meshes nodes. The meshes are refined in the pumping areas to consider the highly varying hydrological properties of these areas (Figure 2). The model consists of 4 aquifers and 3 aquitards (Figure 2).

To represent the system relationship with the surrounding area, a set of appropriate boundary conditions are applied into the model: (1) The Western boundary representing the Thi Vai river, was assigned as river boundary. For this boundary, the time series of river water levels are used as the value for a 3rd kind (*Cauchy-type*) boundary condition. (2) For the Southern boundary, the time series of tidal levels were used as the values for a 1st kind (*Dirichlet-type*) hydraulic head boundary condition. (3) Finally, the pumping rate of 21 wells was assigned as the 4th kind boundary to the model.

4. Model calibration

The calibration is the process of adjusting model parameters and then comparing the simulation results so that calculated head values closely match the observed values at selected points of the aquifer (Roger Gonzalez_Herrera, 2002).

Due to the availability of input data and monitored groundwater levels, the model was calibrated to transient state from April to August 2013 in this study. During the model calibration, the main parameters were adjusted



including hydraulic conductivity, drain/fillable porosity, specific storage, transfer rates, and the pumping rate of wells.

To assess the deviation between observed and simulated results, some statistical parameters consisting of mean absolute error (MAE) and root mean square (RMS) were used in this study. RMS is the square root of the sum of the square of the differences between simulated and observed values, divided by the number of observation wells. The error is expressed as follows:

$$RMS = \sqrt{\frac{\sum_{i=1}^n (H_i - H_i')^2}{n}}$$

where, RMS is root mean square error (m); n is total number of measurements; H_i is simulated value of groundwater at the time i (m); and H_i' is measured value of groundwater at the time i (m).

The MAE and RMS have been widely used to evaluate the performance of groundwater models. If the values of MAE and RMS close to 0, the model simulation is taken as an indication of perfect performance.

5. Results and discussions

In order to assess the development of the groundwater table with time, the computed hydraulic heads have been compared to the measurements at all 12 monitoring points over the calibration period of 5 months (Figure 3). In general, the model simulated well for both the temporal trend and magnitude of groundwater levels. The statistical values of MAE and RMS ranging from 0.1-1.07 and from 0.15-1.32, respectively, demonstrate that the modelled results are reliable for the groundwater levels in different aquifers.

Considering the simulated results at the observation point of DN30 which is close to the Thi Vai river, the magnitude and the trend of simulated values are relatively consistent with the measured values. The fluctuation of simulated values is similar with those of the Thi vai river. This reveals that groundwater depth is strongly influenced by the Thi Vai water levels and it is mainly recharged by seepage from the Thi Vai river bed. The



simulated results also indicate that tidal water levels affect directly the variation of groundwater levels at the points of DN30, VT7a, and VT7b.

At some monitoring points, the heads are slightly underestimated during the period from 20 - 30 August 2013. This is presumably due to the local storm events. Since storm events occurred with high local variation, the amount of rainfall infiltration during the storm is not reflected by the model.

The spatial distribution of groundwater depth at the end of 31 August 2013 is shown in Figure 4. The elevations of groundwater were represented by different colors that the darker color suggests lower groundwater elevations within the domain. The simulated results showed that the higher elevations of groundwater table concentrate in the Northeast boundary of the model, while lower elevations occur in the Western and the Southern boundary. In addition, contour lines of groundwater table elevations have also been drawn at interval of 2 m that cover the elevations plotted on the figure. Contour values ranging from 0-38 m appear on the map. Based on the contour pattern, the groundwater table slopes downward to the coastline (Southwestern boundary) of the model domain in general.

Overall, the results of the numerical model show a moderate to good accordance with the measurements. However, the performance of the model has general limitation due to the following reasons: 1) the knowledge of the aquifer system is still limited. Information regarding the stratigraphy and lithology is not adequate. 2) Information about the vertical and horizontal variations of hydraulic conductivity are missing or very sparse. In addition, some other properties of aquifers such as drain/fillable porosity, specific storage are also missing. Therefore, the rough estimations of these parameters are mainly based on the relevant documents obtained from other catchments with the similar conditions.

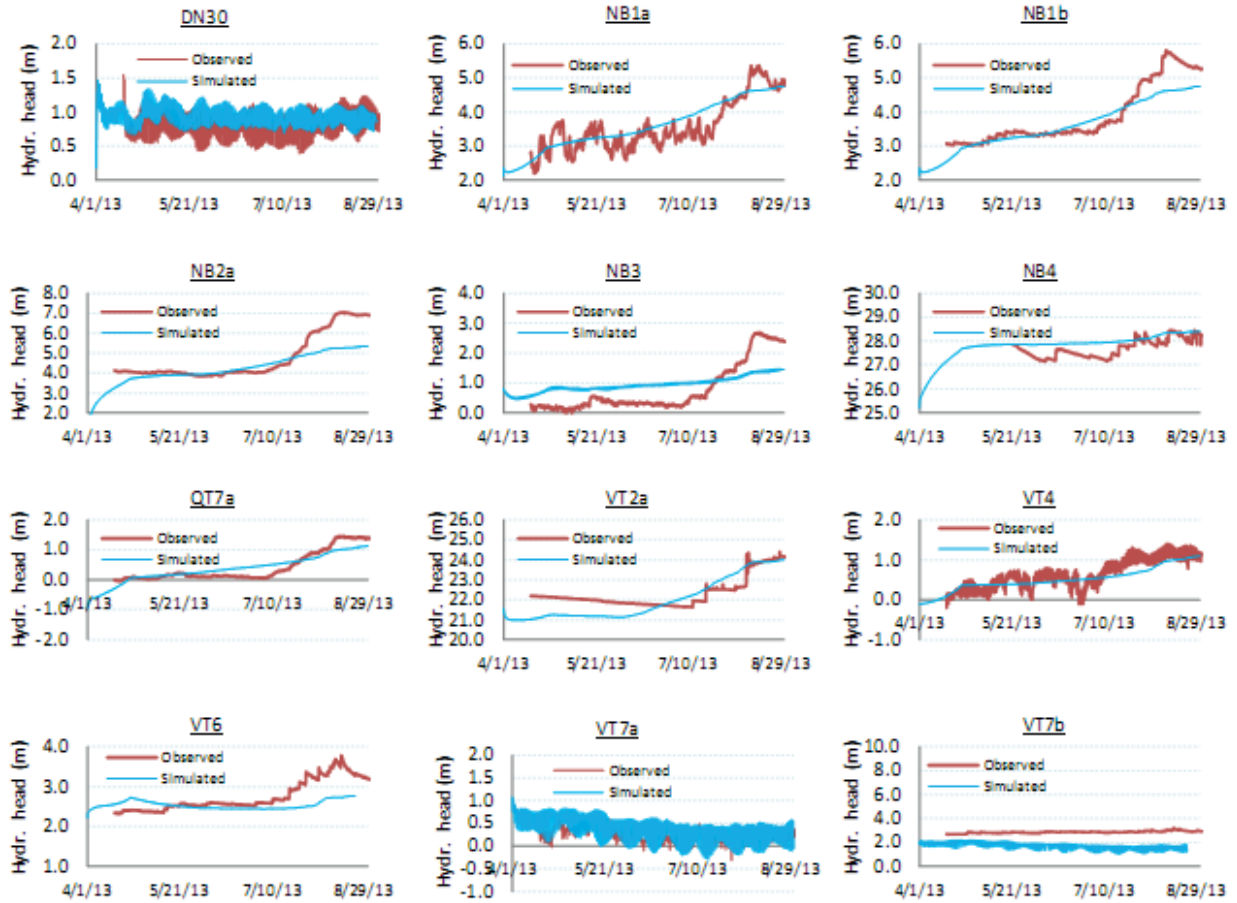


Figure 3. Comparison between the observed and simulated values at different observation points

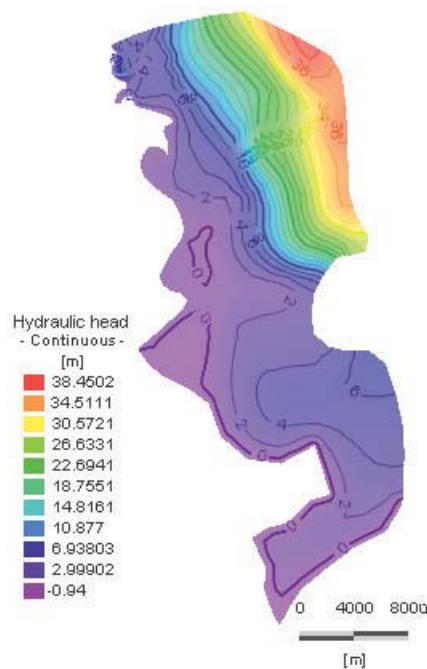


Figure 4. Spatial distribution of computed groundwater level



Besides the stratigraphic and geologic properties of the aquifer, the boundary conditions influence significantly the accuracy of the model results as well. For the determination of the abstractions and pumping rate of private wells, no direct measurement are available. The amount of abstraction have been estimated based on the survey of industrial zones and residential areas. It is obvious that this is a relatively rough estimation when applying to the model. The river-groundwater interactions is also an important boundary impacting on the groundwater flow of areas close to the Thi Vai river. The in-transfer rate and out_transferate have not been sufficiently investigated so far.

6. Conclusion

The numerical model FEFLOW was used to assess the variations of groundwater behavior in the Thi Vai river catchment and its vicinity. The calibration is based on the observation points with high resolution of groundwater data for a short period from April to August 2013. During the calibration, the domain has been separated in zones with different aquifer's properties such as hydraulic conductivity, porosity, specific storage. In general, FEFLOW was performed successfully in simulating groundwater flow in complex porous aquifers. The simulated groundwater levels showed quite good agreement with the observed data, achieving the MAE and RMS ranging from 0.1-1.07 and from 0.15-1.32, respectively. Modeled results also revealed that groundwater levels in this study area are not only affected by rainfall infiltration, but also by the variation of the Thi Vai river water and tidal levels.

In our ongoing research, the measured data of groundwater levels will be continuously expanded and used to increase the calibration and validation period of groundwater levels. In addition, further investigations of the aquifer properties and pumping rate are needed to improve the accuracy of the model results.



References

- [1] Akther, H., Ahmed, M.S., Rasheed, K.B.S., 2009. Spatial and temporal analysis of groundwater level fluctuation in Dhaka City, Bangladesh. *Asian J Earth Sci.* 2, 49-57.
- [2] Almedeij, J., Al-Ruwaih, F., 2006. Periodic behavior of groundwater level fluctuation in residential areas. *J Hydrol.* 328, 677-684.
- [3] Berg, M., Stengel, C., Pham, T.K.T., 2007. Magnitude of arsenic pollution in the Mekong and Re River deltas: Cambodia and Vietnam. *Sci Total Environ.* 372, 413-425.
- [4] Chen, D.B., 2002. Investigation the Balance at North Stradbroke Island with MODFLOW and PEST-ASP. Balancing the Groundwater Budget. 7th IAH National Groundwater Conference, Darwin, Australia.
- [5] Diersch, H.G., 1979. *FEFLOW – Finite element modeling of flow, mass and heat transport in porous and fractured media*, Springer, 2014, Berlin Heidelberg, XXXV, 996p., ISBN 978-3-642-38738-8, ISBN 978-3-642-38739-5 (eBook), doi: 10.1007/978-3-642-38739-5.
- [6] Doherty, J., 2001. *PEST-ASP User's Manual*. Watermark Numerical Computing, Brisbane, Australia.
- [7] DONRE_Ba Ria-Vung Tau, 2010. Study and installation on groundwater monitoring, Ba Ria-Vung Tau.
- [8] Hoque, M.A., Hoque, M.M., Ahmed, K.M., 2007. Declining groundwater level and aquifer dewatering in Dhaka metropolitan area, Bangladesh: causes and quantification. *Hydrogeol. J.* 15, 1523-1534.
- [9] Mende, A., Astorga, A., Neumann, D., 2007. Strategy for groundwater management in developing countries: a case study in northern Costa Rica. *J Hydrol.* 334, 109-124.
- [10] Panicoli, C., Khlaifi, I., Lecca, G., Giacomelli, A., Tarhouni, J., 2001. A modelling study of seawater intrusion in the Korba Coastal Plain, Tunisia. *Phys Chem Earth*, 26(4), 345-351.
- [11] *PCP, 2010*. <http://en.baria-vungtau.gov.vn/web/guest>
- [12] Perera, E.D.P., Jinno, K., Tsutsuni, A., Hiroshiro, Y., 2010. A numerical study of the saline contamination of a coastal aquifer. *Proceedings of the ICE-Water Management*, 163(7), 367-375.
- [13] Phien-wej, N., Giao, P.H., Nutalaya, P., 2006. Land subsidence in Bangkok, Thailand. *Eng Geol.* 82, 187-201.



- [14] Sekhar, M., Rasmi, S.N., Sivapullaiah, P.V., Ruiz, L., 2004. Groundwater Flow Modeling of Gundal Sub-basin in Kabini River Basin, India. *Asian Journal of Water, Environment and Pollution*, Vol. 1, No. 1 & 2, pp. 65.
- [15] McDonald, M.G., Harbaugh, A.W., 1988. A modular three dimensional Finite-Difference Groundwater flow model. U.S Geological Survey Techniques of Water Resources Investigations, book 6, chap. A1, 568 p.
- [16] Roger, G.H., Ismael, S.P., 2002. Groundwater flow modeling in the Yucatan karstic aquifer, Mexico. *Hydrogeol J.* 10, 539-552.
- [17] Shamsudduha, M., Chandler, R.E., Taylor, R.G., 2009. Recent trends in groundwater levels in a highly seasonal hydrological system: the Ganges-Brahmaputra-Meghne Delta. *Hydrol Earth Syst Sci.* 13, 2373-2385.
- [18] Timothy H. D., 2006. Space geodesy: Subsidence and flooding in New Orleans. *Nature* 441, 587-588.
- [19] Uppenberg, S., Wallgren, O., Åhman., 1997. Saturated horizontal hydraulic conductivity in an acid sulphate soil. *Avdelningsmeddelande / Sveriges lantbruksuniversitet, Institutionen för markvetenskap, Avdelningen för lantbrukets hydroteknik (0282-6569).*
- [20] Werner, A.D., Simmons, C.T., 2008. Impact of sea-level rise on sea water intrusion in coastal aquifers. *Ground Water*, 47(2), 197-204.



Accumulation of contaminants in mangrove species *Rhizophora apiculata* along Thi Vai River in the South of Vietnam

Hoang Anh Nguyen¹, Otto Richter¹, Duc Hoan Huynh³, Kim Linh Nguyen²,
Marit Kolb⁴, Van Phuoc Nguyen², Tran Tran Bao²

¹ Institute for Geoecology, Langer Kamp 19c, 38106 Braunschweig, Germany

² Institute for Environment & Resources, 142 To Hien Thanh Str., Ho-Chi-Minh City, Vietnam

³ CanGio Mangrove Forest Protection Management Board, Rung Sac Str., CanGio, Vietnam

⁴ Institute for Ecological Chemistry, Hagenring 30, 38106 Braunschweig, Germany

Abstract

Located at the lower section of Dong Nai River system, Thi Vai River is the main water way connecting Ho-Chi-Minh City in Vietnam with other countries. Water ports and industrial zones along the river therefore were developed and have been operating since the 1990s; these increasing activities have caused severe pollution in the catchment.

The environment along the river has been subjected to pollution loads. The mangroves, one of the most productive ecosystems of the world, are not excluded and suffer enormously from pollution and destruction of their habitat.

This study focuses on analyzing the amount of contaminants absorbed and stored in mangrove species *Rhizophora apiculata* along ThiVai River. The result shows that not all pollutants act in the same destructive way on the plants; the mangroves are very tolerant to high doses of contaminants. The accumulations of PAHs, PCBs and metals show a large variation in tree organs. The highest amounts of PAHs, PCBs and metals are stored in leaves, then in roots, stem barks and lowest are in the stem cores.

Key Words: mangrove, *Rhizophora apiculata*, PAHs, PCBs, heavy metals.



1. Introduction

Pollution has been a major problem in the catchment of Thi Vai River which is located in the downstream of Dong Nai River system in Vietnam, particularly during the last two decades. Emissions of pollutants from industries have already led to damages in natural communities and environments in a wide range of the area.

The Thi Vai has been characterized by a rapid development of industry as well as by serious environmental pollution. The mangrove ecosystems, due to the increasing population growth, the increasing industrial and agricultural areas, have been directly or indirectly affected by many pollutants released into the area. The effects of environmental pollution on mangrove ecosystems aroused the concern of the public and politicians.

This study aims to assess the polluted situation in Thi Vai Catchment by analysing the concentrations of organic and inorganic substances in the soils and in the organs of mangrove species *Rhizophora apiculata* at Thi-Vai River and to relate these to locations within the core of the forest.

Exposure of inorganic substances (heavy metals) may have natural or anthropogenic sources. In which, the anthropogenic sources here are mainly from industrial plants, the main cause, which emit high concentrations in the environment.

Organic compounds, such as polycyclic aromatic hydrocarbons (PAHs) and chlorinated hydrocarbons (PCBs), have a relatively large industrial importance and are produced in large quantities, they are known as relevant to the environmental pollution because they are toxic or persistent in the environment and can accumulate in the food chain. Among the released sources of these harmful organic compounds are mainly from shipping, industry, households and agriculture, from which the pollutants directly or diffusely, released to the rivers or the atmosphere.

There are various ways and means the plants can absorb pollutants, in that the pollutants exist in forms of being dissolved in soil water or trace particles in the air. The introduction of pollutants into the plant is from the soil via the roots and is transported to the upper parts of the plants by xylem or from the atmosphere into the leaves then is translocated to other parts of the plants by phloem.



Other processes are the dry air deposition of dust particles on the plant surface and the absorption of the volatilized bonding chemicals from the ground. The wet deposition, for example, by precipitation, is one entry path, which relates to the above-ground parts of plants.

The bioavailability of these substances in mangroves depends on multiple factors, such as salinity, temperature and redox potential. The bio-concentration of these substances is well documented in mangrove studying and they are different depending on the mangrove species, nevertheless the effects on plant physiology and the toxicity, is still unknown [2].

2. Materials and methods

We examine the types of pollution in the Thi Vai catchment by analyzing the concentrations of substances in different organs of the plants at different positions.

2.1. Site description

Two zones were selected for sampling, one is along the Thi Vai River and the other is inside the Can Gio mangrove forest. Both zones are similar in geo-location and belong to the estuary of the Dong Nai River system.

Thi Vai catchment is one of the most rapidly developed areas dominated by industrial zones during the last two decades, as well as one of the most seriously polluted areas in the Dong Nai river basin. Five sampling positions were chosen along the river. The first position is located on the opposite side of Vedan company, the others are located along the river downward to the sea (Figure 1). The other six positions are located inside the forest, they are used as reference sites.

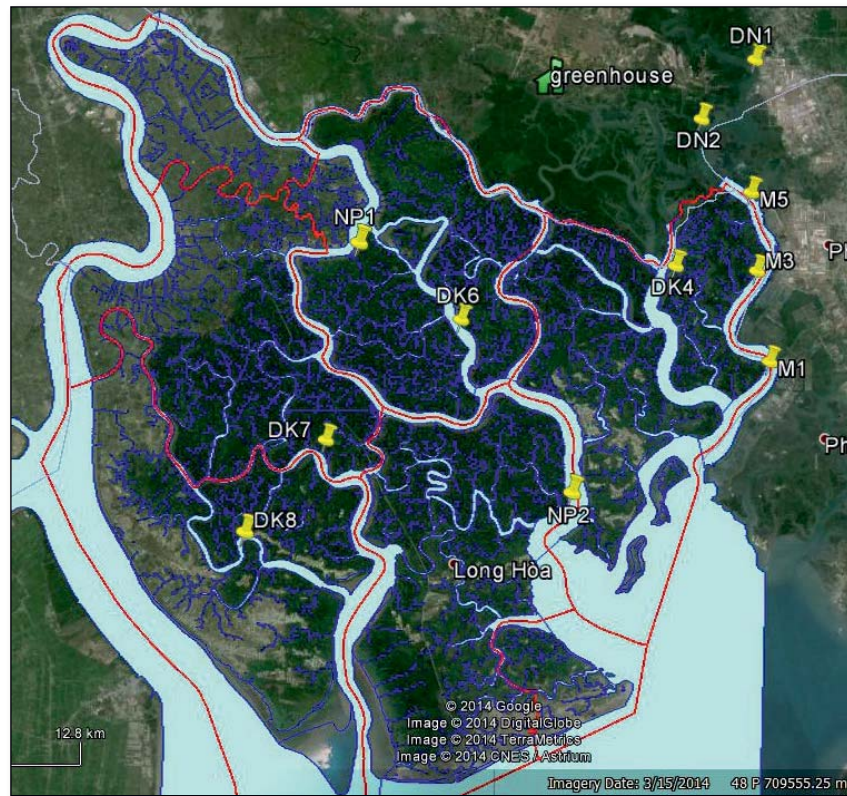


Figure 1. Sampling positions

2.2. Sampling

Healthy and adult trees at 12 locations were sampled include roots, stem cores, stem barks and leaves. Soil samples were also obtained at two depth levels, from the surface to 30 cm and from 30 to 50 cm. The samples were analyzed the parameters PAHs, PCBs and heavy metals.

Measurements of the vegetation were made on the 12 plots (30x30 m²), the following parameters were measured:

- Height, diameter, canopy
- Tree density
- Density of new seedlings

2.3. Sample preparation

Vegetation samples were not washed and were dried in the oven at a temperature of 105°C for about 5h to a constant weight. The dried samples were then ground. To avoid contamination, the mill was thoroughly cleaned and dried after each grinding.



2.4. Data analysis

Statistical analysis was made of the data sets under the assumption that all the concentrations of substances of 12 locations are equal. The data was normalized to mean 0.

Comparison of concentrations between the locations at Thi Vai River and locations at the forest core were made. Correlation between concentrations of substances of different parts of trees and of the soils was analyzed.

3. Results

Based on the assumption that distributions of substances in soils and in tree organs are equal in all positions since the sampling positions are located in the same geological condition. We expect that the distributions of substances concentrations have the same structure in soils and tree organs. Thus, the differentiations in the concentrations among different sites and tree organs are due to the anthropogenic impact.

3.1. Elements (heavy metals) concentrations

Concentrations of elements (metals) in the two zones are shown in Figure 2 for soil and in Figure 3 for tree organs. It is shown that the metals concentrations in the soils located along Thi Vai River (zone 1) are higher than those in the core of the forest (zone 2). The distribution of metals concentrations in zone 1 is more inhomogeneous among different locations compare to those in zone 2.

For plant organs, the accumulation of metals occur highest in the leaves and then the barks and roots, the lowest concentrations occur in the cores of plants. Between the two zones, the accumulation of heavy metals in tree organs at zone 1 is also higher than this in zone 2, especially in the leaves.

The metals are to be found in form of gelatinous, particulate and dissolved in soil water and are available for plants dependent on pH values and redox potential and the chlorine content from the sediment [3]. As mentioned above, there are various sources for the metal pollution and mangroves present themselves as a kind of buffer between the land and the water; they do slow the spread speed of metals. Mangroves show

their ability in storing metal [4]. Their storage capacity is high, especially in the leaves (see also [1]). It should be noted that the roots represent thereby a barrier for metals. Thus, higher metal values were found in sediment and leaves than in the roots (see also the work of [3]).

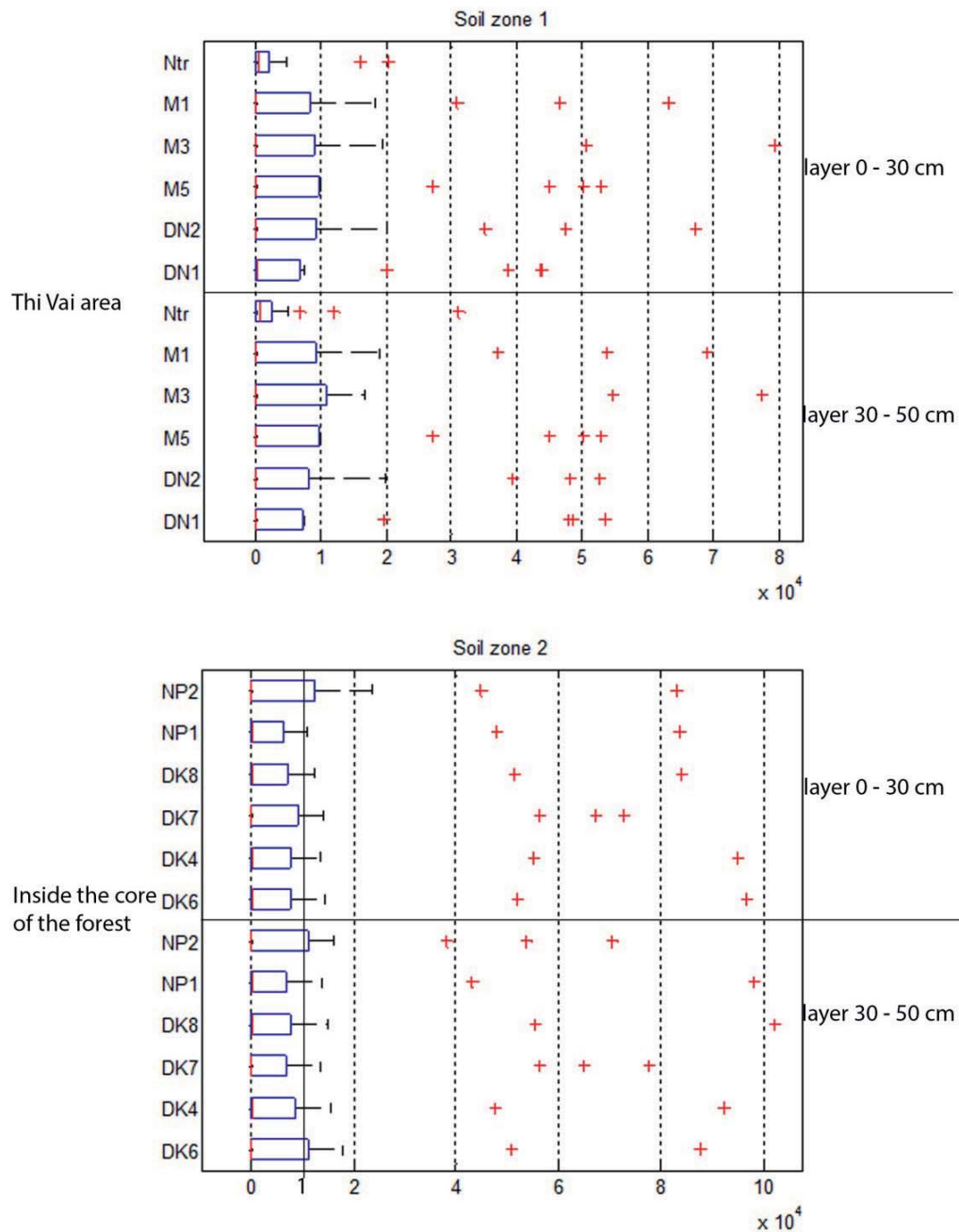


Figure 2. Metal concentrations (mg/kg of dry weight) in the soils at the positions located in two zones. Zone 1 is the Thi Vai area and zone 2 is the core of the forest (Figure 1). It is shown that there are no differences in metal concentrations between the two layers of the soil (layer of 0-30 cm and layer of 30-50 cm) and the concentration distribution at the locations in zone 1 is more varying than this in zone 2.

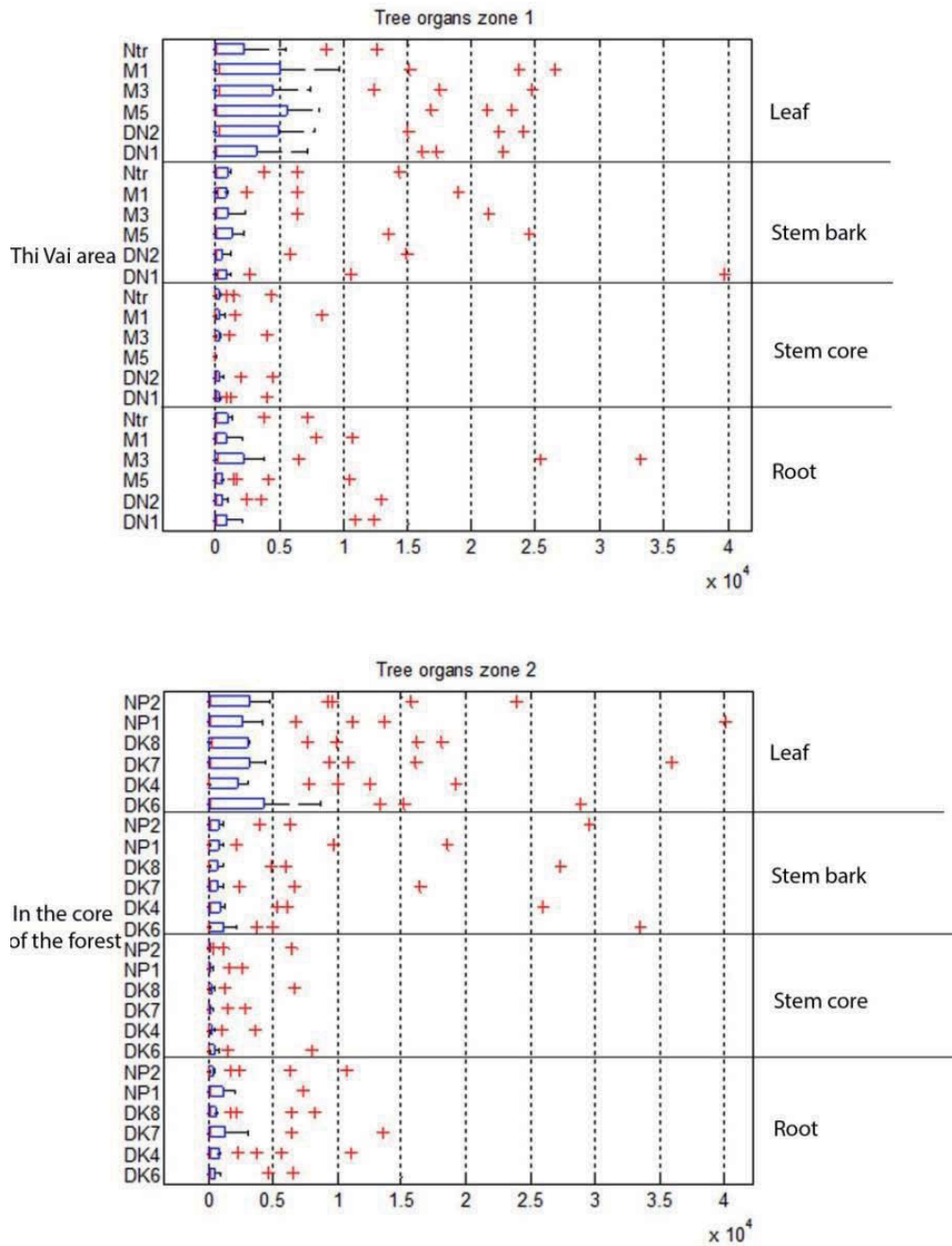


Figure 3. Metal concentrations (mg/kg of dry weight) in the tree organs at the positions located in two zones. Zone 1 is the Thi Vai area and zone 2 is the core of the forest (Figure 1). The leaves are highly accumulated metal concentration much more than the other organs, and their concentrations are even higher at the positions in zone1

Some elements are essential plant nutrients. Plants must obtain the following mineral nutrients from the growing media.

3.1.1. Primary (macro) and secondary nutrients for plants

The macro nutrients are nitrogen, phosphorus and potassium. They are the most frequently required for plants growth. Also, they are needed in the greatest total quantity by plants as fertilizer. The secondary nutrients are calcium, magnesium and sulphur. For most crops, these three are needed in lesser amounts than that the primary nutrients.

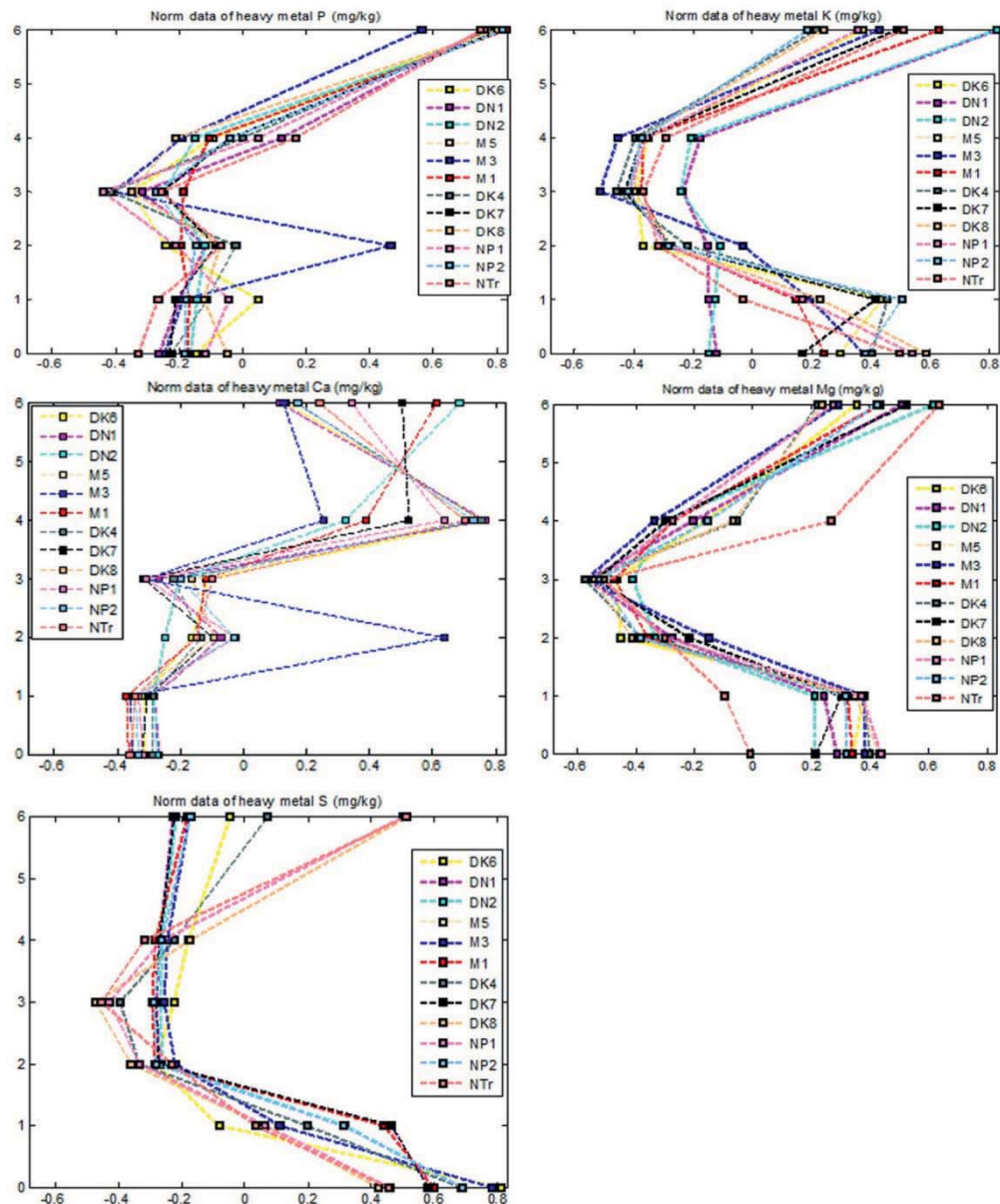


Figure 4. Distribution of essential normalized nutrients concentrations in two layers of soil and in tree organs. The y-axis represents the different objects: 0- soil layer 30-50 cm, 1- soil layer 0-30 cm, 2- tree root, 3- tree stem core, 4- tree stem bark, 6- tree leaves. The x-axis shows the variations of metal concentrations around the mean 0.



The distribution of metals concentrations in different objects of soils and plants as in Figure 4 shows a general tendency for all sampling positions, highest in the leaves and lowest in the stem cores. It is because the primary and secondary nutrients are necessary for the growth processes of plants. They are present in all plant cells and highly concentrate in the leaves, the organ which is responsible for the key growth process of the plants.

There are some outliers in the result. As for sulfur, its concentrations in the leaves at positions along Thi Vai River are lower than the mean value (Figure 4), while these concentrations in the soils and in the roots are higher than the mean value. For Calcium, its concentration is extraordinarily high in the roots at the location M3 (Thi Vai area) while this value is the lowest in the leaves at the same location compare to this value of other locations.

3.1.2. Micronutrients for plants

The micronutrients are boron, chlorine, cooper, iron, manganese, molybdenum, and zinc. These plant food elements are used in very small amounts, but they are just as important to plant development as the major ones. Especially, they work "behind the scene" as activators of many plant functions.

The results show that, among the minor essential nutrients for plants, iron and aluminum have good correlation among different organs of trees and among different positions. The other metals concentrations distributions show the fluctuation among different tree organs and sampling positions, while they still keep the general structure of the distribution curves.

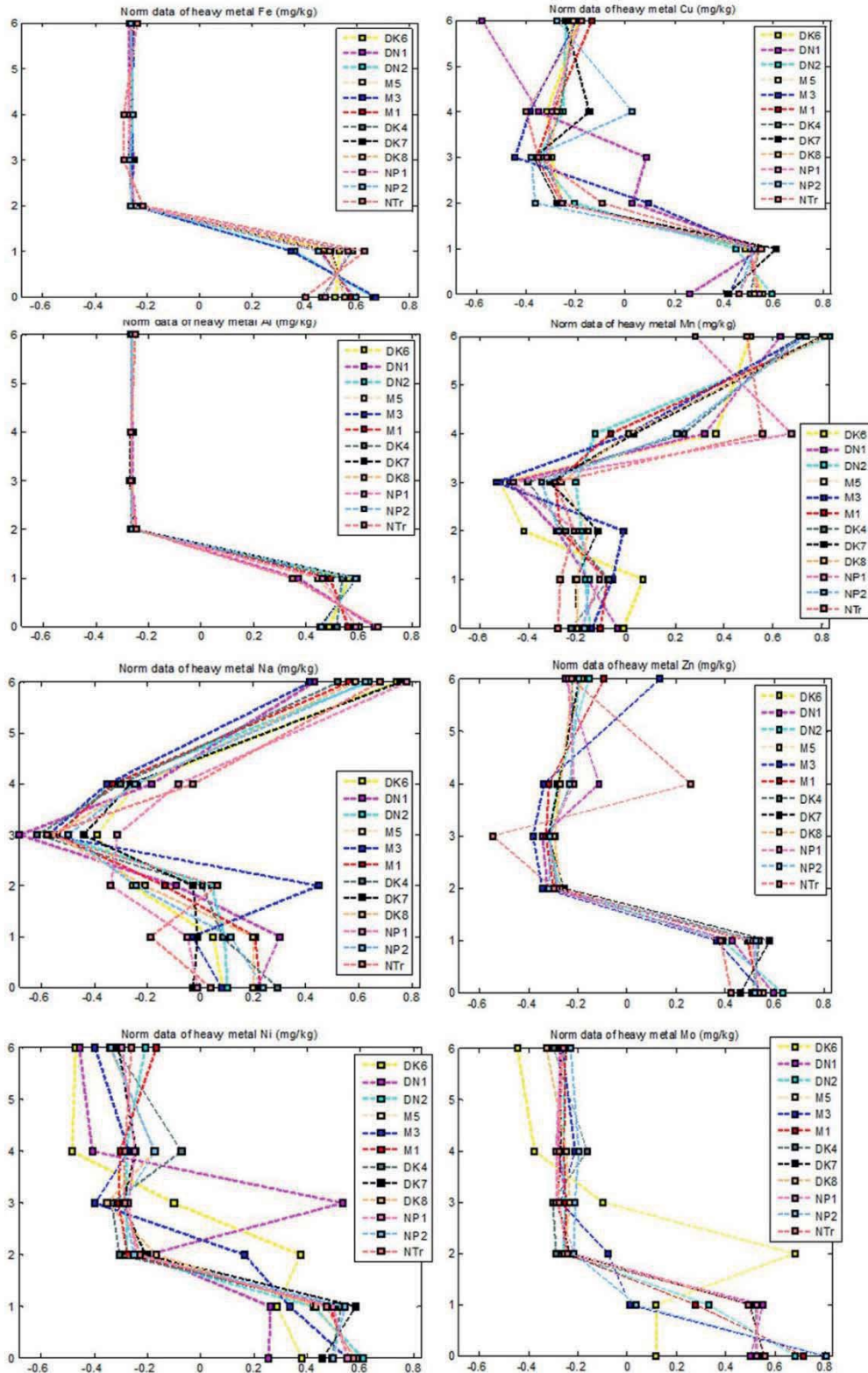


Figure 5. Distribution of minor normalized nutrients concentrations in two layers of soil and in tree organs. The y-axis represents the different objects: 0- soil layer 30-50 cm, 1- soil layer 0-30 cm, 2- tree root, 3- tree stem core, 4- tree stem bark, 6- tree leaves. The x-axis shows the variations of metal concentrations around the mean 0.

3.1.3. Non-essential elements for plants

Chromium, barium, lead and strontium are considered as non-essential elements for plants. Nevertheless, plants uptake them if they exist in the environment. Chromium concentration in tree core at position DN1 located along Thi Vai River is very high (Figure 6), it shows that this substance has been accumulated for a long time and it also proves that the environment in this area is polluted by this substance for a long time.

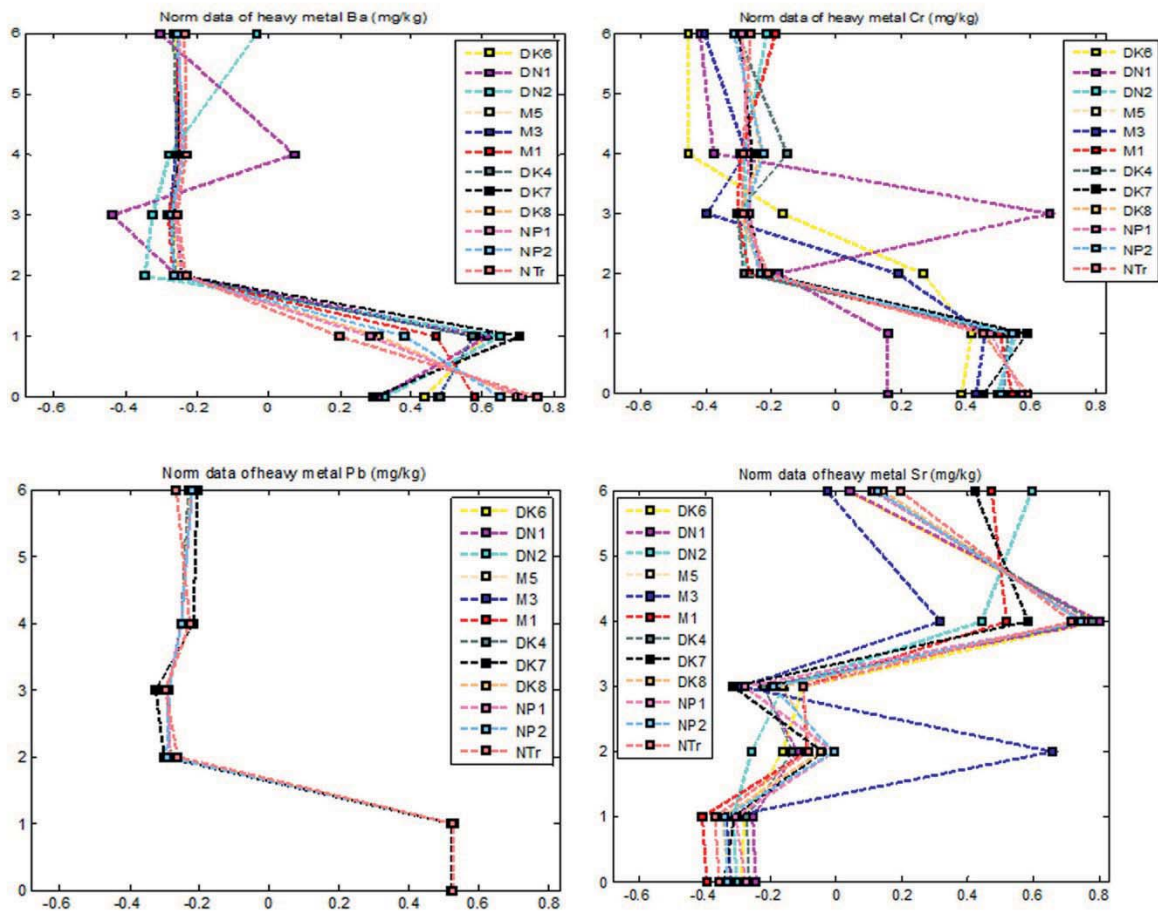


Figure 6. Distribution of non-essential normalized elements concentrations in two layers of soil and in tree organs. The y-axis represents the different objects: 0- soil layer 30-50 cm, 1- soil layer 0-30 cm, 2- tree root, 3- tree stem core, 4- tree stem bark, 6- tree leaves. The x-axis shows the variations of metal concentrations around the mean 0.

3.2. Concentrations of organic substances

The transport of organic substances can be done over the short, medium or long distance transportation. In the short distance transportation, sub-

stances come into the cell through the plasma membrane and the transportation within the cell mainly by diffusion. The middle-distance transportation happens within the tissues without pathways [5].

3.2.1. PAHs concentrations

In soil, PAHs concentrations accumulated highly in zone 1 much more than those in zone 2 (see Figure 7, more than 30 $\mu\text{g}/\text{kg}$ in zone 1 compares to 16 $\mu\text{g}/\text{kg}$ in zone 2). In tree organs (Figure 8) it is similar, the high concentrations of PAHs occur in zone 1, especially in the leaves. It shows that the air is affected by PAHs particles.

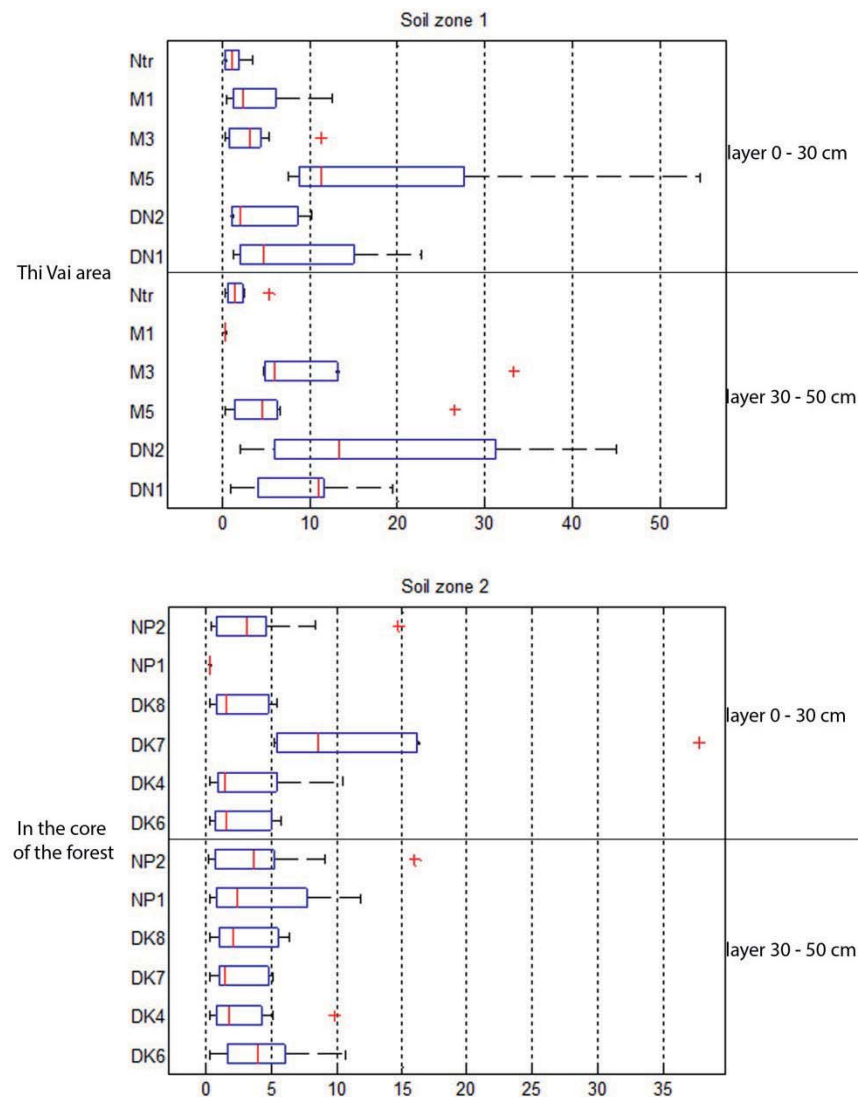


Figure 7. Concentrations of PAHs ($\mu\text{g}/\text{kg}$ dry matter) in the two-layer soils at different positions in zone 1 and zone 2.

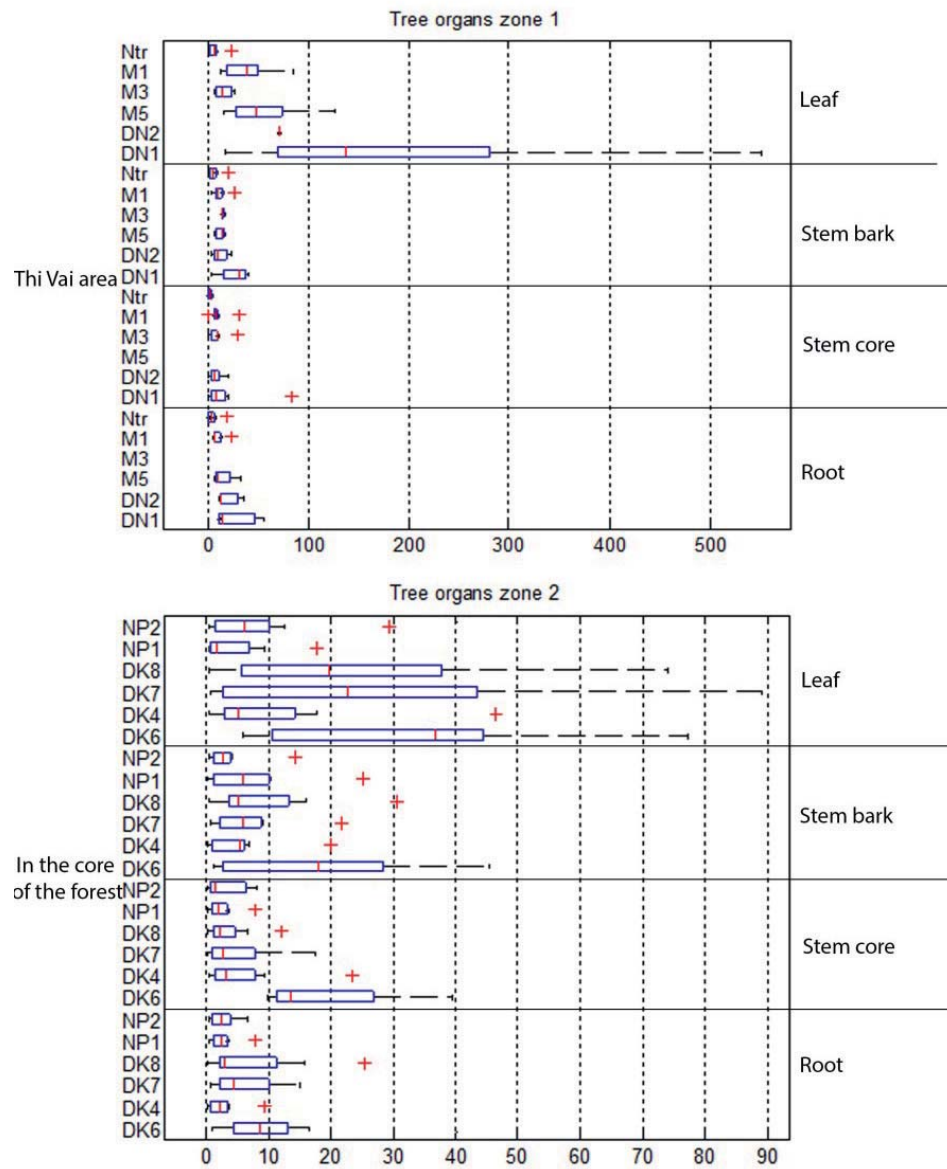


Figure 8. Concentrations of PAHs ($\mu\text{g}/\text{kg}$ dry matter) in the tree organs at different positions in zone 1 and zone 2.

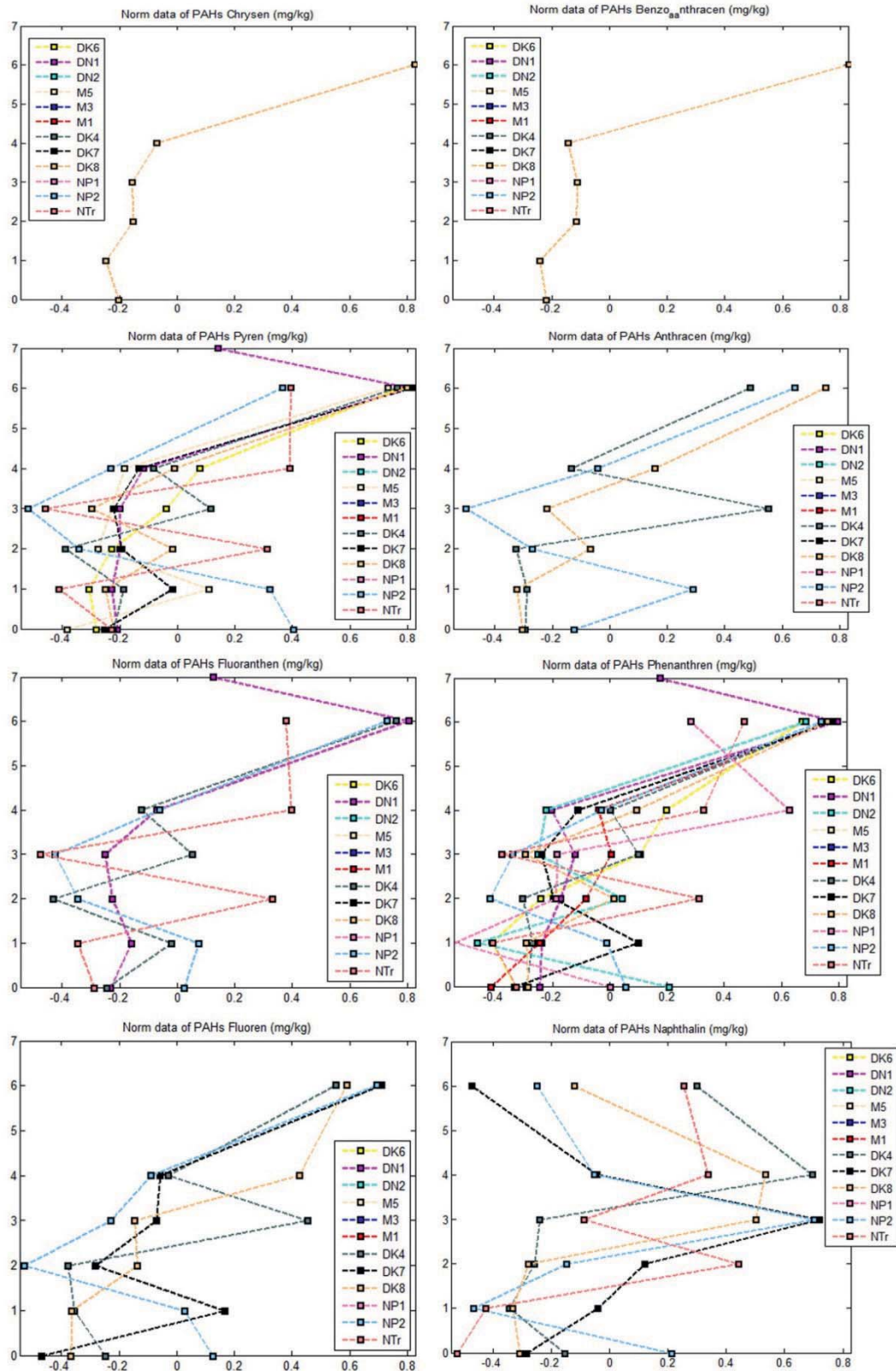


Figure 9. Normalized concentration of each PAH substance in the two-layer soils and in tree organs. The y-axis represents the different objects: 0- soil layer 30-50 cm, 1- soil layer 0-30 cm, 2- tree root, 3- tree stem core, 4- tree stem bark, 6- tree leaves. The x-axis shows the variations of metal concentrations around the mean 0.

3.2.2. PCBs concentrations

In soil, PCBs concentrations accumulated generally similar in zone 1 and zone 2 (see Figure 10) whereas in tree organs (Figure 11) the high concentrations of PCBs occur in zone 1, especially in the leaves. It shows that the air at zone 1 is affected by PCBs particles.

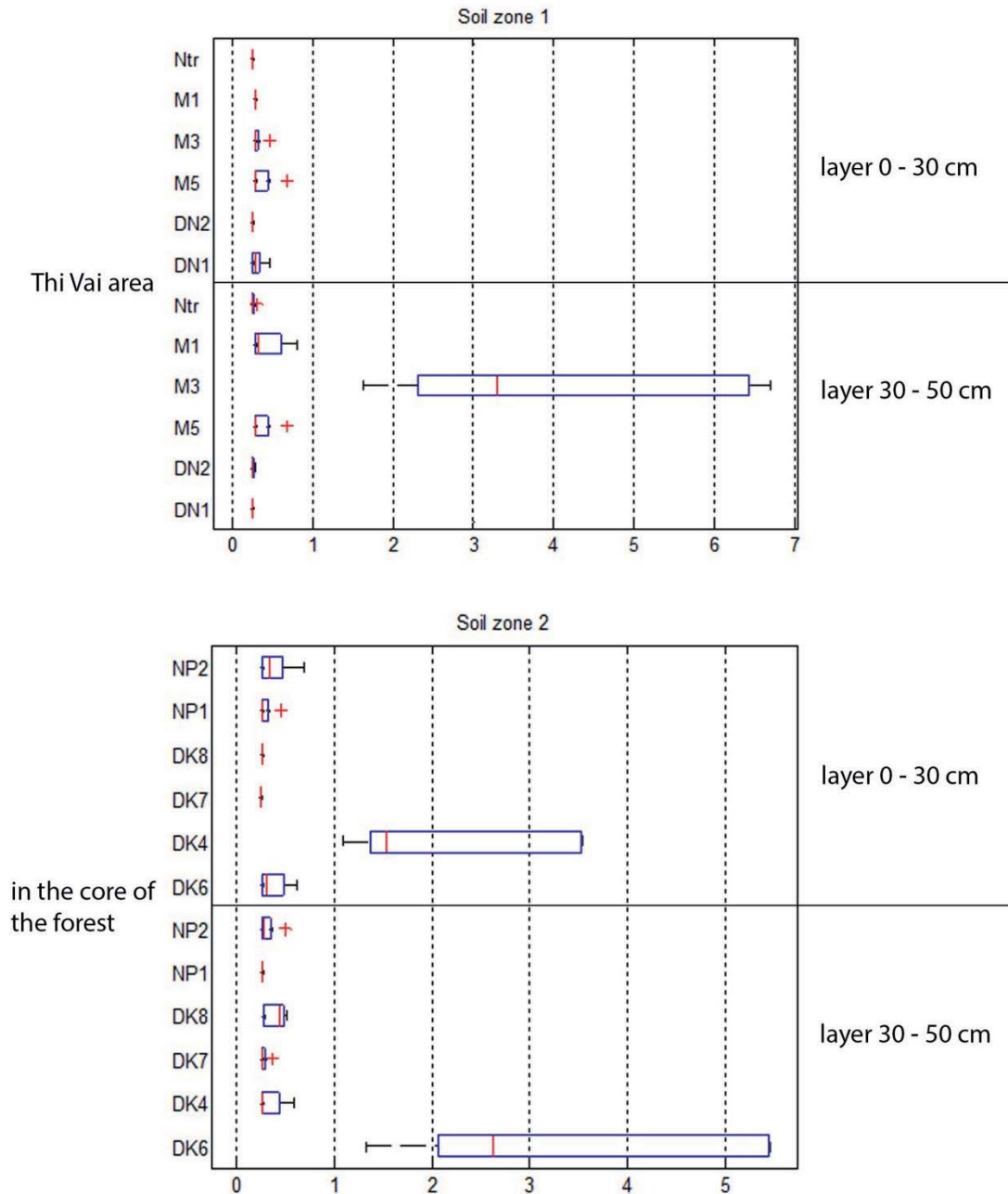


Figure 10. Concentrations of PCBs ($\mu\text{g}/\text{kg}$ dry matter) in the two-layer soils at different positions in zone 1 and zone 2.

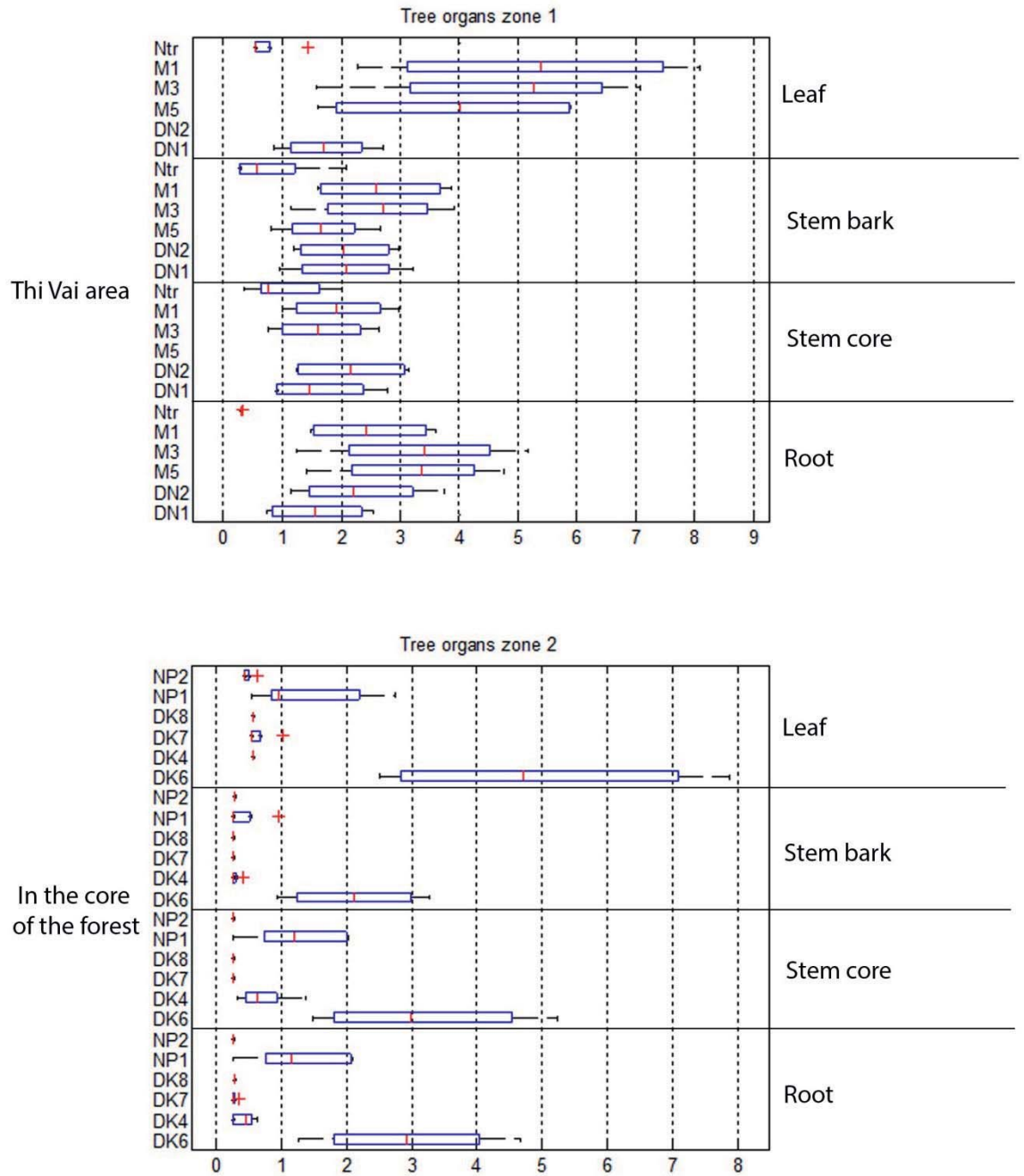


Figure 11. Concentrations of PCBs ($\mu\text{g}/\text{kg}$ dry matter) in the tree organs at different positions in zone 1 and zone 2.

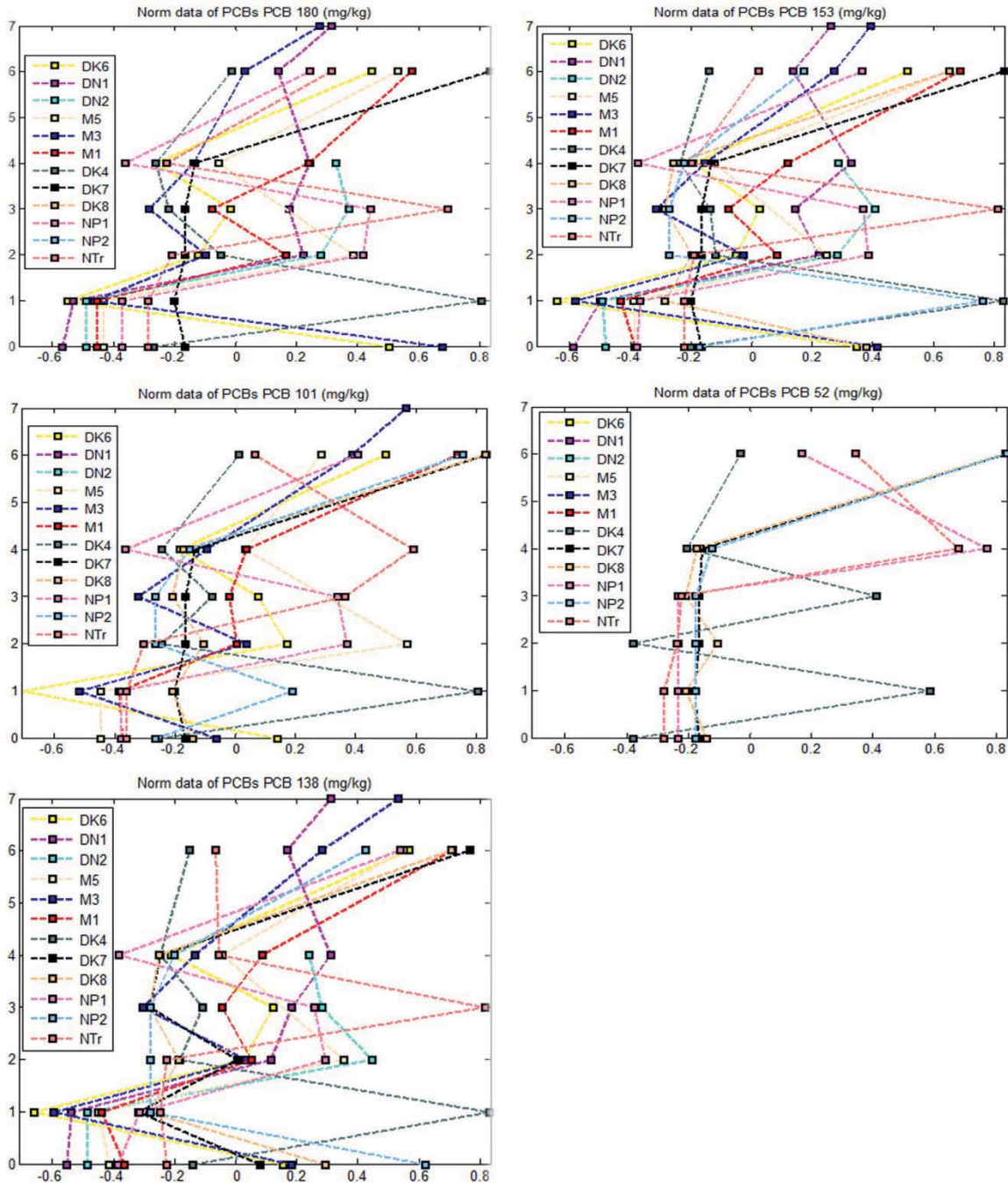


Figure 12. Normalized concentration of each PCB substance in the two-layer soils and in tree organs. The y-axis represents the different objects: 0- soil layer 30-50 cm, 1- soil layer 0-30 cm, 2- tree root, 3- tree stem core, 4- tree stem bark, 6- tree leaves. The x-axis shows the variations of metal concentrations around the mean 0.

In contrast to metals concentrations distributions, PAHs and PCBs concentrations are not distributed correlated, each substance behaves differently from each other among different tree organs positions.



4. Discussion

Mangrove species *Rhizophora apiculata* uptakes the essential elements phosphorus (P), potassium (K), Calcium (Ca), Magnesium (Mg), Sulphur (S) with a high dose which is higher than or equal to that in the soil. The essential elements concentrate highly in the leaves of trees.

For minor nutrients such as iron (Fe), manganese (Mn), zinc (Zn), copper (Cu), aluminum (Al), sodium (Na), nickel (Ni) and molybdenum (Mo), their concentrations inside the tree organs are smaller than those in the soils except Mn and Na which have high concentrations in the leaves. This maybe because of the high concentration of these elements in the ambient air.

There may be a limiting mechanism for the distribution of non-essential metals in the plant.

The upper layer of the soils has somewhat the same concentrations of elements and organic compounds. The concentrations of substances in zone 1 are higher than those in zone 2.

Up to now, there are very few research on PCBs and PAHs in mangroves. Thus there is no statement about their bio-concentration, bioaccumulation and toxicity effects of different types can be made.

5. Conclusion

In conclusion it can be summarized that the bio-concentration and accumulation of organic and inorganic compounds in organs of mangrove species *Rhizophora apiculata* at different locations in the estuary of the Dong Nai River System provide a basic overview.

This result can prove that mangrove vegetation can uptake polluted substances. Up to now, the toxicity thresholds have not been determined yet. Thus, further research is required together with studying the interactions of different substances on the toxicity, the relationships with other factors such as salinity, redox potential etc. and thus comes the theme of the phytoremediation potential of mangroves with the possibility of plants absorb and store pollutants without suffering any damages.



References

- [1] Keshavarz, M., Mohammadikia, D., Gharibpour, F., Dabbagh, A-R., 2012. Accumulation of Heavy Metals (Pb, Cd, V) in Sediment, roots and leaves of Mangrove species in Sirik Creek along the Sea Coasts of Oman, Iran. J. Appl. Sci. Environ. Manage. 2012. 16 (4): p323 -326.
- [2] Michael Lewis, Rachel Pryor und Lynn Wilking (2011). Fate and effects of anthropogenic chemicals in mangrove ecosystems: A review. U.S. Environmental Protection Agency, Office of Research and Development, 1 Sabine Island Drive, Gulf Breeze, FL 32561, USA. Environmental Pollution 159, p2328 – 2346.
- [3] Nazli and Hashim, 2010. Heavy metal concentrations in an important mangrove species *Sonneratia caseolaris* in Peninsular Malaysia. EnvironmentAsia 2010, 3, p50-55.
- [4] Prabhakar, C., Saleshrani, K., Thamaraj, K. and Vellaiyan, M., 2012. Heavy metal pollution in mangrove region: A review. International Journal of Pharmaceutical & Biological Archives 2012; 3(3): p513-518.
- [5] Nultsch, W., 2001. Book of Allgemeine Botanik.



Spatial distribution of diatom assemblages in surface sediments of a deltaic coastal zone in Southern Vietnam

Sandra Costa-Böddeker¹, Lê Xuân Thuyên², Anja Schwarz¹, Hoang Duc Huy², Hoang Trong Khiem² and Antje Schwalb¹

¹ Institut für Geosysteme und Bioindikation, Technische Universität Braunschweig, Technische Universität Braunschweig, Langer Kamp 19c, D-38106 Braunschweig, Germany. E-Mails: s.boeddeker@tu-braunschweig.de, anja.schwarz@tu-bs.de, antje.schwalb@tu-bs.de

² Department of Ecology and Evolutionary Biology, University of Sciences, HCM, Vietnam. E-Mails: lxthuyen@hcmus.edu.vn, hdhuy@hcmus.edu.vn

Abstract

This study aims to evaluate the spatial diatom composition and abundance in surface sediments in the tidal Thi Vai River and the Can Gio mangrove forest in Southern Vietnam in order to evaluate spatial differences in biodiversity as expression of water quality and estuarine dynamics. In January 2013, samples were taken at 33 sites (31 stations in the river and 2 stations in the mangrove forest). A total of 203 diatom taxa belonging to 70 genera were recorded. In both systems, benthic species contributed mostly to species richness. The genus *Nitzschia* contributed with 32% to the total species richness, *Navicula* 20%, *Thalassiosira* 17% and *Gyrosigma* 8%. In general, marine-coastal planktonic species were most abundant with dominance of *Thalassionema nitzschioides* Grunow, a neritic planktonic species, and dominant in 25% of the samples. Minor variations in its spatial distribution probably reflect significant influence of oceanic water in the area. The second most abundant species was *Thalassiosira cerdarkeyensis* Prasad, occurring in 19% of the samples, particularly in the shallow sampling sites upstream. Principal component analysis (PCA) explained 44.8% of the variance, separating diatom assemblages according to the habitat (freshwater/marine species) and longitudinal gradient (upstream/downstream). Canonical correspondence analysis explained 63.3% of the variation in the species-environmental relationship. Total phosphorus was the most significant variable to explain diatom assemblage distribution ($p < 0.001$).



This is the first contribution to the knowledge of diatoms biodiversity in this region, and will provide a key to interpret long-term environmental changes from fossil assemblages archived in sediment cores from this coastal zone.

Key Words: diatoms; surface sediments; coastal zones;
Southern Vietnam.



1. Introduction

Coastal zones are traditionally considered as an important focus of the development of societies. Major cities have developed along coasts. Currently, more than half the world's population lives in coastal areas and this number tends to increase in the coming decades. These areas have an extremely important economic and ecological role, as they provide a number of environmental goods and services. They are among the most productive ecosystems, providing food resources and habitat for commercially important fish and mediate the fluvial delivery of nutrients and other materials to the ocean [1]. Their vulnerability to natural disasters has been increased by human pressure, such as water pollution, eutrophication, deforestation increasing erosion process and climate changes [2]. Vietnam is considered one of the most vulnerable regions in Southeast Asia to climate change impacts, such as sea level increase [3].

Ecological quality can be assessed by the degree to which present-day conditions deviate from reference conditions [4]. Knowledge of the reference condition (or natural baseline) of an ecosystem, prior to disturbance, is fundamental to the design of effective recovery strategies, as it allows a realistic target to be set and provides a benchmark against which managers can evaluate the degree to which their restoration efforts are successful or to define management targets for the future [5-6]. Long-term monitoring data are important for understanding the complexity of environmental change in time and space, but they are rarely available [7]. Therefore, paleoecological approach is an effective tool to evaluate long-term environmental changes [8]. Knowledge of modern assemblages and their relation to environmental variables is fundamental to aid paleoecological interpretation.

Diatom species are powerful indicators and one of the most applied proxy in paleoenvironmental studies. Diatoms (class Bacillariophyceae) are siliceous algae that play a fundamental role in food webs [9]. They have a worldwide distribution and constitute a major component of planktonic and benthic algal communities [10], responding directly and sensitively to many environmental conditions [9]. Diatoms have fast migration rates and colonize new habitats quickly [10], moreover, they are generally well



preserved in sediments due to their siliceous cell wall; different species have different ecological optima and tolerances [8].

In estuarine and shallow coastal benthic environments, diatoms are often the most important and dominant component of the benthic microalgal assemblages [11-12]. Although some work had been done to understand the interactions between diatom populations on mudflats and various environmental factors explaining their spatial and temporal distribution [13,11,14], ecological studies on estuarine and shallow coastal water diatoms are scarce, compared with freshwater and open ocean habitats [15]. Furthermore, studies of the spatial and seasonal distribution of sediment associated diatom assemblages in coastal areas worldwide are mainly restricted to Northern European and North American estuaries [16].

The aim of this study is to assess diatom species composition and distribution in surface sediments and their relation to environmental variables in the Thi Vai River and Can Gio Mangrove Forest (Southern Vietnam) in order to identify main distribution patterns and their relation to the actual ecological state of these systems. This information will provide a key to interpret long-term environmental changes from fossil assemblages archived in sediment cores from this area.

2. Material and methods

2.1. Study area

The study area is located in Southern Vietnam along the Thi Vai River and the Can Gio Mangrove Forest. It is situated in tropical monsoon zone with a single rainy season during the south monsoon from May to October [17]. Annual rainfall exceeds 1000 mm.

The Thi Vai River (Figure 1) has a catchment area of ca. 500km² with irregular semi-diurnal tidal regime with high amplitude (3.3 - 4.1 m). It forms a deltaic estuary (Dong Nai Province) and flows into the South China Sea. It flows for 76 kilometres through Bà Rịa–Vũng Tàu Province and Đồng Nai Province. Because several companies located along the river discharge untreated wastewater into the river it was considered ecologically dead since 1995.

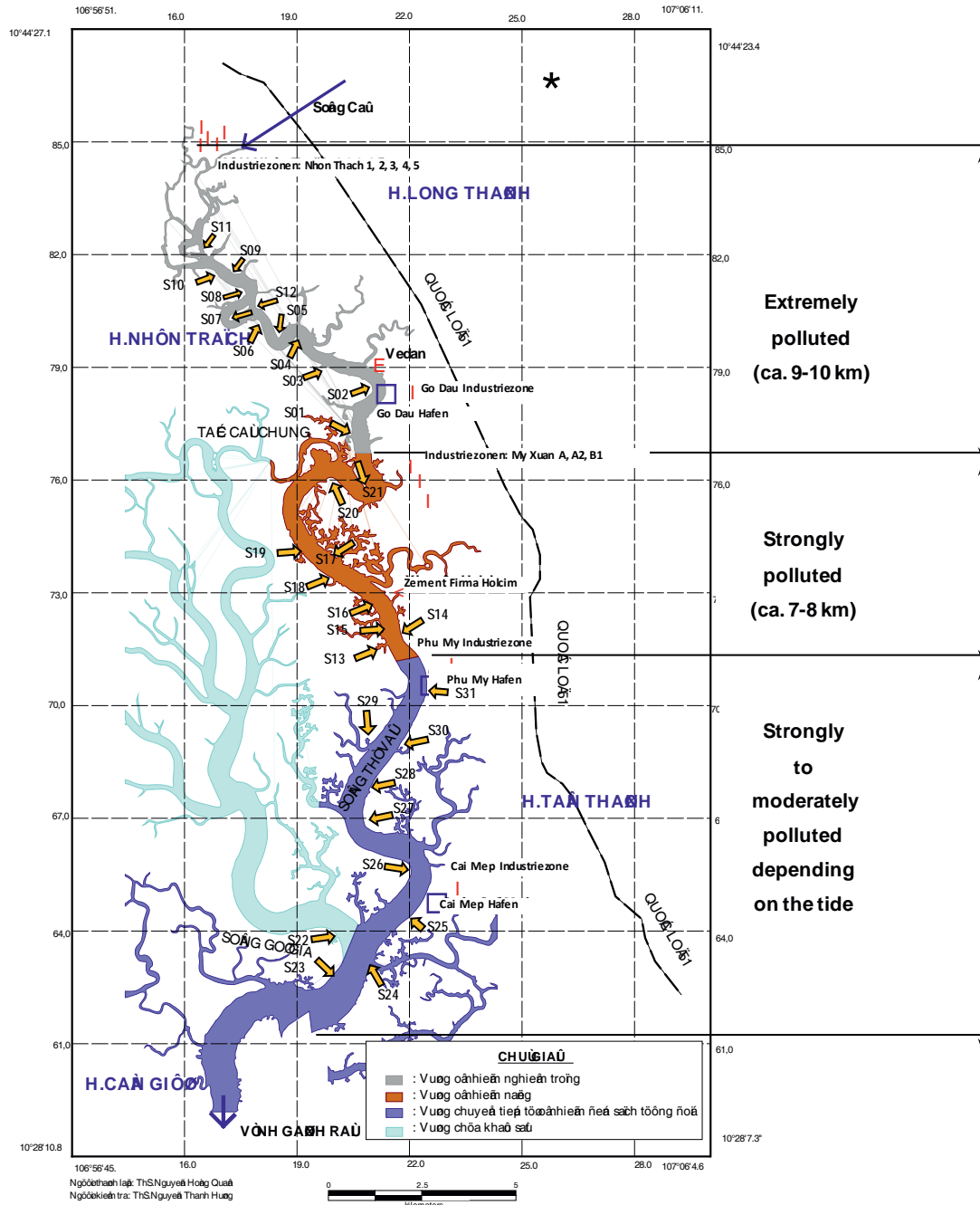


Figure 1. Map of Thi Vai River showing the location of sampling sites. Water quality in 2006 (Source: IER, Vietnam Nat. Uni. HCMC)

Can Gio Mangrove Forest (Figure 2) is located ca. 50 km south of Ho-Chi-Minh City covers an area of 71,964 ha [18] on the delta of the Saigon-Dong Nai River system which is the second largest river system in southern Vietnam after the Mekong Delta [17]. The coordinates of the study area are 10°22' - 10°40' N and 106°46' - 107°01' E [18].

Expanding aquaculture and salt farming, as well as coastal erosion induced by waves particularly during storms (typhoons) threatens mangrove forests in Viet Nam [18].

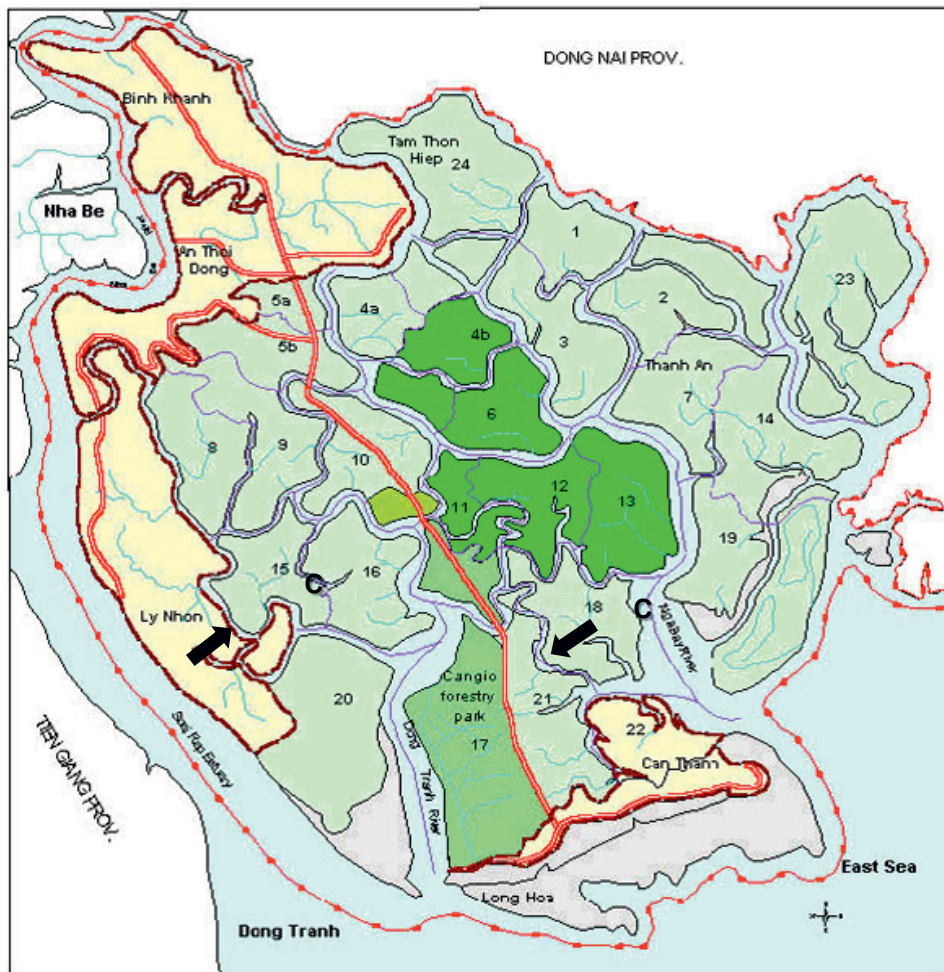


Figure 2. Map of Can Gio Mangrove showing the location of sampling sites. (Source: www.unesco.org)

2.2. Sampling

In January 2013, thirty-three surface sediments were collected using a Petite Ponar[®] grab on the ebb tide, representing 31 samples along the Thi Vai River and 2 samples in representative area of the Can Gio Mangrove forest (Figures 1 and 2). These samples were kept at 4°C until be processed. Using a multi-parameter measurement WTW Multi 350i[®] were measured *in situ* the following water parameters: Temperature (°C), pH, conductivity (mS/cm), salinity (ppt), dissolved oxygen (mg/L) and oxygen saturation (%). Coordinates and water depth were obtained through sonar Lowrance[®]. Water samples were collected from each site for total ni-



trogen (TN), ammonium (NH_4), nitrate (NO_3^-), orthophosphate (PO_4) and total phosphorus (TP) analyses. These analyses were made at Institute Environmental Resources Laboratory (Vietnam National University) using the Standard Methods for Examination of Water and Wastewater (SMEWW) [19].

2.3. Diatom analysis

Diatom samples were processed and analyzed at Institut für Geosysteme und Bioindikation (Technische Universität Braunschweig). Diatom slides were prepared following standard techniques [20]. Samples were previously treated with H_2O_2 30% and HCl 37% in order to remove organic matter and carbonates respectively. Samples were evaporated onto coverslips and mounted with Naphrax[®] (refractive index 1.7) on permanent glass slides. A minimum of 350 valves were counted per sample and counting efficiency of 90% (equation in [20]). Counts were made using a Leica[®] DM 5000 B light microscope with oil immersion objective (1000X magnification). Species abundances were expressed as percentages. Species were identified according to standard works and specific floras [20-21].

2.4. Data analysis

To examine major trends in diatom composition multivariate statistical analyses were performed. Principal component analysis (PCA) was employed to analyze the distribution of surface sediment diatom assemblages [24]. Before computation, diatom data were square root transformed, and environmental variables (except for pH) were logarithmically transformed ($x+1$) in order to stabilize variances. The gradient length of 2.3 SD indicates that unimodal-based numerical techniques would be appropriate to be applied to our data, therefore, direct gradient ordination by canonic correspondence analysis (CCA) and Monte Carlo permutation tests (999 permutations) were used to determine environmental variables that explain significant ($p \leq 5$) patterns in the diatom distribution. Data transformation and ordinations were carried out using the program CANOCO version 5 [25].



3. Results

3.1. Environmental variables

Table 1 shows the water physico-chemical parameters measured at each sampling site and their location.

Sites located upstream of the estuarine section of the Thi Vai River were deeper than downstream ones. The water temperature ($T^{\circ}\text{C}$) range was between 25.2°C und 30.4°C . Minimum pH value (7.1) was measured at both upstream sites TV-SS02 and TV-SS11. Maximum pH (7.8) was recorded at the outermost downstream site TV-SS23. Conductivity mean value was 39.4 mS/cm and salinity 25.3 ppt. Dissolved oxygen concentration (DO) measured at upstream sites (TV-SS01 to TV-SS12) were lower compared to the other sites, ranging between 3.2 and 3.8 mg/L. Oxygen saturation (OSat) values ranged between 25.5% and 73.5%.

In general, nutrients values were higher at the upstream sites. Twenty-three sites had ammonium (NH_4) concentrations below detection limit, particularly towards downstream sites, averaging 0.03 mg/L. The maximum nitrate (NO_3^-) concentration measured was 0.36 mg/L at TV-SS09 sample. Total nitrogen (TN) showed some variation among sites, ranging between 0.92 mg/L(TV-SS22) and 8.48 mg/L (TV-SS09). Total phosphorus (TP) ranged from 0.06 mg/L (TV-SS24, TV-SS26, TV-SS27, TV-SS31 and CG-SS02) to 0.12 mg/L (TV-SS07, TV-SS11 and TV-SS17) averaging 0.08 mg/L. The highest concentration of orthophosphate (PO_4) was measured at TV-SS07 towards upstream (0.06 mg/L) with mean value of 0.04 among sites.



Table 1. Sampling site locations and physicochemical water parameters measured in the Thi Vai River (TV) and Can Gio Mangrove Forest (CG) including minimum, mean, maximum values and standard deviation (SD).

Sites	Depth (m)	Temp. (°C)	pH (-)	Cond. (mS/cm)	Sal. (ppt)	DO (mg/L)	OSat. (%)	Location	
TV-SS01	1.7	27.1	7.5	39.6	25.4	3.3	41.7	N 10°39'09.7"	E107°00'33.9"
TV-SS02	1.1	28.6	7.1	37.0	23.8	3.7	25.5	N 10°39'22.1"	E107°00'57.1"
TV-SS03	2.1	28.5	7.3	35.6	22.6	3.5	41.7	N 10°40'03.1"	E106°59'55.4"
TV-SS04	3.9	29.0	7.4	33.9	21.4	3.7	51.2	N 10°40'10.0"	E 06°59'52.8"
TV-SS05	1.2	28.6	7.4	33.8	21.2	3.5	42.7	N 10°40'08.9"	E 06°59'36.3"
TV-SS06	1.3	29.1	7.5	31.7	20.0	3.7	48.0	N 10°40'20.9"	E106°59'22.0"
TV-SS07	0.6	29.8	7.4	33.3	20.7	4.5	61.4	N 10°40'29.2"	E106°58'55.8"
TV-SS08	5.9	28.4	7.4	34.6	21.9	3.4	43.4	N 10°40'50.9"	E 06°59'08.0"
TV-SS09	2.4	28.6	7.3	33.7	21.2	3.8	48.5	N 10°41'05.0"	E 06°58'59.1"
TV-SS10	0.8	28.3	7.2	34.8	22.1	3.4	44.2	N 10°41'01.1"	E 06°58'47.4"
TV-SS11	0.8	29.0	7.1	33.4	21.0	3.2	40.1	N 10°41'38.2"	E106°58'30.7"
TV-SS12	5.0	28.3	7.3	35.7	22.5	3.3	42.5	N 10°40'38.5"	E106°59'17.9"
TV-SS13	0.8	27.2	7.4	43.4	28.1	3.7	48.0	N 10°33'52.2"	E107°00'37.2"
TV-SS14	1.2	28.4	7.5	43.4	28.1	4.7	60.4	N 10°33'25.8"	E107°00'49.8"
TV-SS15	1.1	28.1	7.4	43.0	27.9	4.3	54.8	N 10°34'23.1"	E107°01'00.1"
TV-SS16	1.1	28.9	7.4	42.6	27.6	4.5	57.8	N 10°35'00.0"	E107°01'27.2"
TV-SS17	1.4	30.4	7.4	41.9	27.1	5.3	70.2	N 10°35'41.2"	E107°01'31.4"
TV-SS18	2.5	30.3	7.4	41.9	27.2	5.2	70.8	N 10°35'43.8"	E107°01'11.6"
TV-SS19	0.6	29.6	7.3	41.6	27.0	4.5	58.9	N 10°36'28.6"	E107°00'36.2"
TV-SS20	0.6	29.5	7.3	40.3	26.0	4.9	62.9	N 10°37'55.7"	E107°00'01.2"
TV-SS21	0.7	28.8	7.2	40.1	25.8	4.2	54.2	N 10°38'03.8"	E107°00'49.6"
TV-SS22	1.6	27.2	7.6	44.1	28.6	4.4	55.4	N 10°31'36.2"	E107°00'09.1"
TV-SS23	0.7	27.6	7.8	45.0	29.1	5.2	67.5	N 10°30'53.8"	E107°00'13.1"
TV-SS24	0.9	25.2	7.7	44.6	29.0	5.4	69.3	N 10°31'05.6"	E107°01'00.6"
TV-SS25	0.5	27.9	7.5	44.4	28.8	4.6	62.0	N 10°31'59.8"	E107°01'06.8"
TV-SS26	0.2	28.6	7.6	43.8	28.4	4.9	62.3	N 10°32'24.9"	E107°01'29.4"
TV-SS27	1.8	29.1	7.6	43.6	28.3	5.2	69.4	N 10°32'59.8"	E107°01'18.0"
TV-SS28	0.9	30.0	7.6	43.2	28.0	5.5	73.5	N 10°33'10.6"	E107°00'48.5"
TV-SS29	0.5	29.8	7.5	42.7	27.7	5.5	72.8	N 10°34'01.0"	E107°00'39.7"
TV-SS30	0.7	30.0	7.5	42.7	27.7	5.5	71.8	N 10°33'52.8"	E 07°01'04.5"
TV-SS31	1.5	28.8	7.6	42.3	27.4	4.9	62.4	N 10°34'36.6"	E107°01'32.8"
CG-SS01	0.7	27.4	7.3	39.2	25.1	4.0	49.4	N 10°30'09.6"	E106°55'54.0"
CG-SS02	0.7	29.2	7.5	37.1	23.6	5.3	69.4	N 10°27'48.3"	E106°49'25.9"
<i>Min.</i>	0.2	25.2	7.1	31.7	20.0	3.2	25.5	—	—
<i>Mean</i>	1.4	28.5	7.4	39.4	25.3	4.3	55.3	—	—
<i>Max.</i>	5.9	30.4	7.8	45.0	29.1	5.5	73.5	—	—
<i>SD</i>	1.27	1.08	0.16	4.22	3.01	0.77	12.06		



Table 2. Concentration of ammonium, nitrate, total nitrogen, total phosphorus and orthophosphate in the Thi Vai River (TV) and Can Gio Mangrove Forest (CG) including minimum, mean, maximum values and standard deviation (SD).

Sites	NH ₄ ⁺ (mg/L)	NO ₃ ⁻ (mg/L)	TN (mg/L)	TP (mg/L)	PO ₄ (mg/L)
TV-SS01	< 0.02	0.29	0.99	0.09	0.04
TV-SS02	< 0.02	0.32	1.77	0.11	0.04
TV-SS03	< 0.02	0.31	3.86	0.10	0.04
TV-SS04	< 0.02	0.32	3.25	0.09	0.04
TV-SS05	0.040	0.34	4.19	0.10	0.05
TV-SS06	0.020	0.33	4.81	0.10	0.05
TV-SS07	0.040	0.31	2.30	0.12	0.06
TV-SS08	0.020	0.33	7.27	0.10	0.05
TV-SS09	0.020	0.36	8.48	0.10	0.05
TV-SS10	< 0.02	0.35	6.04	0.10	0.04
TV-SS11	0.060	0.35	7.80	0.12	0.05
TV-SS12	< 0.02	0.32	6.21	0.08	0.04
TV-SS13	< 0.02	0.27	1.41	0.07	0.03
TV-SS14	< 0.02	0.30	2.37	0.08	0.04
TV-SS15	< 0.02	0.27	1.04	0.10	0.04
TV-SS16	< 0.02	0.29	1.64	0.09	0.04
TV-SS17	0.030	0.29	2.80	0.12	0.05
TV-SS18	< 0.02	0.26	0.97	0.09	0.04
TV-SS19	0.020	0.25	2.54	0.10	0.04
TV-SS20	0.030	0.26	2.72	0.08	0.04
TV-SS21	0.020	0.29	3.38	0.08	0.04
TV-SS22	< 0.02	0.23	0.92	0.07	0.03
TV-SS23	< 0.02	0.20	2.21	0.07	0.03
TV-SS24	< 0.02	0.23	2.50	0.06	0.03
TV-SS25	< 0.02	0.19	1.81	0.07	0.03
TV-SS26	< 0.02	0.26	3.18	0.06	0.03
TV-SS27	< 0.02	0.27	2.08	0.06	0.03
TV-SS28	< 0.02	0.27	2.83	0.08	0.03
TV-SS29	< 0.02	0.27	4.59	0.07	0.03
TV-SS30	< 0.02	0.28	2.94	0.07	0.03
TV-SS31	< 0.02	0.29	2.54	0.06	0.03
CG-SS01	< 0.02	0.18	1.63	0.07	0.03
CG-SS02	< 0.02	0.21	1.35	0.06	0.03
<i>Min.</i>	0.02	0.18	0.92	0.06	0.03
<i>Mean</i>	0.03	0.28	3.10	0.08	0.04
<i>Max.</i>	0.06	0.36	8.48	0.12	0.06
SD	0.01	0.05	2.01	0.02	0.01

3.2. Diatoms

A total of 203 diatom taxa, belonging to 70 genera, were identified in the surface sediments of the Thi Vai River and Can Gio Mangrove forest. Because no diatoms were found at TV-SS30, only 32 samples were included in the subsequent analyses. Only diatom taxa with a relative abundance $\geq 2\%$ in at least two samples were included in the statistical analyses (in total 28 taxa, Table 3). The most abundant taxa was *Thalassionema nitzschioides* Grun., a neritic planktonic species being dominant (relative abundance $\geq 50\%$) in 25% of the samples, particularly at downstream sites. *Thalassiosira cerdarkeyensis* Prasad was the second most abundant species with high relative abundance, mostly in the sites upstream (maximum relative abundance 45% at TV-SS07).

Considering species richness (i.e. number of species in a sample, without taking into account their abundance) the most representative genera in all sampled sites contains benthic species (except *Thalassiosira* Cleve, *Actinocyclus* Ehrenberg and *Coscinodiscus* Ehrenberg). Although the most groups contributed mostly in relation to species number, they had very low abundances compared to planktonic taxa. Figure 3 shows the contribution of the most representative genera identified in the data set in relation to species richness. The genus *Nitzschia* Hassal contributed with 32% to the total species richness in all samples, mostly at upstream sites (35 species). The second most representative genus was *Navicula* Bory de St. Vincent with 20% followed by *Thalassiosira* Cleve (17.7%). *Gyrosigma* Hassal contributed with 8.4% of the specific richness, particularly at upstream sites (14 species).



Table 3. Diatom taxa with relative abundance $\geq 2\%$ in at least two samples of the data set. Maximum abundance (MA) shows the maximum abundance value of the taxa at all sites. Occurrence (Occ) represents the number of sites where the taxa was present.

Species name	Code	MA (%)	Occ.
<i>Bacillaria paxillifera</i> (O.F.Müller) T.Marsson	BPAX	10	4
<i>Coscinodiscus lineatus</i> Ehrenberg	COLI	7	7
<i>Coscinodiscus radiatus</i> Ehrenberg	CORA	20	9
<i>Cymatodiscus planetophorus</i> (Meister) Hendeby	CPLA	3	16
<i>Cymatotheca weissflogii</i> (Grunow) Hendeby	CWEI	7	26
<i>Cyclotella atomus</i> Hustedt	CYAT	16	8
<i>Cyclotella litoralis</i> Lange & Syvertsen	CYLI	7	9
<i>Cyclotella meneghiniana</i> Kützing	CYME	19	10
<i>Cyclotella striata</i> (Kützing) Grunow	CYST	9	30
<i>Cyclotella stylum</i> Brightwell	CYTY	11	26
<i>Delphineis surirella</i> (Ehrenberg) G.W.Andrews	DESU	4	9
<i>Diploneis smithii</i> (Brébisson) Cleve	DSMI	6	13
<i>Diploneis weissflogii</i> (A.W.F.Schmidt) Cleve	DWEI	3	13
<i>Navicula antonii</i> Lange-Bertalot	NANT	2	3
<i>Navicula cryptotenella</i> Lange-Bertalot	NCRY	2	4
<i>Neodelphineis pelagica</i> Takano	NEPE	5	7
<i>Nitzschia amphibia</i> Grunow	NIAM	3	3
<i>Navicula pavillardii</i> Hustedt	NPAV	3	3
<i>Paralia longispina</i> S.Konno & R.W.Jordan	PLON	2	2
<i>Paralia sulcata</i> (Ehrenberg) Cleve	PSUL	9	27
<i>Rhabdonema</i> sp.	RHSP	3	2
<i>Thalassionema frauenfeldii</i> (Grunow) Tempère & Peragallo	TFRA	8	24
<i>Thalassiosira</i> sp.1	THSP	4	10
<i>Thalassiosira</i> sp.2	THSS	4	8
<i>Thalassiosira cedarkeyensis</i> Prasad	THCE	45	22
<i>Thalassiosira ferelineata</i> Hasle & G.A.Fryxell	THFE	3	2
<i>Thalassionema nitzschioides</i> (Grunow) Mereschkowsky	TNIT	57	32
<i>Tryblionella cocconeiformis</i> (Grunow) Hendeby	TRCO	6	24

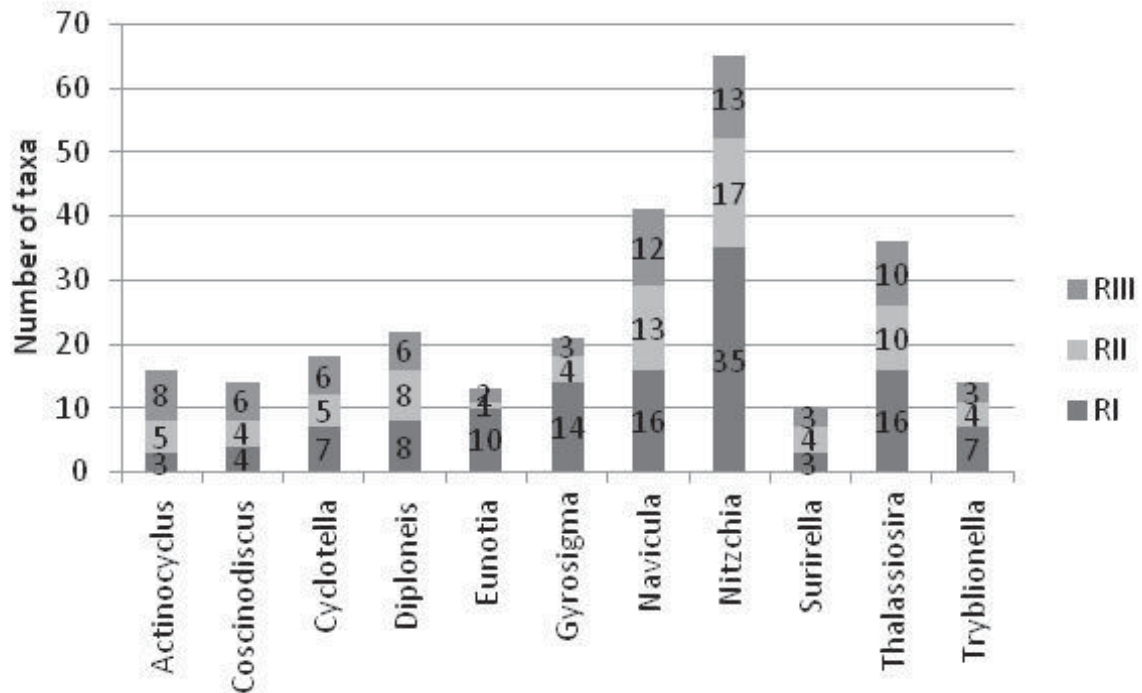


Figure 3. Contribution of the most representative genera identified in the data set in relation to specific richness. RI, RII and RIII correspond to sampling sites upstream, central river section and downstream (mangrove samples are included in RIII).

The eigenvalues ($\lambda_1 = 0.307$, $\lambda_2 = 0.110$) for the first two PCA axes accounted for 44.8% of the total variation of diatom communities. The main variation of diatoms distribution is explained by the first PCA axis. Samples were mainly arranged in relation to diatom affinities of salinity (freshwater/coastal-marine species), benthic/planktonic species and the longitudinal sections of the river (upstream, middle and downstream). Diatom species composition of the Can Gio Mangrove forest was more correlated to the downstream assemblages (Figure 4).

Cyclotella atomus Hustedt, *C. meneghiniana* Kützing, *Thalassiosira cedarkeyensis* Prasad are positively correlated to the axis 1, while *Thalassionema nitzchioides* (Grunow) Mereschkowsky, *T. frauenfeldii* (Grunow) Tempère and Peragallo, *Paralia sulcata* (Ehreneberg) Cleve, *Tryblionella cocconeiformis* (Grunow) Hendey and *Cymatotheca weissflogii* (Grunow) Hendey are negatively correlated. *Neodelphineis pelagica* Takanô, *Diploneis weissflogii* (Schmidt) Cleve are positively correlated to the axis 2, while *Coscinodiscus radiatus* Ehrenberg are negatively correlated to this axis.



According to the PCA results the pattern for the variations in diatom species composition in the samples can be summarized as follows:

Group 1 is composed of 6 samples collected at sites upstream of the river section (TV-SS01, TV-SS03, TV-SS07, TV-SS08, TV-SS10 and TV-SS11) positioned at the positive side of the axis 1. This group is characterized by high abundances of *Cyclotella atomus* Hustedt, *C. meneghiniana* Kützing and *Thalassiosira cedarkeyensis* Prasad. *T. cedarkeyensis* was the most abundant species in this group (45% at TV-SS07, 38% at TV-SS08, 35% at TV-SS10, 28% at TV-SS11 and 19% at TV-SS01), *Cyclotella atomus* (16% at TV-SS03 and 12% at TV-SS10) was the second most abundant one and *C. meneghiniana* (19% at TV-SS11) the third one. Although *C. meneghiniana* had high abundance only in one sample, this species had high correlation to the first PCA axis ordination ($r = 0.88$).

Group 2 is composed of 6 samples collected at sites upstream and in the central section of the Thi Vai River (TV-SS02, TV-SS06, TV-SS09, TV-SS19, TV-SS20 and TV-SS21) positioned mainly at axis 2 (negative side). Although *T. cedarkeyensis* had high abundance in the most samples of this group, it seems that occurrence of *Diploneis smithii*, *Bacillaria paxillifera* and *Nitzschia amphibia* in these samples characterizes this group.

Group 3 is characterized by a higher degree of heterogeneity; it includes all samples collected downstream (TV-SS22 to TV-SS31), samples of Can Gio Mangrove forest (CG-SS01 and CG-SS02), samples from upstream sites (TV-SS04 and TV-SS12) and central section of the river (TV-SS13 to TV-SS18). *Paralia sulcata*, *Thalassionema frauenfeldii*, *Tryblionopsis cocconeiformis*, and *Thalassionema nitzschioides* characterize this group based on their correlation with axis 1 ($r = -0.91$, $r = -0.87$, $r = -0.83$, $r = -0.91$, $r = -0.92$, respectively). *T. nitzschioides* occurred in all samples of the data set (upstream, middle section, downstream and mangrove) with very high abundances, being dominant in 25% of the sampling sites.



Table 4. Results of the PCA for diatom species composition. Species names (for each species code) are given in the table 3.

Species Code	PC	
	Axis 1	Axis 2
BPAX	0.3676	-0.1406
COLI	-0.3045	-0.3529
CORA	-0.2569	-0.6243
CPLA	-0.4655	-0.3637
CWEI	-0.7846	-0.3807
CYAT	0.7863	0.1428
CYLI	0.6061	-0.2162
CYME	0.8779	0.1143
CYST	-0.5848	-0.3145
CYTY	-0.4058	-0.0129
DESU	-0.5046	0.5455
DSMI	0.5194	-0.3207
DWEI	-0.3265	0.6294
NANT	0.4488	0.1287
NEPE	-0.3101	0.6181
NIAM	0.0967	-0.3332
NPAV	-0.0259	0.2325
PLON	-0.2739	0.3661
PSUL	-0.91	-0.1042
RHSP	-0.278	0.5925
TFRA	-0.8764	0.0879
THSP	-0.1406	-0.0347
THSS	-0.39	0.4439
THCE	0.8737	0.0912
TNIT	-0.9244	-0.1123
TRCO	-0.8373	-0.1153
Explained variation % (cumulative)	32.95	44.82

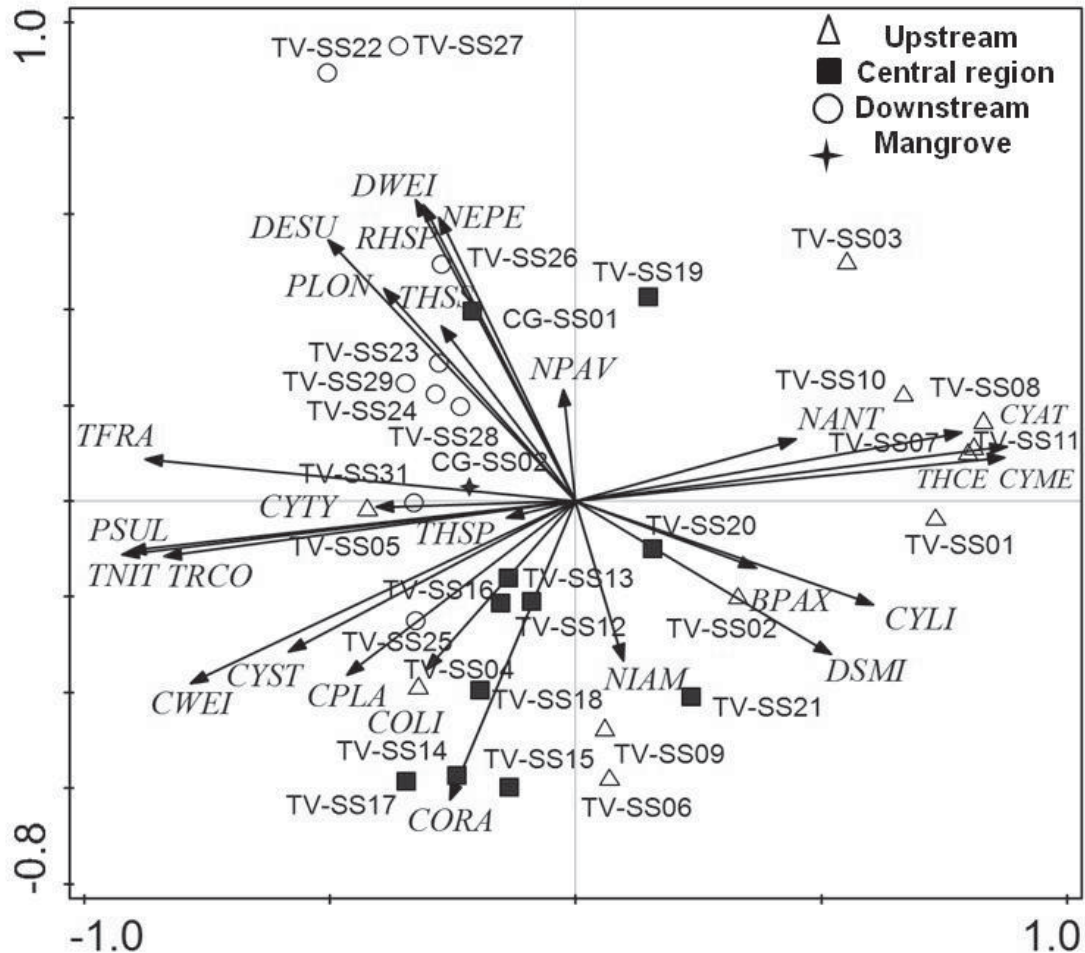


Figure 4. PCA biplot of diatom composition and distribution in surface sediments of the Thi Vai River and Can Gio Mangrove Forest. Species names (for each species code) are given in the table 3.

The result of the final CCA is summarized in table 5 and figure 5. The first two CCA axes ($\lambda_1 = 0.211$, $\lambda_2 = 0.056$) explained 20.4% of the cumulative variance in species composition and 63.3% of the variation in species-environment relationships. Only those environmental variables that seem to explain diatom distribution variations in the data set were included in the analysis. Correlations between species and environmental variables for axis 1 (0.79) and for axis 2 (0.72) were significant. Monte Carlo permutation tests indicated that both axes were significant ($p \leq 0.05$). The first ordination axis is defined by total phosphorus, while the second axis relates to temperature and water depth. Total phosphorus was the most significant variable to explain diatoms composition ($p < 0.001$).



Table 5. Summary of CCA results on diatom species and environmental data.

CCA axes	1	2
Eigenvalues	0.212	0.056
Species-environment correlation	0.795	0.722
Cumulative % variance		
of response data	16.15	20.45
of fitted response data	50.3	63.6
Sum all eigenvalues		1.312

Table 6. Canonical coefficients and correlation coefficients (intra-set correlations) of environmental variables included in the CCA.

	Canonical coefficients		Correlation coefficients	
	Axis 1	Axis 2	Axis 1	Axis 2
Water depth (m)	-0.071	-0.126	0.167	-0.171
Temperature (°C)	-0.228	-0.173	0.140	-0.344
pH	-0.401	-0.713	-0.672	-0.217
Conductivity	0.290	3.677	-0.636	0.301
Salinity (ppt)	-0.570	-2.666	-0.633	0.302
Dissolved oxygen	0.039	-0.651	-0.591	-0.201
Total nitrogen (mg/L)	0.118	-0.138	0.446	-0.245
Total phosphorus (mg/L)	0.526	-0.151	0.689	-0.107

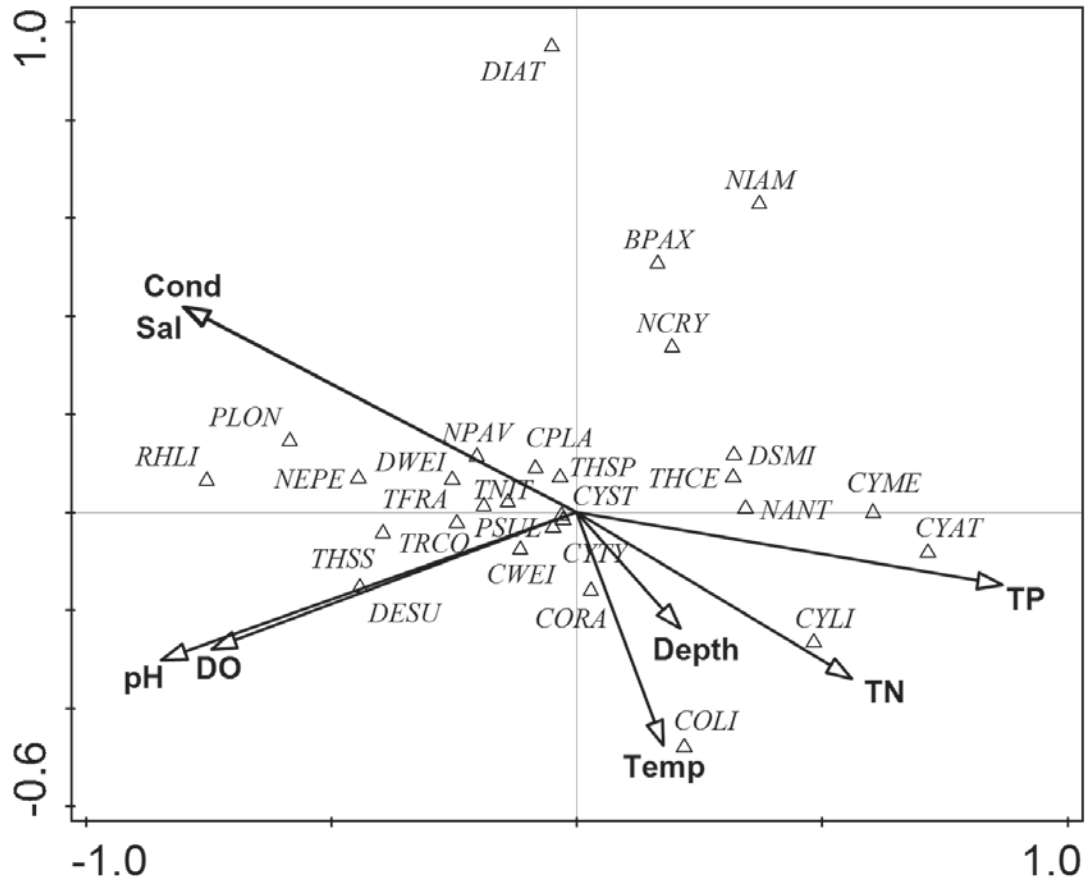


Figure 5. CCA biplot of diatoms and environmental variables. For abbreviations see table 3.

4. Discussion

In this study TP was the most important variable to explain diatom assemblage distribution. Particularly *Cyclotella atomus* and *Cyclotella meneghiniana* - freshwater planktonic species - were well correlated to TP. This result agrees with other studies that showed the strong relationship between *C. atomus* and *C. meneghiniana* with nutrient enrichment [26-27]. *C. meneghiniana* has been widely studied and shown to be tolerant of elevated pollution levels in estuaries and freshwater systems, including lakes that receive urban and industrial wastewater [28-30]. In this study, *C. meneghiniana* was more abundant (19%) in the TV-SS11 sampling site (upstream), one of the sites where the highest TP value was recorded (0.12 mg/L). This result suggests the association of this species with relatively high nutrient levels. *C. atomus* has been recorded as tolerant to high phosphorus and is associated with polluted, eutrophic, warm



harbors and nearshore areas [26]. Although the National Technical Regulation on Coastal Water Quality [31] in Vietnam does not provide guide values for TP, the highest TP concentration (0.12 mg/L) obtained in our study is comparable with TP concentrations in modified and extensively modified estuaries in Australia [30]. This TP concentration value is more than six times above the water quality triggers values in that country [30]. Compared with guide values provided in the Water Quality Guidelines in Brazil for brackish waters (class I) this result is considered the maximum value allowed [31]. On the other hand, TP trigger values proposed by the Environmental Protection Agency (EPA) for estuaries in Florida range from 0.09 mg/L (e.g. St. Andrews Bay) to 0.243 mg (Upper Halifax River), as this criteria is based according to the peculiar characteristics of each estuary [32].

Thalassiosira cedarkeyensis also occurred with very high abundances in the sampling sites upstream contributing up to 45% of the species abundance at TV-SS07. The highest TP concentration in the data set also occurred at this site (0.12 mg/L), and *T. cedarkeyensis* was relatively well correlated to the first CCA axis 1 ($r=0.57$) suggesting that this species variance was driven mainly by TP.

Thalassiosira nitzchioides - a neritic planktonic species - occurred in all samples of the data set (upstream, middle section, downstream and mangrove) with very high abundances (up to 57% at TV-SS12), being dominant in 25% of the sampling sites. However, this species was more associated to sampling sites downstream. This wide distribution and abundance of *T. nitzchioides* suggests that this species is likely not a good indicator to evaluate distribution patterns. *T. nitzchioides* has been reported to be widespread, most abundant diatom with high occurrence in several studies in marine and coastal areas [14, 34-37] or even difficult the view of variation in other components of the assemblages [37]. Nevertheless, its high distribution throughout the sampling sites shows the high influence of oceanic water in that area.

In general, diatom distribution and their relationship with the analyzed environmental variables were mainly explained by the first CCA axis. Diatom species composition downstream is composed mostly by planktonic, marine species. Salinity and conductivity, which are variables strongly correlated (as salinity is a strong contributor to conductivity) both were



well and negatively correlated to the axis 1 ($r = -0.63$). This explains the patterns of the downstream diatom species composition. However, based on the CCA analysis, these variables were not significant (Table 6). Some studies suggest that the interpretation of salinity as an important environmental variable to evaluate diatom composition change, based only on field studies, is very difficult, because most estuarine systems exhibit strong decreasing gradients in nutrient concentrations seawards, therefore it would be not possible to separate the effects of salinity from nutrient concentrations [38].

Regarding water depth, sampling sites upstream were deeper than the downstream sites (Table 1). Water depth is positioned in the second axis with short arrow length. This indicates that this variable does not explain this relationship, because relevant variables tend to be represented by longer arrows [24]. In a study to infer sea level changes in coastal waters of Hong Kong [34] water depth was reported as the most important variable in their data set. The authors recorded the occurrence of *Tryblioptychus cocconeiformis* – a meroplanktonic species - mainly in shallower sites which grain size is large. In fact, in our data this species occurred mainly in shallower sites. Overall, water depth was not well correlated with diatom assemblages (Table 6) and explained only 1.5% of the variance in the species data. Therefore, the distribution of this species might be related to other environmental factors that were not considered in this study.

In summary, based on ordination analysis, the distribution of the diatom species in our study seems to be mostly related to TP concentrations. However, the high abundances and wide distribution of marine planktonic species along the data set also suggests that hydrodynamics has an important role in their distribution, e.g. the influence of oceanic water.

Several studies report the complexity of studying estuaries due their heterogeneity and highly dynamic conditions [30, 39-40]. The relationship between estuarine nutrients and diatom is neither simple nor linear [11]. Therefore, caution is needed to interpretation of driving forces explaining diatoms composition and distribution in coastal environments; as such information is valuable to aid interpretation of diatoms in sediment cores used in reconstruction of past environments [38].



This is the first contribution to the knowledge of diatoms biodiversity in this region, and will provide a key to interpret long-term environmental changes from fossil assemblages archived in sediment cores from this coastal zone.

Acknowledgements

This work was supported by funds provided by the German Federal Ministry of Education and Research (BMBWF) and was undertaken as part of the joint research project “Environmental and Water Protection Technologies of Coastal Zones in Vietnam - EWATEC-COAST” (Grants 02WCL1217A). We deeply appreciate the valuable field work and laboratory assistance in Vietnam of Mr. Nguyen Thai Chung and Emmi Halonen and all colleagues who contributed to this study.

References

- [1] Hobbie JE. (2000): Estuarine science: A synthetic approach to research and practice. Island Press. xi 1 539 p.
- [2] Nicholls RJ, Wong PP, Burkett VR, Codignotto JO, Hay JE, McLean RF, Ragoonaden S., Woodroffe CD. (2007): Coastal systems and low-lying areas. Climate Change 2007: Impacts, Adaptation and Vulnerability. Contribution of Working Group II to the Fourth Assessment Report of the Intergovernmental Panel on Climate Change, Parry ML et al. Eds., Cambridge University Press, Cambridge, UK, 315-356.
- [3] Yusuf AA, Francisco H. (2009): Climate change vulnerability mapping for Southeast Asia. Economy and Environment Program for Southeast Asia (EEPSEA), Singapore with CIDA, IDRC and SIDA. Available from: http://web.idrc.ca/uploads/user-S/12324196651Mapping_Report.pdf
- [4] Hall, R. I. & Smol, J.P. 2010: Diatoms as indicators of lake eutrophication. In: Smol JP, Stoermer EF. (eds). The Diatoms: Applications for the Environmental and Earth Sciences. Cambridge University Press, Cambridge, 122–151.
- [5] Dixit AS, Alpay S, Dixit SS, Smol JP.(2007): Paleolimnological reconstructions of Rouyn-Noranda lakes within the zone of influence of the Horne Smelter, Quebec, Canada. J Paleolimnol 38: 209–226



- [6] Bennion H, Battarbee RW, Sayer CD, Simpson GL, Davidson TA (2011): Defining reference conditions and restoration targets for lake ecosystems using palaeolimnology: a synthesis. *J. Paleolimnol.* 45:533–544
- [7] Battarbee RW, Anderson NJ, Jeppensen E, Leavitt PR. (2005): Combining paleolimnological and limnological approaches in assessing lake ecosystem response to nutrient reduction. *Freshwater Biology* 50 (10):1772-1780.
- [8] Smol JP. (2008): Pollution of lakes and rivers – a paleoenvironmental perspective. 2nd. Oxford: Blackwell Publishing. 362p.
- [9] Stevenson RJ, Yangong P, van Dam H. (2010): Assessing environmental conditions in rivers and streams with diatoms. . In: Smol JP, Stoermer EF. (eds). *The Diatoms: Applications for the Environmental and Earth Sciences*. Cambridge University Press, Cambridge, 57-85.
- [10] Round FE, Crawford RM, Mann DG. (1990): *The Diatoms – biology and morphology of the genera*. Cambridge: University Press. 747 p.
- [11] Admiraal W. (1984): The ecology of estuarine sediment-inhabiting diatoms. *Progres. Phycol. Res.* 3: 269-322.
- [12] Trobajo R, Sullivan MJ. (2001): Applied diatom studies in estuaries and shallow coastal environments. In: Smol JP, Stoermer EF. (eds). *The Diatoms: Applications for the Environmental and Earth Sciences*. Cambridge University Press, Cambridge: 309–323.
- [13] Admiraal W. (1977): Experiments with mixed populations of benthic estuarine diatoms in laboratory microecosystems. *Bot. Mar.* 20:479-485.
- [14] Sylvestre F, Guiral D, Debenay JP. (2004): Modern diatom distribution in mangrove swamps from the Kaw Estuary (French Guiana). *Mar. Geol.* 208: 281-293.
- [15] Trobajo R, Quintana XD, Sabater S. (2004): Factors affecting the periphytic diatom community in Mediterranean coastal wetlands (Emporda wetlands, NE Spain). *Arch. Hydrobiol.* 160: 375-399.
- [16] Ribeiro LLCS (2010): Intertidal benthic diatoms of the Tagus estuary: Taxonomic composition and spatial-temporal variation. PhD Thesis, Universidade de Lisboa, Portugal.
- [17] Nguyen HA (2011): A model for predicting mangrove forest dynamics under variable environmental conditions - A Case study of the Estuary of Dongnai - Saigon River system, Vietnam. PhD Thesis. Technische Universität Braunschweig. 120p.
- [18] Tuan VQ, Kuenzeret C. (2012). *Can Gio Mangrove Biosphere Reserve Evaluation 2012: Current Status, Dynamics, and Ecosystem Services*. Hanoi, Viet Nam: IUCN. 102 pp.



- [19] SMEWW (2005): Standard Methods for the examination of water and wastewater, American Works Association and Water Environmental Federation, 21th Edition, 2005.
- [20] Battarbee RW, Jones V, Flower RJ, Cameron N, Bennion H, Carvalho L, Juggins S. (2001): Diatoms. In: Smol JP, Birks HJB, Last WM (ed.). Tracking Environmental Change Using Lake Sediments. London: Kluwer Academic Publishers.v.3. p.155-203
- [21] Pappas JL, Stoermer EF. (1996): Quantitative method for determining a representative algal sample count. *J. Phycol.* 32 (4): 693-696.
- [22] Witkowski A, Lange-Bertalot H, Metzeltin D. (2000): Diatom flora of marine coasts I. In: Lange-Bertalot H. (ed.) *Iconographia diatomologica*. Vol. 7, 925 p.
- [23] Hasle GR, SYVERTSEN EE. (1997): Marine diatoms. In: (C.R. Tomas, ed.): *Identifying Marine Phytoplankton*. Academic Press, San Diego, California. pp. 5-385.
- [24] ter Braak CJF. (1986): Canonical Correspondence Analysis: a new eigenvector technique for multivariate direct gradient analysis. *Ecology*, 67 (5). p.1167-1179.
- [25] ter Braak CJF, Šmilauer P. (2012): *Canoco reference manual and user's guide: software for ordination, version 5.0*. Microcomputer Power, Ithaca, USA, 496 pp.
- [26] Kipp RM, McCarthy M, Fusaro A. (2014): *Cyclotella atomus*. USGS Nonindigenous Aquatic Species Database, Gainesville, FL. <http://nas.er.usgs.gov>
- [27] Costa-Böddeker S, Bennion H, Jesus TA, Albuquerque ALS, Figueira RCL, Bicudo DC. (2012): Paleolimnologically inferred eutrophication of a shallow, tropical, urban reservoir in southeast Brazil. *J. Paleolimnol.* 48: 751-776.
- [28] Sabater S, Sabater F. (1988): Diatom assemblages in the River Ter. *Archiv für Hydrobiologie*, 111: 397–408.
- [29] van Dam H, Mertens A, Sinkeldam J. (1994): A coded checklist and ecological indicator values of freshwater diatoms from the Netherlands. *Netherlands Journal of Aquatic Ecology*, 28 (1): 117-133.
- [30] Logan B, Taffs KH. (2013): Relationships between diatoms and water quality (TN, TP) in sub-tropical east Australian estuaries. *J. Paleolimnol.* 50: 123-137.
- [31] National Technical Regulation (QCVN 10:2008/BTNMT) (2008): National Technical Regulation on coastal water quality. Ministry of Natural Resources and Environment, Vietnam.



- [32] CONAMA. (2008): Environmental National Brazilian Council . Water Quality Guidelines (CONAMA 397/2008). <http://www.mma.gov.br/conama>.
- [33] Environmental Protection Agency- EPA. (2012): Water Quality Standards for the State of Florida's Estuaries, Coastal Waters and South Florida Inland Flowing Waters.
http://water.epa.gov/lawsregs/rulesregs/florida_coastal.cfm
- [34] Ng SL, Sin FS. (2003): A diatom model for inferring sea level change in the coastal waters of Hong Kong. *J. Paleolimnol.* 30: 427-440.
- [35] Schuette G, Schrader H (1981): Diatom taphocoenoses in the coastal upwelling area off South West Africa. *Mar. Micropaleontol.* 6:131-155.
- [36] Yim WWS, Li J. (2000): Diatom preservation in an inner continental shelf borehole from the South China Sea. *J. Asian Earth Scie.* 18: 471-488
- [37] Jiang H, Zengh Y, Ran L, Seidenkrantz MS. (2004) Diatoms from the surface sediments of the South China Sea and their relationships to modern hydrography. *Mar. Micropaleontol.* 53:279-292.
- [38] Underwood GJC, Phillips J, Saunders K.(1998): Distribution of estuarine benthic diatom species along salinity and nutrient gradients. *Eur. J. Phycol.* 33, 173-183.
- [39] de Jong L, Admiraal W. (1984): Competition between three estuarine benthic diatom species in mixed cultures. *Mar. Ecol. Prog. Ser.* 18: 269-275.
- [40] Rovira L, Trobajo R, Leira M, Ibáñez C. (2012): The effects of hydrological dynamics on benthic diatom community structure in a highly stratified estuary: The case of the Ebro Estuary (Catalonia, Spain). *Estuarine, Coastal and Shelf Science* 101: 1-14.



On analyzing the marine-hydrological boundary conditions for the flood risk in the Thi-Vai region

Sönke Dangendorf¹, Jens Bender¹, Nguyen Hong Quan²,
and Jürgen Jensen¹

¹ Research Institute for Water and Environment, University of Siegen,
Paul-Bonatz-Str. 9-11. soenke.dangendorf@uni-siegen.de

² Institute for Environment and Resources (IER), Vietnam National University,
Ho-Chi-Minh City, 142 To Hien Thanh, Dist. 10. hongquanmt@yahoo.com

Abstract

According to the UNEP (2009) Vietnam is likely to be one of the several countries most adversely affected by climate change. As part of the BMBF project EWATEC-COAST the present study assesses the marine-hydrological boundary conditions for the Thi-Vai River region with a particular focus on the coastal area around Vung-Tau. By combining tidal observations with satellite altimetry data and a long mean sea level reconstruction we characterize the interplay between astronomical tides, storm surges and long-term sea level rise. The astronomical tides dominate the water level elevations with a tidal range alternating between two and four meters, while storm surges play a relatively minor role, with maximum elevations of ~50 cm. Additionally, we find a particular large seasonal cycle in mean sea levels, varying throughout the year by about 50 cm on average (with inter-annual perturbations of 60 to 70cm). On the long-term we find that mean sea levels have risen by about approximately 2.0 ± 0.1 mm/yr since 1950, a rate that is slightly above the global mean. We further find significant inter-annual to multi-decadal variations in mean sea level, which are significantly correlated with the El-Nino-Southern-Oscillation over the central Pacific. Hence, future mean sea level projections need not only account for changes in the global mean, but also for regional variations in the central Pacific.

Furthermore we analyze the development of extreme sea levels by calculating linear trends for annual percentile time series before and after removing the influence of mean sea level changes. While we do not find any evidence for significant changes in the majority of percentiles after removing mean sea level changes, the two most upper percentiles show



significant positive trends. These findings, however, require deeper investigations to identify whether the deviations result from local processes (tides, measurement errors) or changes in storminess.

Key Words: Mean sea levels, extreme sea levels, tides, storm surges



1. Introduction

According to the “Vietnam Assessment Report on Climate Change”, published in 2009 by the United Nations Environmental Programme (UNEP, 2009), Vietnam is likely to be one of the several countries most adversely affected by climate change. This demonstrates that improved knowledge about past, present day and future climate conditions is required to develop adequate adaptation strategies. Within the research project “CLIENT Vietnam – Joint project Environmental and Water Protection Technologies of Coastal Zones in Vietnam” (EWATEC-COAST), funded by the Federal Ministry of Education and Research (BMBF) in Germany, a management system for the development, supply, and the use of water and environmental technologies and service tools in the Thi-Vai River region, covering an area of ~500 km², is developed. The system aims at offering users the capability of sustainable improvement of the environmental and living conditions of the designated coastal zone in South Vietnam, taking anthropogenic influence and natural climate variability into account (<https://www.tu-braunschweig.de/ewatec/index.html>).

The main goal of subproject 7 (Coastal Protection) in EWATEC-COAST is to analyze the present day and future marine-hydrological boundary conditions, the flood risk and the vulnerability of the Thi-Vai River region. This comprises the investigation of (i) mean sea levels (MSL) and storm surges as well as their physical driving factors, (ii) the inland flood risk due to enhanced river discharges, (iii) the combination of (i) and (ii), and (iv) the development of flood risk maps for the Thi-Vai region. In this study we will provide first insights into the present day oceanographic boundary conditions for the Thi-Vai region. We will analyze the importance of different driving mechanisms (e.g. tides and surges) for the development of extreme sea levels (determined by an analysis of tide gauge observations and satellite altimetry) and discuss first estimates of the long-term MSL rise since 1950 (approximated by the means of a high resolution MSL reconstruction). Finally, recommendations for further improvements of the data availability and modelling requirements will be given.



2. Tidal conditions

The Thi-Vai River is located southeasterly of Ho-Chi-Minh City and opens to the South China Sea (SCS) near Vung-Tau, where also the only historical coastal tide gauge in this region is located. Publically available observations from the tide gauge can be derived from the University of Hawaii Sea Level Center (<http://uhslc.soest.hawaii.edu/>). The record available there spans a period from 1986 to 2002 (Research Quality), but non-homogenized measurements are also available for the period from 2002 to 2012. A snap shot of the record for the two years from 1998 and 1999 is given in Figure 1. The figure provides valuable information about the general tidal characteristics in the region. Tidal predictions have been calculated applying a common harmonic analysis to the raw data. The harmonic analysis has been performed using the t-tide package (Pawlowicz et al., 2002) under the consideration of 67 tidal constituents. The tidal regime is mixed (i.e. a mixture between diurnal (once a day) and semi-diurnal tides (twice a day)) and the tidal range (difference between tidal high and low waters) alternates depending on the moon's declination between two and four meters (Figure 1a). In turn, the surges (i.e. the non-tidal residuals computed as the difference between observed and predicted water levels, Figure 1b), which mainly represent the oceanic response to local or remote disturbances in the atmosphere (i.e. wind and sea level pressure fluctuations), vary in a range of ± 50 cm. Hence, tides are up to 8 times larger than surges, demonstrating that the magnitude of extreme sea levels is mainly triggered by the phase and magnitude of the tides. For instance, a tropical cyclone making land fall (with strong onshore winds) near Vung-Tau will only be critical with respect to coastal flooding if it coincides with a simultaneous tidal high water.

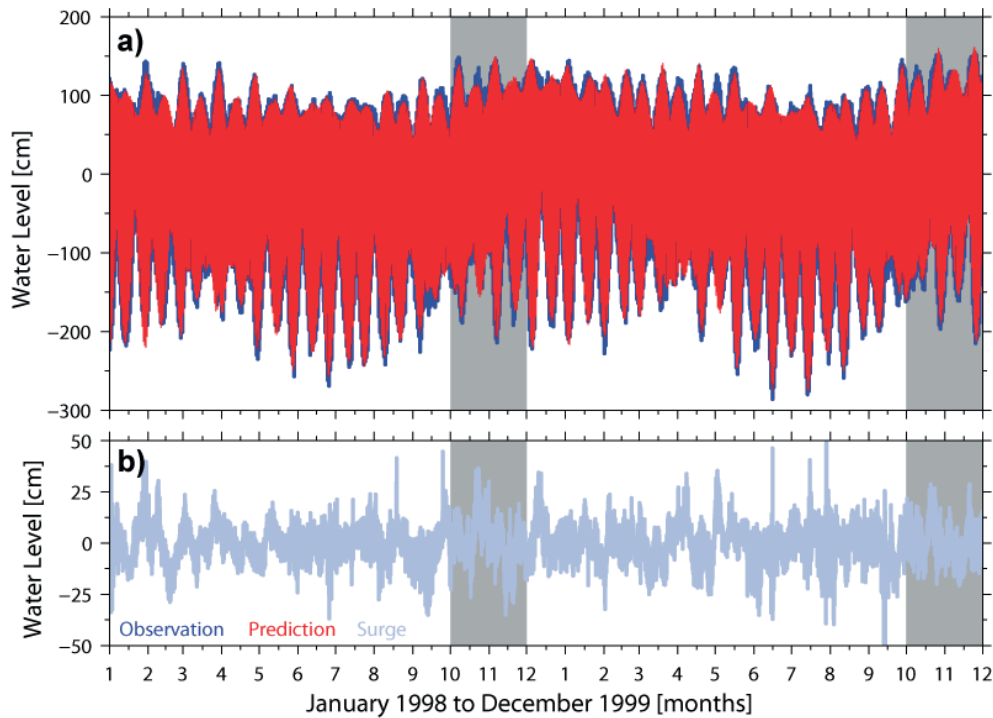


Figure 2. Observed and predicted water levels (a) and the corresponding surges (b) (difference between observed and predicted water levels) measured over the period from 1998 to 1999. The grey shading marks the months in which the annual cycle peaks on average.

From Figure 1 it is also obvious that water levels and tides exhibit a clear seasonal dependence, showing two distinct cycles during the period of the snap shot (Figure 1a). Higher than normal conditions are observed during winter from October to February: with an average peak during November (compare also Figure 2c and d). The seasonal cycle is one of the most energetic components in sea level variability especially on time scales larger than a few hours (Pugh, 2004). To get an insight into the characteristics of the seasonal cycle we have calculated the average amplitudes and phases of the annual and semi-annual cycle for each grid point time series in the SCS from monthly MSL as derived by AVISO (<http://www.aviso.altimetry.fr/en/home.html>) satellite altimetry measurements over the period from 1993 to 2011 (Figure 2). The figure shows a clear spatial pattern in both the amplitudes and the phases of the annual and semi-annual cycle. The amplitudes vary from ~1 cm to over 20 cm for the annual cycle and ~1 to 7 cm for the semi-annual component within the entire basin. For the annual cycle largest amplitudes oc-

curing between November and January appear in the Gulf of Thailand including also the southern coastlines of Vietnam. Near the coast of Vung-Tau, for instance, the amplitudes are around 20 cm and 6 cm for the annual and semi-annual cycle, respectively. This means, that the sea levels vary within one year on average by 50 cm (when combining the annual and semi-annual component), with inter-annual excursions being even much higher (Amiruddin et al., in prep). Hence, the seasonal cycle represents one of the most important components (after high frequency tides, see also Figure 1a) with respect to the magnitude of extreme sea levels in the region.

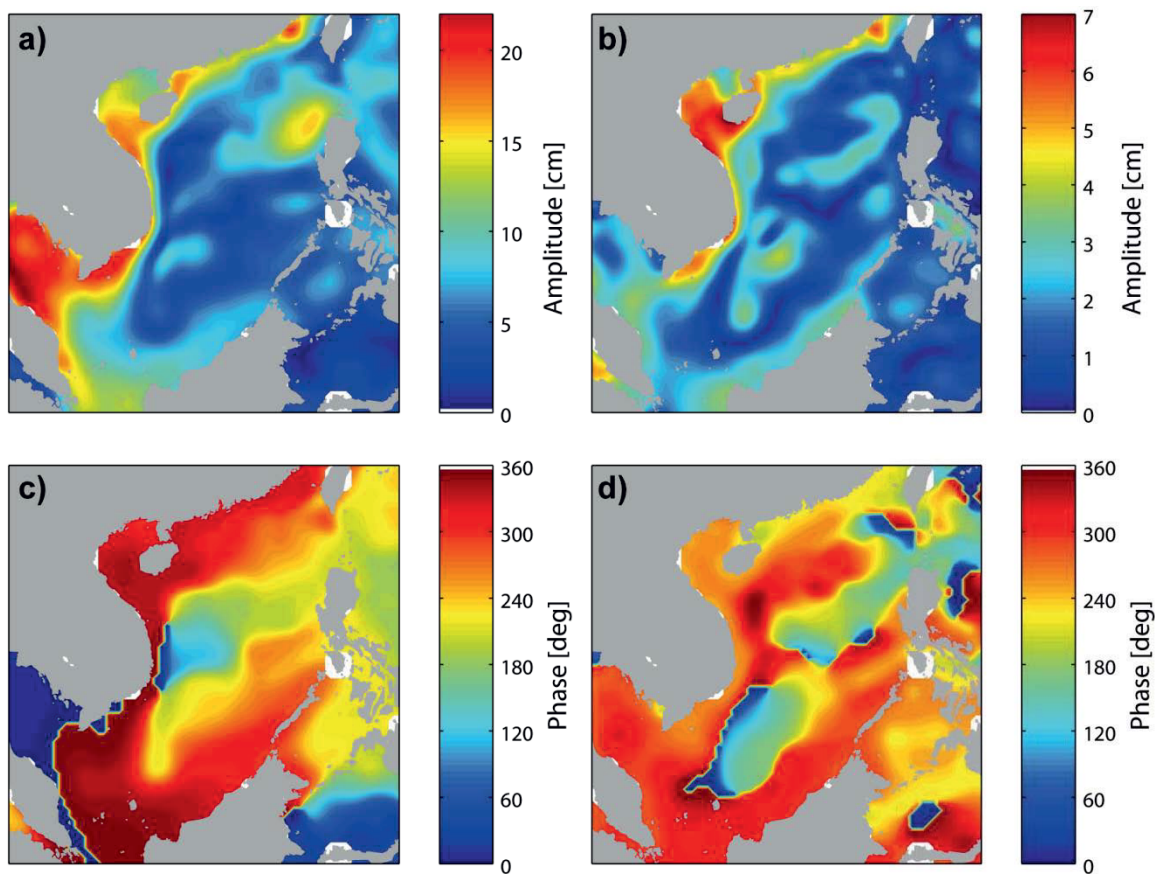


Figure 2. Amplitudes and phases of the annual (a, c) and semi-annual cycle (b, d) as estimated by a harmonic analysis of monthly MSL derived from satellite altimetry data (merged AVISO product) over the period from 1993-2011.

3. Long-term sea level rise and extremes

Beyond the synoptic scale variations clearly visible in sea level (Figure 1 and 2) it is of particular interest whether sea level has changed in the



long term and if so, by how much. Since 1950 global MSL (GMSL) has risen by an average rate of roughly 1.8 mm/yr (Church and White, 2011), with larger rates in the order of 3.2 mm/yr since 1993 (Church et al., 2013). However, it is well known that regional sea level may deviate considerably from the global mean in both variability (e.g. Dangendorf et al., 2013a) and trends (e.g. Cazenave and Nerem, 2004). A common way to infer long-term rates of regional sea level change is to investigate historical tide gauge observations. These are, however, spatially and temporally very limited in the SCS (Amiruddin et al., in prep.), hampering the robust estimation of long-term sea level changes. Another possibility is to use so called sea level reconstructions, which have usually been used to assess sea level changes on basin wide or global scales (e.g. Church and White, 2011). These reconstructions are based on a combination of spatially homogeneous satellite altimetry observations and selective tide gauge records and provide a near global coverage of sea level change. Here, we use a recent reconstruction by Meyssignac et al. (2012, hereafter M12) to analyze the regional MSL in the SCS. Figure 3 shows all available grid point time series from the SCS region, available from the M12 reconstruction, as well as the spatial SCS average and the time series in direct vicinity to Vung-Tau. The SCS average is marked by a steady rise in the order of approximately 2.0 ± 0.1 mm/yr with significant inter-annual to (multi-) decadal excursions. The sea levels near Vung-Tau clearly follow the basin average in both variability and trends. The long-term rate of 2.0 ± 0.1 mm/yr is slightly (but statistically significantly on the 95%-significance level) above the GMSL rate (1.8 ± 0.1 mm/yr) during the same period (Church and White, 2011). The inter-annual to decadal scale fluctuation (reaching ~ 4 cm) around the steady trend are significantly correlated to the El-Nino Southern Oscillation index (Figure 3b), probably due to equatorial Rossby wave forcing in response to changing trades in the equatorial Pacific (Merrifield et al., 2012). This indicates that the sea level in the SCS is mainly a product of global processes (thermal expansion and mass changes) in combination with climate internal variations in the equatorial Pacific.

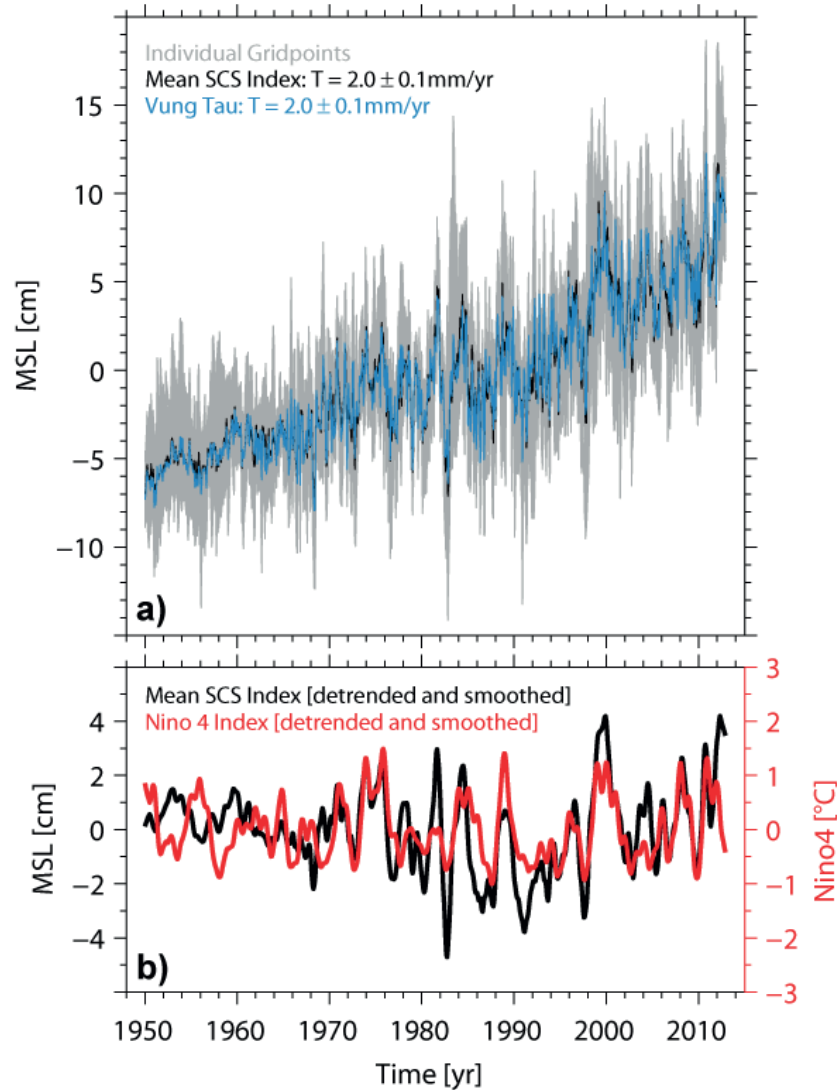


Figure 3. Monthly MSL (a) in the SCS as derived by the M12 reconstruction. Single grid point time are shown in grey, while the spatial average is marked in black. The time series in closest vicinity to Vung-Tau is separately highlighted in blue. The average seasonal cycle has been removed from all time series. (b) The linearly detrended and smoothed (48 months LOWESS filter) M12 SCS average (black) in comparison to the NINO4 index (red).

While the long-term rate of MSL change is important especially in the context of climate change, extreme sea levels are the ones which result in the highest impacts for coastal zones. Therefore, it is vitally important to understand whether extreme sea levels follow in the long-term changes in MSL (Woodworth and Blackman, 2004). There have been numerous investigations on that topic around the world, some focussing on quasi-global data sets (e.g. Menendez and Woodworth, 2010) and others with a

more regional focus (e.g. Dangendorf et al., 2013b). While the quasi-global assessments show less evidence for significant changes in the extremes (relative to the MSL), there are a few studies reporting differing trends in both parameters on a regional scale (e.g. Dangendorf et al., 2013b; Mudersbach et al., 2013). These assessments have been mostly conducted by analyzing annual or seasonal percentile time series before and after removing the MSL (or the median). We followed these studies and made a similar analysis for the hourly observations at the Vung-Tau tide gauge over the period from 1980 to 2007. The results are visualized in Figure 4. The time series (Figure 4a) are characterized by a considerable temporal variability and significantly increasing trends in the majority of the percentiles (Figure 4b). There is also a tendency visible that higher percentiles show larger trends compared to those observed for the lower percentiles. However, when removing the median sea levels from each percentile time series (Figure 4b) these significant trends disappear in most percentiles with exception of the upper most (>98. percentile). This suggests that there are (at least during the investigation period) other mechanisms than the MSL also influencing the long-term changes in extreme sea levels. These findings require deeper investigations in future and could be either related to changes in extreme winds or changes in the local tidal regime.

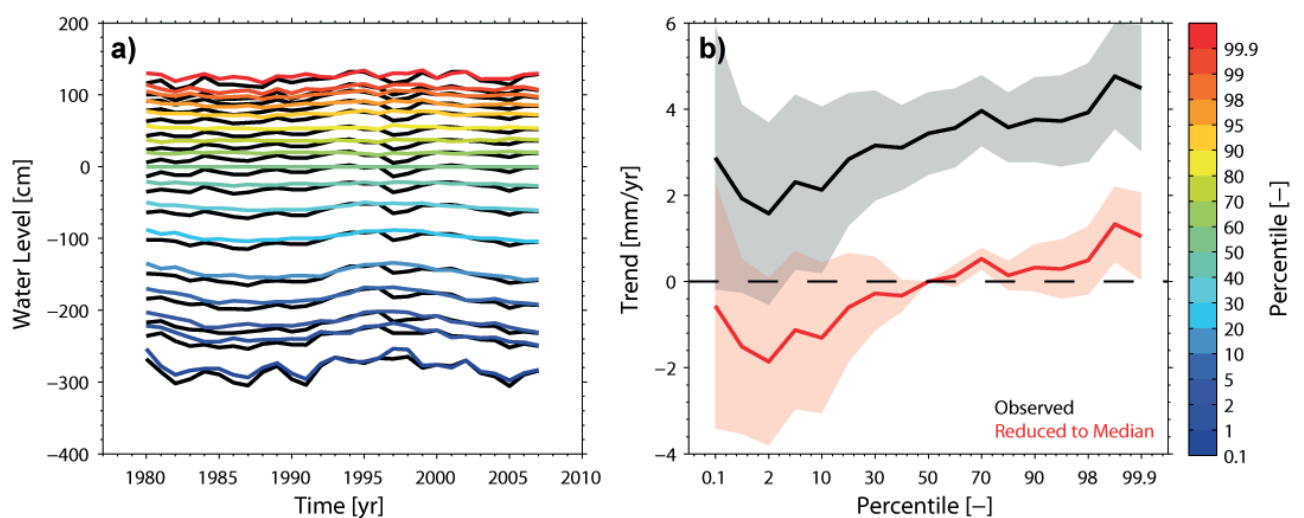


Figure 4. Annual percentile time series of sea level as obtained from the hourly Vung-Tau tide gauge over the period from 1980 to 2007 (a) as absolute values (black) and reduced to the median sea level (colored). The corresponding linear trends are shown with 95%-confidence bounds in (b).



4. Discussion and conclusions

In this study we have briefly assessed the marine-hydrological boundary conditions for the Thi-Vai region with a particular focus on the location of Vung-Tau, a city at the mouth of the Thi-Vai River, which harbours the only historical tide gauge in the region. From all currently available data sources (including tide gauge observations, satellite altimetry and a MSL reconstruction) we have made some first assessments of the present day conditions in mean and extreme sea levels. The sea levels are mainly controlled by astronomical forces with a mixed tidal regime characterized by an alternating tidal range between approximately two and four meters. Surges, which are mainly driven by strong on-/offshore winds, play a comparably small role for the flood risk, since their maximal elevation usually does not exceeds 50 cm. This results in a tide/surge ratio of approximately eight, i.e. the influence of tides is up to eight times larger than that of surges. Hence, the impact of tropical cyclones (which are rather rare events in the region) making landfall near the coast of Vung-Tau is limited to the phase and magnitude of high tides. As an additional factor influencing the timing of extreme sea levels, we found that the seasonal cycle of MSL varies on average by about 50 cm within one year and peaking in November, a value that can be even larger in some particular years (Amiruddin et al., in prep).

We further found that MSL has increased since 1950 by roughly 2.0 mm/yr, a rate close to but slightly larger than the global mean during the same period. Simultaneously, we have observed slightly larger trends in the extreme sea levels (>98. Percentile), pointing to some other forcing factors than MSL alone showing distinctive positive trends in the recent years. However, this finding is based on only a few years of tidal observations publically available from the webpage of the University of Hawaii, demonstrating the urgent need of longer and more homogeneous measurements in the region. To this end, it is important to notice that the tide gauge of Vung-Tau was originally installed in 1918. During our search for the data, we found log books (Figure 5, top) providing observations of tidal high and low water levels from 1918 up to the 1950s and since then hourly measurements for a couple of years, extending the present day data base significantly. These data sets have recently been digitized at the Southern Regional Hydro Meteorological Center in Ho-Chi-Minh City

and are currently under inspection. If homogeneous, the data may provide valuable information about long term changes in mean and extreme sea levels.

As a complementary tool, we are currently further developing a two-dimensional fully barotropic tide+surge model covering the entire SCS (based on Delft 3D), to hindcast storm surge water levels over the past approximately 60 years (Figure 5, top and bottom). The model is forced with eight main tidal constituents at the model boundaries in the Taiwan Strait, at the boundary to the West Pacific, and the Java Sea. The model will allow us to produce a more homogenous hindcast of sea levels which can be used as dynamic boundary conditions for the Thi-Vai River model, which is simultaneously also in progress at the University of Braunschweig, Germany.

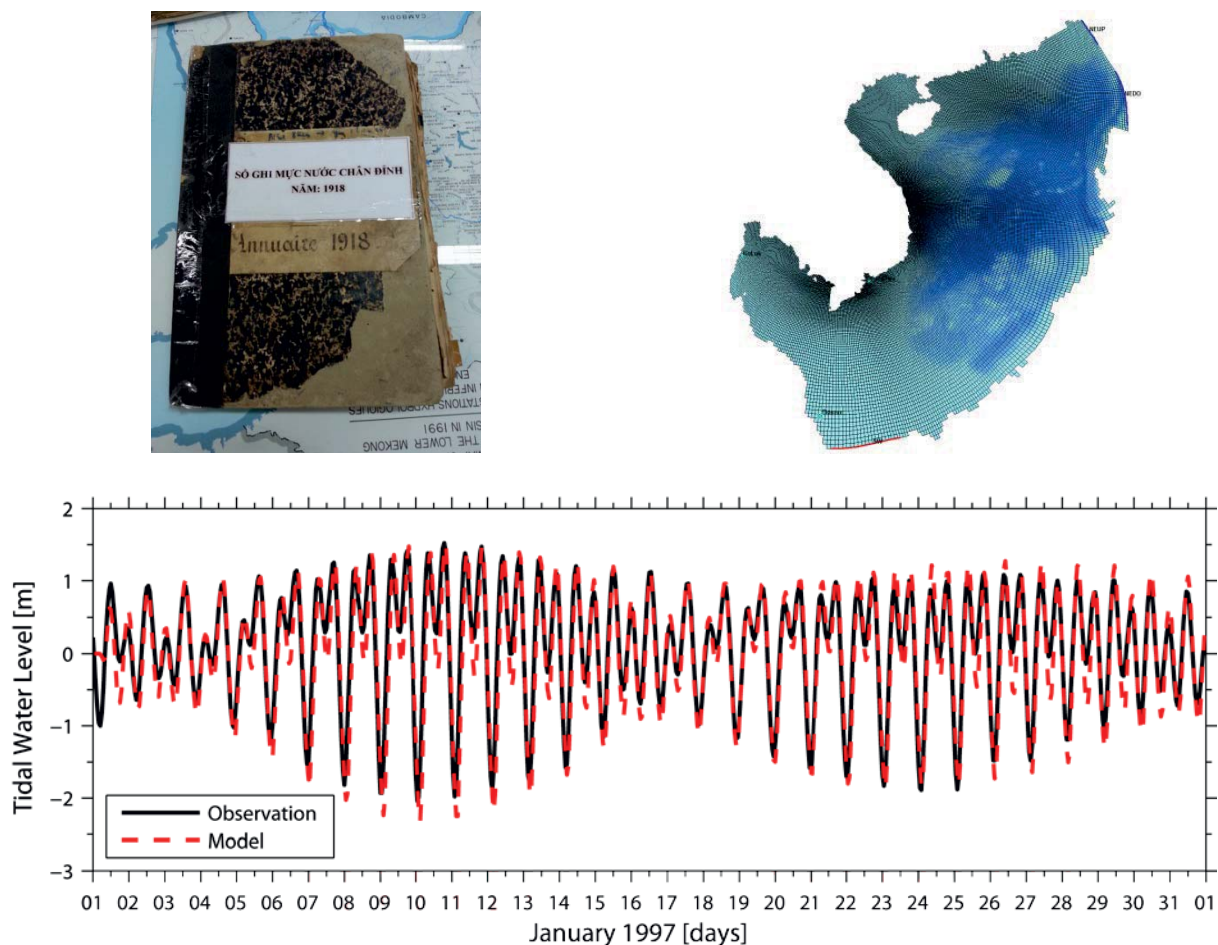


Figure 5. (top, left) Log book with tidal observations from Vung Tau since AD 1918. (top, right) Bathymetrie of the two-dimensional tide+surge model based on Delft 3D. (bottom) Observed versus modelled tides.



References

- [1] Amiruddin AM, Haigh ID, Tsimplis MN, Calafat FM, Dangendorf S (in prep): Seasonal Cycle and Variability of Sea Level around the South China Sea. To be submitted to *J. Geophys. Res.*.
- [2] Cazenave A, Nerem RS (2004): Present-day sea level change: observations and causes. *Rev. Geophys.*, 42, RG3001, doi:10.1029/2003RG000139.
- [3] Church JA, White NJ (2011): Sea-level rise from the late 19th to the early 21st century. *Surv. Geophys.*, doi:10.1007/s10712-011-9119-1.
- [4] Church JA, Clark PU, Cazenave A, Gregory JM, Jevrejeva S, Merrifield MA, Milne GA, Nerem RS, Nunn PD, Payne AJ, Pfeffer WT, Stammer D, Unnikrishnan AS (2013): Sea level change, *Climate Change 2013: The Physical Science Basis. Contribution of Working Group I to the Fifth Assessment Report of the Intergovernmental Panel on Climate Change* [Stocker et al. (eds.)], Cambridge University Press, Cambridge, United Kingdom and New York, NY, USA.
- [5] Dangendorf S, Mudersbach C, Wahl T, Jensen J (2013a): Characteristics of intra-, inter-annual and decadal sea-level variability and the role of meteorological forcing: the long record of Cuxhaven. *Ocean. Dyn.*, 63(2-3), 209-224, doi:10.1007/s10236-013-0598-0.
- [6] Dangendorf S, Mudersbach C, Jensen J, Ganske A, Heinrich H (2013b): Seasonal to decadal forcing of high water level percentiles in the German Bight throughout the past century. *Ocean Dyn.*, 63, 533-548, doi:10.1007/s10236-013-0614-4.
- [7] Menendez M, Woodworth PL (2004): Changes in extreme high water levels based on a quasi- global tide gauge data set. *J. Geophys. Res.*, 115:C10.
- [8] Merrifield MA, Thompson PR, Lander M (2012): Multidecadal sea level anomalies and trends in the western tropical Pacific. *Geophys. Res. Lett.*, 39, 13, L13602.
- [9] Meyssignac B, Salas y Melia D, Becker M, Llovel W, Cazenave A (2012): Tropical Pacific spatial trend patterns in observed sea level: Internal variability and/or anthropogenic signature. *Clim. Past. Discuss.*, 8, 349-389.
- [10] Mudersbach C, Wahl T, Haigh ID, Jensen J (2013): Trends in high sea levels along the German North Sea coastline compared to regional mean sea level changes. *Cont. Shelf Res.*, 65, 111-120, doi: <http://dx.doi.org/10.1016/j.csr.2013.06.016>.



- [11] Pawlowicz R, Beardley B, Lentz S (2002): Classical harmonic analysis including error estimates in MATLAB using T_TIDE. *Computers and Geosciences*, Vol. 28(8), pp. 929-937.
- [12] Pugh D (2004): *Changing Sea Levels: Effects of Tides, Weather and Climate*. 1st ed., Cambridge University Press, Cambridge, UK.
- [13] UNEP (2009): *Vietnam Assessment Report on Climate Change*. ISBN: 0-893507-770124.
- [14] Woodworth PL, Blackman DL (2004): Evidence for systematic changes in extreme high waters since the Mid-1970s. *J. Climate*, 17, 1190-1197.



Treatment of tannery wastewater by enhanced biological processes – preliminary results

Joachim Fettig¹ and Volker Pick²

¹ University of Applied Sciences Ostwestfalen-Lippe, An der Wilhelmshöhe 44, D-37671 Höxter, joachim.fettig@hs-owl.de

² University of Applied Sciences Ostwestfalen-Lippe, An der Wilhelmshöhe 44, D-37671 Höxter, volker.pick@hs-owl.de

Abstract

As a part of the joint Vietnamese-German research project EWATEC-COAST the treatment of wastewater from a leather producing company in Greater Ho-Chi-Minh City is currently investigated on a pilot-scale. The treatment train includes a pH-adjustment and pre-precipitation stage, sedimentation and dissolved air flotation (DAF) for particle removal, and a membrane bioreactor (MBR) for the aerobic biological degradation of dissolved organic substances as well as the removal of nitrogen components. Data from the first weeks of regular operation are presented where reactor operation still had to be adapted to the wastewater. In addition, the possibilities for the removal of organic substances by anaerobic pre-treatment are investigated by operating an EGSB reactor in parallel. The preliminary results are discussed in the context of findings from other studies on biological treatment of tannery wastewater.

Key Words: tannery wastewater, dissolved air flotation, membrane bioreactor



1. Introduction

The leather and footwear industry in Vietnam is an important economical branch that has produced 8-10% of Vietnam's total export volume in recent years [1]. This branch includes the tanneries where the raw hides are processed and converted into wet-blue or final leather pieces. While Hao [1] refers to a number of 42 tanneries in the whole country, Thanh [2] specifies that there are 33 industrial tanneries and, in addition, about 27 household enterprises in some leather craft villages.

Tanneries need a lot of water for different process steps. According to EU's reference documents up to 40 m³ of fresh water per t of raw hides (corresponding to 200-250 kg of final leather) are required in tanneries which have not taken steps to reduce water consumption [3]. The resulting wastewater streams contain particulates and both easily and hardly degradable organic substances and, in addition, inorganic pollutants like chromium and sulphide. Figure 1 shows the basic scheme of leather production and the main pollutants found in the wastewater streams.

Some large tanneries are located in industrial zones that have been built during the past ten years. These zones are usually equipped with centralised wastewater treatment plants. However, even then an on-site pre-treatment is required for the removal of hazardous substances. For other tanneries which are not embedded in such an infrastructure the situation is different in the way that they must treat their wastewater according to the final effluent standards.

Since the tanning industry has been categorized as one of the most polluting industries in the country, the environmental regulations require that each company must (i) submit environmental impact assessment reports, (ii) install wastewater treatment systems, and (iii) pay wastewater fees [2]. In 2010 about 65% of the tanneries did comply with the regulation to install a wastewater treatment system. However, almost all tanneries have been fined for various environmental violations in recent years [2] indicating that there is still a lack of appropriate technologies to fulfil the discharge requirements in accordance with the Vietnamese standard TCVN 5945-2005 on industrial wastewater.

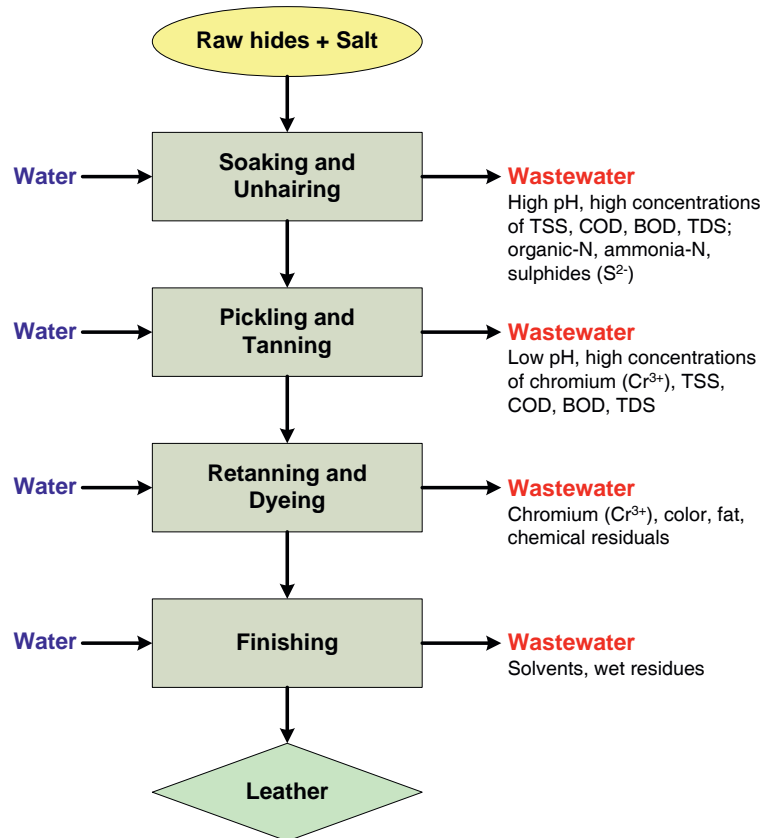


Figure 1. Basic scheme of the production of leather and resulting wastewater pollutants

The conventional way to deal with tannery wastewater is to apply chemical precipitation and aerobic biological treatment in activated sludge stages [3]. During the past years it has also been shown that sequencing batch reactors (SBR) are suited for the removal of COD and nitrogen compounds [4, 5]. Most recently the application of membrane bioreactors (MBR) was studied on a lab-scale [6]. It was concluded that the MBR gave higher COD removal efficiencies (+4%) and provided more stable and complete nitrification than an activated sludge system [7].

Since tannery wastewater is characterised by a high load of dissolved organic substances anaerobic processes have also been applied as a pre-treatment stage [8, 9]. However, if the concentration of sulphate is too high the activity of methane producing archaea can be strongly inhibited by sulphate reducing bacteria [10, 11].



As a part of the joint Vietnamese-German research project EWATEC-COAST a treatment concept comprising improved mechanical pre-treatment and enhanced biological processes has been suggested that is implemented on a pilot-scale at the tannery Dang Tu Ky in the Nhơn Trạch 1 Industrial Zone (Đồng Nai Province). Preliminary results are described in this paper.

2. Material and methods

The wastewater to be investigated has to be taken from the sedimentation basin of the technical-scale plant after physico-chemical pre-treatment because there is no basin for flow and concentration equalisation prior to that stage. Therefore the treatment concept studied does not include such a pre-treatment stage. In the technical-scale plant the incoming wastewater streams are strained and then collected in a rectangular basin where they undergo batch coagulation and pH-adjustment. Sulphuric acid, ferrous sulphate, poly-aluminium chloride and an organic polymer are added in order to precipitate both chromium and sulphide and remove particulate matter by flocculation. After some hours of slow mixing the coagulated wastewater enters a sedimentation stage with an average hydraulic retention time of more than one day. The feed to the pilot plant is withdrawn from the supernatant in this stage. Mean values of some important wastewater parameters are given in Table 1.

Table 1. Raw wastewater parameters (Mean values)

Parameter	This study (Inflow to pilot plant)	Data from tanneries in Europe [3]
Conductivity	20.6 ± 2.8 mS/cm	
pH	7.75 ± 0.44	
Temperature	30.2 ± 2.1 °C	
Total COD	2,600 ± 370 mg/l	5,200 – 14,000 mg/l
TKN	n.a.	320 – 460 mg/l
Ammonium-N	910 ± 246 mg/l	
Nitrate-N	< 1 mg/l	
Phosphate-P	< 2 mg/l	
Total Chromium	1.2 mg/l	6.6 – 87 mg/l
Sulphide	5.6 mg/l	47 – 184 mg/l
Sulphate	3,400 mg/l	770 – 1,850 mg/l
Chloride	n.a.	1,800 – 7,100 mg/l

n.a. = not analysed

According to the data the TDS content is quite high due to salts used for conserving and processing the raw material with chloride and sulphate being the predominant anions. The wastewater investigated in this study contains 2-4 times more sulphate than found in typical tanneries in Europe. However, the data also prove that the pre-treatment applied has reduced the COD significantly due to the removal of particulate organic material. This is in accordance with the findings described in [3] that the combination of mixing + coagulation/precipitation + sedimentation can remove up to 65% of the COD in raw wastewater. Moreover, both chromium and sulphide have been removed efficiently. The remaining load of the wastewater is primarily made up of dissolved organic substances and nitrogen compounds.

When planning the pilot plant study in 2011 wastewater samples were taken at this location and analysed in order to obtain orientating data for the experimental set-up. At that time the COD concentrations were much higher, therefore the idea was to combine anaerobic biological pre-treatment and aerobic post-treatment. When the pilot plant went in operation in autumn 2013 the situation was different, and it was decided to run both biological stages in parallel. Figure 2 depicts the scheme of the pilot plant.

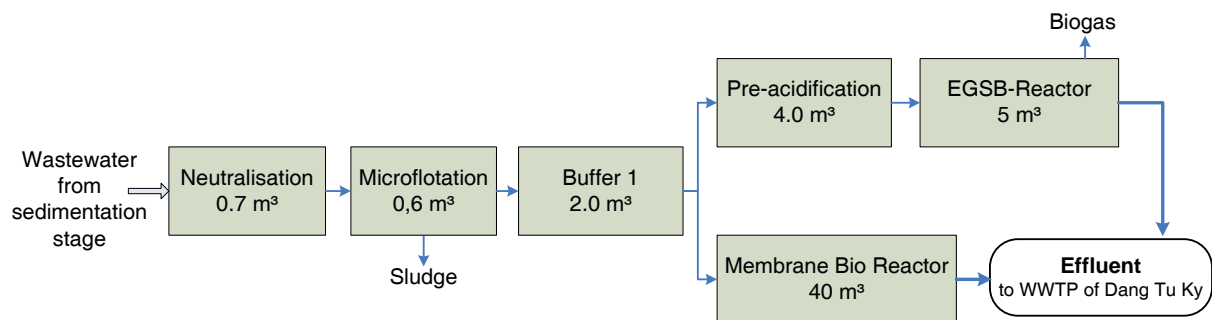


Figure 2. Scheme of the pilot plant

The incoming wastewater is pre-treated by dissolved air flotation (DAF) in order to remove suspended solids still present after the sedimentation stage. An Aquatector[®] Microfloat[®] device (Enviplan Company) is applied for that purpose. Prior to the DAF unit, additional pH-adjustment could be done but this measure was not applied so far. Then the flow is divided in-



to one stream (500 l/h) that enters the membrane bioreactor (A3 Water Solutions Company), and another stream (100 – 150 l/h) directed to the acidification column of the anaerobic stage (EGSB reactor, type ANAFIT-AC, Hager+Elsässer Company). Samples are taken at the inlet and the outlet of both biological stages and analysed onsite with respect to the parameters COD, NH₄-N, NO₃-N, PO₄-P, S²⁻, SO₄ and Total-Cr with Merck Spectroquant test kits. Total suspended solids are determined according to the German standard DIN 38409 H2.

3. Results and discussion

The main task of the DAF system is to prevent the membrane bioreactor from being loaded with fat particles that do not settle during pre-treatment. Fat could cause severe membrane fouling therefore it has to be removed before the wastewater enters the MBR. It was observed that some material is separated by the DAF unit, however, the amount varies and due to the short period of regular operation, it could not be quantified yet.

The influent and effluent COD concentrations of the membrane bioreactor are shown in Figure 3 for the first weeks of regular operation. Activated sludge from the technical treatment plant at the tannery was used to seed the reactor with biomass. However, during the first part of the starting-up phase several technical problems had to be solved, therefore regular operation started with some delay.

According to the data obtained so far, the removal efficiency was less than 50% during the first three weeks when the sludge concentration in the reactor was below 4 g/l TSS. In the meantime the sludge concentration could be increased to more than 10 g/l TSS. This is probably the main reason that COD removal efficiency has increased to about 90% in the second month of operation. This result which must be confirmed during the next couple of weeks is in agreement with data reported in [6] for a MBR while it is higher than removal efficiencies obtained for a sequencing batch reactor (SBR) system [12]. Because of the very low phosphate content of the wastewater it has been decided to add some phosphorous salt to the influent in the future.

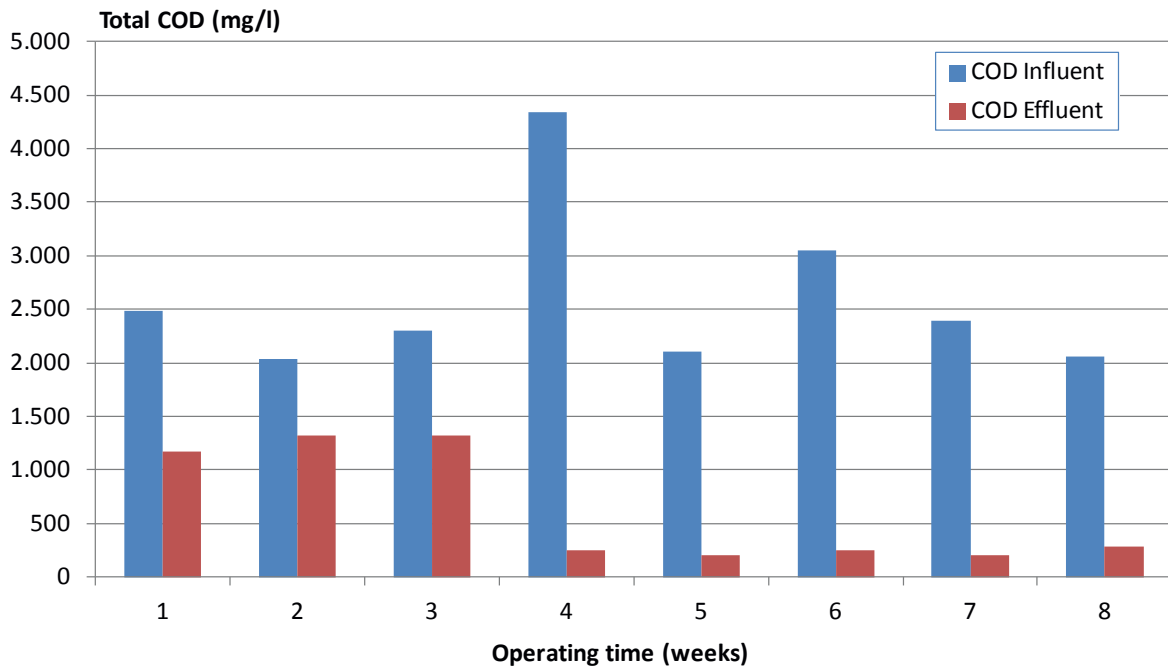


Figure 3. Total COD concentrations for the membrane bioreactor during the first weeks of regular operation

In the technical plant at the tannery no nitrification occurs. Therefore the seeding sludge did not contain significant amounts of nitrifying bacteria. One of the future tasks will be to put a focus on nitrogen removal. The membrane bioreactor is equipped with an anoxic zone, and both the nitrification and the denitrification process will be investigated. According to a study published by Orhon et al. [13], tannery wastewater can have a strong inhibitory effect on nitrifying bacteria. On the other hand the removal of nitrogen from tannery wastewater including denitrification has been studied and modelled successfully [14, 15, 16].

As already mentioned the composition of the wastewater at the study site has changed since the experimental set-up was designed. While the COD concentration is considerably lower now, the concentration of sulphate has increased. It was tried to pre-treat the tannery wastewater anaerobically using granular biomass adapted to starch wastewater. However, the biomass did not degrade the new substrate but rather, after some months of operation, new bacteria developed in the reactor that reduced sulphate to sulphide producing H_2S as a gaseous product instead of methane. Such effects have also been observed in another investigation [11] where it was concluded that the COD:SO₄ ratio is the most crucial factor.



It was decided then to seed the reactor with new biomass from the anaerobic stage of a technical treatment plant for brewery wastewater and to add sugar as a co-substrate to the influent in order to increase the COD:SO₄ ratio. Such an operation mode on a technical scale would be possible if there was an appropriate company in the neighborhood of the tannery that could provide wastewater with a high COD concentration for this type of combined treatment.

The first data show that organic matter is converted to methane now, however, it is still too early to quantify the results. The objective of further work will be to find out which COD removal efficiency can be obtained for the anaerobic reactor and whether a limiting COD:SO₄ ratio can be defined.

4. Conclusions

1. Tannery wastewater pre-treated by coagulation/precipitation and sedimentation is currently treated further by dissolved air flotation and aerobic degradation using a membrane bioreactor. Results from the first period of regular operation show that about 90% of dissolved organic substances measured as COD can be removed. Nitrogen removal has not been observed yet, probably because there were too few nitrifying bacteria in the activated sludge used for seeding.
2. Anaerobic pre-treatment of pure tannery wastewater was not successful because the COD:SO₄ ratio was too low. As a result, sulphate reducing bacteria developed that displaced the methane producing organisms.
3. Future work with the membrane bioreactor will focus on the stability of COD removal, on the maximum loading of the reactor, and on nitrogen removal. Besides, operational experiences with respect to fouling prevention will be collected.
4. Further studies on anaerobic pre-treatment will be related to COD removal efficiency and the volumetric loading of the reactor. Moreover the process stability has to be investigated as a function of the COD:SO₄ ratio. It is also planned to evaluate the aerobic degrada-



tion of the effluent from the anaerobic stage by conducting lab-scale tests.

Acknowledgements

The project funding by the German Federal Ministry of Education and Research (BMBF) under grant no 02WCL1217B, and by the National University of Vietnam (VNU HMC) is gratefully acknowledged. The authors like to thank Prof. N. V. Phuoc for his support and Nguyen Cong Vu, Stefan Nordbruch, Thomas Lücking, Tilman Steinert and Henning Zeich for their technical help.

References

- [1] Hao, N. D. (2009): *Leather and Footwear Industry in Vietnam: The Labour Markets and Gender Impact of the Global Economic Slowdown on Value Chains*. GTZ, Eschborn, Germany 2009.
- [2] Than, L.H. (2011): *Greening the Leather Tanning Industry in Vietnam*. Research Report No. 2011-RR8, Economy and Environment Program for Southeast Asia (EEPSEA), Singapore.
- [3] European Integrated Pollution Prevention and Control Bureau (2013): *Best Available Techniques (BAT) Reference Document for the Tanning of Hides and Skins*. EIPPCB, Sevilla, Spain 2013.
- [4] Murat, S., Ateş Gencell, E., Taşlı, R., Artan, N., Orhon, D. (2002): Sequencing batch reactor treatment of tannery wastewater for carbon and nitrogen removal. *Water Sci. Technol.* **46** (9), 219-227.
- [5] Farabegoli, G., Carucci, A., Majone, M., Rolle, E. (2004): Biological treatment of tannery wastewater in the presence of chromium. *J. Environm. Managem.* **71** (4), 345-349.
- [6] Goltara, A., Martinez, J., Mendez, R. (2003): Carbon and nitrogen removal from tannery wastewater with a membrane bioreactor. *Water Sci. Technol.* **48** (1), 207-214.
- [7] Munz, G., Mori, G., Laura, S., Barberio, C., Lubello, C. (2008): Process efficiency and microbial monitoring in MBR (membrane bioreactor) and CASP (conventional activated sludge process) treatment of tannery wastewater. *Bioresource Technol.* **99** (18), 8559-8564.
- [8] Mannucci, A., Munz, G., Mori, G., Lubello, C. (2010): Anaerobic treatment of vegetable tannery Wastewaters: A review. *Desalination* **264** (1-2), 1-8.



- [9] Durai, G., Rajasimman, M. (2011): Biological Treatment of Tannery Wastewater: A Review. *J. Environm. Sci. Technol.* **4** (1), 1-17.
- [10] Shin, H.S., Oh, S.E., Lee, C.Y. (1997) Influence of sulfur compounds and heavy metals on the methanization of tannery wastewater. *Water Sci. Technol.* **35** (8), 239-245.
- [11] Tadesse, I., Green, F.B., Puhakka, J.A. (2003): The role of sulphidogenesis in anaerobic treatment phase of tannery wastewater treatment in advanced integrated wastewater pond system. *Biodegradation* **14** (3), 219-227.
- [12] Ganesh, R., Balaji, G., Ramanujam, R.A. (2006): Biodegradation of tannery wastewater using sequencing batch reactor – Respirometric assessment. *Bioresource Technol.* **97** (15), 1815-1821.
- [13] Orhon, D., Ates Genceli, E., Sözen, S. (2000): Experimental evaluation of the nitrification kinetics for tannery wastewaters. *Water SA* **26** (1), 43-50.
- [14] Murat, S., Insel, G., Artan, N., Orhon, D. (2003): Effect of temperature on the nitrogen removal performance of a sequencing batch reactor treating tannery wastewater. *Water Sci. Technol.* **48** (11-12), 319-325.
- [15] Chung, Y.J., Choi, H.N., Lee, S.E., Cho, J.B. (2004): Treatment of tannery wastewater with high nitrogen content using anoxic/oxic membrane bio-reactor (MBR). *J. Environm. Sci: Health, Part A. Toxic/hazardous substances & environm. enrg.* **39** (7), 1881-1890.
- [16] Moussa, M.S., Rojas, A.R., Hooijmans, C.M., Gijzen, H.J., van Loosdrecht, M.C.M.. (2004): Model-based evaluation of nitrogen removal in a tannery wastewater treatment plant. *Water Sci. Technol.* **50** (6), 251-260.



Membrane bio-reactors for wastewater treatment

Principles and Design

Martin Oldenburg

¹ University of Applied Sciences Ostwestfalen-Lippe, An der Wilhelmshöhe 44, D-37671 Höxter, martin.oldenburg@hs-owl.de

Abstract

Membrane bio-reactors as a substitute for activated sludge plants with secondary clarifiers are much more in the focus than years before. The benefits of MBRs like enhanced sludge concentrations, solid-free effluents, retention of pathogens and better efficiency of the effluent values are proven by a number of technical applications. Furthermore pharmaceutical residues can be retained in part. On the other hand an higher energy consumption for the treatment in the wastewater as well as additional oxygen demand and an additional maintenance of the membranes have to be taken into account.

Nevertheless membranes for the separation of sludge in combination with biological reactors are in the focus of interest. Herein an overview of the the principles of membrane bio-reactors and their application as well as basics for the design of these units will be given.

Key Words: membrane bio-reactor, membrane, aeration



1. Introduction

The most common process for biological wastewater treatment is the activated sludge process. Various bacteria and other microorganisms are forming the activated sludge and degrade the substances from wastewater under different conditions depending on the demand of effluent quality. Due to long generation times of the microorganisms separation of hydraulic retention time from sludge retention time (sludge age) is necessary. Separation of activated sludge is one of the main tasks of the secondary clarifier behind the activated sludge tank. Beside this concentration of sludge and safety versus the sludge deposition during high hydraulic loadings are other tasks and are taken into consideration during the design process.

Activated sludge systems are dependent by the sedimentation characteristics of activated sludge. Sludge with high specific volumes (Sludge volumetric indices SVI) demands larger areas for sedimentation due to higher sedimentation times and lower surface loading rates. Nevertheless the sludge concentration in activated sludge systems is limited to a sludge concentration of approx. 5 kg MLSS/m³. Treatment stages with higher sludge retention times which are designed for nitrification and denitrification need high specific volumes due to the restriction of the operation of the secondary clarifier system. In addition these sedimentation units are sensitive to changes in the sludge characteristics (increasing SVI) and to maximum peak flows. In both cases the sludge level in the clarifiers may increase and the risk of a solids concentration in the effluent increases. For water bodies in which the effluent of wastewater treatment plants is discharged this will result in higher loadings of sludge and oxygen consumption as well as in higher load of nutrients. Both issues may increase eutrophication in the water environment. Nevertheless the efficiency of secondary clarifiers is high for the removal of suspended solids but very low regarding pathogens, virus and micropollutants (e.g. pharmaceutical residues).

Membrane systems can work as a substitute for settler systems and are able to avoid most of the disadvantages connected with secondary clarifiers. They may act as a replacement for settler, filtration and UV-disinfection and are able to reduce the required treatment volume to ap-

prox. 30 % compared with conventional treatment. Beside this effluent values can be much lower by establishing microorganisms with higher sludge age and their ability of removal of slowly biodegradable organic compounds.

2. Principle of Membrane bio-reactors

Separation of solids by a membrane is a physical process similar to filtration processes. Membranes have pores of specific sizes. Loaded by the feed, which contains liquid (e.g. wastewater) and solids (e.g. sludge), particles smaller than the pores of the membrane are able to pass the membrane (Figure 1). Larger particles remain in the liquid and leave the system in a concentrated solution as retentate (concentrate). The flow passing the membrane is named as permeate or filtrate and its quality depends mainly on the pore size of the membrane. The flux is the flow passing the membrane and can be controlled by the pressure difference between the feed and permeate site.

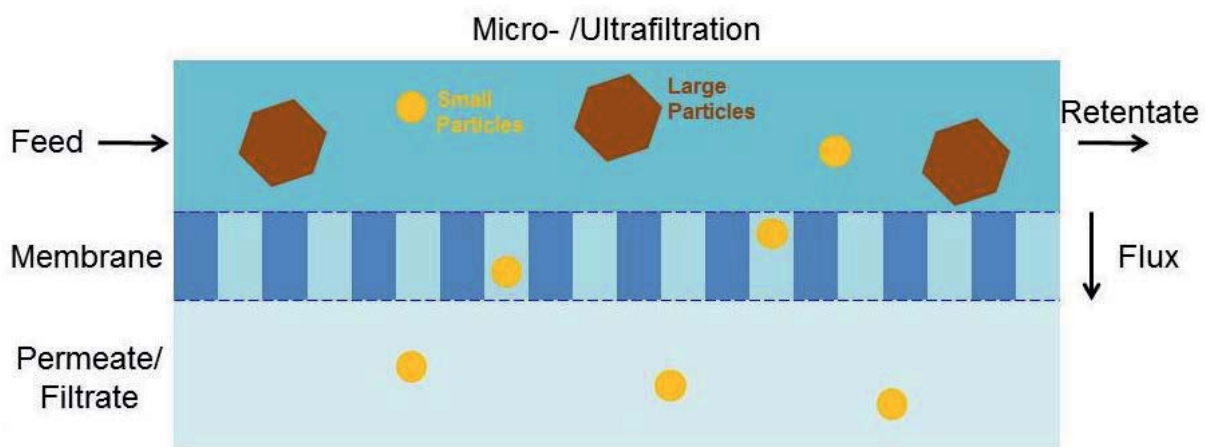


Figure 1. Principle of Micro- and Ultrafiltrationmembranes

Pollutions and substance in wastewater may occur in different ways; either dissolved (salts, organic substances, org. macromolecules etc.) or undissolved (bacteria, protozoa, sludge etc.). Membrane filtration systems are separated into microfiltration (MF), ultrafiltration (UF), nanofiltration (NF) and reverse osmosis (RO) by the limit of separation.

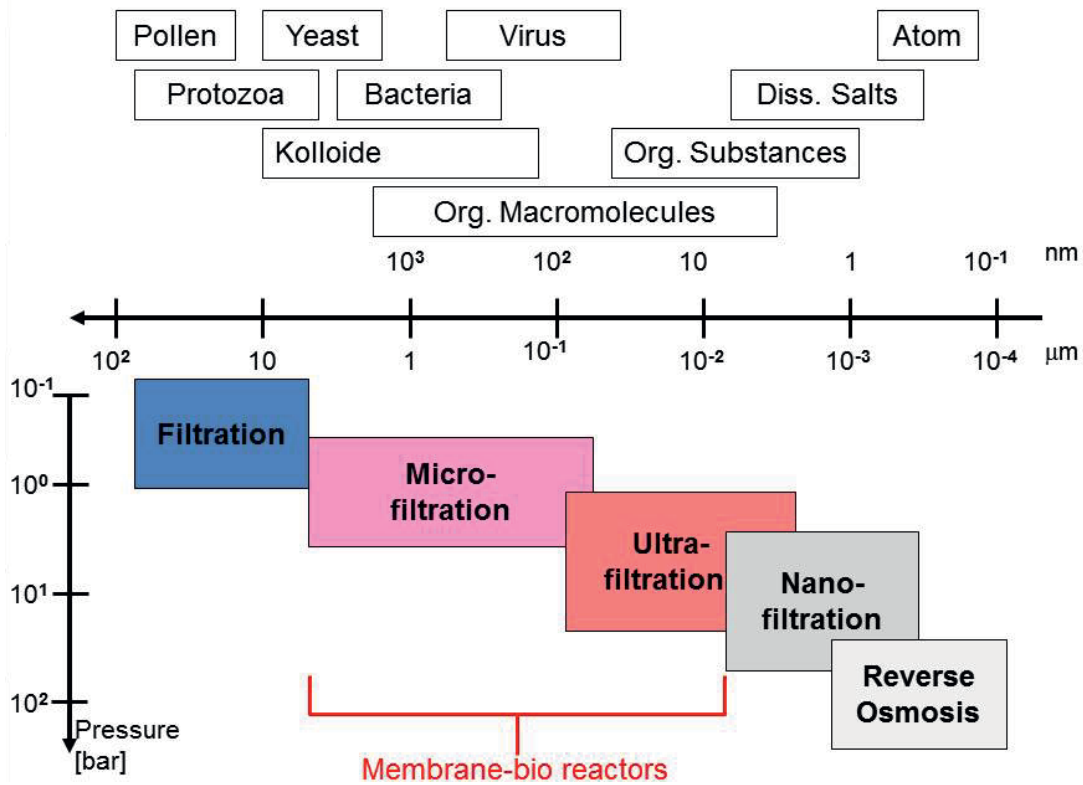


Figure 2. Overview on membrane systems

In Figure 2 sizes of substances originated from wastewater and membrane systems for separating them is given. In membrane bio-reactors micro- of ultrafiltration membranes are in use mainly. Separation limit is in the range of max. 0.4 μm particle size.

Membranes for separation of activated sludge in membrane bio-reactors can be located in different positions and are replacing the secondary clarifier of the activated sludge system (A in Figure 4). Membranes can be located outside of the activated sludge basin either in a separate basin or in a dry position in which sludge is pumped through the membrane units (B). The most common location of membranes in membrane bio-reactors is inside of the activated sludge basin as submersed membrane units (C). The location behind the activated sludge system is possible (C) but not realised at the moment.

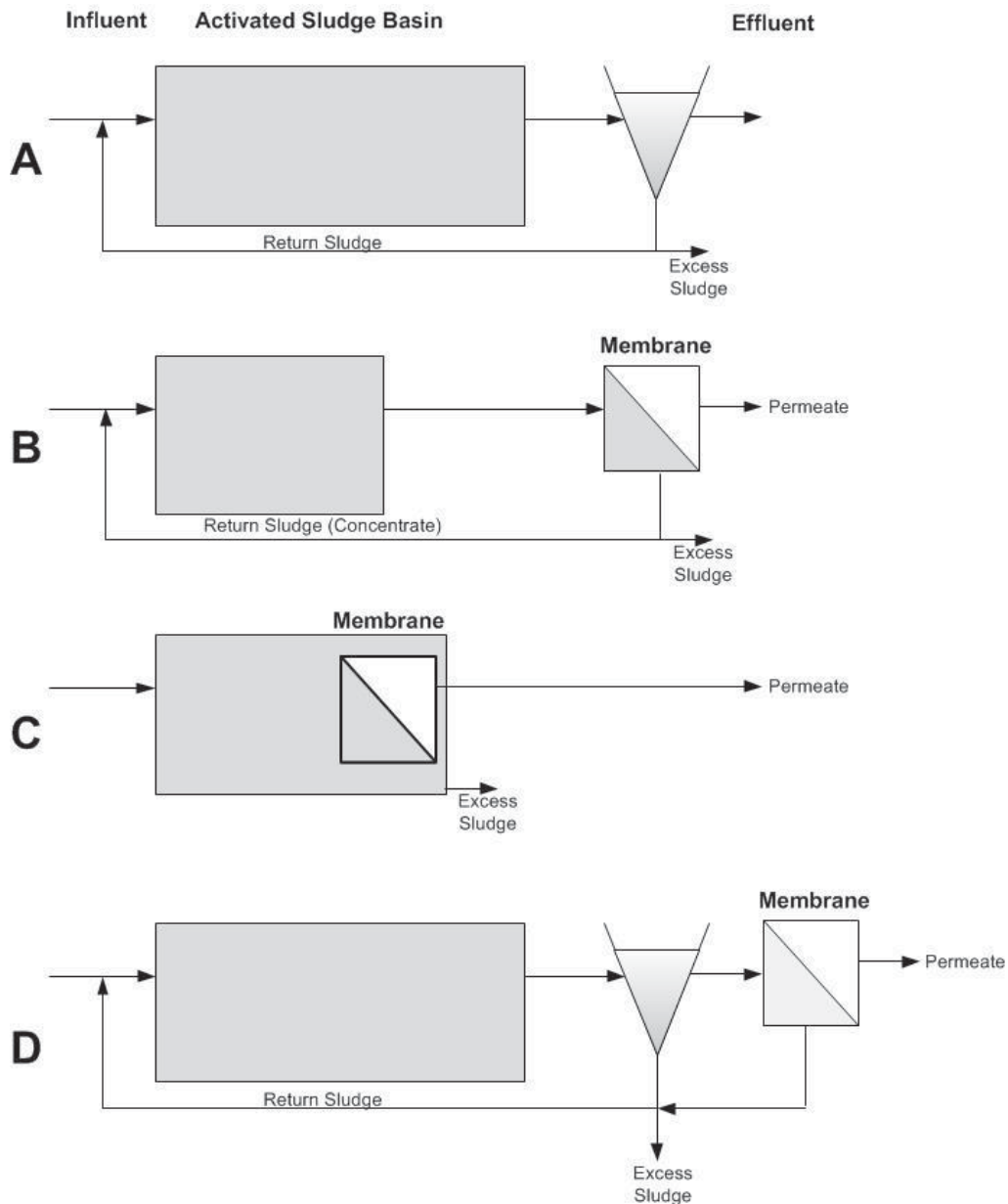


Figure 3. Position of membranes in membrane bio-reactors

For membrane bio-reactors the following demands have to be fulfilled for a proper operation: mixing and aeration of sludge by aerators in combination with turbulences for the control of the boundary layer of the membranes for an enhanced activation of the membrane surface. Pressure difference between feed and permeate side is mainly induced by permeate pumps or by hydrostatic pressure.

Membranes for membrane bio-reactors are used in different forms, the most common ones are membrane-plates as well as capillaries mainly

bundled to packages. Both are fabricated as modules and integrated into the reactors. Figure 4 shows examples for these membrane systems.

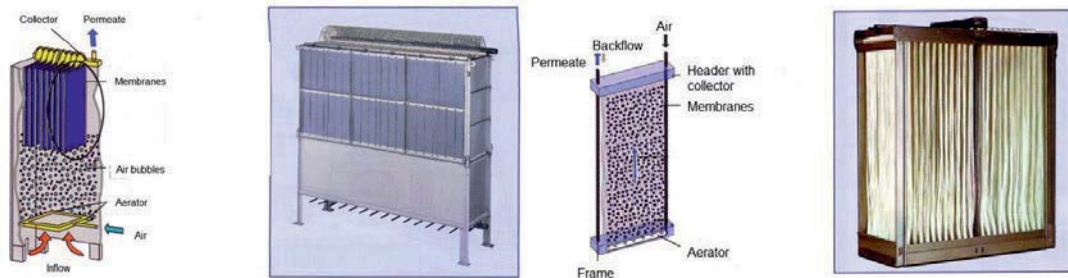


Figure 4. Examples for membrane systems (flat membranes, capillary membrane) [1, modified]

Flat membranes are installed as parallel units on a carrier material with drainage construction. Membrane material is located on both sides of the plate and the flow runs from outside to the inner part of the membrane. Permeate is sucked off by a pump. Aerators under the membrane produce an upflow by uprising air bubbles, which are responsible for a continuous mass exchange at the boundary layer. A modification of the system is the installation of membranes on a drum, which rotations are replacing the boundary layer on the surface of the membrane.

Capillary membranes are fibers with one or more channels in which permeate is infiltrated from outside. Sometimes the membrane layer is installed on a support layer. Position of the capillary can be vertical as well as horizontal. Also here an aerator is installed under the membrane units to increase the velocity in the membrane units.

Materials of the membrane are mainly organic materials, mostly polyethersulfones or polyethylenes. Ceramic materials have been in investigation in research projects, but are not in technical application at the moment.

For minimising the membrane's top layer backflushing with permeate by reverting the flow direction is in use and is scheduled regularly.



3. Design

Membrane systems are very sensitive to fibres and fat originated from wastewater, mainly domestic wastewater. For the protection of membranes and avoiding of accumulation of fibres, hairs and other material inside of the membrane installations and units sieves with a mesh size of 1 – 3 mm are recommended.

Operation with higher MLSS concentrations compared to conventional activated sludge systems is one of the benefits of the membrane bio-reactor systems. Concentrations up to 20 kg/m³ MLSS are possible but result in lower operations times for membranes and in a reduction of oxygen transfer rates. Therefore sludge concentrations of approx. 12 kg/m³ in the activated sludge basin has been proved as an optimum.

The aeration of membrane is necessary for achievement of turbulences on the top layer of the membrane. While the oxygen supply in the activated sludge basin has to be optimised by an maximum of oxygen transfer from gas to liquid with fine bubble aeration membrane units can be aerated with coarse bubble aeration systems.

Due to higher the increase of sludge concentration the oxygen transfer coefficient is significantly reduced. While oxygen transfer coefficient α (ratio of oxygen uptake in wastewater and oxygen uptake in tap water) for conventional system is in the range of $\alpha = 0.7 - 0.8$, for membrane bio-reactors show a transfer coefficient $\alpha = 0.5$. Therefore the oxygen demand is much higher and has to be taken into consideration by the design process.

Design criteria are given in the table 1 below.



Table 1. Parameters for membrane bio-reactors

Parameter	Unit	Dimension
Pore size membrane	μm	0,1 – 0,4
Material membrane	-	Polyvinylidenfluoride, PVDF Polyvinylchloride PVC Polyethersulfon PES Polyacrylnitril PAN Polyethylene PE
Flux (Q_M/A_M)	$\text{m}^3/(\text{m}^2 \cdot \text{h})$	8 – 30
MLSS	kg/m^3	8 – 20
max pressure membrane	mbar	300 – 400
Medium pressure membrane	mbar	20 – 200
Specific membrane area	m^2/m^2	70 – 165
Energy demand aeration membrane module	$\text{kWh}/\text{m}^3_{\text{IN}}$	0,25 – 0,80
Energy demand permeate pump	$\text{kWh}/\text{m}^3_{\text{IN}}$	0,06 – 0,07

4. Experiences

Despite of regular backflushing of membranes flux is reduced during the operation time. For maintaining an acceptable permeability of the membrane a chemical treatment is necessary. Chemicals are used for the removal of organic residues on the membranes to reduce the effect by fouling and scaling. Chemicals used for cleaning are acids like citric acid, oxalic acid or other oxidising substances like hypochlorite. Often the cleaning with two substances step by step is done dependant from the membrane material.

Cleaning of the membrane can take place in-situ; here the addition of cleaning substances takes place from the permeate side. Other possibilities are the filling of the basins with cleaning substances or the external



cleaning. With this method the modules are removed and are submerged into the cleaning substances externally.

Each supplier of membrane systems has his own recommendations for cleaning procedures which have to be taken into consideration.

Due to the short time of implementation of membrane bio-systems information concerning the total lifetime of membranes is very poor and has to be expected in the next years.

Compared to conventional wastewater treatment plants membrane bio-reactors have much better effluent qualities (see table 2). In addition pathogens can be removed by membranes significantly. In general effluent quality of membrane bio-reactors fulfill the criteria of the EU directive for bathing water qualities in most of the application cases.

The removal rate of xenobiotics depends on the quality and the pore size of the membrane. Pharmaceutical residues can be reduced with nanofiltration membranes which are not very common for bio-reactors at the moment, because the treatment is connected with higher energy demands and more membrane area required.

Other benefits are much smaller reactor volumes due to higher sludge concentrations and better degradation rates of slowly biodegradable organic substance due to the high sludge age which results in an accumulation of slowly growing microorganisms as well.

Table 2. Examples for effluent qualities for membrane bio-reactors

Parameter	Unit	Conventional wastewater treatment	Membrane bio-reactor
Suspended solids	g/m ³	10 – 15	0
COD	g/m ³	40 – 50	< 30
N _{total}	g/m ³	< 13	< 13
Spec. energy consumption	kWh/m ³	0.3 – 0.5	1 – 2



Reactor volumes can be reduced significantly due to much higher sludge concentrations. Although in systems with bulking sludge which affects the sedimentation in secondary clarifiers significantly membrane systems are very robust to negative sludge sedimentation characteristics.

Disadvantages are the higher investment costs and the higher operations costs compared to conventional activated sludge systems. Nevertheless the economic investigations with lifetime cycle cost have to be investigated for the decision for membrane bio-reactors.

5. Outlook

Membrane bio-reactors will have an increased implementation in the future due to changes in the effluent qualities for treatment of wastewater. In the future focus will be much more given to the removal of pathogens and slowly or non-biodegradable substances, which can only be removed by membrane separation systems. Due to the development of better membranes and the decrease of costs (e.g. membranes etc.) the disadvantage of slightly higher costs will disappear in the future.

References

- [1] Pinnekamp, J., Friedrich, H. (2003) Membrantechnik für die Abwasserreinigung, ISBN 3-939377-01-5, (in German) Germany 2003
- [2] DWA Working group „membrane bio-reactor systems“ report (in German) January 2005



Municipal and Industrial Wastewater Treatment by Microflotation

Roland Damann

enviplan® Ingenieurgesellschaft mbH, Dammstr. 21, D-33165 Lichtenau-Henglar, E-Mail: damann@enviplan.de

Abstract

In nature, water treatment takes place slowly. Human made treatment processes imitate the processes taking place in nature are affected in controlled conditions, with selected functions and with accelerated speed. Treatment processes are mechanical, physical, chemical or biological and their combinations. Treatments are combinations of two processes, transformation and separation.

Microflotation is an enhanced separation method to float particles to the surface of a tank or basin with the aid of adherent air bubbles.

A sludge bed is formed on the surface and removed hydraulically and/or mechanically. Micro bubbles of 30-50 μm in size are used to separate fragile chemical, biological or non-flocculated flocks in drinking water, industrial process water, municipal wastewater, and industrial effluent and sludge treatment.

Microflotation requires mostly not more than 10-20Wh/m³ of wastewater being treated.

The paper will describe a low pressure and low energy Microflotation technique which has successfully been used over 270 times in national and international projects treating quantities from 1m³/h to 1200m³/h.

It is technically appropriately and primarily economic to substitute classic technology like sand filtration and sedimentation.

Beyond there are several applications at which low pressure Microflotation even outmatch membrane technology or represents a convincing addition.

Key Words: microflotation, membrane technology, wastewater



1. Introduction

At the stage of transformation, dissolved and colloidal substances are transformed by addition of chemicals or by microbiological conversion to form suspended particles called flocks of character to allow separation in sedimentation, filtration or flotation processes or in their combinations. The acceleration needs energy when introducing oxygen or chemicals to the water, generating micro bubbles, mixing, transporting, collecting and lifting the water and sludges. By help of the accelerating technologies the residence times in chemical precipitation in sedimentation processes are 3-4, in dissolved air flotation, DAF processes 0.2-1 and in biological processes 8-18 hours.

Sedimentation processes are normally used to separate settleable suspended solids. Suspended solids inferior to 100 μm and light density solids are considered to create problems when using sedimentation as separation process. Sandfilters succeed sedimentation to capture solids of these characters in drinking water and high-grade wastewater treatment processes. In dissolved air flotation, DAF processes conditions for separation of suspended solids in all density ranges can be created. The function of air-bubbles can be described as follows:

Bubbles act as nuclei for the attachment of suspended and part of the colloidal hydrophobic solids or solids with hydrophobic spots providing a transport mechanism for the movement of the agglomerates of solids to the surface.

2. The process of microflotation

Microflotation is an enhanced method to float particles to the surface with the aid of adherent air bubbles. A sludge bed is formed on the surface and removed hydraulically and/or mechanically. Micro bubbles of 10-80 μm in size are used to separate fragile chemical, biological or non-flocculated flocks in drinking water, high-quality industrial process water, municipal wastewater, industrial effluent and sludge treatment. A difference has to be made to dispersed flotation used in mining industry in mineral segregation processes where the bubble are bigger being 500-2000 μm in size and volume of air is many fold compared to the water volume. Traditional DAF mainly oper-



ates with bubble sizes ranging from 80-300 μm with very inhomogeneous bubble size distribution.

Microflotation requires mostly not more than 10-20Wh/m³ of wastewater being treated.

Bubbles in size 40-70 μm have rise rates from 3-10 m/h. The rise rate is slow enough not to destroy the fragile flocks forming an agglomeration of particles with weak mutual bonding and high enough to allow time for separation of the agglomeration. With the attachment of particles to bubbles the size range of "flock-bubble" grows, and the rise velocities grow simultaneously. The separation rate is accelerated leading to residence times of combined chemical precipitation and flotation from 10 to 60 minutes with need of small footprint areas of treatment plants and decreasing the cost structures of treatment processes.

The micro bubbles are introduced and mixed evenly with the flocculated water. The distance between bubbles is 30-50 μm . The micro bubbles and flocks as well as flock-bubble agglomerates form a suspension. The suspension contains 0.5-1.2 % air in surface water treatment.

In the flotation technology the control elements are effective and a high separation range can be maintained on constant basis. Removal of flocks and small particles takes place effectively, resulting in small coagulant residuals, like ~0.3 mg/l and low turbidity ~0.3 NTU after flotation before the filtration.

Any Flotation processes include liquid, solid and gaseous where physical, chemical, electrical reactions take place at both micro and macro levels. Variations in water quality, quantity, temperature and other factors increase the number of variants. To evaluate the flotation mechanism it is necessary to study the effect of all variables simultaneously.

Flotation requires special design skills. Design faults have led to many plants not working in an optimal way. DAF processes have large safety margins, are forgiving and many mistakes stay hidden. This fact is presented well in a study of 34 drinking water works in Finland: "Despite the good treatment results, some criticism of the waterworks can be made. The design parameters are far from ideal and have resulted in unnecessary high construction costs. The

concept of good engineering has been forgotten. In the author's opinion, this is because the research institutes have not played their part in the design work. Their role is to conduct investigations and publish the results, thus directing development in the right direction. " This paper will describe a next generation low pressure and low energy Microflotation technique which has successfully been used over 270 times in national and international projects treating quantities from 1 m³/h to 1200 m³/h.

It is technically appropriately and primarily economic to substitute classic technology like sand filtration and sedimentation. Beyond there are several applications at which low pressure Microflotation even outmatch membrane technology or represents a convincing addition.

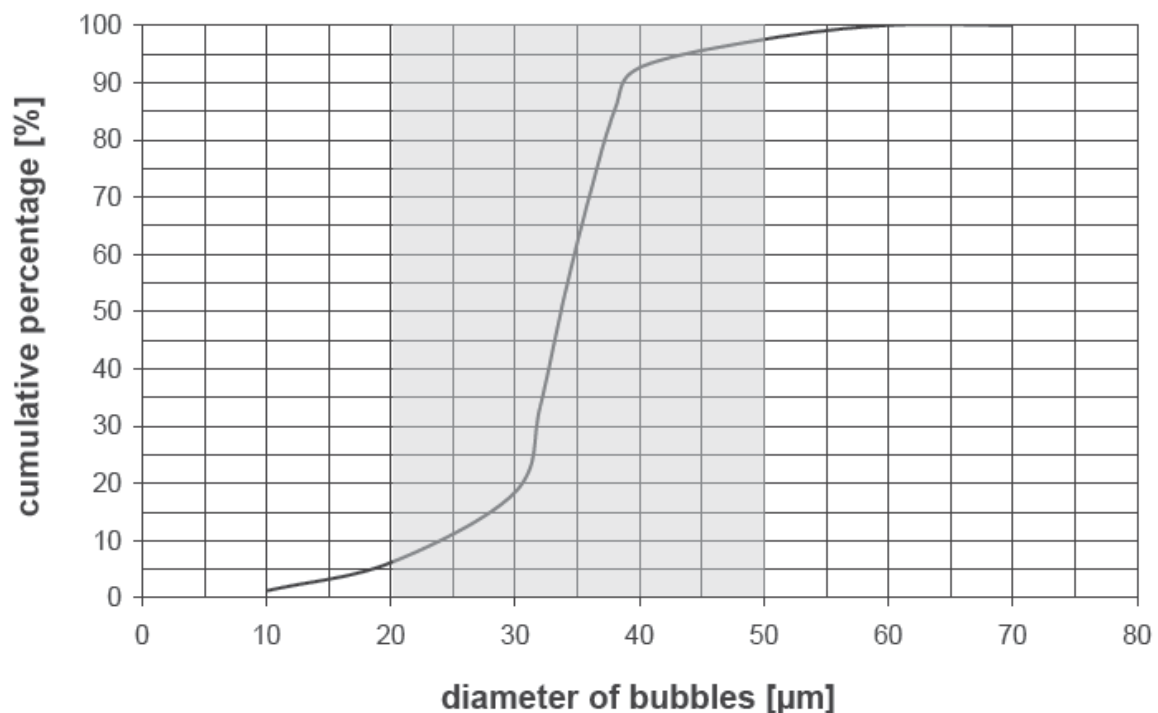


Figure 1. Distribution of Micro-Bubbles according to [Hempel (1994), University of Paderborn]

A major difference of low pressure dissolved air flotation and other flotation processes lies in the volumes of bubbles, amount of air and raising speeds. One macro bubble can be 1000 times bigger in volume compared to one micro bubble. And vice versa the number of micro bubbles



can be 1000 fold in number compared to one macro bubble having same volume.

A distribution of bubble sizes between 20 and 50 microns (see figure 1) is the necessary requirement for an optimum flotation result. Even a small number of bubbles with diameters of above 100 microns can disable a flotation separation process, because larger bubbles rise more quickly and cause turbulence, which severely destroys already build air-flocks-agglomerates. Re-equipping of settling units of secondary clarification in case the separation of active sludge by flotation in order to achieve in overloaded wastewater treatment plants performance improvements.

With an unfavourable adjustment of the bubble spectrum these disturbances can take place in the liquid as well as at the sub-area of the flotation blanket. Inhomogeneous bubble distribution and varying sizes decrease the efficiency of the separation tremendously. Because of this Microflotation technology uses a homogeneous distribution of bubble size, which is realised though the following methods:

Avoidance of bigger bubbles and turbulence before entering of the wastewater stream in the flotation cell,

Usage of a special technique to assemble the pipes to prevent the formation of air pockets, which uncontrollably create bigger bubbles and usage of special injector nozzles (iFloat[®] Technology²) and pressure release valves with integrated selfcleaning system.

It should clearly be pointed out, that self-cleaning systems of injectors and pressure release valves are mandatory to keep the operation of the nozzles permanently under optimal condition. Without self-cleaning system it is impossible to use required small nozzle diameters and cross section of expansion valves, as they are required for the formation of an optimum bubble spectrum.



3. Comparison between microflotation and sand-filtration

Microflotation is characterized by following advantages as compared to sedimentation:

- Shorter sludge residence time in secondary clarifier stage,
- Flexibility in changing operation situation,
- Very low foot print requirement,
- High solid content of the separated sludge so that the total energy requirement is not higher than in the case of a secondary clarification with sedimentation.

A comparison of bubbles in different size ranges indicates big variations as follows (table 1):

Table 1. Size of Micro-bubbles

Size in μm	20	50	100
Number of bubbles per ml	1,250,000	100,000	14,000
Surface area cm^2 in one cm^3	23	12	6,6
Distances in μm	100-150	250-350	500

A proper size range for different waters can be optimised and is one of the control elements.

As a result of these advantages Microflotation is increasingly used as a high performance separation process in wastewater treatment. Investigations in pilot purification plants and large-scale plants in industry (e.g. BAYER AG, BP, Kimberly-Clark...) showed that it is reasonable to substitute classic therapies like gravity sedimentation or filtration.

Improved efficiency of biological treatment plant can be provided with Microflotation as tertiary treatment.

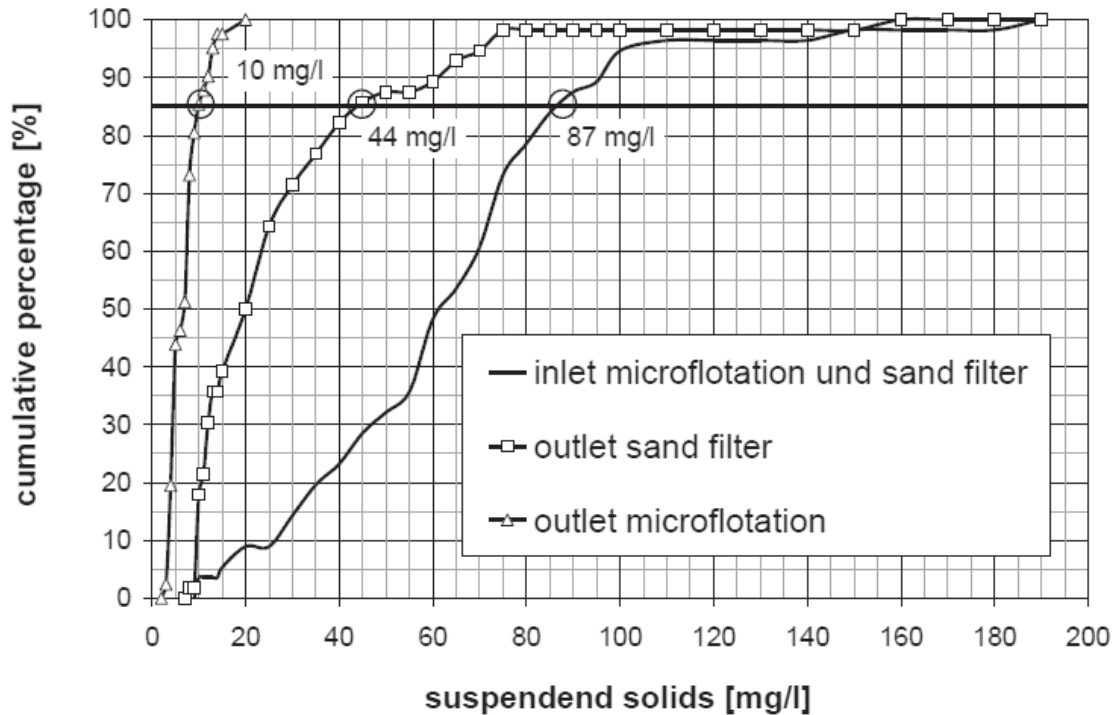


Figure 2. Comparison Microflotation vs. Sandfiltration

The above diagram (figure 2) shows a field test comparison between a Sandfilter and Microflotation. The large-scale Microflotation plant with a capacity of 1500 m³/h has been erected in the chemical industry. The treated water oxygen saturation level is 95-100 %. This is an important fact when the goal is phosphorus reduction. Suspended phosphorus will not dissolve at low oxygen levels.

The parameters bubble generation and bubble-inflow do characterize flotation systems as objectively assessable system parameters.

An operational pressure between 2 and 4 bar, the pressure re-saturation process continuously generates micro-bubbles of 20-50 µm diameter which finely floats in the form of a fog-like bubble filter-cushion unaccessed by suspended and solid matter.

The rising speed of the bubbles is approx. 1mm/s. The process achieves almost 100% level of resaturation.





Thanks. Cám ơn nhiều.